Transport and biodegradation of volatile organic compounds: influence on vapor intrusion into buildings

Sara Picone

Thesis committee
Thesis supervisor
Prof. Dr. Ir. H.H.M. Rijnaarts
Professor of Environmental Technology
Wageningen University, NL

Thesis co-supervisors
Dr. Ir. J.T.C. Grotenhuis
Assistant professor at the sub-department of Environmental Technology
Wageningen University, NL

Dr. P.F.M. van Gaans
Senior Consultant Soil Management at Deltares
Utrecht, NL

Other members
Prof. A. Gargini, University of Bologna, IT
Prof. Dr. A.M. Breure, RIVM/Radboud University, NL
Prof. Dr. Ir. S.E.A.T.M. van der Zee, Wageningen University, NL
Prof. Dr. H. Smidt, Wageningen University, NL

This research was conducted under the auspices of the Netherlands Research School for Socio-Economic and Natural Sciences of the Environment (SENSE)

Transport and biodegradation of volatile organic compounds: influence on vapor intrusion into buildings

Sara Picone

Thesis
submitted in fulfilment of the requirements for the degree of doctor
at Wageningen University
by the authority of the Rector Magnificus
Prof. dr. M.J. Kropff,
in the presence of the
Thesis Committee appointed by the Academic Board
to be defended in public
on Monday 18 June 2012
at 11 a.m. in the Aula.

Sara Picone
Transport and biodegradation of volatile organic compounds: influence on vapor intrusion into buildings, 151 pages

PhD Thesis Wageningen University, Wageningen, the Netherlands (2012)
With references, with summaries in Dutch, English and Italian

ISBN: 978-94-6173-276-7

More and more I have come to admire resilience.
Not the simple resistance of a pillow,
whose foam returns over and over to the same shape,
but the sinuous tenacity of a tree:
finding the light newly blocked on one side,
it turns in another.
(J. Hirshfield)

Summary

Vapor intrusion occurs when volatile subsurface contaminants, migrating from the saturated zone through the unsaturated zone, accumulate in buildings. It is often the most relevant pathway for human health risks at contaminated sites, especially in urban areas; yet its assessment is controversial. Field assessment of vapor intrusion risk is complicated by two interrelated main factors that are controlled by the contaminant's properties: transport processes in the unsaturated zone and biodegradation in the unsaturated zone. Commonly available vapor intrusion models either overlook significant properties at the field scale or, conversely, are too complex to be applicable at this scale. Specifically, moisture variation, liquid diffusion, dynamic processes such as water table variations, and biodegradation are not adequately accounted for. As a result, the soil gas and indoor air concentrations predicted by existing models frequently overestimate measured concentrations by several orders of magnitude.

This thesis addressed transport and biodegradation processes of volatile organic compounds, focusing on aerobic unsaturated zones. The main aims were to i) characterize significant transport processes influencing vapor intrusion and ii) quantify and mechanistically describe biodegradation in unsaturated soils. Field experience, numerical modeling and laboratory experiments were combined to separate out the relevant processes influencing vapor intrusion.

Firstly, state of the art monitoring techniques and available analytical models were applied to a site where groundwater contamination from vinyl chloride poses vapor intrusion risk (Chapter 2). A discrepancy between predictions from commonly used risk assessment models and monitored indoor air concentrations was observed up to several orders of magnitude. The presence of a less permeable layer and the occurrence of biodegradation were likely interrupting the vapor intrusion pathway. These factors could not be taken into account by available risk assessment models.

Therefore, to investigate the effects of physical and chemical properties on vapor intrusion risks, a one-dimensional numerical model including vertical variations of soil moisture, biodegradation and dynamic processes was developed (Chapter 3). A sensitivity analysis performed with the model showed that two factors controlled the predicted concentrations: i) the vertical distribution of the contaminant ruled by variable water-filled porosity, and ii) aerobic biodegradation. The influence of vertical moisture variations was due to liquid diffusion, which significantly retards contaminant transport, confirming the findings of other studies.

In order to obtain biodegradation rates in unsaturated soils, laboratory experiments were conducted with toluene (Chapter 4) and vinyl chloride (Chapter 5) under conditions of no oxygen limitations. For toluene, liquid batches, unsaturated soil microcosm and unsaturated soil column experiments were performed. For vinyl chloride, liquid batches and soil microcosms were compared. In the latter, a new molecular tool based on the quantification of the abundance of the functional gene involved in the aerobic metabolism of vinyl chloride (etnE) was applied to soil and liquid samples. Results from both contaminant showed that the use of liquid phase removal rates as derived from liquid mixed batches significantly underestimates the role of microbial degradation. Microbial conversion in liquid batches appears to be

affected by mass transfer limitations not occurring under unsaturated soil conditions. In unsaturated soil microcosms, liquid phase biodegradation rates for toluene were not related to water content variations. In contrast, vinyl chloride liquid phase degradation rates decreased with increased water content. It was therefore postulated that the influence of water content on micro-scale mass transfer depends on contaminant chemical properties, which control partitioning amongst soil phases. Molecular quantification of the etnE gene showed a linear correlation with the amount of chemical degraded. Hence, it has high potential for application in the field.

The main conclusions from this thesis indicate that soil moisture variations (Chapter 3) and aerobic biodegradation (Chapter 4 and 5) are crucial aspects to be jointly considered for the assessment of vapor intrusion. These may contribute to a significant reduction in the risk associated with dissolved volatile organic contaminants. Specific and relevant implications for modeling and monitoring vapor intrusion can be derived. With respect to vapor intrusion modeling, when including unsaturated zone biodegradation, the use of liquid phase biodegradation rates as derived from liquid mixed batches may underestimate by several orders of magnitude the liquid degradation rates in the unsaturated system. Therefore, biodegradation rates derived from unsaturated system appear more appropriate. With respect to monitoring, vertical soil moisture variations and contaminant/oxygen concentration profiles need to be measured in the field, in order to account for the above processes.

Contents

1 General Introduction

1.1 Background

Accidental release of petroleum hydrocarbons and chlorinated hydrocarbons due to leakages, spills or improper disposal, has deteriorated large volumes of soil and groundwater in all industrial and urban regions in the world (Clement et al., 2000; Lundegard and Johnson, 2004; Wang et al., 1998). Growing awareness on this subject has called for specific regulations issued by environmental authorities. In Europe, protection of water resources has been regulated by the Water Framework Directive, setting common quality objectives for water systems (EC, 2000). Furthermore, soil and groundwater contamination is recognized as one of the major threats in the European soil thematic strategy (EC, 2006 a), aimed at "protecting, preserving and restoring" (EC, 2006 a) soil and subsurface across Europe. Following this document, a draft Soil Framework Directive was issued in 2007 (EC, 2006 b) shaping common procedures to identify and manage threats to soil quality, including soil contamination (Rodrigues et al., 2009). Overall, in Europe, it is estimated that 3.5 million sites are potentially contaminated (EEA, 2007).

The main cause of contamination is industrial activities, followed by municipal or industrial waste disposal. About 10% of European contaminated sites is polluted by petroleum hydrocarbons and chlorinated hydrocarbons (EEA, 2005). Since 2003, in the Netherlands alone, 41 sites affected by this type of contaminants have been remediated (www.soilection.nl). Petroleum hydrocarbons and chlorinated hydrocarbons are known as volatile organic compounds (VOCs) due to their tendency to volatilize at atmospheric pressure. These compounds are generally well soluble in water and thus easily migrate in groundwater, to form large plumes of contaminated groundwater and contaminated soil vapor phase in the unsaturated zone above.

It is often economically unfeasible to reduce contaminant concentrations to background levels required to fit all soil uses because of the extent of the soil and groundwater contamination problem. Instead, remediation strategies are increasingly based on a risk approach and aim at a "fitness-for-use" specific for that

location (Swartjes, 2011). This concept implies that the management of the contaminated site refers to a specific type of land use, and that quality standards for soil, groundwater and vapor phase can vary with these different functions. By restricting the actual use of a site to certain types of land use, acceptable risks levels can be reached without clean up to rigorous, multi-functional soil quality levels.

In Europe, the Netherlands is a pioneer country in contaminated soil management since the case of Lekkerkerk in 1979 (Swartjes, 2011), which triggered the initiation of a specific policy addressing soil and groundwater contamination. Nowadays, in the majority of European countries (Austria, Belgium, Czech Republic, Denmark, Finland, France, Germany, Italy, Norway, the Netherlands, United Kingdom, Spain, Sweden) as well as in the US and Canada, a risk-based regulation on contaminated sites is enforced (Rodrigues et al., 2009). According to a risk-based approach, a site requires remediation when, while having the designated use, it poses unacceptable risks for human health or the environment for the designated use. The level of acceptable risk is defined by regulators and, as such, may vary from country to country (Swartjes, 2011). Risk assessment is a framework to derive a range of specific criteria protecting a certain target from adverse effects that could be caused by exposure to contaminants. Both environmental risks and human health risks can be taken into account. However, in Europe, human health is recognized as the main protection target of soil contamination management (Carlon and Swartjes, 2007).

One of the components of human health risk assessment is the exposure assessment (van Leeuwen and Vermeire, 2007). It involves the identification and quantification of the possible ways the receptor can be exposed to a contaminant. In the case of human health risk assessment, receptors may be residents (adults or children), or workers. With respect to VOCs, two main exposure pathways are considered: transport to groundwater generating extensive groundwater plumes (Christophersen et al., 2005; Pasteris et al., 2002) and migration as gas phase into buildings (Fischer and Uchrin, 1996; Hers et al., 2000; Patterson and Davis, 2009). The latter pathway is known as vapor intrusion (Johnson and Ettinger, 1991) and is schematized in Figure 1.1.

Contaminant vapors in indoor spaces are of concern due to both potential immediate threats to safety (e.g., explosive concentrations of petroleum vapors) as well as possible adverse health effects from lifelong inhalation exposure to toxic chemicals. Risks from vapor intrusion are assessed by means of modeling or measurements. Vapor intrusion is recognized as one of the most controversial risk pathway to be assessed due to i) the low indoor air limit concentrations and the variability of measured indoor air concentrations (McAlary et al., 2011), ii) the frequent overestimation of measured concentrations by the available models (Provoost et al., 2009), and iii) conceptual models neglecting the role of biological processes (Hers et al., 2000). These shortcomings suggest that knowledge gaps on the fundamental processes involved in vapor intrusion are still present.

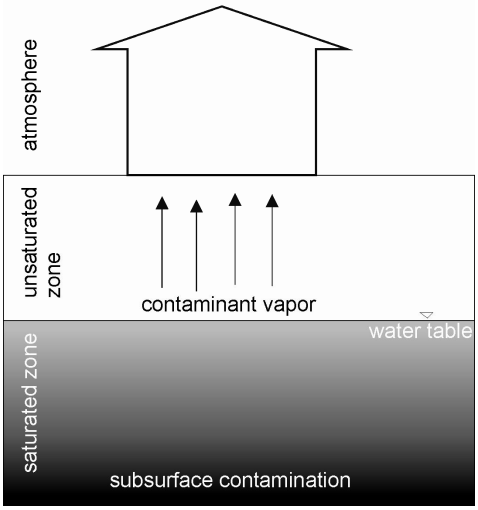

Figure 1.1 – Conceptual model of vapor intrusion.

1.2 Volatile organic compounds

1.2.1 Sources and impacts

Various definitions of volatile organic compounds (VOCs) are available. Here, we restrict the definition of VOC to organic compounds that have a vapor pressure higher than 0.01 KPa at 20°C (EC, 1999). This definition identifies organic compounds that easily evaporate under normal pressure and temperature conditions (USEPA, 2011). As mentioned above, petroleum hydrocarbons (PH) and chlorinated hydrocarbons (CHC) are VOCs. Relevant physical and chemical parameters of the most common contaminants belonging to these groups are shown in Table 1.1.

Petroleum hydrocarbons are the primary constituents in oil, gasoline, diesel, and a variety of solvents and penetrating oils. Benzene, toluene, ethylbenzene and three isomers of xylene (orto-meta-para), together known as BTEX, are the most commonly encountered subsurface contaminants among the various PH. BTEX make up about 11% of petroleum products (Serrano and Gallego, 2004). These are aromatic hydrocarbons, consisting of alkene rings containing double carbon bonds within the chain. Their higher solubility with respect to other gasoline components (i.e. the aliphatic fraction) makes them more mobile (Farhadian et al., 2008). BTEX enter the environment primarily through processes associated with gasoline and petroleum fuels, but also from a number of other industrial activities, such as wood processing, and the manufacturing of pesticides, detergents, chemicals, paints, and varnishes (Andreoni and Gianfreda, 2007). Associated with BTEX contamination, fuel additives such as methyl tert-butyl ether (MtBE) and ethanol might be present.

Table 1.1 – Relevant chemical properties and biodegradation rates of selected VOCs, including oxygenated fuel additives.

Compound	Formula	Density (1)	H (2)	Solubility (2)	Koc (2)	Vapor Pressure(2)	First order Biodegradation rate (3)	
							Aerobic	Anaerobic
		g cm^{-3}	-	g L^{-1}	cm^{-3} g	Pa	d^{-1}	d^{-1}
Benzene	C_6H_6	0.88	0.23	1.79	59	12675	0.389	0.045
Toluene	C_7H_8	0.87	0.27	0.53	182	3990	0.372	0.522
Ethylbenzene	C_8H_{10}	0.87	0.95	0.17	363	1330	0.208	0.283
Xylene (orto)	C_8H_{10}	0.88	0.68	0.18	363	1168	0.263	0.035
Ethanol	C_2H_6O	0.79	$<3x10^{-4}$	completely soluble	16	5866	0.10-0.53 (4)	0.230 (4)
Methyl tert-butyl ether - MtBE	$C_5H_{12}O$	0.74	0.03	51	12	32664	0.001 (5)	0.001 (5)
Tetrachloroethylene PCE	C_2Cl_4	1.61	0.75	0.20	155	9882	0.003*	0.212
Trichloroethylene TCE	C_2HCl_3	1.46	0.42	1.47	166	2527	0.946	0.107†
Dichloroethylene (cis) - cis DCE	$C_2H_2Cl_2$	1.26	0.38	6.30	53	26999	0.399	0.117
Dichloroethylene (trans) - trans DCE	$C_2H_2Cl_2$	1.28	0.17	3.50	36	43890	0.521‡	0.220‡
Vinyl Chloride VC	C_3H_2Cl	0.91	1.10	8.80	19	353780	5.59	0.1

* Aerobic Oxidation rate

† Anaerobic Oxidation rate

‡ Rate for Dichloroethylene (trans) equals to the rate for Dichloroethylene (all other isomers)

Reported rates correspond to the 90th percentile of laboratory studies in aerobic and anaerobic conditions. For CHC, anaerobic first order biodegradation rates correspond to reductive dechlorination rates, whereas aerobic first order biodegradation rates correspond to cometabolic degradation rates where not differently specified.

References:

1) CRC Handbook of Chemistry and Physics, Weast R.C., Astle M., 1981, CRC Press, Florida

2) USEPA, 2004. User's guide for evaluating vapor intrusion into buildings. Washington, DC, Office of Emergency and Remedial Response, 133 p. H : Henry's Law constant at 20°C; Vapor pressure at 25°C

3) Suarez M.P., Rifai H.S., 1999. Biodegradation Rates for Fuel Hydrocarbons and Chlorinated Ethenes in Groundwater. Bioremediation Journal, 3:4, 337-362

4) Corseuil H.X., Alvarez P.J.J, 1996. Natural bioremediation perspective for BTX-contaminated groundwater in Brazil: Effect of ethanol. Water Science and Technology, 34:7, 311-318.

5) Fiorenza S., Rifai H.S., 2003. Review of MtBE Biodegradation and Bioremediation. Bioremediation Journal, 7:1, 1-35

BTEX contamination significantly impacts both ecosystem functions as well as human health. Data on the impact of BTEX on the ecosystem indicate inhibition effects on earthworms survival (Vaajasaari et al., 2002). With respect to human health effects, exposure to BTEX occurs mostly from inhalation and has both acute and long-term toxic effects. Benzene is known to cause leukemia and other blood related types of cancer; it is therefore classified as a known human carcinogen (IARC, 1987). Toluene, ethylbenzene and xylenes have lower toxicity but may still cause adverse health effects. Prolonged exposure to toluene can damage the central nervous system (ATSDR, 1994).

Chronic exposure to xylenes has impacts on the respiratory and the nervous systems (ATDSR, 1995). Finally, the health effects of ethylbenzene are controversial, but the compound is not classified as a carcinogen (ATSDR, 1999). Chronic exposure to these chemicals leads to amnesia and other illnesses, often called "painters disease" as has come to be known from professional fields where solvents were extensively used, such as painting or in the metal industry (Indulski et al., 1996; Wieslander et al., 1994). Also in scientific research, care must be taken to limit exposure to such compounds. Therefore, in this thesis, toluene is used as a model compound for PH in laboratory experiments, since it has similar chemical properties

as the risk driver compound benzene but has no carcinogenic effect and a much lower chronic toxicity.

The other category of VOC is chlorinated hydrocarbons (CHC) (Table 1.1). These compounds are hydrocarbon molecules in which one up to four carbon atoms may be displaced by chlorine. They include tetrachloroethylene (PCE), trichloroethylene (TCE), dichloroethlyene (DCE) and vinyl chloride (VC), in order of decreasing chlorine atoms. These chemicals were intensively used as intermediate for plastic production, degreasers in metal industry and solvents in dry cleaning facilities. Production of TCE and PCE, used as chemical intermediate product and solvents, began in the 1920's. Their market size in Europe amounted to 25,000 tons and 56,000 tons, respectively, in 2006 (ECSA, 2007). Recently, the demand for TCE and PCE has shrunk as a consequence of their declared carcinogenicity (EuroChlor, 2008). Vinyl chloride is used for polyvinylchloride (PVC) production; VC monomer is produced by thermal cracking of 1,2-dichloroethane. In 2008, european VC production capacity was 9 million tons per year (ChemWeek, 2008). Besides industrial production, VC occurs in landfill gas (WHO, 1999), or may accumulate in groundwater at contaminated sites as a result of incomplete biodegradation of PCE and TCE (Bradley and Chapelle, 2000; Lorah and Voytek, 2004). Incomplete biodegradation commonly occurs since only specific bacterial strains are able to perform the complete dechlorination reaction from PCE or TCE to ethene (Maymo-Gatell, 1997). These bacteria are frequently absent or inactive due to environmental conditions or competition in the subsurface of contaminated sites (Dowideit et al., 2010; Lee et al., 2008; Tas et al., 2009; Van Der Zaan et al., 2010).

Contamination from CHC negatively affects ecosystems and human health. Even though data on the environmental effects of exposure to chlorinated solvents are limited, experiments with aquatic invertebrates showed effects on reproduction (Niederlehner et al., 1998). As for health effects, TCE and PCE are classified as probably carcinogenic to humans (IARC, 1995). Prolonged exposure to TCE and PCE may lead to kidney, liver, cervix, and lymphatic system cancer (USEPA, 2001). Based on evidence both from experimental animal studies (Grosse et al., 2007) and epidemiological studies on humans (Gennaro et al., 2008), VC is classified as known human carcinogen (IARC, 1979), and correlated to liver and lung cancer. The toxicity of VC is related to its metabolism in the liver. In particular, a very reactive expoxide (chlorooxyrane) is formed by addition of one oxygen atom while breaking down the double carbon bond of VC. This epoxide can combine with DNA and has mutagenic effects leading to cancer (Melnick, 2002).

Unlike for PH, there is no moderately harmful compound for CHC which can be considered representative of the whole group, as they have different physical and chemical properties. In this thesis, VC is used as focal compound for CHC, since it is the main risk driver amongst this group of contaminants due to its carcinogenicity. In addition, research on VC is needed since information regarding its biodegradation rate in aerobic unsaturated soils is lacking. Because in the case of VC more stringent safety measures needed to be adhered to, the experimental design for VC in part differed from that for the other model compound toluene.

1.3 Fate and transport of VOCs from the subsurface to buildings

1.3.1 VOCs in the subsurface

The presence of VOCs as subsurface contaminants is often related to a separate pure phase immiscible with water, commonly defined as "non-aqueous phase liquid" (NAPL) (Rivett et al., 2011). In the case of PH, the pure phase is lighter than water and floats on the groundwater table migrating in the direction of the groundwater flow (Marinelli and Durnford, 1996). Conversely, TCE and PCE pure phases tend to sink in the aquifer as they are denser than water and form pure product pools on top of low-permeable layers, that may be present at a depth of one to a few meters, to even hundreds of meters in deep sandy aquifers (Hunt et al., 1988; Johnson and Pankow, 1992). From the NAPL source, contaminant dissolution will form a plume. Advection, dispersion and liquid diffusion contribute to contaminant spreading in the water-saturated area, with the last being the slowest process.

Advective transport driven by groundwater flow depends on groundwater velocity. Mechanical dispersion causes migration in both a parallel as well as in a perpendicular direction with respect to the main groundwater flow direction. Dispersion dominates over diffusion at groundwater velocities higher than 0.1 m day^{-1} (McCarthy and Johnson, 1993). Diffusion, driven by solute concentration gradients over space, may dominate at low groundwater velocities.

At the pore scale, a contaminant will partition among soil phases: solid, liquid, gas phase, and, at concentrations above the solubility, a NAPL phase (Mayer and Hassanizadeh, 2005). Under equilibrium assumptions, partitioning is determined by four constants: Henry's law constant (H, vapor/liquid partitioning), K_d (soil/liquid partitioning), vapor pressure and solubility. These compound specific properties may have profound effects on the contaminant mobility and transport (Batterman et al., 1995). The derivation of these constants will be briefly explained here. Henry's Law constant defines the partitioning between dissolved (C_{liq}) and vapor concentration (C_{gas})

$$C_{gas} = H'\left(\frac{C_{liq}}{RT}\right) \tag{1}$$

where H' is expressed in Pa L mol^{-1}, R is the universal gas constant (8.31 J mol^{-1} K^{-1}) and T is the absolute temperature (K). Henry's Law constant can also be expressed as dimensionless by

$$H = \frac{H'}{RT} \tag{2}$$

(Yaron et al., 1996). Henry's law constant for volatile compounds holds for diluted solutions, i.e. solution approximately below a concentration of 10,000 mg L^{-1} (Staudinger and Roberts, 2001). It is mostly temperature dependent because of the temperature dependency of vapor pressure and solubility of the compounds (Goss, 2006).

The solid to liquid partition coefficient K_d for organic compounds is mostly related to sorption to the organic matter fraction of the soil as:

$$K_d^{'} = K_{oc} * f_{oc} \tag{3}$$

where K'_d is the partitioning coefficient in L kg^{-1}, K_{oc} (L kg^{-1}) is the organic carbon-water partitioning coefficient, and f_{oc} is the mass fraction of organic carbon (Appelo and Postma, 1994).

The K'_d relates the concentration in the liquid phase to the sorbed concentration C_{soil} in mg kg^{-1}

$$C_{soil} = C_{liq} * K'_d \quad (4).$$

By correcting for bulk density (kg L^{-1}) and porosity (Lpores/Ltotal), K_d can be expressed as dimensionless.

1.3.2 Transport of VOCs in buildings

Once a dissolved contaminant has reached the unsaturated zone, volatilization may lead to migration of the compound as vapor and cause it to enter buildings through the building foundations. The main transport mechanism leading to contaminant transport into buildings is gas diffusion (McAlary et al., 2011). Diffusion fluxes are driven by the concentration gradient between the source zone in the groundwater and the ground surface, where the volatile compound concentration is close to zero.

Additionally, an advective gas flux through the gas filled pores of the soil may contribute to the overall vapor intrusion flux as a response to pressure differentials. Pressure differentials can arise from i) a positive pressure gradient between the building foundation and the soil gas pressure, ii) effects of wind and heating (stack effect), or iii) barometric pressure fluctuations. The first process is referred to as a suction flow (Krylov and Ferguson, 1998). The wind pressure on one side of a building may also generate pressure differentials causing gas entering and leaving the subsurface (McAlary et al., 2011). The stack effect, particularly important in winter months, describes an air flux directed upwards and resulting from the pressure difference between the columns of warm and cold air respectively inside and outside a house (Krylov and Ferguson, 1998). Barometric pressure variations may cause fluxes in and out of the soil (Massmann and Farrier, 1992). Generally, pressure fluctuations are not significant in determining vapor fluxes (Atteia and Hoehener, 2010; Parker, 2003), as diffusion fluxes are often found several orders of magnitude larger than advection fluxes due to pressure fluctuations (Choi and Smith, 2005). Since larger unsaturated zone thicknesses, or gas permeabilities, increase the importance of advective fluxes (Choi and Smith, 2005), these fluxes may contribute significantly in specific cases.

Besides advection and diffusion through the unsaturated zone, an often overlooked vapor transport mechanism is created by preferential pathways through which vapor may migrate faster (McAlary et al., 2011). Preferential pathways might be e.g. utility drains filled with coarser material in an otherwise low air permeable soil.

Another factor influencing vapor transport is the type of building foundation. Buildings with a basement have an underground floor which is separated from the soil surface by a concrete layer (type a in Figure 1.2). In this case, vapors may enter the building by cracks in the basement floor or walls or by diffusing through the

walls. Buildings with a crawl space (type b in Figure 1.2) lack a separation surface between the soil surface and the enclosed space. The crawl space is below the building floor, and is normally not higher than 50-60 cm. In this space, utilities like heating pipes or electricity are usually installed. Because of the absence of a separating surface, houses with a crawl space are most sensitive in terms of potential risks from vapor intrusion. Finally, buildings with a slab foundation (type c in Figure 1.2) lie on top of a concrete surface which is in contact with the soil. The contaminated vapors can intrude the building by diffusion through concrete, and by cracks in the concrete layer.

In case of vapor intrusion, once the contaminant has entered the building, its concentration in indoor air is additionally determined by the building ventilation, normally expressed as a bulk air exchange rate (Krylov and Ferguson, 1998).

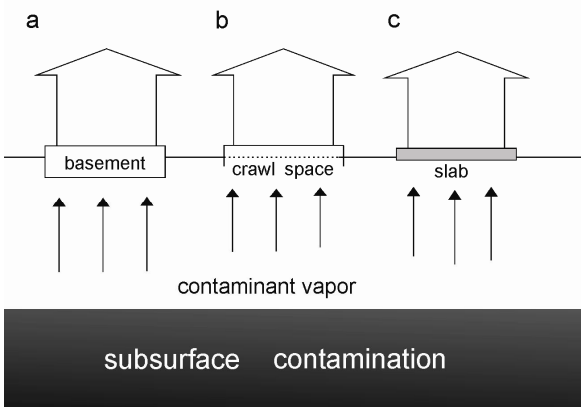

Figure 1.2 – Types of building foundation.

1.3.3 Available vapor intrusion models

Several analytical and numerical models have been developed to predict vapor intrusion into buildings. An overview of available models for vapor intrusion is presented in Table 1.2. They range from analytical models requiring a simpler data input to numerical models which demand a more thorough site characterization. Most of the analytical models rely on the work of Jury et al. (1983; 1984a,b,c; 1990), who developed a one dimensional screening model for leaching and volatilization of organic compounds in the unsaturated zone. The main conceptual understanding was derived from previous studies on radon transport (Garbesi and Sextro, 1989; Loureiro et al., 1990; Nazaroff and Cass, 1989; Nazaroff et al., 1987).

In the case of analytical models, the fate and transport model is in general a steady state model, and in most cases is one dimensional (vertical direction). Steady state models assume linearity and time invariant partitioning between different soil phases. Most models in use are deterministic. They rely on reference parameters for compounds and for soil type that are provided as defaults in the model. Some analytical models also allow a probabilistic approach, accounting for the variability

and the uncertainty related to the parameters used in the calculations. Once the volatile compound enters the building, the building is generally assumed as a well-mixed container (Turczynowicz and Robinson, 2001).

The most commonly used models in practice are analytical one dimensional models which account for gas diffusion and advection, and neglect biodegradation (Johnson and Ettinger, 1991; Waitz et al., 1996). All the available models take into account gas phase diffusion and advection due to pressure gradients (Johnson and Ettinger, 1991; Jury et al., 1990; Jury et al., 1984c; Little et al., 1992). The Johnson and Ettinger model (Johnson and Ettinger, 1991) couples steady-state diffusion from a planar source to vapor intrusion into basements of buildings by diffusion and advection processes. It is the most widely applied model for vapor intrusion in practice. The VOLASOIL model developed by Waitz et al. (1996), updated by Bakker et al. (2008), also considers pressure differentials due to atmospheric pressure gradients or water infiltration. The Johnson and Ettinger model as well as VOLASOIL assume a homogeneous soil profile. Both models can include a pure phase (NAPL) as a separate source feeding the vapor phase. They differ in the types of building scenarios considered and in the possibility to be used as site specific or generic risk assessment tools (McAlary et al., 2011). More recently, aerobic biodegradation including oxygen consumption has been incorporated in analytical models (DeVaull, 2007).

Besides analytical models, a number of numerical models have been developed, which take into account variation in soil properties or specific processes (Table 1.2). The numerical models may account for i) specific physical factors including ventilation, barriers, heterogeneities, or the presence of a NAPL phase (Davis et al., 2005; Fischer and Uchrin, 1996; Mendoza and Frind, 1990a; Mendoza and McAlary, 1990; Tillman and Weaver, 2007); ii) transient conditions such as variations in atmospheric pressure or water table (Garbesi and Sextro, 1989; Little et al., 1992; Massmann and Farrier, 1992); and iii) biochemical processes and factors influencing these, including the presence of peat layers, anaerobic soils, and seals preventing oxygen influx (Abreu and Johnson, 2006; Hers et al., 2000; Johnson et al., 1999).

Analytical models such as those introduced by Johnson and Ettinger (1991) and Waitz et al. (1996) provide screening tools for risk estimates, but neglect significant properties and processes. Conversely, three dimensional numerical models such as those presented by Abreu and Johnson, and Bozkurt (Abreu and Johnson, 2005; Bozkurt et al., 2009) are often too complex and too demanding with respect to specific input-data that may be unavailable in real world field situations. Therefore, there is a clear need for transport models which adequately describe the heterogeneous bio-physical subsurface system using parameters such as organic matter content, concentration at a specific depth, and soil type (peat, clay, silt, sand, gravel) that can be readily obtained from the field.

1.3.4 VOCs biodegradation pathways

Biodegradation is the process by which soil microorganisms transform hazardous contaminants to harmless products (Alexander, 1999). The biodegradation

processes that are likely to occur in the environment are determined by a combination of biotic factors, i.e. presence and activity of the appropriate microorganisms, and environmental factors, such as redox conditions, pH, moisture content, temperature, nutrient availability (Van der Zaan, 2010). Here a brief overview of possible biodegradation pathways for BTEX and CHC is presented.

Under aerobic conditions, BTEX are considered relatively easily degradable compounds. These chemicals are degraded aerobically by means of oxygenase catalyzed reactions, which require molecular oxygen for the hydroxylation of the aromatic ring, or an alkyl substitution (Kim and Jaffe, 2008). Oxygen serves not only as electron acceptor, but it is also used in the initial enzymatic activation (Weelink et al., 2008). Many bacteria species, as well as fungi, are capable of using BTEX as carbon and energy source (Attaway and Schmidt, 2002; Deeb and Alvarez-Cohen, 1999; Lee and Lee, 2001; Prenafeta-Boldu' et al., 2004; Shim and Yang, 1999). Under anaerobic conditions, toluene and ethylbenzene can be degraded by denitrifying and sulfate-reducing bacteria (Chakraborty and Coates, 2004). Anaerobic benzene degradation has been reported under iron reducing (Anderson et al., 1998), sulfate reducing (Vogt et al., 2007), and methanogenic conditions (Kazumi et al., 1997). Recently, Weelink et al. (2008) have isolated a culture which is able to degrade benzene under chlorate reducing conditions. Literature values of BTEX biodegradation rates are reported in Table 1.1 for aerobic and anaerobic conditions.

For CHC, three main biodegradation pathways are possible: i) reductive dechlorination, ii) oxidative reactions, iii) oxygenase mediated reactions. In general, for more chlorinated compounds, reductive dechlorination becomes more favorable than oxidation (Vogel, Criddle et al. 1987), as it can be seen from reported biodegradation rates in aerobic and anaerobic conditions in Table 1.1. Reductive dechlorination is favorable under sulfate reducing and methanogenic conditions (Vogel and McCarty 1985; Suarez and Rifai, 1999), and requires the presence of electron donors. However, complete reductive dechlorination from PCE to ethene has been found to this moment to be only performed by specific bacteria belonging to the species *Dehalococcoides* (He et al., 2005). Due to the absence of the appropriate microorganism, or to the insufficient amounts of electron donors, incomplete reductive dechlorination at many sites leads to the accumulation of DCE and VC (Lorah and Voytek, 2004). Oxidative reactions require electron acceptors in aerobic or anaerobic environments and are favorable for the less chlorinated compounds (Bradley and Chapelle, 1997; 1998; Davis and Carpenter, 1990). Finally, indirect biodegradation via cometabolic reactions, i.e. non energy yielding reactions, has been reported (Alvarez-Cohen and McCarty 1991).

Table 1.2 – Selected overview of available models for vapor intrusion (not intended to be exhaustive).Type indicates the dimensions of the model (1,2 or 3D).

Type	Reference	Contaminant Source	Transport processes	Biodegradation	Building	Time Dependency/Seasonal effects/Indoor contaminant sources
Analytical 1D	Jury et al.1983, 1984a;1984c	Infinite dissolved or NAPL source	Volatilization, diffusion, advection, leaching	Yes	No	No
	Johnson and Ettinger, 1991	Infinite dissolved or NAPL source	Diffusion, advection	No	Crawl space, slab on grade, basement	No
	Little et al., 1992	Infinite dissolved or NAPL source	Diffusion, advection	No	No	No
	Sanders and Stern, 1994; Sanders and Talimcioglu, 1997	Finite source	Diffusion, advection, based on behavior assessment model	Yes	Yes	Yes
	Ferguson et al., 1995; Krylov and Ferguson, 1998	Finite source	Vaporization, diffusion, suction flow, advection due to pressure differentials	Yes	Crawl space, basement	Indoor sources of contaminant
	Bakker et al., 2008; Waitz et al., 1996	Infinite dissolved or NAPL source	Diffusion, volatilization, advection, sorption	No	Crawl space, slab on grade, basement	No
	Johnson et al., 1999	Infinite, dissolved source/NAPL finite source	Diffusion, advection, sorption	Yes	Yes	No
	Olson and Corsi, 2001	Finite source	Diffusion, advection due to pressure gradients between soil/basement	No	Yes	No
	Parker, 2002	Finite NAPL or dissolved source	Diffusion, advection	Yes	Yes	Barometric pumping
	Mills et al., 2007	Infinite or finite source	Diffusion advection, sorption, decay	Yes	Crawl space, basement	Yes
	Atteia and Hoehener, 2010	Infinite dissolved source	Diffusion, advection, variable soil moisture	No	No	Barometric pumping
	Murphy and Chan, 2011	Dissolved or NAPL source	Diffusion, advection, ventilation	No	Crawl space, basement,slab	No
Numerical 1D	Turczynowicz and Robinson, 2001	Infinite dissolved source	Diffusion, advection, ventilation, coupled with risk calculation based on Jury et al., 1984	Yes	Crawl space	No
	Choi and Smith, 2005	Vapor source	Diffusion advection	No	Slab/ basement	Temperature variation, variable water table
Numerical 2D	Hers et al., 2000	Vapor or dissolved source	Diffusion, advection, sorption	Yes	Slab	No
	Tillman and Weaver, 2007	Infinte source	Diffusion, advection	No	Yes	Time variable moisture
Numerical 3D	Abreu et al., 2009; Abreu and Johnson, 2005; Abreu and Johnson, 2006	Vapor or dissolved source	Volatilization, diffusion, advection through building cracks	Yes	Slab	Transient indoor and ambient pressure
	Bozkurt et al., 2009; Yao et al., 2011	Finite source	Diffusion, advection, sorption	No	Yes	No
	Yu et al., 2009	Dissolved or NAPL source	Dissolution, diffusion, advection, heterogeneous permeability distribution	No	Slab	Barometric pressure

Some of the primary substrates that support cometabolism of chlorinated solvents are methane, ethene, propane, toluene, and phenol (Suarez and Rifai, 1999).

Other compounds like ethanol, methyl tert buthyl ether (MtBE) can be present in fuel or solvent spills which might affect biodegradation of PH and CHC (Freitas and Barker, 2011; Jewell and Wilson, 2011; Sanders and Hers, 2006). Ethanol was shown to increase the extension of BTEX plumes (Ruiz-Aguilar et al., 2003). This is due to two mechanisms: the enhanced solubility of BTEX in presence of ethanol, and the reduced aerobic biodegradation due to competing oxygen consumption for ethanol fermentation, which produces methane (Jewell and Wilson, 2011). Presence of ethanol-derived methane can generate pressure gradients which might drive contaminated vapor fluxes (MPA, 2010).

MtBE was shown to impact indoor air although only at high dissolved concentrations (Sanders and Hers, 2006). This compound can be aerobically biodegraded but the presence of other aromatics inhibits its degradation (Deeb et al., 2000), thus in general relatively low degradation rates are observed (Table 1.1). Bioconversion may occur independently from molecular oxygen. Moreover, due to the high solubility of fuel oxygenates, the dissolved concentrations might reach values at which biodegradation is strongly inhibited. It was decided to focus this thesis on two model compounds, toluene and VC representing aromatic and chlorinated hydrocarbon group, respectively.

1.4 Knowledge gaps in assessing vapor intrusion

Vapor intrusion may occur from subsurface contamination if the interplay between transport mechanisms and biodegradation processes, controlled by contaminant properties, results in a net flux of contaminant to the built environment above (Figure 1.3). Once the compound has reached the top of the unsaturated zone, additional variability and uncertainty in determining the effective risk is related to building-specific parameters.

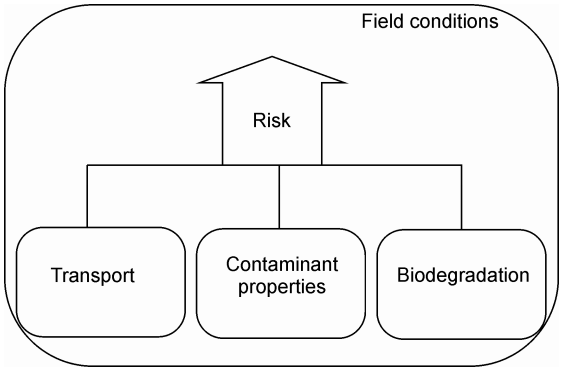

Figure 1.3 - Schematic overview of main factors in vapor intrusion.

Risks as deduced from concentrations in the top of the unsaturated zone can be assessed by measurements or by modeling. Provoost et al. (2009; 2010) compared measured and predicted concentrations with seven commonly used models for vapor intrusion. These authors showed that predicted soil air concentrations are up to two orders of magnitude larger than measured values (Figure 1.4).

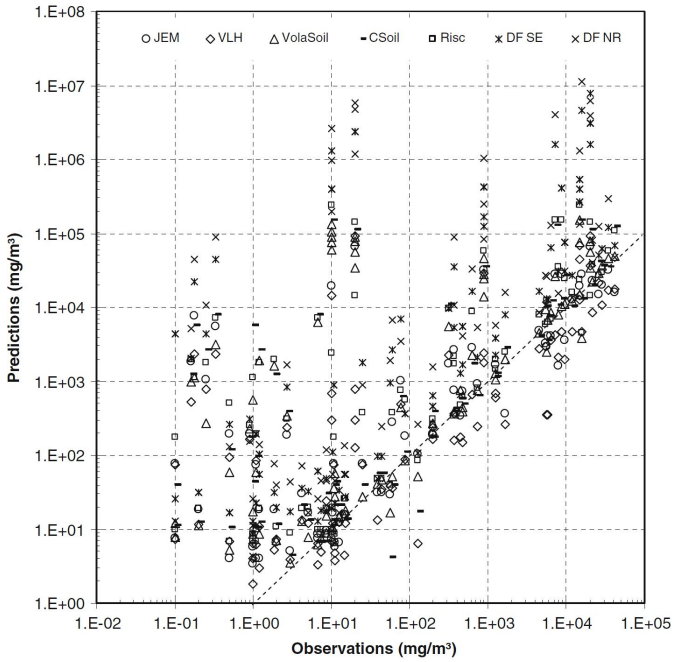

Figure 1.4 – Comparison between observed and predicted soil air concentrations with seven vapor intrusion models (Provoost et al., 2010).

Moreover, for a single model predicted concentration, measured concentrations span over two or three orders of magnitude, indicating that risks are not correctly ranked by the model predictions. Apparently, the models contain assumptions and bio-physical descriptions of the soil system that significantly deviate from the actual situations in the field. This indicates that knowledge gaps related to an adequate understanding, description and measuring of the essential processes and parameters in the unsaturated zone are still present. These will be discussed hereafter in detail in relation to field monitoring (Section 1.4.1), transport in the unsaturated zone (Section 1.4.2), and biodegradation in the unsaturated zone (Section 1.4.3).

1.4.1 Field measurements

In the field, monitoring to assess vapor intrusion consists normally of a combination of groundwater, soil gas, and indoor air measurements. Reported literature about field studies is mostly related to North American sites (e.g. Fitzpatrick and Fitzgerald, 2002; Hers et al., 2001; Sanders and Hers, 2006). For all

compartments (groundwater/soil gas/indoor air) two types of methods can be alternatively or simultaneously applied: active or passive. Active measurements imply pumping out a certain volume of groundwater, soil air or indoor air into a sample collection device. Conversely, passive methods consist of sorbent materials left in the target compartment so that contaminant can be selectively adsorbed over time, using the natural advective and diffusive processes for delivery. Typically, active measurements can be performed within a shorter time, in which peak concentrations may or may not occur, whereas passive methods can take several days or weeks and thereby give averaged results.

Unresolved issues regarding field measurements to assess vapor intrusion are mostly related to two considerations: i) sample representativeness, and ii) indoor air background concentrations (McAlary et al., 2011). Sample representativeness is problematic for groundwater and soil gas measurements due to spatial and temporal variations (Luo et al., 2009; McDonald and Wertz, 2007). Regarding groundwater measurements, depth averaged samples integrate vertical concentration gradients that may be present in groundwater (Fitzpatrick and Fitzgerald, 2002). For soil gas measurements, it is not straightforward to relate concentrations measured in close proximity to a building to the actual concentrations below the building, due to soil heterogeneity (McAlary et al., 2011). In addition to that, volatile organics background concentrations due to household activities or outdoor air input are a major limitation in correlating indoor air measurements with subsurface contamination (Dawson and McAlary, 2009; Doucette et al., 2010; McHugh et al., 2006; Sanders and Hers, 2006). Moreover, detection of low levels of VC, which is particularly important due to its carcinogenicity, remains an analytical challenge (Ochiai et al., 2003).

The above mentioned critical points complicate the comparison between measurements and vapor intrusion model predictions. Therefore, a more thorough understanding of the mechanisms involved can i) provide indications about which measurements need to be performed in the field, and ii) support the interpretation of field data and comparison with predictions.

1.4.2 Transport through the unsaturated zone

The transport processes occurring between the upper centimeters of a contaminated water-saturated zone and the ground surface are relevant for vapor intrusion. In this portion of the soil profile, depending on soil type, water content varies from full water saturation at the top of the capillary fringe to residual moisture content at the top of the soil surface. Here, we define the capillary fringe as the portion of the soil profile above the groundwater table in which the pore space is tension saturated but the pressure may be lower than atmospheric pressure (Silliman et al., 2002). Typically, the capillary fringe is relatively thin for sandy soils and relatively thick for more clayey soils, due to prevailing surface tension in relation to pore size (Koorevaar et al., 1983).

The unsaturated zone is characterized by decreasing amounts of liquid phase in upward direction and consequently by the presence of an additional gas phase within soil pores. At the interface between water saturated and the first air-filled

pores the volatile contaminant will volatilize and partition into the gas phase, where diffusion and advection will drive the mass transfer. Simultaneously, sorption will occur on soil surfaces. Sorption of gaseous organic compounds is driven by three mechanisms i) adsorption on mineral surfaces, ii) partitioning into surface bond water, and iii) partitioning into soil organic matter (Farrell and Reinhard, 1994). In dry soil conditions, i.e. water contents below 2%, sorption onto mineral surfaces prevails, and competition between water and the organic compound for mineral surfaces occurs (Batterman et al., 1995). In contrast, in wet soils (>4% moisture) VOC adsorption is mostly related to the organic matter as driven by the hydrophobicity of many organic compounds (Batterman et al., 1995). Adsorption decreases at increasing moisture content (Chiou and Shoup, 1985; Ong and Lion, 1991; Smith et al., 1990).

Diffusion is the dominant transport mechanism in unsaturated soil. Diffusion is of greater significance in the gas phase since gas phase diffusion coefficients are larger than aqueous phase diffusion coefficients, with factors in the order of $1x10^3$ to $1x10^4$ (Pasteris et al., 2002; Wiedemeier et al., 1999). However, diffusion is influenced by soil properties, as it is hindered by the tortuous nature of the pores, the diminished cross-sectional area available for movement, and by the pore size (Grathwohl, 1998).

The effective diffusion coefficients can be calculated as a function of the porosity and soil water content of the medium, as proposed by Millington and Quirk (1959):

$$D_{eff} = D_a \frac{\theta_a^{10/3}}{\theta_T^2} + \frac{D_w}{H} \frac{\theta_w^{10/3}}{\theta_T^2} \tag{5}$$

where D_{eff} is the effective diffusion coefficient, D_a is the compound diffusion coefficient in air, θ is the porosity (subscripts T for total, a for air-filled, and w for water-filled), D_w is the compound diffusion coefficient in water, H is the Henry's Law constant.

It is well known that slow liquid diffusion acts as a resistance barrier to volatilization fluxes under water saturated conditions (Brusseau, 1991; Sanders and Talimcioglu, 1997). Also, Murphy and Chan (2011) showed that the resistance to mass transfer by water saturated portions cannot be neglected. Thus, soil moisture is one of the most crucial parameters regulating transport of volatile compounds (Johnson et al., 1999). However, until this moment variable soil moisture is not included in any of the much used vapor transport and vapor intrusion models. An attempt has been made by Atteia and Hoehener (2010), who introduced a semi analytical model considering vertical soil moisture variations. These authors showed that incorporation of variable soil moisture content decreases the predicted value of the concentration reaching the surface by a factor of six. Considering that moisture variations in a soil profile can be present at the centimeter scale, the impact of such variations could be significant.

Findings on the effects on transport mechanisms of dynamic processes such as water table variations are controversial. The modeling work by Thomson et al. (1997) showed that magnitude and frequency of water table fluctuations had significant influence on gas phase concentrations above VOC plumes. Moreover, Werner and

Hoehener (2001) observed significant effects on gas concentration of 20 cm water table variations over a 15 day period in laboratory experiments. In contrast, Parker (2002) inferred only a marginal effect of annual water table variations of 3.6 m based on modeling. No field evidence of the influence of water table fluctuations on vapor emissions has been found. As long as the impacts of these dynamic processes remain unclear, so does the importance of monitoring them in the field.

1.4.3 Biodegradation in the unsaturated zone

Microorganisms in the unsaturated zone are exposed to conditions of reduced water availability compared to water-saturated conditions (Holden and Fierer, 2005) because part of the soil pore volume is occupied by the gas phase. Soil water content can be expressed as water potential, which is the sum of matric, osmotic and gravitational potential. While the gravitational potential is constant, matric and osmotic potential can vary and therefore affect microorganisms (Chowdhury et al., 2011). Matric potential is the dominant component in non-saline soils. At decreasing matric potentials, water availability decreases because water is held more tightly to the aggregate surfaces (Ilstedt et al., 2000). At the pore scale, the primary substrate supply mechanism is diffusion through almost stagnant water films, thus a reduction of water films implies reduced substrate availability (Or et al., 2007). At this scale, due to hydrophobicity, bacteria may absorb preferentially to air/water interfaces over soil/water interfaces (Powelson and Mills, 1996; Rijnaarts et al., 1993; Wan and Wilson, 1994). Despite the importance of these mechanisms, pore scale mechanisms determining attachment and retention at interfaces in the unsaturated zone are still poorly understood (Sen, 2011).

At the macro-scale, liquid convection and gas diffusion dominate as transport mechanisms (Or et al., 2007). The primary effect of changes in water content at the macro-scale is on gaseous diffusion and on convective supply of substrates. As water content decreases, the increased air-filled porosity and the increased surface area produce a net enhancement of gas diffusion and improve gaseous exchange with the atmosphere (Or et al., 2007). This originates from the order of magnitude differences between liquid and gas diffusion coefficient; in the case of oxygen 2.0×10^{-5} m^2 s^{-1} versus 2.5×10^{-9} $m^2 s^{-1}$ in water. Concurrently, liquid diffusion pathways will reduce. Skopp et al. (1990) and Schjønning et al. (2003) have analyzed the interplay between enhanced gas diffusion and the decrease in liquid diffusion pathways as a function of soil porosity and water content. Biological activity was measured by the rate of CO_2 production, and showed an optimum between values of 0.5-0.6 for θ_w, the volumetric water content (Figure 1.5 a), which corresponds to approximately 60 – 70% of the water-filled porosity (Figure 1.5 b) (Skopp et al., 1990). If the matric potential decreases further, physiological stress becomes the main factor limiting microbial activity (Stark and Firestone, 1995). The physiological impacts of reduced water availability are related to reduced cell motility, control of growth rates, cell mechanisms, and ultimately survival (Potts, 1994).

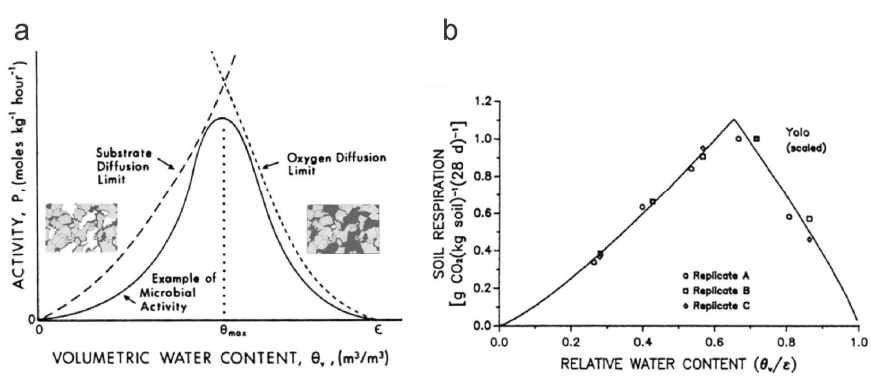

Figure 1.5 a, b – Relationship between water content and microbial activity (from Or et al. 2007); a) conceptual scheme showing the trend of microbial activity versus soil water content; b) measured soil respiration versus relative water content.

Reduced cell motility has been observed by Dechesne et al. (2008) at water contents below 15%. The occurrence of fragmented aquatic habitats in which interactions with mineral and air interfaces dominate significantly restricts cell motility (Wang and Or, 2010). Studies have shown that water stress impacts the microbial genes that regulate stationary phase-growth phases, and those that regulate oxygen scavenging mechanisms, as reactive oxygen species can damage the DNA (Potts, 1994).

Most of the available literature on the effects of water content on microbial activity focuses on nitrification (Linn and Doran, 1984; Schjønning et al., 2003; Skopp et al., 1990; Stark and Firestone, 1995) and soil respiration (Chowdhury et al., 2011; Ilstedt et al., 2000).

The large majority of studies investigating the effects of water content on the biodegradation of organic contaminants focused on toluene. An overview of rates obtained from batch and column experiments is shown in Table 1.3. The table illustrates the large variation in observed biodegradation rates, types of biomass assessed, and in the definition and calculation of the biodegradation rates. These factors complicate the choice of a specific value to predict field biodegradation rates.

Conflicting results have been presented on the effect of soil moisture content. There are indications of a threshold water content below which no biodegradation occurs (Fan and Scow, 1993; Holden et al., 1997), and that observed biodegradation rates vary with water content (Schoefs, 2004; Kirstensen et al., 2010). However, Freijer et al. (1996) found respiration rates from mineral oil degradation not to be affected by soil moisture content variation above 10% relative water content. Conversely, batch experiments with unsaturated soil (from 13% to 40% water-filled porosity) and toluene, decane and hexadecane as contaminants, showed a lower biodegradation rate at the highest water content tested (Malina et al., 1998; Schoefs et al., 2004).

In the context of vapor intrusion, a more accurate description of biodegradation processes and associated mechanisms needs to be incorporated in the models to adequately predict contaminant fate and transport. For this, better insights and better model descriptions are needed on how biodegradation of VOCs is influenced by the

specific properties of the unsaturated zone and their variation within the soil profile. For the two reference compounds selected, toluene and VC, this was therefore chosen as a focal point in the experimental and modeling work of this thesis.

Table 1.3 – Overview of laboratory experiments reporting biodegradation rates in unsaturated soil; D: diameter (cm), L: length (cm); C_{liq}: dissolved initial concentration.

Compound (Reference)	Experimental set-up	Dimension (cm or L)	Soil water content (% water-filled porosity – WFP)	^{iq} g L^{-1})	Type of bacterial culture	Biodegradation rate
Toluene TCE (Fan and Scow, 1993)	Batch	250 mL bottles 50 g soil	2.5% - 5%, 16%, 25%, 30%	5 - 20	uncontaminated soil	No biodegradation at 2.5 and 5%, 0.03 - 0.1 mg $(L\ h)^{-1}$
Toluene (Allen-King et al., 1994)	Batch slurry, mixed pure phase	1.1 L gas bottle 90g soil/60 g groundwater	-	2.5	indigenous from contaminated site	0.07 mg $(kg\ h)^{-1}$
Toluene (Malina et al., 1998)	Batch	500 mL 75 g soil	13 - 40%	144	indigenous uncontaminated soil	51.11 - 150.64 mg $(L\ h)^{-1}$
Toluene (Holden et al., 2001)	Batch	a) 40 mL vials 10 g soil b) 250 mL bottles 20 g soil	a) 100%- 50% b)20%	1	arid volcanic soil indigenous population	a) 0.03 mg $(Lh)^{-1}$ b) 1-7 x10^6 mg $(gOD_{soil}\ h)^{-1}$
MtBE, VOCs (inc. Toluene) (Hoehener et al., 2003)	Batch	63 mL bottles, no headspace	31%	14.46	indigenous	0.12 h^{-1}
Benzene (Kristensen et al., 2010)	Slurry, mixed gas phase benzene	120 mL bottles	50% - 100%	3	indigenous from contaminated site at different depths	0.21 h^{-1}
Toluene (Holden et al., 1997)	Biofilm membrane reactor	14.8 L reactor volume	matric potential from 0 to -1.5 MPa	25	adapted culture of *P.putida* biofilms	18 - 55 mg toluene (mg protein $h)^{-1}$
BTEX -Toluene (Baker et al., 2000)	Bioreactor	D: 3.8 L: 30.48	14% - 20.5%	0.1 -1 -9.6	contaminated site	0.11 mg $(L\ h)^{-1}$
Toluene (Jin et al., 1994)	Unsaturated column	D: 25 L: 20- 30	15% - 12% - 8%	11.1 - 140 - 25.1	indigenous	1.42 h^{-1}
Toluene (Allen-King et al., 1996)	Unsaturated column infiltration	D: 10 L:170	65%	4 - 46	indigenous	0.33 - 1.46 mg $(kg\ h)^{-1}$
Toluene, Decane (Malina et al., 1998)	Unsaturated column gas advection pure phase	D: 9.6 L: 45	40%	250	indigenous uncontaminated soil	25.11 mg $(L\ h)^{-1}$
MtBE, VOCs (inc. Toluene) (Hoehener et al., 2003)	Horizontal unsaturated column diffusion	D: 8.1 L:114	28%	14.46	indigenous	0.06 h^{-1}
Toluene (Tindall et al., 2005)	Unsaturated column liquid	L: 150 D: 30	70%	25.5	indigenous uncontaminated soil	0.04 -0.08 h^{-1}

1.5 Scope and outline of the thesis

In summary, field assessment of vapor intrusion risk is complicated by several interrelated factors: contaminant properties, transport processes in the unsaturated zone, and biodegradation in the unsaturated zone. The direct assessment of vapor intrusion risks by means of measurements is complicated by these factors, as they give rise to difficulties in obtaining the measurements and interpreting them. Commonly available vapor intrusion models still have limitations in including essential processes and system characteristics. They either overlook significant properties at the field scale or, conversely, are too complex to be applicable at this scale of practical application. Specifically, moisture variation, liquid diffusion, dynamic processes, and biodegradation are not adequately taken into account in the present models. Regarding biodegradation in the unsaturated zone, the lack of well-defined rate parameters is a major source of uncertainty in model prediction, as evidenced by the wide variety of rates reported and ways of expressing them.

This thesis addresses the knowledge gaps summarized above. It combines field experience, numerical modeling, and laboratory experiments to separate out the relevant processes involved in vapor intrusion from subsurface contaminant sources to buildings. The focus is on aerobic unsaturated zones.The thesis approach includes three tiers, each zooming in on a smaller scale (Figure 1.6), and consists of:

i) applying available knowledge on a case study of VC contamination potentially posing vapor intrusion risks,

ii) simulating vapor intrusion in a vertical section in the field by numerical modeling,

iii) performing biodegradation experiments with thin slices of unsaturated soil.

First, state of the art monitoring techniques and available analytical models were applied to a site where contamination from VC in groundwater could potentially pose risks for vapor intrusion (Chapter 2). This chapter further illustrates the limitations of the current vapor intrusion approaches in complicated field settings.

To investigate the effects of physical and chemical properties on vapor intrusion a risk, a one-dimensional numerical model including vertical variations of soil moisture was developed (Chapter 3). The model accounts for gas and liquid diffusion, advection, sorption and aerobic biodegradation. Moreover, it allows simulating dynamic processes. By means of a sensitivity analysis, the model was used to identify the relative importance of processes and parameters affecting vapor emissions.

In order to obtain insights in biodegradation rates in unsaturated soils, laboratory experiments were conducted under aerobic conditions with toluene (Chapter 4) and VC (Chapter 5) as model compounds. In the case of toluene, which was chosen as model compound for volatile PH, different unsaturated soil laboratory set-ups were compared in order to simulate different conditions of substrate supply. Interpretation of the experimental data was supported by the numerical model predictions. For VC, risk driver compound for volatile CHC, biodegradation experiments in liquid batch experiments and soil microcosms were performed with a known aerobic VC degrader. This allowed monitoring VC biodegradation by analytical as well as by molecular techniques. Also for VC, numerical modeling was

used for data interpretation. The molecular techniques were tested as monitoring tools for aerobic VC biodegradation in the field (Chapter 5).

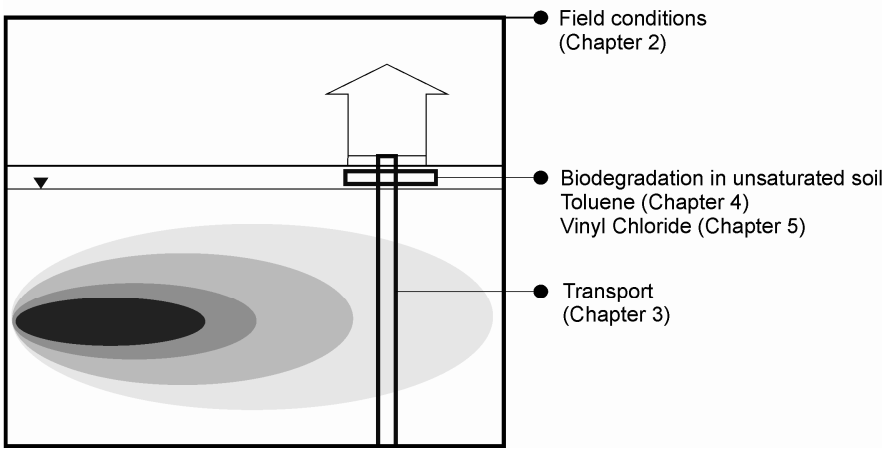

Figure 1.6 – The approach adopted in the thesis.

The outcomes are discussed in the general discussion (Chapter 6). An improved mechanistic understanding resulted from combining modeling and biodegradation experiments, including the identification of the key processes and parameters controlling contaminant transport and unsaturated zone biodegradation. This newly obtained knowledge is framed in a broader perspective, leading to important conclusions regarding monitoring, prediction and mitigation of vapor intrusion risks, and gives an outlook to further research and application.

2 Vapor Intrusion risk from subsurface contamination: a case study

Abstract

This case study deals with groundwater contamination by chlorinated ethenes and ethanes in an urban area in northern Italy. The sources of contamination are two waste dumps not secluded by a liner, located inside abandoned clay quarries and filled, during the 1960's -70's, by a mixture of urban solid waste and chlorinated pitches originated from the chloromethane distillation process of nearby petrochemical plants. Results from a multi-step site characterization show that contaminant plumes of mainly vinyl chloride (VC) occur in the two shallowest aquifers (down to a maximum depth of about 25 m b.g.l), with maximum concentrations at the source of $2x10^4$ $\mu g\ L^{-1}$ (maximum allowed concentration equals 0.5 $\mu g\ L^{-1}$). Contaminants migrated to a maximum distance of 500 m from the source below the houses at the site. In addition to VC, concentrations of PCE, TCE, DCE (1,1 and *cis*1,2), 1,1,2,2 PCA and chloromethanes were detected up to a thousand times higher than maximum allowed concentrations. Ethenes concentrations dominated over those of ethanes and VC concentrations were higher than all other contaminants along the plumes.

Based on the concentrations as measured in the groundwater and conventional risk models, the contamination potentially poses a serious threat to on-site receptors (inhabitants) by indoor and outdoor vapor inhalation. Thus, for vapor intrusion assessment, indoor air measurements were performed by means of sorption tubes by combining active and passive techniques, in two different sampling campaigns in the ground floor and the first floor of the buildings. Seasonal measurements of groundwater concentrations were also performed at four wells located in close proximity to the houses.

A slightly modified version of this chapter has been published as:
Gargini A., Pasini M., Picone S., Van Gaans P., Rijnaarts H. (2010). Chlorinated hydrocarbons plumes in a residential area. Site investigation to assess indoor vapor intrusion and human health risks. In: Saponaro S., Sezenna E., Bonomo L. eds., Vapor emission to outdoor air and enclosed spaces for human health risk assessment: site characterization, monitoring and modeling. Nova Science Publishers, Inc., pp. 211-233.

Two different analytical risk assessment models (RISC and VOLASOIL) were applied with available site specific data to predict indoor air concentrations and estimate risks for adults and children as receptors.

In contrast to such a severe groundwater contamination, and to predictions by analytical risk assessment models, low and spotty contaminant vapor concentrations were measured either in soil or in indoor gas. Toluene (up to 0.31 mg m^{-3}) and PCE (up to 0.07 mg m^{-3}) were measured in soil gas. In indoor air PCE (11.74 μg m^{-3}), benzene (4.75 μg m^{-3}), and VC (0.04 μg m^{-3}) were detected. Benzene was not present in the contaminated aquifers, and the other compounds were well below risk based limits in indoor air. Thus, no direct link between indoor air contaminants and the subsurface contamination could be established.

The occurrence of fine grained sediments (clays and silts) overlying the shallowest aquifer appears to interrupt the vapor intrusion pathway. Alternatively, biodegradation processes occurring at the interface between the saturated and the (oxygen rich) unsaturated zone may degrade the contaminant fluxes which could potentially reach the receptors. Detailed process-oriented and modeling studies are needed to elucidate these phenomena and improve site investigation tools and risk models. The case presented illustrates the complications arising from interpretation of monitoring data and suggests that a more extensive multiple line of evidence approach is needed to adequately estimate the risks and, as was shown in this specific case, to prevent large overestimations.

2.1 Introduction

2.1.1 Origin of the subsurface contamination at the site

In the urban area of Ferrara (Emilia-Romagna region, northern Italy), groundwater contamination by chlorinated solvent reaches concentrations up to hundreds of mg L^{-1}. The most commonly encountered contaminants are chlorinated aliphatic hydrocarbons, and amongst those VC is the risk driver due to its mobility and carcinogenity.

The origin of the contamination in the area is related to the presence of a large petrochemical plant (250 ha) at about 2 km NW to the center of the city, in operation since after World War II. Amongst other industrial processes, PVC production from VC monomer and distillation of halomethanes took place at the plant between 1951 until 1998. The production of halomethanes formed chlorinated ethenes (PCE and TCE) and ethanes (1,1,2,2 TECA) as pyrolisis by-products. These waste compounds are known as “chlorinated pitches” or “heavy ends” and were commonly disposed into special waste landfills or, as was the case in the Ferrara area, improperly dumped in available pits or dismissed quarries not secluded by a liner.

According to available data, groundwater below at least three urban sites around the historical center of Ferrara, became contaminated by the residues of heavy ends (Figure 2.1).

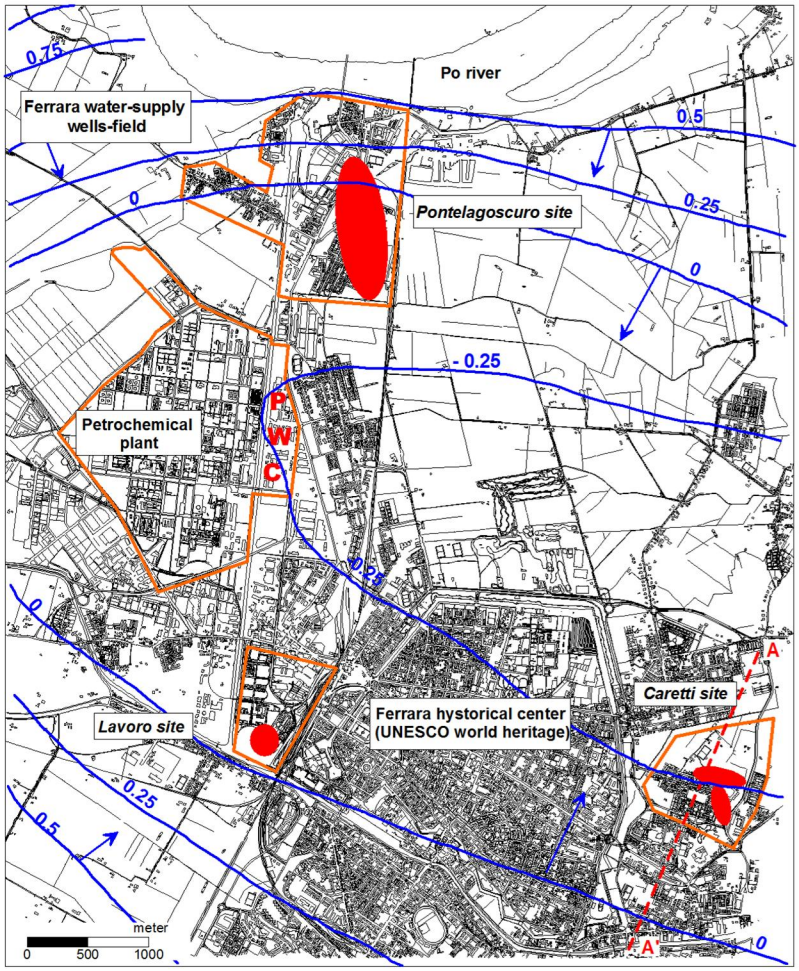

Figure 2.1 – Geographical map of the urban area of Ferrara with locations (in red) of areas with aquifers contaminated by chlorinated solvents outside the petrochemical plant and head contours (in blue) of A1 aquifer groundwater (m a.s.l.; spacing 0.25 m, redrawn from Molinari et al., 2007). Explanation of symbols: P: location of PVC production facility; C: location of chloromethanes production facility; W: pump & treat in A1 aquifer.

At the Pontelagoscuro site, to the North of the city center, a plume of only VC migrates in a confined alluvial sand aquifer, between about 10 and 30 m b.g.l., below a residential and agricultural area (Gargini et al., 2006). At the Lavoro site, to the West, a contaminant plume of mainly cis-1,2-DCE, with occurrence of VC, migrates in unconfined groundwater hosted in a sandy paleo-channel below a mostly industrial and residential area. At the Caretti site, to the East, a severe contamination from chlorinated ethenes and ethanes, with VC dominant in the off-source plumes,

affects both the unconfined to leaky-confined shallow aquifer (3-10 m b.g.l.) and the first confined aquifer (between 13-14 and 26 m b.g.l.), immediately beneath a residential area.

In all these cases, the contaminant sources are located in old dump sites, active during the 1960's-70's, inside dismissed pits for sugar-beet washing (Pontelagoscuro and Lavoro sites) or for clay excavation (Caretti site). The direct relationship between the disposal of chlorinated pitches and the contaminant plumes has been confirmed by means of isotopic fingerprinting (Pasini et al., 2008).

At Pontelagoscuro and Lavoro site, notwithstanding the impact on groundwater resources, direct exposure to receptors is impeded by the confining clay layer above the aquifer (Pontelagoscuro), or by the current land use (Lavoro site). Conversely, at the Caretti site, concerns for human health risks from direct exposure by vapor intrusion arise from the shallow contamination and the proximity to the buildings.

The area where the Caretti site is located was mostly agricultural until World War II. A brick-factory was active at the site, exploiting clay from two nearby quarries located to the east, excavated down to 6-7 m b.g.l. Meanwhile urbanization of the area took off. At the end of the 1950's the furnace activity stopped and, as it was not uncommon for the period, the dismissed clay pits were used for urban wastes disposal by the municipality of Ferrara. They are referred to as South Dump (SD) and North Dump (ND), coinciding with the two former clay-pits (Figure 2.2). Industrial wastes were dumped along with municipal and inert wastes during this period. The waste disposal activity also implied large ground works in the two areas, so that reworking of the soil and filling of depressions was more widespread than just being confined to the original pits. The waste disposal lasted for a decade, until the beginning of the 1970's. Afterwards, urban development in the area proceeded 1990's, in close proximity to ND and west of SD.

In December 2000 the local environmental protection authority (ARPA) detected an excavated soil mound contaminated by TPH (Total Petroleum Hydrocarbons) within a construction site immediately to the west of SD. The subsequent site screening, detected a severe contamination by metals and chlorinated solvents in soil and by chlorinated solvents in shallow groundwater (May-June 2003). The waste in the pits consisted of a highly heterogeneous mixture of urban wastes, inerts, sludge, ashes, and metallic objects, more or less dispersed in a silty-clayey matrix originating from the ground works connected to the clay quarrying and dumping operations in the past. Analyses of the silty-clayey matrix mixed with the wastes, performed in some samples collected over the 2001-2003 period, show concentrations exceeding regulatory limits of metals (As, total Cr, Ni), chlorinated ethenes and PAH (Polycyclic Aromatic Hydrocarbons).

This blocked further urban development. As a consequence, since 2004 the municipality of Ferrara took over the responsibility of the site characterization. A multi-step investigation strategy started and was conducted along five years (2004-2008), with the scientific support of the Hydrogeology Group of the University of Ferrara (Hydro-UNIFE). Support of the Deltares-TNO Subsurface and Groundwater Unit (NL) was requested in 2007 to monitor indoor gas and evaluate the human health risks for on-site residents. The investigation approach and strategy were

complicated by the dense urbanization of the area (with occurrence of houses, courtyards, public gardens, orchards and even a kindergarten) and by the geological heterogeneity of the site, different from other well known sectors of the Ferrara area.

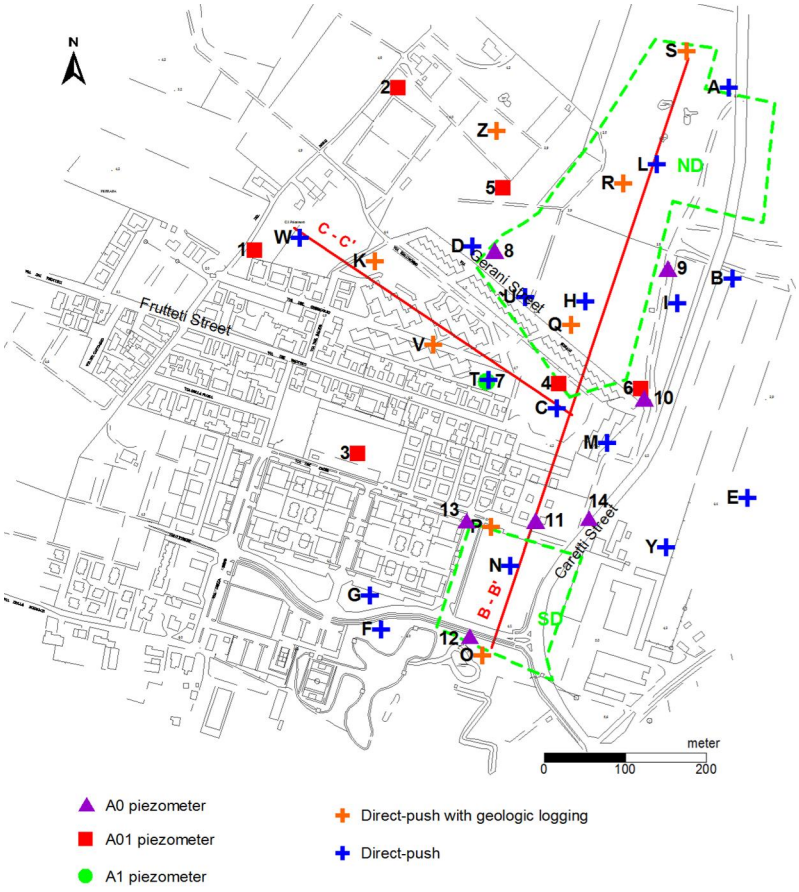

Figure 2.2 – Overview of the Caretti site. SD and ND are the two waste dumps source of contamination. Monitoring points relevant for site characterization are shown: piezometers (numbers) and direct-push drillings (letters).

2.1.2 Human health risk assessment

Risk assessment describes the magnitude and characteristics of an undesired event with respect to a certain receptor, based on the analysis of scientific data (van Leeuwen and Vermeire, 2007). Risk assessment consists of four main steps: a) hazard identification, b) exposure assessment, c) dose-response assessment, d) risk characterization. The hazard identification consists of the identification of agents that may cause adverse effects. The exposure assessment is the estimation of the intensity, frequency and duration of exposure to the hazardous agents in question. This can

include transport and fate of contaminants in groundwater and surface waters. The three main routes of exposure to humans are ingestion, dermal contact and inhalation (van Leeuwen and Vermeire, 2007). The dose-response assessment determines the quantitative relationship between exposure (or dose) and adverse effect from laboratory experiments or epidemiological studies. This assessment leads to the definition of a no adverse health effect level, to a chronic dose, or to a limit concentration. Finally, the risk characterization results from the integration of the previous steps and provides an estimation of the incidence and severity of the adverse effects likely to occur on a certain receptor as a result of exposure (van Leeuwen and Vermeire, 2007). Risk is expressed as risk quotient, which corresponds to the ratio between the actual exposure and the limits.

Due to the amount and level of complexity required of the input data, risk assessment normally consists of a tiered approach. The tiered approach constrains the risk-assessment process, focusing effort on areas where risks are potentially unacceptable (Ferguson et al., 1998). This is essentially an iterative process where the earlier the exit from the process, the higher the likely remedial costs. Generally, three tiers are scrutinized, namely preliminary (tier I), generic (tier II) and site specific (tier III) (van Leeuwen and Vermeire, 2007). Preliminary risk assessment includes the gathering of existing information in order to build a conceptual site model which summarizes the source-pathway-receptor model at the site, and identifies knowledge gaps to guide further characterization. Generic risk assessment (tier II) implies comparison of measured groundwater/soil concentrations with generic standards. These are typically conservative to ensure their applicability to the majority of sites. Finally, site specific risk assessment (tier III), makes greater use of site-specific data to conduct a more accurate assessment of risks. It often involves the use of models to derive site specific standards which are then compared to measured concentrations in environmental compartments. Here, a tier II risk assessment was performed in order to compare data from field monitoring with analytical models.

2.1.3 Geological and hydrogeological settings of the area

The site is located in the eastern and lowest sector of the Po river plain (Padana plain), about 7 km southward of the Po river (Figure 2.1) at an average elevation of 3 - 4 m a.s.l. The Po river basin is a rapidly subsiding foreland basin bounded by the Alps to the north and the Apennines to the south. The sedimentary sequence consists of a cyclic transgressive-regressive alternation of two major types of deposits: i) fluvial-channel deposits, mostly sandy, and ii) overbank deposits, as floodplain muds with subordinate sand bodies (Amorosi et al., 2008; Stefani and Vincenzi, 2005).

Fluvial-channel sedimentary facies were deposited during the glacial period. They form medium to coarse grained sandy layers of up to 30 m thick. During interglacial periods, development of swamp areas and poorly drained floodplains took place in the study area in response to rapid sea-level rise. In such conditions mostly silty-clayey units, with intercalation of peat horizons were deposited. Sandy intercalations within this unit identify minor paleo-channels, natural levees and

crevasse deposits. After the Flandrian transgression, during the Holocene period, a deltaic-alluvial sedimentation occurred with dominance of silty-clayey organic rich sediments. Encapsulated in these fine-grained units are scattered, ribbon-shaped, medium to fine grained sandy paleo-river channels, related to recent and modern deposition of the Po delta (Amorosi et al., 2008; Stefani and Vincenzi, 2005). The river channels, being essentially non-migrating, display a strongly lenticular geometry.

The hydrogeological structure mirrors the architecture of the sedimentary bodies. An hydrogeological profile at the Caretti site (Figure 2.3) and the main geohydrological units (Table 2.1) are given.

Down to a depth of about 200 m b.g.l., a multi-aquifer system is present with four sandy confined aquifers (glacial sheet-like layers), coded downward from A1 to A4, capped by interglacial silty-clayey units acting as aquitards/aquicludes (Table 2.1). At the top of the succession, the shallowest, locally unconfined to leaky-confined aquifer called A0 (Regione Emilia Romagna&ENI-AGIP, 1998; Molinari et al., 2007), consists of ribbon and lens-shaped sandy lithosomes. A0 has low continuity and transmissivity, with the exception of major paleo-river channels. In contrast, the A1 and A2 aquifers display good lateral continuity and hydraulic transmissivity.

Table 2.1 – Main stratigraphic and hydrogeologic features of the multi-aquifer sandy system at the site. Surface level at the Caretti site is 3-4 m a.s.l. Data are derived from Molinari et al. (2007) and from the site characterization.

Aquifer unit	Top (m a.s.l.)	Bottom (m a.s.l.)	Thickness (m)	Aquifer type
A0	1 / -2	-3 / -7	0 / 8	Leaky confined
A01	-8 / -17	- 12/-23	4/15	Leaky-confined
A1	-22 / -29	-32 / -49	12 /20	Confined
A2	-58 / -60	-82 / -84	24	Confined
A3	- 105	- 133	28	Confined
A4	- 160	- 176	16	Confined

Recharge differs amongst the different aquifer units. Unit A0 is in connection with direct recharge, particularly where paleo-river channels outcrop or where they are intersected by canals. A1 is recharged laterally from the Po river and is the main groundwater resource for the municipal water supply. A2 is recharged from the foot-hills of the Apennines about 30 km to the south. Besides, downward seepage occurs from A0 to A1 and, to a much lesser extent, from A1 to A2.

At the site (see Figures 2.4 and 2.5), three mainly sandy units (aquifers) are present from the surface at elevation between 4 and 5 m a.s.l., to a depth of about -50 m a.s.l. (53 m b.g.l.). The first aquifer A0 has a variable thickness of on average around 3-4 m, never exceeding 8 m but locally lacking (Figure 2.4 and 2.5). This sand body is always covered by at least 3 m of silts and clayey silts. The sandy unit below A0 displays a higher average thickness, of around 12 m, but also with large variation, down to a minimum of 4 m thickness. It is separated from A0 by a layer of silt and clay, which thins out and becomes more silt-rich below ND (Figure 2.4). In some locations, A0 and the lower unit coalesce. The third sandy unit of the succession is

encountered (in only one drilling) at -29 m a.s.l., extending down to -49 m and separated from the upper aquifers by 6 m of a mainly clayey horizon.

Comparing expected and measured top and bottom elevations, the sandy aquifer detected at -29 m is most probably A1 and not A2, as A2 is only expected at much larger depths (Table 2.1). A main sandy body located in an intermediate position between A0 and the regional A1 unit seems to exist at the site: it was identified as A01 in Table 2.2 and in Figure 2.4. Its large variation in thickness, the frequent occurrence of fine-grained lenses and intercalations and the erosive character of the top surface suggest a main paleo-channel as origin for this unit. A01 maximum thickness is oriented along a W-S axis more or less coincident with the profile in Figure 2.5.

Table 2.2 – Features of the multi-aquifer sandy system below the Caretti site as derived from the current site characterization. Estimated groundwater velocity is based on hydraulic conductivity of $1x10^{-4}$ m s^{-1} and effective porosity of 0.2 values. EC: electric conductivity.

Unit	Hydraulic head (m a.s.l.)	Head excursion (m)	Depth to water-table (m)	Average flow direction	Hydraulic gradient	Estimated effective groundwater velocity (m y^{-1})	Use	EC@25°C (µS cm^{-1})
A0	1.70-2.90	0.4 - 0.72	0.45-1.42	NW	$1x10^{-3}$	16	Irrigation of private gardens far from the site	2500
A01	1.89-2.85	0.83 -1.18	-	N	$4x10^{-4}$	6	No use in the area	1000-1600
A1	1.62-2.66	1.05	-	-	-	-	Used for irrigation	600

Further evidences from groundwater flow and chemistry confirm the presence of this additional intermediate unit. Hydraulic head and head variation in A0 and A01 are comparable at the site, whereas A1 has a slightly lower hydraulic head. This differs from other sectors of the Ferrara plain where the full hydrodynamic confinement of the A1 aquifer is reflected by a head value significantly lower than that of the shallower aquifer A0. Flow direction is northward for both the A0 and A01 aquifers, topographically controlled by lateral recharge induced from the outcropping paleo-river channel of Volano to the south (left-hand of profile in Figure 2.3). However, the expected regional flow direction for the A1 aquifer is also northward, due to the effects of pumping in the industrial area of the city (Figure 2.1). A relatively higher electrical conductivity was observed in A0 and A01 (Table 2.2), resulting from direct recharge through fine-grained cover (ion enrichment from crossing aquitards), as compared to that in A1, laterally recharged by Po fresh-water.

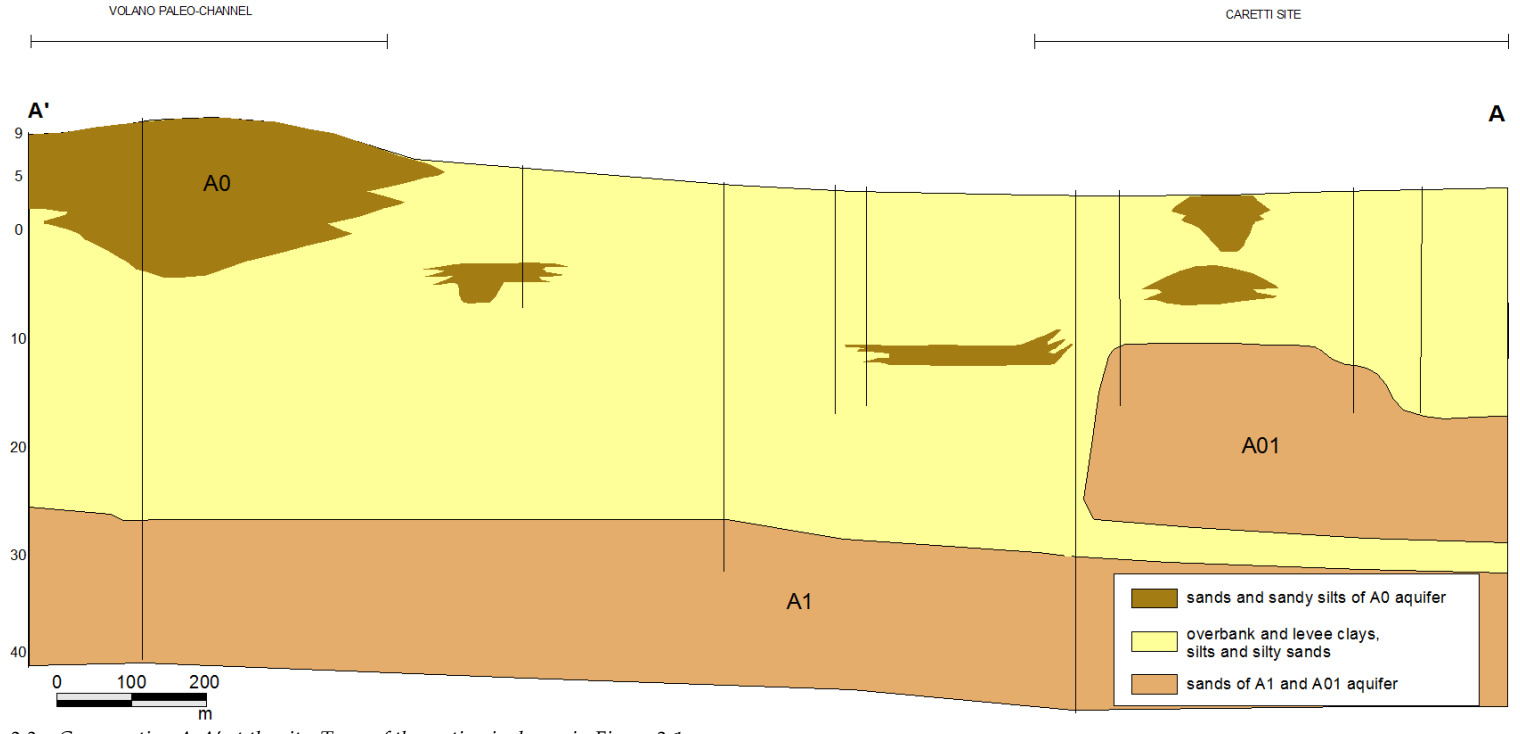

Figure 2.3 – Cross section A-A′ at the site. Trace of the section is shown in Figure 2.1.

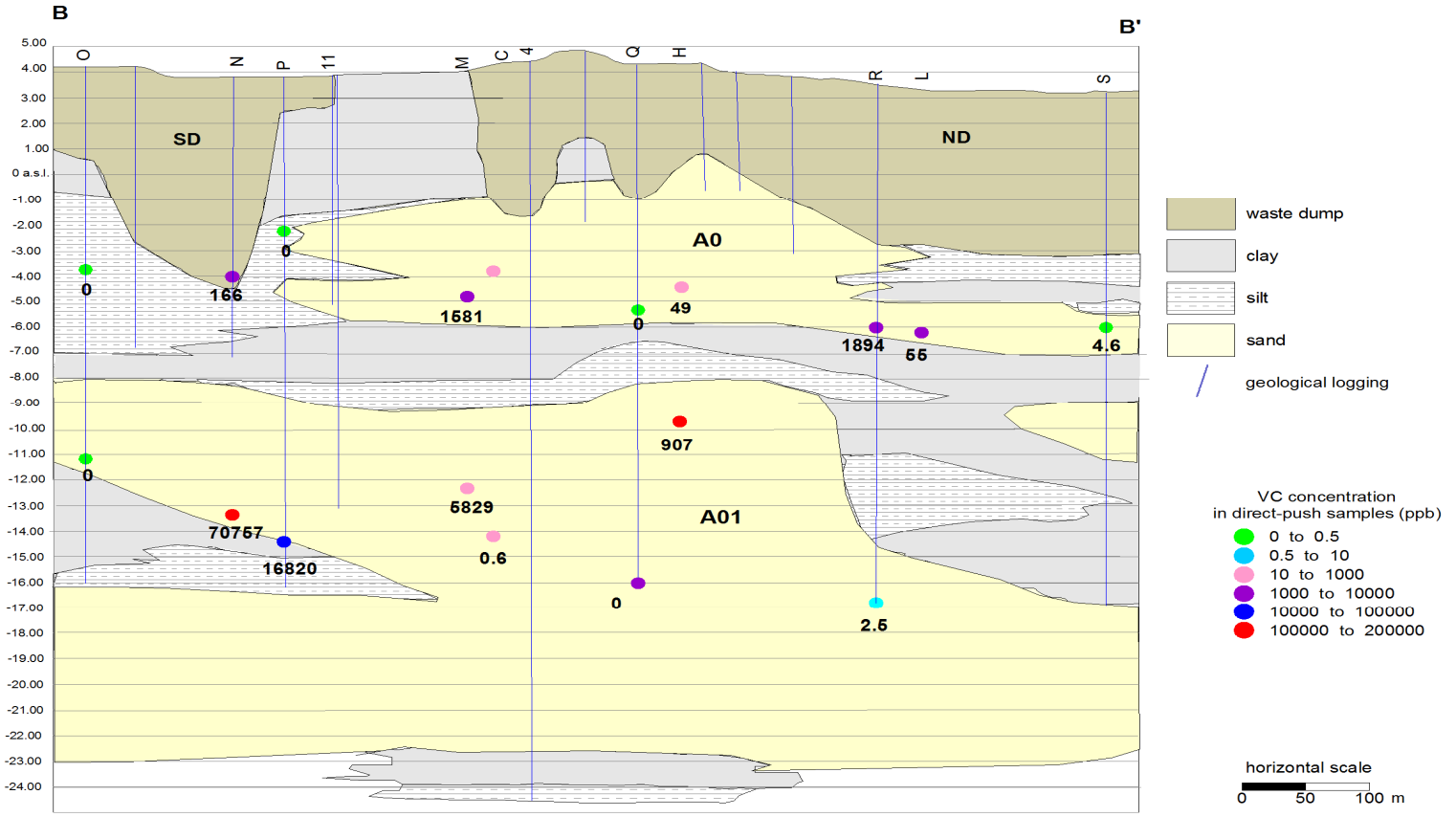

Figure 2.4 – Hydrogeological cross section B-B′ across ND and SD with contaminants concentrations in direct-push groundwater samples. Colored dots refer to VC concentration; numbers refer to PCE+TCE concentrations, both in µg L^{-1}. Trace of the section is given in Figure 2.2.

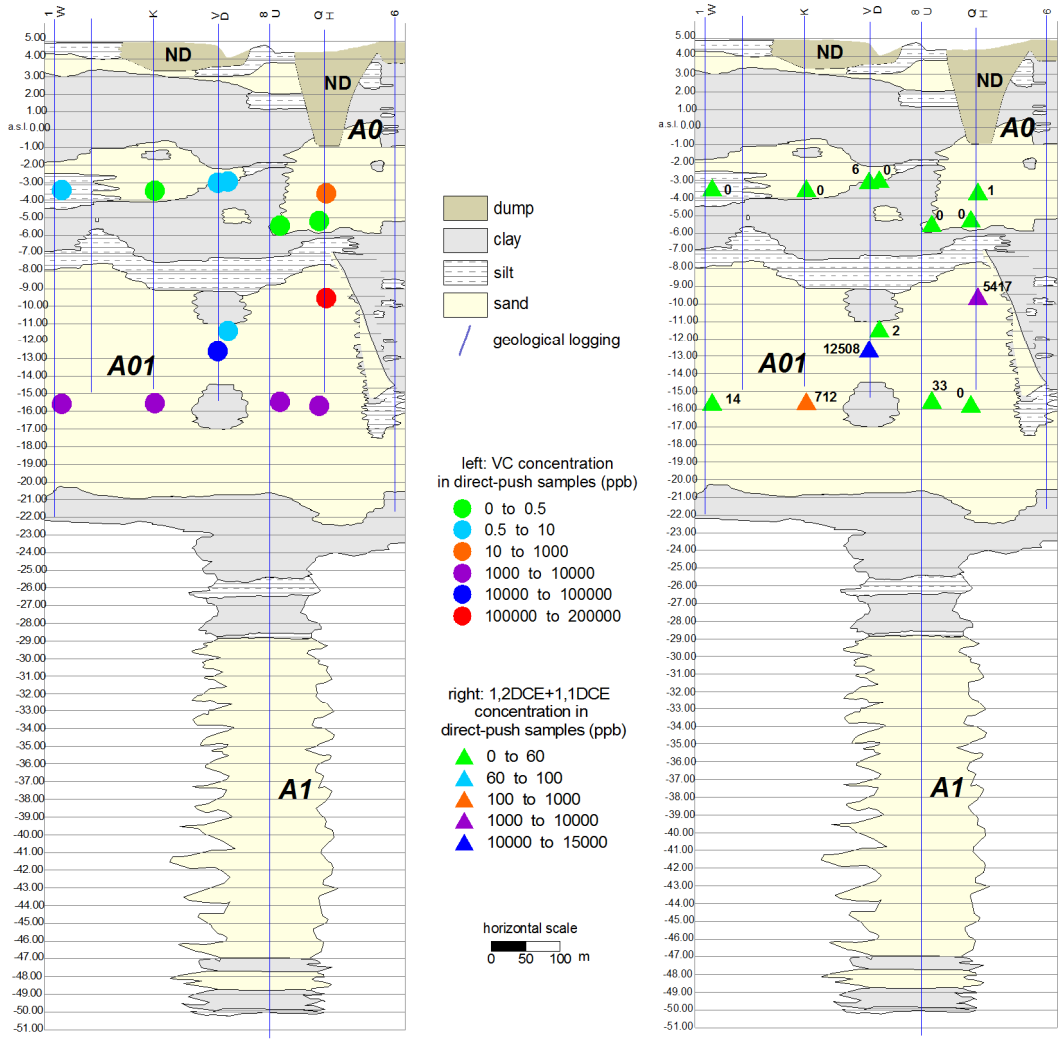

Figure 2.5 – Hydrogeological cross section C-C', transversal to Figure 2.4 with VC concentrations (to the left) ad 1,1DCE+1,2DCE (to the right) concentrations in direct-push groundwater samples. Trace of the section given in Figure 2.2.

2.2 Site characterization: groundwater contamination

Since the beginning of the site characterization in 2004, groundwater samples from the A0, A01 and A1 aquifers at via Caretti were obtained through 24 direct-push drillings (identified with letters in Figure 2.2) and 14 bore-hole piezometers (identified with numbers in Figure 2.2). The direct-push drillings (28 m maximum attainable depth b.g.l.) were performed in two sampling rounds (12 in 2004/2005 and 12 in 2007); groundwater was sampled at two discrete depths (in the A0 and A01 aquifers) through 0.6 long screens. In this way time snapshots of the contaminant occurrence were obtained. Groundwater sampling in piezometers was always conducted after low-flow borehole purging. The analytical method complied with USEPA protocols for purge and trap (EPA 5030 b) and gas chromatoghraphy mass spectrometry (EPA8260 b).

The sources of contamination are two waste dumps not secluded by a liner, identified as ND (north dump) and SD (south dump) in Figure 2.2. Total waste dump thickness varies between 1 and 8 m, depending on the location within the original clay pit; above the waste a 0.4 - 1.8 m thick man-made cover is present. Due to the depth of the pits (A0 aquifer sandy lenses intersecting the pit bottom), and due to the reduced thickness of (1-4 m) the silty aquitard separating the A0 and A01 units (Figure 2.4), both aquifers were easily and severely contaminated. In contrast, a thicker (Table 2.1) and clay richer layer between A01 and A1 impaired contaminant migration between A01 and A1. This is shown by the complete absence of contamination in two irrigation wells screened in A1 and by the only occurrence of 3 μg L^{-1} of TCE and 0.35 μg L^{-1} of 1,1-DCE in piezometer n°7, screened in A1 too.

Given this conceptual model, contaminant concentrations in the A0 and A01 units immediately below the dumps (Table 2.3) are expected to closely reflect the original composition of the source material (although possibly altered by chemical and biological degradation). Both aquifers show reducing conditions with permanent negative redox potential (Eh) values.

Table 2.3 – Maximum concentrations (in μg L^{-1}) for contaminants of concern detected below the sources at the site in the A0 and A01 aquifers. Maximum Allowed Concentrations (MAC) according to Italian national law for contaminated sites are given in brackets. For drilling locations see Figure 2.2. nd: measure below detection limit.

Group	Species (MAC)	ND		SD	
		A0 aquifer Drilling: L, R, 9	A01 aquifer Drilling: H,U,Q	A0 aquifer Drilling: N	A01 aquifer Drilling: N,P
Chlorinated Ethenes	VC (*0.5*)	$2.9x10^{4}$	$1.1x10^{5}$	$5x10^{3}$	$1.7x10^{5}$
	1,1-DCE (*0.05*)	$7.3x10^{2}$	$1.8x10^{2}$	$7.4x10^{0}$	$3.1x10^{3}$
	1,2-*cis*DCE (*60*)	$3.3x10^{3}$	$5.3x10^{3}$	$9.4x10^{1}$	$1.3x10^{4}$
	1,2-*trans*DCE	$4.4x10^{1}$	$1.4x10^{2}$	$5.0x10^{0}$	$7.7x10^{2}$
	TCE (*1.5*)	$6.1x10^{3}$	$6.8x10^{2}$	$5.2x10^{1}$	$3.9x10^{4}$
	PCE (*1.1*)	$1.0x10^{3}$	$2.3x10^{2}$	$1.1x10^{2}$	$3.2x10^{4}$
	TOTAL	$4.3x10^{4}$	$1.2x10^{5}$	$5.2x10^{3}$	$3.2x10^{5}$
Chlorinated Ethanes	1,1,2-TCA (*0.2*)	$8.6x10^{2}$	$1.5x10^{2}$	$4.0x10^{-1}$	$6.7x10^{3}$
	1,1,2,2-PCA (*0.05*)	$1.4x10^{3}$	$3.2x10^{2}$	$3.9x10^{0}$	$2.6x10^{4}$
	TOTAL	$2.3x10^{3}$	$4.7x10^{2}$	$4.3x10^{0}$	$3.5x10^{4}$
Halo-alkanes	TCM (*0.15*)	$1.7x10^{3}$	$6.0x10^{1}$	$2.1x10^{0}$	$1.0x10^{4}$
	BDCM (*0.17*)	$1.2x10^{3}$	nd	nd	$1.5x10^{1}$
	1,2-DCP (*0.15*)	$2.0x10^{-1}$	$1.9x10^{0}$	$1.8x10^{0}$	$1.3x10^{1}$

Chlorinated ethenes generally dominate by one or two orders of magnitude over ethanes; VC dominates over all other ethenes, with the exception of A01 aquifer below SD. Here the other ethenes (PCE, TCE, 1,2-DCEcis) and ethanes occur at concentrations comparable to VC, reflecting either a different DNAPL (Dense Non Aqueous Phase Liquid) source composition or a different degradation process.

Migration of dissolved contaminant from the source was rather slow within the A0 and A01 aquifers, with an average groundwater velocity of less than 20 m per year (Table 2.2). Plume migration was controlled by i) the density-driven initial downward percolation of the NAPL phase down to the A01 aquifer, ii) the groundwater flow direction, on average northward, iii) the limited northward extension of the sandy units (Figure 2.4) and iv) the occurrence of higher transmissivity zones in the A01 aquifer. As a consequence, the highest concentrations in the A0 aquifer are distributed along a mainly N-S direction and are restricted to the proximity of the sources (Figure 2.4) whereas the maximum plume spreading is in A01 aquifer in a westward direction (Figure 2.5).

The contaminant plume in the A0 aquifer is shown in Figure 2.6 migrating from SD for about 200 m, immediately below the residential buildings. Its maximum concentration are 1,430 $\mu g\ L^{-1}$ for PCE in M and 3,860 $\mu g\ L^{-1}$ for VC in 11 (Figure 2.6).

Concerning ND, the very limited lateral continuity of the lens-shaped A0 unit induced contaminant migration to occur mainly in the lower A01 aquifer (as reflected from the concentrations in Table 2.3). The migration potential of the dissolved contaminants is higher in the A01 aquifer due to the greater thickness and lateral continuity. As a result, a rather well defined mainly VC and cis-1,2-DCE plume has been formed, which migrates in a west-northwest direction up to about 500 m away from the sources. Complete disappearance of higher chlorinated ethenes and all ethanes in the migrating plume within A01 is probably due to natural attenuation.

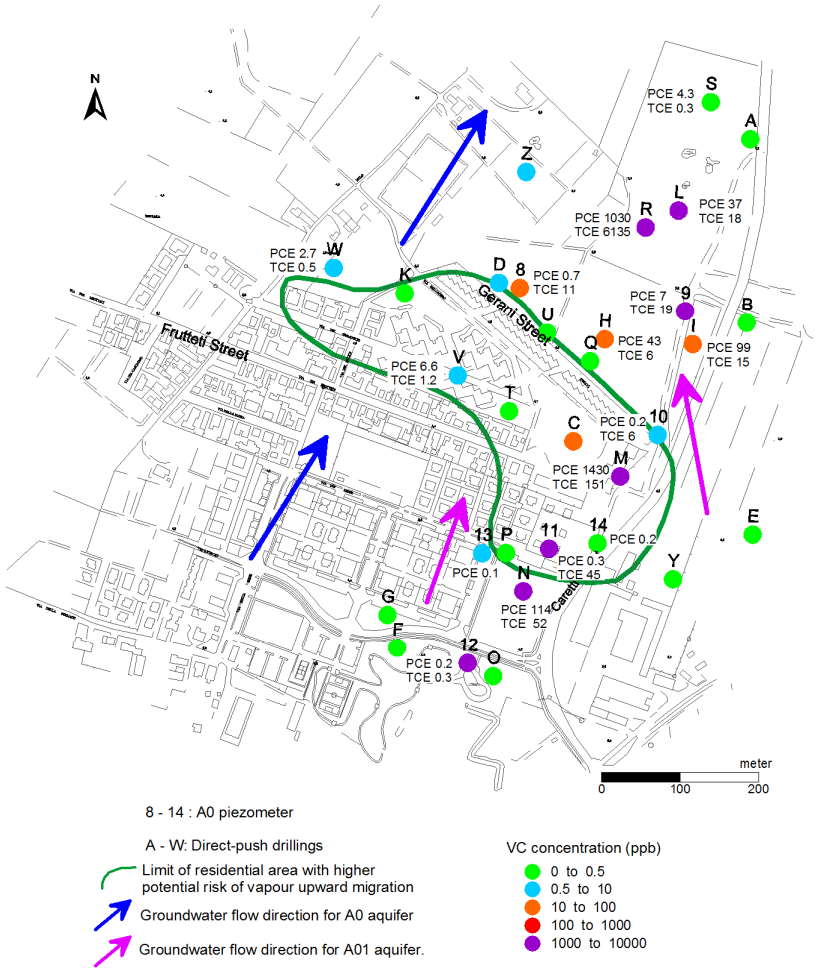

Figure 2.6 - Classed post-map of maximum VC and PCE-TCE concentrations in the A0 aquifer in µg L^{-1}, PCE-TCE are given on the map.

With respect to human health risk assessment, the most important information concern maximum contaminant concentrations at the site, with specific focus on the shallowest A0 aquifer. Below the residential area, defined by the green line in Figure 2.6, patch wise high contaminant concentrations occur in the A0 unit just a few meters below the houses (Table 2.4).

Contaminant concentrations appear not to be constant over time. Groundwater monitoring in four A0 piezometers (8, 9, 10, 11) during 2007-2008 showed large concentration variability over 1-2 orders of magnitude. For example, the maximum measured VC concentration in piezometer n°9 (near ND source) was 28,561 µg L^{-1} in July 2004 whereas in June 2008 the observed concentration was only 1,117 µg L^{-1}.

These variations, probably due to environmental (air temperature), hydrological (soil moisture, hydraulic head), or borehole purging conditions among different sampling rounds, do not change the hazard assessment for the site, in terms of potential exposure to receptors.

Table 2.4 – Maximum concentrations (in μg L^{-1}) of contaminants detected below the houses at the site in the A0 aquifer (sampling depth in the sandy layers between 2 and 9 m b.g.l.). nd: measure below detection limit; -: Not Analyzed. For drilling location see Figure 2.2. Regulatory limits for groundwater concentrations are given in Table 2.3.

Drilling ID	PCE	TCE	1,2-DCE	1,1-DCE	VC	Benzene	Toluene
C	nd	nd	nd	nd	34	-	-
D	nd	nd	nd	nd	6	-	-
M	1430	151	279	2.5	1065	-	-
V	6.6	1.2	6	nd	3.3	nd	nd
W	2.7	0.5	nd	nd	0.8	nd	nd
8	0.7	11	52	0.7	100	1	6
10	0.2	6	1.4	nd	0.15	2	nd
11	0.3	45	405	9.9	3860	9	4
12	0.2	0.3	4.8	0.4	2615	-	-
13	0.1	nd	0.9	nd	8.9	-	-

2.3 Soil gas and indoor air monitoring

Soil gas and indoor air were monitored to assess whether the subsurface contamination adversely affected the indoor air quality, resulting in exceeding of risk limits. Active and passive monitoring methods were combined to obtain information about both a daily and an averaged weekly exposure. As already discussed, the main contaminant of concern at the site is VC, for which adequate indoor air monitoring is still hampered by a lack of proven techniques for sampling and analytics. The monitoring of VC is very sensitive to air moisture content -which is commonly highly variable in indoor environments- due to two chemical properties: the gas status of the pure phase at normal temperature and pressure and its high solubility in water. In part for these reasons, a screening method was performed with a passive sampling technique of indoor air, prior to the actual monitoring campaign in which VC was monitored by a combination of passive and active sampling. While active sampling consists of withdrawing a certain air volume by means of suction pumps, passive diffusive sampling relies on molecular diffusion of gaseous compounds through a stagnant diffusion layer followed by sorption onto an adsorbent. In terms of information, active sampling delivers a snapshot of the contaminant concentration, while passive samplers provide a time-averaged concentration.

Ten buildings located in proximity to the highest groundwater concentration of contaminants were selected for indoor air monitoring (July 2007), of which three

were previously selected for the screening (March 2007). The indoor air was measured at the ground floor and also in the cellar when present. In 2004 and 2006, two soil gas surveys (Russel Bouling and Ginn, 2003), with active soil gas sampling, were performed in a total of 44 locations by Hydro-UNIFE and the Municipality of Ferrara. Soil gas was sampled at a depth of 1 m b.g.l. with activated carbon tubes. In 2007, soil gas was sampled by the Netherlands Organization for Applied Scientific Research (TNO) with a passive method at four locations positioned within 10 meters from two of the buildings (IS1 and IS2) where indoor air was monitored. A questionnaire was submitted to the residents to identify possible indoor sources such as smoking and recent paint. Indoor air samplers were positioned in places with a sufficient air circulation in order to observe average conditions, as recommended by Otte et al. (2007).

Active sampling of indoor air was performed according to USEPA Compendium Method TO-17 (USEPA, 1999), using sorption tubes (Markes International, 89 mm long x 6.4 mm diameter) filled with 300 mg Unicarb, carbon molecular sieve. Tubes were conditioned prior to sampling according to the manufacturer's protocols. This sorbent was chosen for its ability to trap the most volatile organics such as vinyl chloride, which are only poorly sorbed by ordinary adsorbents such as TENAX or charcoal (Chiriac et al., 2007). Active samples were collected in duplicate at each location by means of a Gilian GilAir-5 Constant Flow Sampling pump at two different flow rates for one hour: 30 mL min^{-1} and 40 mL min^{-1} (Figure 2.7 a). A laboratory blank was included in the analysis.

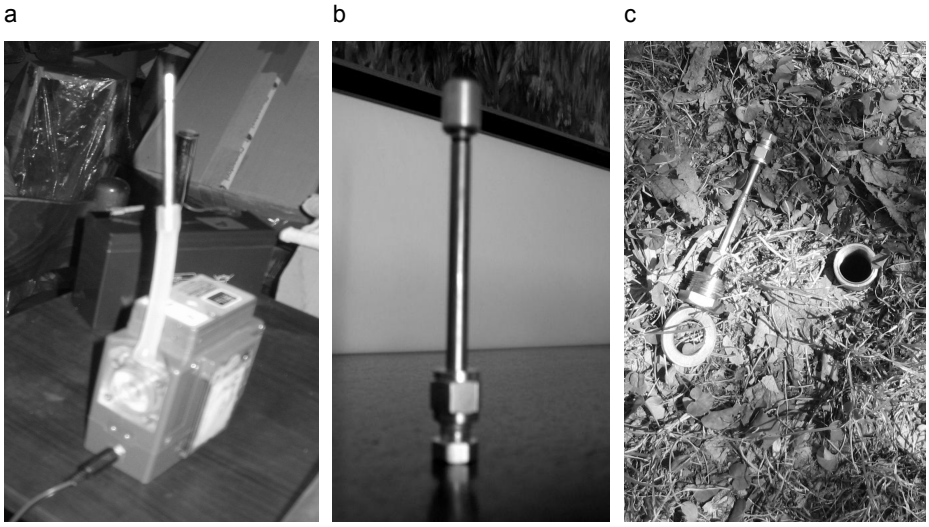

Figure 2.7 a,b,c – Sampling tools used for indoor air and soil gas monitoring (2007). a) indoor air active sampling, b) indoor air passive diffusive sampler, c) soil gas probes.

Passive sampling of indoor air and soil gas was performed by means of the same sorption tubes as used for active sampling, provided with a diffusion cap (Figure 2.7 b). For soil gas passive sampling 25 cm long metal probes (VOC-Mole™ from

Markes International) were used, in which the sorption tube was installed (Figure 2.7 c). The indoor air samplers were left in place for one week. In case of the soil gas passive samples, this was reduced to two days as analytical problems were encountered during the screening monitoring due to adsorption of water from the soil gas phase onto the adsorbent. Water affects the GC/MS analyses methods normally used.

Soil gas analysis for volatile organic compounds in the samples were performed by CSA laboratories (Rimini, IT), for the 2004 and 2006 soil gas surveys. In 2007, analysis of indoor air samples was performed in TNO laboratories (Apeldoorn, NL) with thermal desorption (Thermal Desorption Perkin Elmer ATD 400) and gas chromatography/mass spectrometry (GC/MS, Hewlett Packard 6980 Gas Chromatograph) techniques (Picone et al., 2007). Monitored buildings and soil gas sampled locations are shown in Figure 2.8.

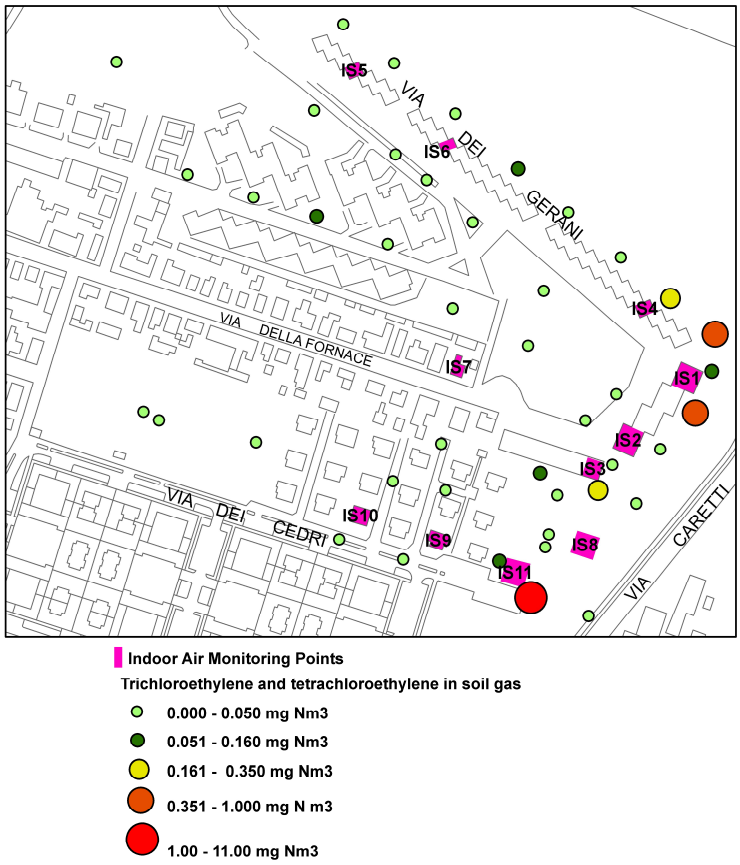

Figure 2.8 – Indoor air and soil gas monitoring points, results from soil gas surveys of 2004 and 2006.

2.4 Risk assessment models

Most of the groundwater contaminants at the site have a dimensionless Henry's law partition coefficient exceeding $2.5x10^{-5}$ (Jury et al., 1983). Therefore, they tend to volatilize and may migrate upwards as vapors, potentially accumulating in buildings. Vapor intrusion risks are controlled by diffusion (Johnson and Ettinger, 1991), pressure gradients (Hers et al., 2001; McHugh et al., 2006), building specific factors (Fugler and Adomait, 1997) and biodegradation in the unsaturated zone (Hers et al., 2000; Johnson et al., 1999; Lahvis, 2005).

Two risk assessment models were used for tier II risk assessment at the site, namely RISC BP (BP, 2001) and VOLASOIL (Waitz et al., 1996). RISC BP is based on the model by Johnson and Ettinger (1991). At the site, risk is driven by the carcinogenic vinyl chloride (IARC, 1979) as most hazardous compound.

For a conservative assessment, the maximum detected concentrations were taken into account to evaluate the potential indoor vapor intrusion risks from the contamination in A0. Between SD and ND, the buildings near drillings M,11,12 (Figure 2.6) are located immediately above the maximum contaminant hot spot in A0 (>100 μg L^{-1} VC and >1000 μg L^{-1} PCE). Besides VC, risk calculations were performed also for TCE and PCE which exceeded regulatory limits in groundwater and were measured in soil gas surveys. Input groundwater concentrations of VC, TCE and PCE were 3.34, 0.04 and 0.01 mg L^{-1} respectively. A residential scenario, with lifelong exposure for adult and child as receptors was modeled. The available site-specific parameters for soil and for buildings were used for the assessment. These included soil type and groundwater levels. For conservativeness, no biodegradation was taken into account. In both models, the soil was modeled as silty sand.

VOLASOIL (Waitz et al., 1996) allows the user to choose amongst different conceptual models of the subsurface at the site. Due to the lack of depth specific pore-water measurements, the most conservative model scenario (groundwater as a mixed container) was used. This scenario assumes that the whole water column, up to the water table, had the same concentration as the one measured at the depth of the sample collection (7 m b.g.l.).

2.5 Results and discussion

2.5.1 Comparison with risk based limits

Results from soil gas (2004 and 2006) and indoor air (2007) monitoring are presented in Figure 2.8, Table 2.5 (screening) and Table 2.6 (monitoring), where Table 2.5 shows the total range of analyzed compounds in 2007. In Figure 2.8, the sum of the measured PCE and TCE concentrations is shown per monitoring point as these compounds might be related to the groundwater contamination. In soil gas, toluene and PCE were detected in both surveys with maximum concentrations of 0.51 mg Nm^{-3} and 1.37 mg Nm^{-3} measured in 2004. The pattern of PCE in the soil gas clearly follows the pattern of the contamination in the A0 aquifer.

Table 2.5 – Measured concentrations (μg m^{-3}) in indoor air with passive sampling (screening) March 2007 (IS1 to IS3 and IS11 in Fig. 2.8). Values in brackets indicate reference risk limits. Figures in bold exceed reference limits. C: cellar; G: ground floor; nd: measure below detection limit.

**USEPA limits, **RIVM TAC*

Sampling Point	Dichloro methane (21)*	VC (1)*	cis-1,2 DCE (30)**	TCE (200)**	PCE (200)**	Benzene (0.45)*	Toluene (5000)*	Ethyl benzene (1000)*	p,m-xylene (100)*	o-xylene (100)*
IS1 C	0.42	nd	nd	0.94	0.7	nd	9.92	1.34	5.68	1.89
G	0.05	0.04	0.02	0.13	0.06	0.22	0.59	0.02	0.07	0.05
IS2 C	**79.79**	nd	7.7	0.61	11.74	**0.73**	**12.8**	0.16	0.5	0.28
IS3 C	1.08	nd	nd	0.12	0.43	**2.32**	8.51	0.47	2.66	0.86
G	nd	nd	5.3	0.22	2.62	0.97	12.49	1.20	4.36	1.36
IS11 G	0.03	0.03	nd	0.55	0.03	0.36	0.29	0.02	0.04	0.03

In indoor air dichloromethane, VC, 1,2 cis-DCE, TCE, PCE and BTEX were detected in the screening (Table 2.5). However, in the monitoring only benzene and VC were detected (Table 2.6). Considering that identical sampling and analytical methods were applied, no apparent reason for this discrepancy could be identified.

Measured concentrations in indoor air were compared with USEPA reference limits for chronic inhalation exposure and with RIVM (National Institute for Public Health and the Environment, NL) tolerable air concentrations (TAC). In the screening campaign, several groundwater contaminants such as PCE and TCE were detected in the indoor air but at concentrations lower than risk-based thresholds (Table 2.5).

Conversely, 1,1-DCE and 1,2 trans-DCE which were groundwater contaminants, were not detected in indoor air samples. Maximum concentrations detected (MCD) were 11.74 μg m^{-3}, 7.7 μg m^{-3} and 0.04 μg m^{-3} for PCE, DCE and VC, respectively.

In the monitoring campaign (Table 2.6) VC was only detected by active sampling at two locations, yet at concentrations below regulatory limits (0.19 and 0.23 μg m^{-3}) . However, no VC was detected with passive sampling in the monitoring. Benzene was the only compound exceeding USEPA indoor air risk limits (0.45 μg m^{-3}) at almost all locations in both monitoring rounds, independently from the sampling technique. At the ground floor of one building (IS8, Table 2.6), the MCD's for benzene were 4.75 μg m^{-3} and 4.42 μg m^{-3}, measured by active sampling at rates of 30 and 40 mL min^{-1} respectively, and 1.80 μg m^{-3} with passive sampling. Taking into account that benzene concentrations in groundwater at the site were in the order of 1 to 9 μg L^{-1} (Table 2.4), and that measured indoor concentrations were comparable with average outdoor air values (3.2 μg m^{-3}) as monitored in nearby weather stations for vehicle traffic monitoring, it is assumed that benzene originated from outdoor sources.

The concentrations of benzene detected with passive sampling are in good agreement with the ones measured actively in cellars, but in the ground floors, passively sampled concentrations are on average between 25% and 90% lower than the actively sampled ones.

Results from soil gas passive sampling (samples SG1 to SG4 in Table 2.6) show that benzene was detected in concentrations lower than 1 μg m^{-3} and that VC was not detected.

Table 2.6 - Measured concentrations (μg m^{-3}) in indoor air (IS1- IS10: Indoor Sampling locations -see Fig. 2.8) and soil gas (SG1-4: Soil Gas) with active and passive sampling (monitoring) of June-July 2007. In brackets risk limits for benzene and VC are indicated. Figures in bold exceed reference limits. For abbreviations see Table 2.5.

**USEPA limits*

Sampling Point	Passive Sampling	1 hour active sampling 30 ml min^{-1}	1 hour active sampling 40 ml min^{-1}	
	Benzene (0.45)*	Benzene (0.45)*	VC (1)*	Benzene (0.45)*
IS1 G	**1.48**	**1.97**	nd	**1.33**
IS1 C	-	**1.91**	nd	**2.69**
IS2 G	**1.80**	**3.55**	nd	**1.45**
IS2 C	-	**1.39**	nd	0.02
IS3 G	-	-	-	-
IS3 C	-	**3.28**	nd	**1.66**
IS4 G	-	**1.47**	nd	**1.58**
IS4 C	0.004	0.03	nd	0.05
IS5 G	**1.05**	**3.27**	nd	**2.25**
IS5 C	**0.80**	**3.30**	nd	**1.95**
IS6 G	**1.80**	**3.41**	nd	**1.40**
IS6 C	**0.55**	**3.05**	nd	**1.38**
IS7 G	**1.62**	0.10	nd	**2.22**
IS8 G	**1.69**	**4.75**	0.19	**4.42**
IS9 G	**1.01**	**2.69**	nd	0.002
IS9 C	**0.78**	**3.04**	nd	**1.39**
IS10 G	**1.79**	**1.37**	0.23	nd
IS 10 C	-	**2.64**	nd	**0.93**
SG1	0.20			
SG2	0.35			
SG3	0.26			
SG4	**0.91**			

2.5.2 Comparison between model predictions and measurements

Vapor intrusion is the critical risk pathway for this residential area, as the contaminated aquifer is not used for drinking water purposes. High concentrations of volatile compounds were present in the groundwater and a shallow groundwater table could have represented a short migration pathway for contaminant vapors.

Results from the modeling are shown in Table 2.7. According to the RISC calculations, a VC concentration of 3.34 mg L^{-1} in groundwater produces a

carcinogenic risk of one in 4.5 million ($2.2x10^{-7}$) for an adult and one in 1.1 million ($8.9x10^{-7}$) for a child, which are acceptable when compared with the $1x10^{-6}$ target risk value. Conversely, with the same input data, VOLASOIL predicts a significant risk for VC (91 times above TAC). Model predictions for TCE and PCE from both models resulted in acceptable risk (lower than $1x10^{-6}$).

Table 2.7 – Results from Tier II risk assessment models (RISC BP and VOLASOIL) and comparison with MCD maximum concentrations detected (Table 2.5). C p: predicted concentration; C m: measured concentration; TAC: tolerable air concentration.

	Contaminant	C predicted mg m^{-3}	Carcinogenic risk (adult)	Carcinogenic risk (child)
RISC Site Specific	VC	$3.49x10^{-4}$	$2.20x10^{-7}$	$8.90x10^{-7}$
	TCE	$2.23\ x10^{-5}$	$2.70\ x10^{-9}$	$1.10\ x10^{-8}$
	PCE	$3.34\ x10^{-6}$	$1.30\ x10^{-10}$	$5.50\ x10^{-10}$
		C predicted mg m^{-3}	TAC mg m^{-3}	Cp/TAC
VOLASOIL Site Specific	VC	**9.12**	0.10	**91.23**
	TCE	$3.46\ x10^{-3}$	1.90	$1.82\ x10^{-3}$
	PCE	$1.06\ x10^{-3}$	2.50	$4.24\ x10^{-4}$
		C measured mg m^{-3}	C m/C p RISC	C m/Cp VOLASOIL
Measured and predicted concentrations	VC	$3.80x10^{-5}$	0.11	$4.17x10^{-6}$
	TCE	$9.40x10^{-4}$	42	$2.72x10^{-1}$
	PCE	$1.17x10^{-2}$	3515	$1.11\ x10^{-1}$

The predicted concentrations were compared with those from passive sampling, as in that campaign all compounds modeled for risk assessment were detected (Table 2.5). The comparison is presented in Table 2.7. As for VC, VOLASOIL calculated a VC concentration five orders of magnitude higher than the MCD, RISC overestimated VC by one order of magnitude. VOLASOIL also overestimated TCE concentrations by two orders of magnitude, but provided a PCE value comparable to the measured one. In contrast, RISC-predicted TCE concentrations were two orders of magnitude lower than the measured values and the PCE concentrations were overestimated.

From comparison between measured values and risk targets, the level of risks at the site was acceptable, which was confirmed by RISC but not by VOLASOIL. However, when predicted concentrations were compared with measurements, a significant discrepancy was observed for all compounds with both models, especially for VC that was the main contaminant of concern at the site.

The discrepancy between vapor intrusion model predictions and measured values has been previously observed elsewhere (Hers et al., 2003; McHugh et al., 2004; van Wijnen and Lijzen, 2006). These discrepancies complicate adequate communication of risks to the citizens concerned. Reasons for the discrepancy have not been clarified yet and research is currently conducted to elucidate these phenomena. It is hypothesized that either physical processes which are relevant at

the field scale are not taken into account by the models, or biodegradation occurs at the site.

2.6 Conclusions

Chlorinated hydrocarbons were present at concentrations in the order of magnitude of mg L^{-1} to g L^{-1} in an aquifer located below a residential area at a shallow depth. An updated conceptual model of the geological framework of the area was needed for a comprehensive understanding of the contamination dynamics, plumes migration potential, and on site human health risk issues. Two sandy aquifer units, called A0 and A01, both to be considered as leaky-confined, occur from 3 m to about 20 m b.g.l., hydraulically closely interconnected. Groundwater flow inside these units is rather low due to poor lateral continuity of the permeable bodies. The A0 aquifer, the shallowest one, never crops out at the site but it is always covered by a fine-grained layer.

The original source material (solid-liquid mixture of chlorinated pitches with unknown composition), once disposed in two dumps, induced gravity-driven percolation of DNAPL down to the bottom of original clay pits (down to 6-7 m b.g.l.). Due to the depth of the pits, a direct connection occurred with the A0 aquifer and free phase easily migrated further downwards also into the A01 unit.

Due to the close proximity to buildings and the shallow occurrence of the contamination, vapor intrusion is the most relevant risk pathway at the site. However, soil gas and indoor air monitoring data show that the pathway is not complete, as groundwater contaminants were scarcely present in the soil gas and almost never detected in indoor air. This can be due to the physical separation represented by the clayey cover (partly consisting of earth filling) that separates the ground surface from the top of the A0 aquifer. The continuity of the A0 unit below the residential area, however, is to be assessed. Alternatively, degradation processes occurring in the unsaturated part of the soil profile could be responsible for preventing vapor intrusion. Such (bio)degradation processes in unsaturated soil layers are not yet well understood and cannot be accounted for field monitoring in current risk models. In this specific case, the use of tier II risk assessment models was inadequate, as the predictions based on aquifer concentrations in general overestimated the risks, as compared to assessments based on indoor air measurements.

The complexity of this case study highlights the need for improvements in conceptual models and monitoring techniques for vapor intrusion, especially in support of better risk perception from the citizen perspective.

3 Sensitivity analysis on processes and parameters affecting vapor intrusion risk

Abstract

A one-dimensional numerical model was developed and used to identify the key processes controlling vapor intrusion risks by means of a sensitivity analysis. The model simulates the fate of a dissolved volatile organic compound present below the ventilated crawl space of a house. In contrast with the vast majority of previous studies, it accounts for vertical variation of soil water saturation and includes aerobic biodegradation. The attenuation factor (ratio between concentration in the crawl space and source concentration) and the characteristic time (to approach maximum concentrations) were calculated and compared for a variety of scenarios. These concepts enable the understanding of controlling mechanisms and aid in the identification of critical parameters to be collected for field situations.

The relative distance of the source to the nearest gas-filled pores of the unsaturated zone is the most critical parameter, as diffusive contaminant transport is significantly slower in water-filled pores than in gas-filled pores. Therefore, attenuation factors decrease and characteristic times increase with increasing relative distance of the contaminant dissolved source to the nearest gas diffusion front.

Aerobic biodegradation may decrease the attenuation factor by up to three orders of magnitude. Moreover, the occurrence of water table oscillations is of importance. Dynamic processes leading to a retreating water table increase the attenuation factor by two orders of magnitude because of the enhanced gas phase diffusion.

This chapter has been published as:
Picone, S., Valstar, J., Grotenhuis, T., Gaans van, P., Rijnaarts, H. 2012. Sensitivity analysis on processes and parameters affecting vapor intrusion risk. Environmental Toxicology and Chemistry, 31:5, 1042 - 1052.

3.1 Introduction

Vapor intrusion is known as the volatilization of subsurface contaminants, migration in the vapor phase through the unsaturated part of the soil, and the subsequent accumulation in buildings. Volatile groundwater pollutants such as BTEX and chlorinated hydrocarbons form extensive dissolved plumes which may cause vapor intrusion. Vapor intrusion is a main driver of human health risks and often a reason to abandon or remediate polluted sites. Adequate risk assessment aims at sufficient protection of receptors, while keeping the societal costs of remediation within limits. Modeling or monitoring can be used to assess exposure to contaminants. In case of volatile contaminants, vapor intrusion is recognized as the most critical yet the most uncertain exposure pathway to be addressed because of unresolved difficulties in both measuring and modeling (McAlary et al., 2011). Quantifying the contribution of vapor intrusion to indoor air concentrations by measurements is hampered by the effects of seasonality and spatial variability (Folkes et al., 2009) and the presence of indoor sources of contamination (McHugh et al., 2006).

Two types of models are currently available for vapor intrusion: analytical and numerical models. Analytical models are simpler in their use and in the data input required, and are therefore mostly applied in practice. Examples are RISC BP (BP, 2001) based on Johnson and Ettinger (1991) and VOLASOIL (Waitz et al., 1996). These are one dimensional analytical models that include diffusive and advective transport of dissolved contaminants. These models do not allow for ranking of risks (Provoost et al., 2009) and may significantly over and underestimate measured concentrations (McHugh et al., 2004; van Wijnen and Lijzen, 2006). Beside these, a number of more complex numerical models have been developed in the past decades, investigating the effects of dissolved, gaseous, or pure phase (Non Aqueous Phase Liquid, NAPL) sources of volatile contaminants. Those models may account for specific physical factors, like ventilation, barriers, heterogeneities, presence of a NAPL phase (Davis et al., 2005; Mendoza and McAlary, 1990; Tillman and Weaver, 2007); transient conditions, such as variations in atmospheric pressure or water table (Garbesi and Sextro, 1989; Massmann and Farrier, 1992); biochemical processes and factors influencing these, including the presence of peat layers, anaerobic soils, and seals preventing oxygen influx (Abreu and Johnson, 2006; Hers et al., 2000).

Notwithstanding the abundance of one up to three dimensional numerical models, their practical use is often limited in that the required data input cannot be obtained due to feasibility or economic reasons (McAlary et al., 2011). Thus, there is a clear need for adequate models that are applicable to real world situations and yield sufficiently accurate risk predictions based on critical parameters and their dynamics that can be assessed with an adequate accuracy. This is the objective of the model study presented here.

Overall, most of the available models assume a constant water saturation along the soil profile and neglect biodegradation processes (Abreu and Johnson, 2006; Mendoza and Frind, 1990 b). Soil moisture was recognized as a critical parameter influencing vapor transport by Johnson et al. (1999) but only recently, Atteia and Hoehener (2010) proposed a semi-analytical model including variable soil moisture

for a homogeneous soil. These authors showed that variable soil moisture content can decrease the predicted concentrations reaching the surface by a factor of six. Furthermore, recent modeling studies (Abreu et al., 2006; 2009) showed that biodegradation may as well significantly reduce contaminant concentrations, provided that no oxygen limitations occur.

Here we concentrate on chemical parameters and physical processes affecting vapor intrusion, and compare their influence with that of aerobic biodegradation, taking into account spatially variable soil moisture and retardation. The focus is on shallow groundwater situations frequently occurring in lowland urbanized settings and potentially posing the highest risks due to short migration paths. The model calculates time-dependent vapor concentrations in a crawl space above a variably water saturated soil. It is a tool for mechanistic understanding of the system response to variations of i) soil and contaminant properties (soil organic matter content, temperature, contaminant type), ii) aquifer properties (position of the source with respect to the water table, unsaturated zone thickness), iii) dynamic processes (variable atmospheric pressure, depleting source, water table fluctuations), iv) crawl space ventilation rates, and v) aerobic biodegradation.

3.2 Material and methods

3.2.1 Conceptual model

The principal modeled system is a one-dimensional 1.5 m long soil column below a headspace of 50 cm, simulating the crawl space of a building located above contaminated groundwater. An infinite dissolved source of a volatile organic compound is present in the soil column beneath a defined depth. Soil moisture in the unsaturated zone varies vertically as a function of pressure. The contaminant diffuses in the liquid phase, volatilizes, and diffuses in the gas phase, while being partially sorbed onto soil surfaces, finally reaching the crawl space. For scenarios including biodegradation, the dissolved contaminant is degraded with oxygen as electron acceptor.

Oxygen is assumed to diffuse downwards from atmospheric concentrations. In the headspace of the column, which mimics the crawl space of a building, gas advection due to ventilation is included, but turbulence effects are neglected. It was chosen to limit the model to a crawl space as extension to the first floor of a building would make the outcomes very sensitive to the permeability of the surface between the crawl space and the first floor and the ventilation in the building itself. For example, Parker (2002) showed that the value chosen for the building foundation permeability contributed alone to 32% of variance in predicted risk. We therefore deliberately excluded very site-specific parameters, which are less fit to describe generic processes related to risk prediction.

The groundwater level is assumed to be constant and no flow occurs in the saturated zone, except for the scenarios with a fluctuating water table. Water table fluctuations are assumed to be related to hydraulic head variations from lateral

recharge or draining which generate a predominantly vertical one-dimensional flow. Water infiltration is neglected as the upper surface is built on or paved. Such a one-dimensional diffusion approximation is adequate when groundwater flow is less than 0.5 m d^{-1}, predominantly horizontal, and horizontal gradients in permeability are small (McCarthy and Johnson, 1993).

In the whole domain, interphase mass transfer is instantaneous as local equilibrium is assumed. The local equilibrium assumption was checked by analytically solving a standard equation for one-dimensional liquid diffusion, which is the limiting step in contaminant transport (Popovicova and Brusseau, 1998). The characteristic time for benzene liquid diffusion in soil pores was computed for the most abundant granulometric fraction of the soil type used in the present study, namely fine sand (average particle size <210 μm). An average pore diameter of 53 μm was calculated according to Hamamoto et al. (2009). The calculated characteristic time (<10 s) for liquid diffusion of benzene within a fully water saturated pore was found negligible compared to the minimum characteristic time within all the considered scenarios (8,640 s). Therefore, the local equilibrium assumption for interphase mass transfer holds.

In case of water table fluctuations, mixing and dispersivity might be enhanced by entrapment of gas bubbles in the capillary fringe (Klenk and Grathwohl, 2002) or by physical heterogeneities such as fully water saturated portions (e.g. clay lenses within the unsaturated zone (Silliman et al., 2002)); however, these two factors were not taken into account to reduce the complexity of the model.

Biodegradation is assumed to take place in the liquid phase only (Bouwer and Zehnder, 1993), following first order kinetics. A Monod-like term accounts for oxygen limitations. The resulting equation for the rate is:

$$r = -k\left[HC\right]\frac{\left[O_2\right]}{K_{O_2} + \left[O_2\right]} \tag{1}$$

where r is the biodegradation rate, k is the hydrocarbon first order aerobic biodegradation rate (d^{-1}), K_{O2} is the oxygen half saturation constant (mg L^{-1}), [HC] is the hydrocarbon concentration in the liquid phase (mg L^{-1}), and $[O_2]$ is the oxygen concentration in the liquid phase (mg L^{-1}). Oxygen consumption is related stoichiometrically to the mass of hydrocarbon degraded assuming its complete conversion into carbon dioxide and water. Other oxygen consuming processes than the contaminant biodegradation, such as organic matter degradation, are neglected.

3.2.2 Model code and governing equations

The model developed uses the Subsurface Transport Over Multiple Phases (STOMP) code (White and Oostrom, 2004), a finite differences numerical model solving differential equations by means of Newton-Raphson iterations. Other codes available for unsaturated zone modeling, such as R-UNSAT (Lahvis and Baehr, 1998) or HYDRUS (Simunek et al., 1999), do not enable the coupling of diffusion, advection in gas and liquid phase, and biodegradation processes together with the presence of a pure phase. The code used in the present study also supports extension to three

dimensional cases and biodegradation processes; the code has been previously used for the modeling of dense TCE vapor movement (Oostrom et al., 2007), but not yet for vapor intrusion modeling.

Governing equations are the component mass conservation equations and flow over two phases from which gas phase and water vapor pressure are derived. Transport equations are solved after governing equations and provide volumetric concentrations. The simulator uses the Millington and Quirk method (1959) to calculate phase tortuosities and hence aqueous and gas effective diffusion coefficients. The water retention curve of Brooks and Corey (1966) was chosen as it is stable under saturated conditions. The method of Lenhard et al. (1989) was used to derive the input entry head (ψ_a), pore size distribution index (λ), and residual water saturation (θ_r) from Van Genuchten parameters. For water and gas relative permeability functions, the Mualem (1976) pore distribution model was used. The simulations assume isothermal conditions (T = 20°C where not indicated otherwise).

3.2.3 Model discretization and parameter values

The model consists of 200 squared 7 by 7 m cells with a vertical thickness of 1 cm (Figure 3.1). The crawl space height is 0.5 m, and the resulting volume of 25 m^3 equals the average crawl space size for a house in the Netherlands (Waitz et al., 1996). The modeled soil type is a characterized real soil from an uncontaminated area consisting of 73% fine sand, 11% coarse sand, 12% silt, and 4% clay. The crawl space is modeled as an additional soil type with a porosity of 0.999 and a null distribution coefficient.

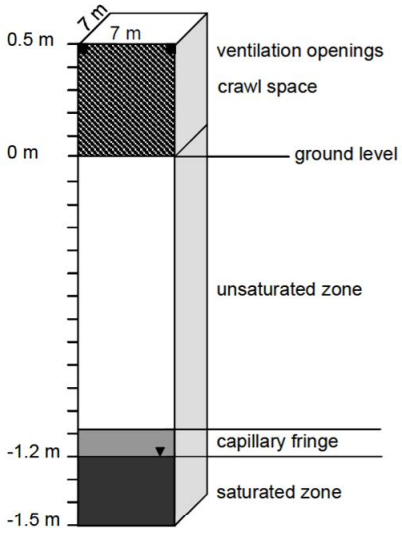

Figure 3.1 - The modeled system, x and y dimensions are not in scale.

Relevant input parameters for soil type and contaminant properties are shown in Table 3.1. Diffusion coefficients at different temperatures were derived from those at 25°C according to Bird et al. (1960). The pressure is hydrostatic, with the upper boundary condition equal to atmospheric pressure.

*Table 3.1 - Constant and variable model input parameters. TCE Trichloroethylene, VC Vinyl chloride. * dissolved source concentration was varied only in the scenarios including biodegradation, as the model is otherwise linear.*

Soil physical properties					
	Unit	Soil		Crawl Space	
Soil porosity	(-)	0.30		0.999	
Soil particle density	kg m^{-3}	2650		-	
Hydraulic conductivity	m day^{-1}	2.30		$1x10^{7}$	
Entry head	(m)	0.16		0.1	
λ parameter	(-)	0.63		5	
Residual water content	(-)	0.02		$1x10^{-7}$	
Contaminant chemical properties (USEPA, 2004)					
	Unit	Benzene	Toluene	TCE	VC
H_c at 20°C	(-)	0.18	0.21	0.34	0.98
K_{oc}	$m^3 kg^{-1}$	$5.89x10^{-2}$	$1.82x10^{-1}$	$1.66x10^{-1}$	$1.86x10^{-2}$
D_{air} at 20°C	$m^2 s^{-1}$	$8.58x10^{-6}$	$8.48x10^{-6}$	$7.70x10^{-6}$	$1.03x10^{-5}$
D_w at 20°C	$m^2 s^{-1}$	$9.55x10^{-10}$	$8.38x10^{-10}$	$8.87x10^{-10}$	$1.20x10^{-9}$
Solubility in water at 20°C	g L^{-1}	1.75	0.53	1.10	2.76
Indoor air risk limit (VROM, 2009)	mg L^{-1}	$2.00x10^{-5}$	$4.00x10^{-4}$	$2.00x10^{-4}$	$3.60x10^{-6}$
Algorithm parameters					
Numerical scheme		Euler backward			
Variable time step range		1 - 30 hours			
Time step acceleration factor		1.25			
Max number of iterations		16			
Convergence criteria		$1x10^{-6}$			
Variable input parameters					
		Reference Scenario		Variations	
Dissolved source concentration *		1 mg L^{-1}		1 - 10 - 20 - 50 - 150 - 400	
Source position		1.19 m b.g.l.		1.49 m b.g.l. - 0.01 m b.g.l.	
Unsaturated zone thickness		1.15 m		3 -5 -10- 15 m	
Temperature		20		5 - 10 -15	
Soil organic matter content		0.1 %		1% - 10%	
Chemical properties		Benzene		Toluene, TCE, PCE, VC	
Crawl space ventilation rate		1 h^{-1}		0.1-0.2-0.5-0.7-1.5-2	
First order biodegradation rate		0 d^{-1}		0.028 - 0.335 - 0.445 - 2.5	
Oxygen half saturation constant		0 mg L^{-1}		0.5 - 5	

Water table fluctuations were modeled by applying a square wave variable Dirichlet type boundary condition to the lower boundary of the modeled system. Semi-annual water table variations of 20 cm were modeled, corresponding to the average water table oscillations in the Netherlands (Van der Sluijs and De Gruijter, 1985). For scenarios including longitudinal dispersion, longitudinal dispersivities were calculated from the empirical equation proposed by Schulze-Makuch (2005) for unconsolidated sands.

For scenarios including biodegradation, the boundary condition for oxygen transport was an atmospheric concentration of 20% volume at the inward ventilation

flux. Upper, mean and lower bound biodegradation rates were derived from literature review of field and laboratory data (Suarez and Rifai, 1999). Where not differently indicated, an oxygen half saturation constant of 0.5 mg L^{-1} was used (Clement, 1997).

To simulate an infinite source, the liquid concentration in all cells of the source zone was kept constant by an additional module in the code. This module overwrites the total mass in the predefined cells of the source zone after the transport calculation of each time step with the fixed mass at the start of the simulation. To avoid a significant decrease of the liquid concentration in these cells within transport calculations of each time step, the distribution coefficient (K_d) in the source zone was increased by several orders of magnitude.

Ventilation was simulated as an airflow at atmospheric composition through one of the ventilation openings located at the top of the crawl space (see Figure 3.1) while on the other side a constant atmospheric pressure boundary condition is applied. At all other boundaries, zero flow conditions were prescribed. The ventilation rate (h^{-1}) is defined as the ratio between the airflow ($m^3\ h^{-1}$) and the volume of the crawl space (m^3). A ventilation rate of 1 h^{-1} (equivalent to a gas flow of 25 $m^3\ h^{-1}$) was applied where not indicated otherwise, equivalent to the average rate measured in crawl spaces in the Netherlands (Stoop et al., 1998).

3.2.4 Model scenarios and output analysis

Model simulations considered a reference scenario with an infinite dissolved benzene source up to the groundwater table, located at 1.2 m below ground level. Scenario variations were performed with respect to i) soil properties, ii) contaminant properties, iii) aquifer properties, iv) crawl space ventilation rate, v) dynamic processes, and vi) aerobic biodegradation (Table 3.2). An arbitrary source concentration of 1 mg L^{-1} was chosen in all main scenarios. This concentration is representative of commonly encountered low source concentrations in groundwater plumes. As the transport model is linear, results from different source concentrations can be easily derived. For simulations including biodegradation, where oxygen limitation could come into play, the influence of variable source concentration on the attenuation was additionally tested, in a concentration range from 1 to 400 mg L^{-1}, which encompasses dissolved low concentration in groundwater plumes up to NAPL related concentrations.

The developed model predicts a concentration gradient in the crawl space which is in contrast with the generally accepted concept of a well mixed container (Turczynowicz and Robinson, 2001); therefore, it was chosen to use as a reference the concentration leaving the crawl space, namely the one predicted at the middle of the upper two cells of the crawl space (49.5 cm height). Based on this reference concentration, each scenario was characterized by two parameters that are independent from the source concentration: the characteristic time (t_c) and the attenuation factor (α). The characteristic time gives an indication of the response time of the system to an input concentration in the groundwater. In practice, it can give an

indication of the urgency of remedial actions. The characteristic time t_c is calculated as the time at which the contaminant concentration at 49.5 cm in the crawl space equals

$$C_{(tc)} = C_{\max}\left(1 - e^{-1}\right) \quad (2)$$

where $C_{(tc)}$ is the gas concentration at the characteristic time (mg L^{-1}) and C_{max} is the maximum gas concentration at 49.5 cm in the crawl space (mg L^{-1}). The dimensionless attenuation factor α represents the ratio between the maximum gaseous concentration at 49.5 cm in the crawl space and the equivalent gas concentration at the source of contamination (Abreu and Johnson, 2006). This value indicates the fraction of the contamination reaching the receptor. It is calculated as

$$\alpha = \frac{C_{gas}^{crawlspace}}{C_{liq}^{source} * H} \quad (3)$$

where $C_{gas}^{crawlspace}$ is the gas concentration at 49.5 cm in the crawl space, C_{liq}^{source} is the liquid concentration at the source depth, and H is the dimensionless Henry constant at the defined temperature.

The Johnson and Ettinger model (Johnson and Ettinger, 1991) was used as comparison for the output of the presented model, as it is the most widely used model for vapor intrusion. It was recently shown that predictions from Johnson and Ettinger were within an order of magnitude agreement with three-dimensional numerical modeling results (Yao et al., 2011), which proves its robustness. Characteristic times and attenuation factors were compared with the Johnson and Ettinger model using the analytical solutions proposed by Johnson et al. (1999) which account for variable soil moisture. Based on the soil moisture profile calculated by STOMP, the water and air-filled porosity were averaged over 10 cm intervals. Advective transport through cracks was neglected.

Furthermore, the obtained attenuation factors were used to calculate the maximum dissolved source concentration for which the indoor air limit is not exceeded based on the reference limits for indoor air quality in the Netherlands (VROM, 2009). This concentration is indicated in Table 3.2 as C_{liq}^{critic}. In terms of risk assessment, this is a conservative approach, as further dilution will occur when crawl space air is mixed with indoor air. Namely, crawl space air constitutes 20% up to 50% of indoor air in case of high and poor ventilation of the crawl space, respectively (Janssen, 2003).

3.3 Results and discussion

Numerical results for all main scenarios are given in Table 3.2. Figure 3.2 a shows the volumetric water content as a function of depth in the modeled soil column. The relative water saturation decreases upward, according to the water retention curve, from full saturation at and below the top of the capillary fringe to a value of 0.3 at the ground level. Here, we define the capillary fringe as the portion of the soil profile above the groundwater table in which the pore space is tension

saturated, but the pressure may be lower than atmospheric pressure (Silliman et al., 2002). In the modeled soil, the capillary fringe thickness is 15 cm.

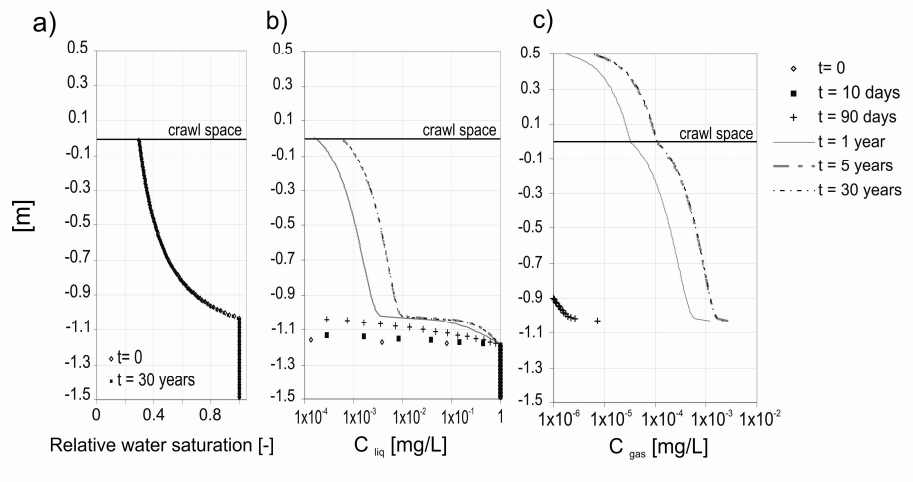

Figure 3.2 a, b, c - Reference scenario: a) relative soil water saturation, b) benzene aqueous and c) gas concentrations in mg L^{-1} both in log scale, versus depth at different time steps.

Reference scenario

Dissolved benzene concentration profiles in time for the reference case are shown in Figure 3.2 b. A three orders of magnitude difference between the dissolved concentration at the water table (1 mg L^{-1}) and the concentration at the depth corresponding to the residual moisture content (1.88 $x10^{-4}$ mg L^{-1}) is present at steady state after one year, similar to what was found experimentally by McCarthy and Johnson (1993). Dissolved benzene diffuses through the water saturated zone in the first 90 d, reaching a concentration above 10^{-5} mg L^{-1} in the liquid phase (lowest concentration displayed) at the top of the capillary fringe. Only after that time benzene exceeds $1x10^{-6}$ mg L^{-1} in the first air-filled pores above the capillary fringe (see Figure 3.2 c). The gaseous concentration at the top of the crawl space increases in time before reaching an asymptotic value of $6.27x10^{-6}$ mg L^{-1} at steady state conditions. The corresponding attenuation factor is $3.48x10^{-5}$. The system has a characteristic time of 1.60 years (Table 3.2). For this scenario, the maximum concentration predicted at the top of the crawl space remains one order of magnitude lower than risk limits (see Table 3.1).

3.3.1 Effect of soil properties

Organic matter content

The chosen range of organic matter content (0.1%, 1%, and 10%, scenarios 2, 1, and 3, respectively, in Table 3.2) spans from average mineral soils to peaty soils, which are common in floodplain areas. Soil organic matter content directly influences contaminant partitioning amongst soil phases: indeed, increasing organic matter increases the characteristic time of the vapor transport process (Table 3.2).

Table 3.2 – Model results. Column headings: D distance from ground surface, C_{gas}^{max} maximum contaminant gas concentration at 49.5 cm in the crawl space, t_c characteristic time, α attenuation factor, C_{liq}^{critic} critical liquid concentration.

Scenarios		N.	Description	D m	C_{gas}^{max} mg L^{-1}	t_c years	α -	C_{liq}^{critic} mg L^{-1}
Reference		1	Benzene OM 1%	1.19	$6.27x10^{-6}$	1.60	$3.48x10^{-5}$	3.19
Soil properties		2	OM 0.1%	1.19	$6.27x10^{-6}$	0.46	$3.48x10^{-5}$	3.19
		3	OM 10%	1.19	$6.10x10^{-6}$	12.54	$3.39x10^{-5}$	3.28
		4	T = 5°C	1.19	$2.15x10^{-6}$	2.62	$2.33x10^{-5}$	4.77
		5	T = 10°C	1.19	$4.44x10^{-6}$	2.37	$2.47x10^{-5}$	4.50
		6	T = 15°C	1.19	$5.30x10^{-6}$	1.93	$2.95x10^{-5}$	3.77
Contaminant properties		7	toluene	1.19	$5.09x10^{-6}$	4.63	$2.83x10^{-5}$	67.32
		8	trichloroethylene	1.19	$5.84x10^{-6}$	3.88	$3.25x10^{-5}$	18.13
		9	vinyl Chloride	1.19	$7.97x10^{-6}$	0.52	$4.43x10^{-5}$	0.08
Contaminated aquifer properties	Source position	10	30 cm below gw table	1.49	$2.15x10^{-6}$	11.20	$1.19x10^{-5}$	9.31
		11	20 cm below gw table	1.39	$2.80x10^{-6}$	7.10	$1.56x10^{-5}$	7.14
		12	10 cm below gw table	1.29	$3.88x10^{-6}$	3.83	$2.15x10^{-5}$	5.16
		13	1 cm above gw table	1.18	$6.68x10^{-6}$	1.43	$3.71x10^{-5}$	2.99
		14	Middle capillary fringe	1.11	$1.24x10^{-5}$	0.57	$6.88x10^{-5}$	1.62
		15	At capillary fringe	1.04	$8.47x10^{-5}$	0.20	$4.70x10^{-4}$	0.24
		16	18 cm above gw table	1.02	$6.46x10^{-4}$	0.09	$3.59x10^{-3}$	0.03
		17	20cm above gw table	0.99	$7.54x10^{-4}$	0.08	$4.19x10^{-3}$	0.03
		18	30 cm above gw table	0.89	$9.45x10^{-4}$	0.05	$5.25x10^{-3}$	0.02
		19	40 cm above gw table	0.79	$1.11x10^{-3}$	0.04	$6.19x10^{-3}$	0.02
		20	50 cm above gw table	0.69	$1.30x10^{-3}$	0.03	$7.23x10^{-3}$	0.02
		21	70 cm above gw table	0.49	$1.83x10^{-3}$	0.016	$1.00x10^{-2}$	0.01
		22	100 cm above gw table	0.19	$3.84x10^{-3}$	0.004	$2.13x10^{-2}$	0.005
		23	110 cm above gw table	0.09	$5.85x10^{-3}$	0.001	$3.25x10^{-2}$	0.003
		24	top of soil column	0.01	$9.91x10^{-3}$	0.0004	$5.50x10^{-2}$	0.002
	Vadose zone thickness	25	unsaturated zone 1.2 m	1.19	$6.27x10^{-6}$	1.62	$3.48x10^{-5}$	3.19
		26	unsaturated zone 3 m	2.99	$6.18x10^{-6}$	2.48	$3.44x10^{-5}$	3.23
		27	unsaturated zone 5 m	4.99	$6.16x10^{-6}$	3.94	$3.42x10^{-5}$	3.24
		28	unsaturated zone 10 m	9.99	$5.87x10^{-6}$	10.34	$3.26x10^{-5}$	3.40
		29	unsaturated zone 15 m	14.99	$4.39x10^{-6}$	16.51	$2.44x10^{-5}$	4.56

Table 3.2 – continued

** for dynamic scenarios with water table variations (retreating and rising water table), the average gas concentration in the crawl space at 49.5 cm is reported*

Crawl space ventilation rate		30	ventilation rate 0.1h^{-1}	1.19	$3.79x10^{-5}$	1.61	$2.00x10^{-4}$	0.53
		31	ventilation rate 0.2h^{-1}	1.19	$2.91x10^{-5}$	1.61	$1.62x10^{-4}$	0.69
		32	ventilation rate 0.5 h^{-1}	1.19	$1.25x10^{-5}$	1.60	$6.96x10^{-5}$	1.60
		33	ventilation rate 0.7 h^{-1}	1.19	$8.95x10^{-6}$	1.60	$4.97x10^{-5}$	2.24
		34	ventilation rate 1.5 h^{-1}	1.19	$4.63x10^{-6}$	1.60	$2.57x10^{-5}$	4.32
		35	ventilation rate 2 h^{-1}	1.19	$3.14x10^{-6}$	1.60	$1.74x10^{-5}$	6.37
Dynamic processes		36	depleting source	1.19	$3.12x10^{-6}$	1.47	$1.73x10^{-5}$	6.42
	Rising gw table	37	groundwater table source	1.19	$1.34x10^{-5}$	$2.81x10^{-6}$ *	$7.45x10^{-5}$	1.49
		38	capillary fringe source	1.04	$8.59x10^{-5}$	$2.26x10^{-4}$ *	$4.77x10^{-4}$	0.23
		39	capillary fringe source longitudinal dispersivity 0.01 m	1.04	$8.78x10^{-5}$	$3.02x10^{-5}$ *	$4.88x10^{-4}$	0.23
		40	capillary fringe source longitudinal dispersivity 0.1 m	1.04	$1.48x10^{-4}$	$3.79x10^{-4}$ *	$8.20x10^{-4}$	0.14
	Retreating gw table	41	groundwater table source	1.19	$6.29x10^{-4}$	$3.16x10^{-5}$ *	$3.50x10^{-3}$	0.03
		42	capillary fringe source	1.04	$8.85x10^{-4}$	$3.79x10^{-4}$ *	$4.92x10^{-3}$	0.02
		43	capillary fringe source longitudinal dispersivity 0.01 m	1.04	$8.85x10^{-4}$	$4.21x10^{-5}$ *	$4.92x10^{-3}$	0.02
		44	capillary fringe source longitudinal dispersivity 0.1 m	1.04	$8.88x10^{-4}$	$3.81x10^{-4}$ *	$4.94x10^{-3}$	0.02
Biodegradation		45	k = 0.028 d^{-1} K_{O2} = 0.5 mg L^{-1}	1.04	$3.89x10^{-5}$	0.20	$2.16x10^{-4}$	0.51
		46	k = 0.335 d^{-1} K_{O2} = 0.5 mg L^{-1}	1.04	$9.07x10^{-6}$	0.10	$5.04x10^{-5}$	2.21
		47	k = 0.445 d^{-1} K_{O2} = 0.5 mg L^{-1}	1.04	$6.29x10^{-6}$	0.10	$3.50x10^{-5}$	3.18
		48	k = 2.5 d^{-1} K_{O2} = 0.5 mg L^{-1}	1.04	$1.25x10^{-7}$	0.04	$6.95x10^{-7}$	159.80

This ranges from 0.46 year (0.1% organic matter) to 12.54 years (10% organic matter), when benzene is the modeled compound. All scenarios asymptotically reach an identical equilibrium concentration lower than the risk limit and have thus equal attenuation factor.

Soil temperature

A temperature variation may influence vapor migration as this parameter affects partitioning and diffusion coefficients. Temperature values of 5, 10, and 15 °C were tested (scenarios 4, 5 and 6 in Table 3.2). At lower temperature, the dimensionless Henry constant of benzene (C_{liq}/C_{gas}) decreases from 0.18 at 20 °C (reference scenario) up to 0.09 at 5 °C. As the gas concentration is indirectly reduced because of the partitioning, the characteristic time increases with decreasing temperature. The modeled temperature decrease causes a 20% lowering of the attenuation factor. A variation in the same order of magnitude was observed by Atteia and Hoehener (2010). The temperature variation moderately increases the maximum aqueous concentration that should not be exceeded to comply with risk limits compared to the reference scenario, which varies between 0.18% and 0.26% of benzene maximum aqueous solubility.

3.3.2 Effect of contaminant properties

Scenarios 7, 8, and 9 in Table 3.2 consider trichloroethylene, toluene, and vinyl chloride as contaminants. Benzene, vinyl chloride, and trichloroethylene are risk-driving compounds in many polluted groundwater situations, as they are known human carcinogens. Toluene is commonly found in combination with benzene at BTEX contaminated sites. These compounds differ mainly in their partition coefficients (see Table 3.1). Vinyl chloride is a gas at normal temperature and pressure (H = 0.98) and is the most soluble compound (solubility = 2760 mg L^{-1}).

Toluene displays the largest soil/organic carbon partition coefficient (K_{oc} = 1.82×10^{-3} m^3 kg^{-1}) and therefore the strongest retardation due to sorption. The mobility of these compounds in air and water due to diffusion is similar as their diffusion coefficients differ less than one order of magnitude.

The main effect of chemical properties is on the characteristic time (Table 3.2). The high organic carbon partition coefficient of toluene and trichloroethylene explains the longer time required to approach maximum concentrations (characteristic times of 4.63 and 3.88 years for toluene and trichloroethylene, respectively). The high Henry constant and diffusion coefficients of vinyl chloride justify the short characteristic time (0.52 year). The maximum contaminant concentrations of each compound at the top of the crawl space remain within the same order of magnitude, with the one of vinyl chloride being the highest (7.97×10^{-6} mg L^{-1}). Considering the calculated attenuation factors, maximum dissolved concentrations in compliance with risk limits are 0.003%, 0.18%, 1.63%, and 12.70% of the aqueous solubility for vinyl chloride, benzene, trichloroethylene, and toluene, respectively. For this system, assuming a dissolved concentration of 1 mg L^{-1} at the groundwater table, risk limits are exceeded only for vinyl chloride.

3.3.3 Effect of variable aquifer properties

Source position

The distance of the non-depleting contaminant source from the top of the soil surface was varied between 30 cm below the groundwater table and the top of the soil surface. The steady state concentration increased with decreasing distance of the contamination from the ground level (scenarios 10 to 24 in Table 3.2). The attenuation factors varied from 1.19×10^{-5} in case of contamination at 30 cm below the groundwater table (scenario 10) to 4.70×10^{-4} (scenario 15) in case of contamination at the top of the capillary fringe. Up to the middle of the capillary fringe (scenario 14), a dissolved benzene concentration of 1 mg L^{-1} did not lead to concentrations higher than the risk limit at the top of the crawl space. It is evident from these data that a decrease in the depth of the contaminant source results in exceeding the risk limit i) at lower dissolved source concentrations, and ii) in a significantly shorter time.

Figure 3.3 a shows how the characteristic time decreases with decreasing depth of the contaminant source, while the attenuation factor increases. Two different regions can be identified in the figure, characterized by increasing air-filled porosity: one up to the top of the capillary fringe and one up to the soil surface. Considering the water table as $d = 0$, until soil pores are water saturated (i.e., $\theta_w = 1$; namely until the top of the capillary fringe as defined above, $d \le d_{cf} = 15$ cm in Figure 3.3), liquid diffusion is limiting. In unsaturated soil ($d > d_{cf} = 15$ cm in Figure 3.3), gas diffusion dominates, causing the break in the curve of Figure 3.3. The fitting function relating the characteristic time, t_c, to the relative distance to the groundwater table (d) is the following quadratic function:

$$t_c(d) = a(d_{cf} - d)^2 + t_c^{cf} \qquad \text{for } d \le d_{cf}$$

$$t_c(d) = b(d_s - d)^2 + t_c^{s} \qquad \text{for } d > d_{cf}$$

where a and b are constants (years cm^{-2}) , d_{cf} and d_s (cm) are the position of the capillary fringe and of the upper soil surface, and t_c^{cf} and t_c^{s} (years) are the characteristic time of the vapor migration process when the source is at the top of the capillary fringe (d_{cf}) and the soil surface (d_s), respectively. Parameter values for the fitted functions are the following: for $d < d_{cf}$, a equals 6.00×10^{-3} years cm^{-2} and t_c^{cf} equals 0.20 years, and for $d \ge d_{cf}$, b equals 7.5×10^{-6} years cm^{-2} and t_c^{s} equals 3.01×10^{-4} years.

The increase of the attenuation factors and the decrease of characteristic times with decreased depth of the contaminant source can be explained by the role of aqueous diffusion in limiting vapor transport. The diffusion coefficient for benzene in water is almost four orders of magnitude lower than that in air (Table 3.1), which strongly limits diffusive transport. As concluded by Parker (2003), vertical mixing within the water saturated zone significantly affects volatilization rates. Experimental work from Arands et al. (1997) also showed that increasing moisture content retarded the rise to steady state concentrations in breakthrough column experiments due to the relatively large capacity of the liquid phase to retain the contaminant.

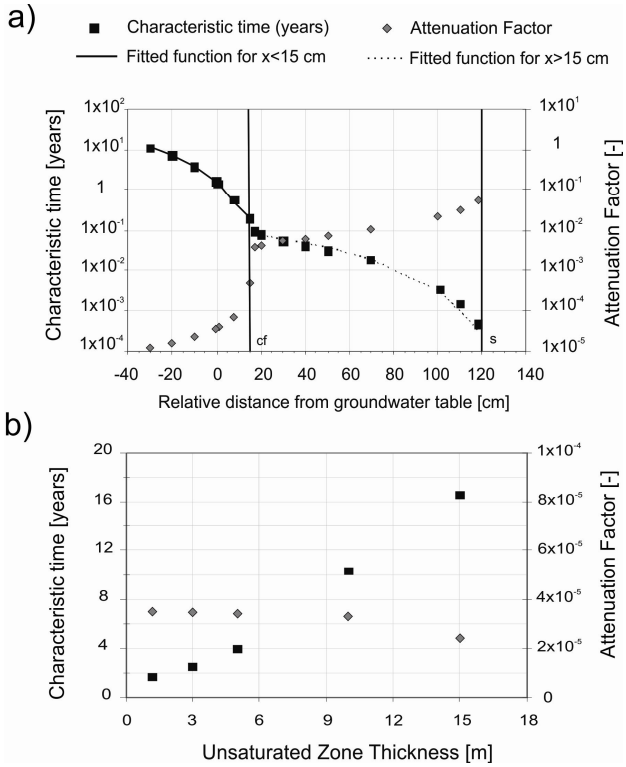

Figure 3.3 a, b - Characteristic time (black squares, left y-axis) and attenuation factor (grey diamonds, right y-axis) for different aquifer properties. a) Characteristic time and attenuation factor versus relative distance of the contaminant source from the groundwater table. Both y-axes are in logarithmic scale. Along the horizontal axis, x=0 represents the groundwater table depth, a negative distance indicates a source located below the water table and a positive distance indicates a source above the water table. The vertical lines represent the top of the capillary fringe (cf) and the top of the soil surface (s). The squares and diamonds represent model results; the lines represent the fitted functions for the characteristic time (see text). Data refer to scenarios 1 and 10 to 24 in Table 3.2. b) Characteristic time and attenuation factor for different unsaturated zone thicknesses. Data from scenarios 25 to 29 in Table 3.2.

Unsaturated zone thickness

In scenarios 25 to 29, the soil column was extended to a total thickness of 19.5 m plus a 0.5 m crawl space to account for the effect of unsaturated zone thickness. The spatial discretization and the time step were unchanged. Varying unsaturated zone thickness between 1.2, 3, 5, 10, and 15 meters causes only a 13% decrease of the attenuation factor, while the characteristic time is approximately linearly correlated to the thickness of the unsaturated zone (Figure 3.3 b).

We acknowledge that the validity of this set of simulations is theoretical, as in practice horizontal concentration gradients would play a role for such deep systems. Nevertheless, the results show that the influence of the unsaturated zone thickness on the attenuation factor is negligible compared to the influence of a fully water saturated zone above the source. In fact, one order of magnitude increase of the characteristic time compared to the reference scenario (t_c = 1.60 years) is observed

when the source is moved to 30 cm below the water table (scenario 10, t_c = 11.20 years), and a comparable effect is produced by a tenfold increase of unsaturated zone thickness (scenario 28, t_c = 10.34 years).

3.3.4 Effect of crawl space ventilation rate

In scenarios 30 to 35, the effect of different crawl space ventilation rates was evaluated. A tenfold increase of the ventilation rate produces a tenfold decrease of the maximum concentrations at the top of the crawl space (e.g., from 2.91×10^{-5} to 3.14×10^{-6} mg L^{-1} for ventilation rates of 0.2 h^{-1} and 2 h^{-1}, respectively), while the characteristic time is unchanged (Table 3.2). Remarkably, for the case of benzene and for the reference scenario considered, a crawl space ventilation rate higher than 0.5 h^{-1} alone is sufficient to maintain vapor concentrations below risk limits.

3.3.5 Effects of dynamic processes

Atmospheric pressure fluctuations

We expected barometric pumping effects to be only minor, based on the findings of Parker (2002). Daily atmospheric pressure variations were simulated for the reference case with a pressure gradient of 3,000 hPa d^{-1}, derived from maximum barometric pressure variations in the Netherlands, as measured by a meteorological station located in Wageningen. The effect of a pressure drop produced a rise on the concentration in the crawl space, but the characteristic time and the attenuation factor did not vary with respect to the constant atmospheric pressure case (results not shown). This is therefore in agreement with the findings of Parker (2002) for benzene indoor air concentrations. However, it is important to stress that when pressure differentials are considered between building foundations and indoor space, low pressure differentials of only –12 Pa are sufficient to generate advective transport through cracks as the dominant mechanism (Patterson and Davis, 2009).

Depleting source

Here the effect of source attenuation due to diffusion, as infinite versus finite source, was evaluated (scenario 36 in Table 3.2). An infinite source situation like the reference scenario pertains to areas where the groundwater flow continuously dissolves and dilutes an upstream NAPL phase supplying a static groundwater plume above which the building of our model is located. A finite source situation is a contaminant plume that is not replenished by a horizontal inflow of contaminated groundwater and therefore undergoes mass depletion due to diffusion and volatilization. The attenuation factor for the finite source scenario (1.73×10^{-5}) is half that of the reference case, and the characteristic time is slightly lower (1.47 years). Benzene removal due to volatilization results in the gradual depletion of the source and a constant decrease of the gas concentration in the crawl space. Provided that the advective replacement of the contaminated groundwater volume underneath the building has a characteristic time much longer than 1.47 years, the source will undergo depletion from diffusion and ventilation.

Water table fluctuations

Water table fluctuations might play a role on vapor emissions because of two main processes: i) an increased volatilization flux at retreating water table conditions, and ii) an increased mixing due to longitudinal dispersion during water table oscillations. However, conflictive findings are reported in literature: while Werner and Hoehener (2001) described significant effects of 20 cm variation water table variations in 15 d; Parker (2002) found only a marginal effect of annual water table variations of 3.6 m. This suggests the influence of water table fluctuations to depend upon the period of the oscillations more than on their amplitude. We therefore chose to simulate semiannual water table fluctuations of 20 cm starting from two scenarios, for which the characteristic time is respectively higher (reference scenario, t_c = 1.60 years) and lower (scenario 15, t_c = 0.20 years) than the period of the water table variations (1 year).

Overall, crawl space concentrations show phases of increasing vapor concentration during water table retreating phases, and decreasing or stationary concentrations during water table rise phases (Figure 3.4 a, b).

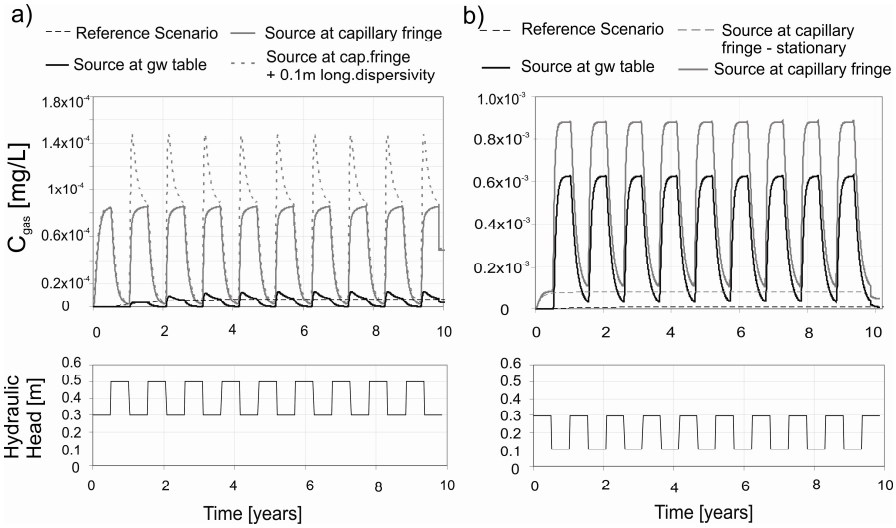

Figure 3.4 a, b - Benzene gas concentration in time at the top of the crawl space for dynamic scenarios with semi annual water table fluctuations. a) rising water table: reference scenario (black dotted line), source located at the groundwater table with water table variation (black line), source at the capillary fringe with water table variation (grey line), source located at the capillary fringe, water table variation and 0.1 m longitudinal dispersivity (dotted grey line). b) retreating water table: reference scenario (black dotted line), source located at the groundwater table (black line), source at the capillary fringe with a stationary water table (grey dotted line), source at the capillary fringe with a retreating water table. The lower plots show the hydraulic head at the bottom of the soil column in time for a rising and retreating water table respectively.

A 20 cm water table rise for a contaminant source located at the water table doubles the maximum crawl space concentration compared to the stationary reference scenario (scenarios 1 and 37). However, the maximum benzene concentration is still lower than risk limit (Table 3.1: $2x10^{-5}$ mg L^{-1}), and the average

concentration in the crawl space is 2.3 times lower than the maximum of the stationary case. In contrast, a water table retreat of the same amplitude produces a two orders of magnitude increase of the maximum and the average crawl space concentration (scenario 41 in Table 3.2). The first water table rising cycle has a loading effect on the pores above the water table, which afterward deliver a higher mass of benzene to the unsaturated zone (Figure 3.4 a). This effect was noticed by Werner and Hoehener (2001) in experimental set-ups.

For a contaminant source at the capillary fringe, a 20 cm water table rise lowers the average crawl space concentration approximately 2.8 times compared to the stationary case. However, the maximum benzene concentration at the top of the crawl space is slightly higher (1.4%, scenarios 15 and 38). Including longitudinal dispersivity in this scenario (water table rise and source at the capillary fringe) does not have a significant effect considering the lower bound value for longitudinal dispersivity of 0.01 m (scenario 39). In contrast, the higher bound longitudinal dispersivity value of 0.1 m leads to a 74% higher maximum concentration and a 50% higher average concentration compared to the stationary case (scenario 15 and 40); both values exceed risk limits. Therefore, dispersion might significantly contrast the protective effect of an increased water-filled porosity due to a rising water table.

A retreating water table for a contaminant source located at the capillary fringe leads to one order of magnitude increase of the maximum concentrations in the crawl space compared to the stationary case (scenarios 15 and 42). This can be mostly ascribed to increased air-filled porosity, as higher longitudinal dispersivities do not have a significant impact on maximum and average concentrations (scenarios 42, 43 and 44). The enhanced gas diffusion caused by a water table drop has relatively more impact on vapor emissions from a contaminant source located at the groundwater table than for a source located at the capillary fringe.

3.3.6 Effect of aerobic biodegradation

The effect of biodegradation was tested for a dissolved contaminant source at fixed concentration present up to the capillary fringe, as this is the first source depth at which the risk limit was exceeded. The range of first order biodegradation rates used (0.028, 0.355, 0.445, 2.5 d^{-1}) reduced the attenuation factor by up to three orders of magnitude and the characteristic time by up to one order of magnitude (Figure 3.5 a). The lower bound biodegradation rate (0.028 d^{-1}) does not keep maximum concentrations below the risk limit (scenario 45 in Table 3.2). At the highest biodegradation rate modeled (2.5 d^{-1}), a dissolved source concentration of 160 mg L^{-1} at the capillary fringe can be attenuated below risk limits.

At increasing source concentration from 1 mg L^{-1} up to 400 mg L^{-1}, and constant biodegradation rate (2.5 d^{-1}), the predicted attenuation factor is constant and equals to 6.95x 10^{-7}. It is questionable whether biodegradation will occur at benzene concentrations higher than 200 mg L^{-1}, as high concentrations might restrict enzymatic activity (Inoue and Horikoshi, 1991). However, these results indicate that no oxygen limitations occur, probably because the diffusion distance from the

oxygen source (i.e. atmosphere) is rather short (1 m), as shown by the oxygen concentration profiles in Figure 3.5 b.

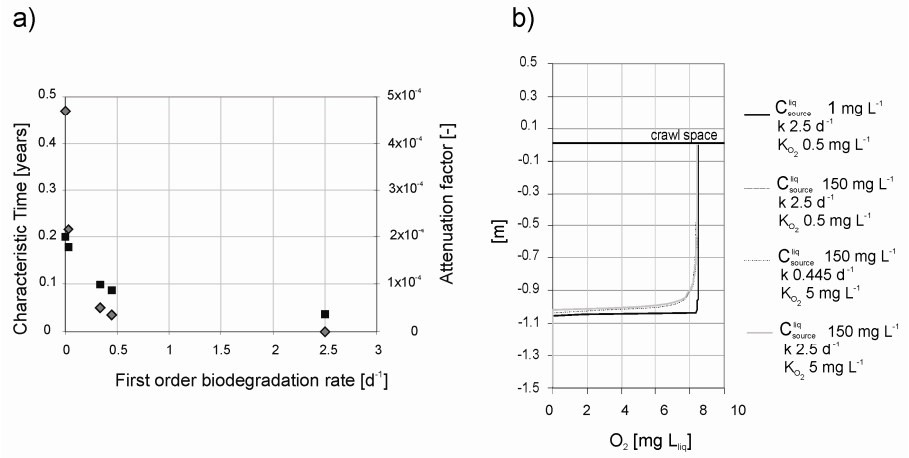

Figure 3.5 a,b - Scenarios including biodegradation. a) characteristic time (black squares, left y-axis) and attenuation factor (grey diamonds, right y-axis) at increasing first order biodegradation rate (k) for a dissolved source concentration of 1 mg L-1. Data from scenarios 45 to 48 in Table 3.2; b) dissolved oxygen concentration profiles at source concentrations of 1 and 150 mg L-1, and variable first order biodegradation rate (k) and oxygen half saturation constant (KO2).

When lowering biodegradation rates, by changing the oxygen half saturation constant from 0.5 mg L^{-1} to the unrealistically high value of 5 mg L^{-1}, higher maximum crawl space concentrations are predicted and the attenuation factor increases by approximately a factor of four ($\alpha = 2.60 \times 10^{-6}$).

The conditions tested here were more conservative than previous studies (Abreu et al., 2006; 2009) in three aspects: i) the source depth was shallower (1.04 m compared to 5 and 8 m), ii) the biodegradation rates used here were on the lower bound range, iii) the oxygen half saturation constant was higher by a factor two. Nevertheless, biodegradation caused a three order of magnitude decrease of the attenuation factor, which proves that it is a significant process to be taken into account when assessing vapor intrusion.

3.3.7 Comparison with the Johnson and Ettinger model

The comparison with the widely applied Johnson and Ettinger model (Johnson and Ettinger, 1991) showed a fair agreement. The calculated attenuation factors at the top of the crawl space reasonably match with the analytical results for the same source-building separation distance (Figure 3.6 a). However, the attenuation factors calculated with STOMP are almost one order of magnitude higher than those calculated with the analytical solution of Johnson et al. (1999) when the contaminant source is situated in the unsaturated zone. This can be explained by the difference in water-filled and air-filled porosity descriptions. These were averaged in the

analytical Johnson and Ettinger model calculations, while according to capillary fringe physics in the STOMP model.

The characteristic times calculated from the developed model are lower than those calculated with the equations from Johnson et al. (1999). At increasing distance from the soil surface, hence at higher water-filled porosity, the difference between the characteristic times increases (Figure 3.6 b).

The maximum difference is one order of magnitude for a contaminant located at the groundwater table. This difference can be justified by the type of equation which is used by Johnson et al. (1999) to estimate the characteristic time. Their equation assumes diffusion into a semi-infinite domain without ventilation. The two assumptions are in contradiction with the system that both the Johnson and Ettinger model and the one presented in this paper consider.

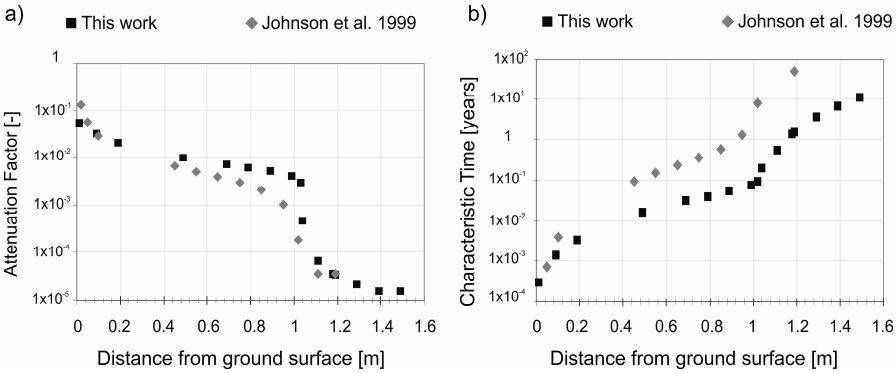

Figure 3.6 a, b - Comparison between the developed model and the Johnson and Ettinger model. a) calculated attenuation factors with the developed model (black squares) and calculated attenuation factors with the analytical equations of Johnson et al., 1999 (grey diamonds) for variable distance of the source from the ground surface; b) calculated characteristic times with the developed model (black squares) and the analytical equation of Johnson et al., 1999 (grey diamonds) for variable distance of the source from the ground surface. In both plots, y-axes are in logarithmic scale.

3.4 Conclusions

Amongst the tested parameters, aquifer properties, dynamic processes, and aerobic biodegradation mostly control the attenuation factor and the characteristic time. Three main system characteristics are dominant: the relative distance from the dissolved source to the first gas diffusion front, biodegradation in the unsaturated zone, and the occurrence of water table oscillations.

First, vertical variations of soil moisture even within a homogeneous soil layer significantly impact vapor intrusion due to transport limitations by liquid diffusion, which substantially lowers the attenuation factor and increases the characteristic time. Conversely, volatilization and rapid diffusion in the vapor phase occur as soon as the dissolved contaminant reaches partially air-filled pores (i.e., right above the

capillary fringe), leading to opposite effects on attenuation factor and characteristic time. Thus, a non-contaminated water saturated layer between the source and the receptor will significantly reduce vapor fluxes.

Second, aerobic biodegradation may result in similar levels of attenuation as depth of the contamination below the saturated/unsaturated zone interface. Biodegradation is thus expected to be especially significant in cases where contaminant sources are shallow, with oxygen fluxes from atmospheric sources being able to enter the soil gas. Nevertheless, limiting factors other than oxygen need to be further investigated to fully assess the potential of biodegradation in risk reduction. Moreover, studies assessing biodegradation rates in variably saturated soils are lacking.

Third, temporal variations of the water table have a stronger influence on vapor emissions when their period is larger than the system characteristic time. A water table drop is the most unfavorable situation, because of the enhanced diffusive gas transport due to increased gas filled porosity. However, a water table rise may as well lead to higher vapor concentrations at the top of the crawl space if dispersivity is taken into account, as it reduces the transport limitations due to liquid diffusion.

Variable soil and compound specific properties mainly influence the characteristic time. Chemical properties shifting the chemical equilibrium towards the gas phase lower the characteristic time and increase the attenuation factor, as shown when vinyl chloride is compared to benzene, trichloroethylene and toluene. Amongst aquifer properties, although unsaturated zone thickness increases the characteristic time, it does not significantly lower the attenuation factor. Source depletion by volatilization and diffusion produces an identical source attenuation as a doubled crawl space ventilation rate. Furthermore, the effects of cyclic barometric pressure variations are limited in magnitude and not persistent, as also concluded by previous literature.

These results have main implications for field characterization in the assessment of vapor intrusion risks. Given the current practice of using sporadic measurements of depth averaged groundwater concentrations as input, the quality of risk evaluation could be greatly improved. It is crucial to verify that vertical mixing throughout the water saturated part of the soil profile is a realistic assumption, through measurements of pore water concentrations at different discrete depths. Additionally, the potential for biodegradation in reducing contaminant diffusion fluxes needs to be assessed, through repeated oxygen and contaminant measurements. Finally, it is also important to monitor water table variations with time.

4 Toluene biodegradation rates in unsaturated soil systems versus liquid batches and their relevance to field conditions

Abstract

Biodegradation of contaminant vapor fluxes in unsaturated soils might reduce emissions from subsurface sources to above ground receptors. However, reported rates show a large variability. Prediction of biodegradation is often based on rates obtained from soil slurry experiments that as such are not representative of unsaturated soil conditions. In order to translate laboratory obtained biodegradation rates to parameters which are meaningful for the field, the role of limiting processes needs to be accounted for. This paper discusses the use of different laboratory set-ups to describe the biodegradation capacity of an in-situ unsaturated soil layer through which gaseous toluene migrates from the water table to the unsaturated zone above. The objectives were to: i) compare biodegradation rates derived from laboratory experiments with unsaturated soil with those from liquid batches, and ii) test whether the observations could be modeled by a liquid phase first order biodegradation rate constant independent from water content, which could be used to predict unsaturated zone biodegradation for the studied culture.

Aerobic toluene biodegradation experiments were performed in static unsaturated soil microcosms ranging from 6% to 30% water-filled porosity (WFP) and unsaturated soil columns at 9, 14 and 27% WFP, inoculated with *Alicycliphilus denitrificans*. These were compared with liquid batches with the same culture. Calculated zero order biodegradation rates were expressed as mass removal rates (r_m), liquid phase biodegradation rates (r_w), and bulk volume biodegradation rates (r_{bulk}). Overall, zero order liquid phase biodegradation rates for unsaturated soil microcosms and soil columns were orders of magnitude higher than rates for liquid mixed batches.

This chapter has been submitted for publication as: Picone, S., Grotenhuis, T., Gaans van, P., Valstar, J., Langenhoff, A., Rijnaarts, H. Toluene biodegradation rates in unsaturated soil systems versus liquid batches and their relevance to field conditions.

Rates were found to be limited by mass supply for the column setup. For the liquid batches, either oxygen or toluene mass transfer at the cell scale, or absence of soil-water-air interfaces seemed to be limiting for bacterial activity. The data from the microcosms could also be fitted by apparent constants for first order biodegradation, that increased with WFP. Apparent rate constants derived from the data compared well with predictions from a numerical model, that included biodegradation in absence of oxygen and nutrient limitations as a first order process taking place in the liquid phase only. Liquid phase first order rates which adequately described the data varied between 6.25 h^{-1} and 20 h^{-1}. They were not related to water content variations. Thus, substrate availability was the primary factor limiting bioactivity here, with evidence for physiological stress at very low water-filled porosity.

Results show that liquid batches do not necessarily reflect optimal conditions for bacteria. Toluene biodegradation in unsaturated soil microcosms appeared to be adequately described by liquid phase first order rate constants derived from apparent first order constants obtained at no oxygen or nutrient limitations.

This work confirms the significant role of unsaturated soil aerobic biodegradation in controlling vapor intrusion risks, providing that adapted or easily adaptable biomass and sufficient oxygen are present. The proposed modeling approach can be used to derive liquid phase biodegradation rates from experimental data and to model biodegradation in vapor intrusion scenarios.

4.1 Introduction

Aromatic hydrocarbons such as benzene, toluene, ethylbenzene and xylene (BTEX) are fuel components and widely used as industrial solvents (Mercer and Cohen, 1990). Besides affecting soil and groundwater quality by generating extended contaminant plumes (Poulsen et al., 1992), hydrocarbon spills in urban areas may cause accumulation of contaminant vapors in buildings – i.e. vapor intrusion (Sanders and Hers, 2006). The main process causing vapor intrusion is gas diffusion through the unsaturated zone (Johnson and Ettinger, 1991). Under abrupt pressure gradients, gas advection might be dominant and generate even higher fluxes (Patterson and Davis, 2009). As numerous bacterial species can degrade aromatic hydrocarbons under aerobic conditions (Smith et al., 1990), their role in reducing vapor emissions in the unsaturated zone has been recognized (Hers et al., 2000; Molins et al., 2010; Ostendorf and Kampbell, 1991). Generally, numerical models describing vapor intrusion include biodegradation as a first order process and literature values from laboratory experiments are used as rate constants (Abreu et al., 2009; DeVaull, 2007; Lahvis et al., 1999). If mass transfer processes are modeled separately and biodegradation is modeled as a process occurring in the liquid phase only, biodegradation rates refer exclusively to the liquid phase (Abreu and Johnson, 2005; 2006; Hoehener et al., 2006; Rathfelder et al., 2000). Alternatively, biodegradation rates are apparent rates referring to the gas phase or overall system (Hoehener et al., 2003; Pasteris et al., 2002).

Reported biodegradation rates show a large variation despite the use of similar experimental set-ups (Suarez and Rifai, 1999). For example, reported toluene first order rate constants in batch experiments range from 0.09 d^{-1}(Nielsen et al., 1996) to 8.3 d^{-1} (Alvarez et al., 1991). In soil slurries, zero order rates for toluene vary from 0.33 mg $(L\ d)^{-1}$ (Zhang and Bouwer, 1997) to 53.8 mg $(L\ d)^{-1}$ (Nielsen et al., 1996). Similarly, specific aerobic toluene degradation rates in liquid batches range from 10.68 mg_{tol} $(mg_{biomass}\ d)^{-1}$ (Chang et al., 1993) to 27.9 mg_{tol} $(mg_{biomass}\ d)^{-1}$(Reardon et al., 2000). Several factors can explain the variability of reported toluene biodegradation rates, such as: a) biomass properties (type of biomass, initial biomass concentration), b) intermittent or continuous substrate feeding, c) the phase distribution of the contaminant (different soil/water/air ratios). The role of these and other potentially rate-limiting factors in controlling biodegradation needs to be understood and explicitly accounted for in order to translate laboratory obtained parameters to meaningful biodegradation rates for field conditions.

Typically, laboratory degradation rates are derived from liquid batches or soil slurries, which as such do not represent unsaturated soil conditions. Variable water content and presence of water/air interfaces characterize the unsaturated zone as opposed to water saturated conditions. On the one hand, variable water content impacts contaminant and oxygen availability (Schoefs et al., 2004) as it affects partitioning and effective diffusion coefficients (Holden et al., 2001; Skopp et al., 1990). A lower water potential may impair bacterial physiology due to the effect on growth and enzyme activity (Potts, 1994). On the other hand, water/air interfaces could potentially retain more bacteria than water saturated soils (Rijnaarts et al., 1993; Schaefer et al., 1998), thus providing intrinsically higher biodegradation capacity. While the effect of water content has been investigated for soil respiration (e.g. Bastida et al., 2006; Khan and Joergensen, 2006; Linn and Doran, 1984), hardly any data are available about contaminant biodegradation rates in unsaturated soils.

This study investigates the performance of an aerobic toluene degrading culture in unsaturated soil microcosms and columns with sufficient oxygen in comparison with liquid batches. The objective was two-fold: i) compare biodegradation rates obtained from the different experimental set-ups, and ii) test whether the observed rates could be explained by a liquid phase first order biodegradation rate independent from water content, which could be used to predict unsaturated zone biodegradation for the studied culture. Toluene was chosen as a model compound for aromatic hydrocarbons as it is a well-studied and relatively easily degradable compound under aerobic conditions.

4.2 Materials and methods

4.2.1 Inoculum and medium

Experiments were performed with a culture of *Alicycliphilus denitrificans* (Weelink et al., 2008). This strain is able to degrade toluene with oxygen as electron acceptor, but not with common soil or groundwater electron acceptors such as

nitrate. The culture was grown in mineral medium under aerobic conditions. The mineral salts medium consisted of (per liter demineralized water): 3.5 g $Na_2HPO_4 \bullet 2H_2O$, 1 g KH_2PO_4, 0.07 g $Ca(NO_3)_2 \bullet 4H_2O$, 1 g $(NH_4)_2SO_4$, 0.2 g $MgSO_4 \bullet 7H_2O$. The pH was adjusted to 7 after autoclaving for one hour at 120°C. After autoclaving, the following filter sterilized solutions were added per liter medium: 1 mL trace elements solution SL10 (DSMZ, medium 320) and 1 mL vitamins (Heijthuijsen and Hansen, 1986). Mineral salts medium was used for all microcosms, batch and column experiments.

4.2.2 Unsaturated soil microcosms and liquid batches

Unsaturated soil microcosms were used to simulate conditions of non-advective transport of toluene and oxygen. Thirty grams wet weight of moist soil, corresponding to about 20 mL volume, were incubated in 250 mL serum bottles under aerobic conditions. The remaining headspace of more than 230 mL with air at atmospheric composition ensured excess oxygen. The soil was prepared by mixing a known amount of an air dry uncontaminated sandy soil (93.3% sand, 2.8% silt, 3.9% clay, 3% organic matter – 43% porosity) previously sieved at 2 mm, with a calculated volume of mineral medium up to a specific water-filled porosity. The total soil pore volume in each microcosm amounted to 8.55 mL. Soil water content is expressed as percentage of water-filled porosity (%WFP), where 100% WFP indicates that the whole soil pore volume is water-filled. This expression makes water content comparable for soils at different density as it is independent from mass (Ilstedt et al., 2000). Soil microcosms inoculated with *A. denitrificans* were tested at 6, 9, 15, 18, 21, 30% WFP, while non inoculated batches were tested at 3, 6, 9, 19% WFP (Table 4.1). Bottles were closed with autoclaved Viton rubber stoppers (Rubber bv., NL) and aluminum crimp caps.

After two hours acclimatization at 20°C, live microcosms were inoculated with an active *A. denitrificans* culture. Biomass concentration was measured by optical density at 600 nm in the source culture, which was diluted if necessary and used as inoculum (Table 4.1).

The activity of the inoculum source was tested by toluene consumption. Sterile controls were prepared in triplicate by adding 1.6 mg NaN_3 and 0.2 mg $HgCl_2$ in 1mL medium per bottle. All inoculated tests and sterile controls were performed in triplicate. The microcosms were incubated statically at 20°C in the dark.

With each triplicate set of unsaturated soil microcosms, one liquid batch was prepared simultaneously. The liquid batches were intended to represent biomass activity under optimal mass transfer conditions, as incubated at 20°C and shaking at 125 rpm on an orbital shaker. 125 mL serum bottles were filled with 25 mL mineral medium and inoculated with the same biomass amount as the soil microcosms (4.13 μg), leading to an initial biomass concentration of 0.17 mg $_{biomass}$ L^{-1}. Additionally, data were obtained from four liquid batches at initial biomass concentration of 4.13 mg $_{biomass}$ L^{-1}.

At t = 0, the microcosms and the liquid batches received respectively 7 and 3.5 mL gas volume from a toluene saturated gas phase, leading to a dissolved toluene

concentration at equilibrium of approximately 5 mg L^{-1} in the soil microcosms and 8 mg L^{-1} in the liquid batches. These concentrations are higher than the intervention value for groundwater contamination in the Netherlands of 1 mg L^{-1} (VROM, 2009) but below toxic concentrations for bacteria (Davis and Madsen, 1996). Soil microcosms without *A. denitrificans* inoculum were spiked once, all others three times. When the first toluene spike was degraded, the inoculated microcosms were re-spiked twice with a similar amount of toluene and the headspace was monitored once per hour for a minimum of eight days. Degradation of the first spike was not used in the evaluation of biodegradation rates as it is affected by adaptation.

Table 4.1 – Experimental set-up.

System	%WFP	Liquid volume	Air-filled pore volume	Total batch gas volume	Initial inoculated biomass concentration	f_M
		mL	mL	mL	mg biomass L^{-1}	%
Unsaturated Soil Microcosm	6	0.53	8.02	238.15	4.13	0.39
	9	0.79	7.76	237.89	4.13	0.59
	15	1.26	7.29	237.42	3.27	0.93
	18	1.53	7.02	237.15	2.70	1.13
	21	1.79	6.76	236.89	2.31	1.32
	30	2.59	5.96	236.09	1.59	1.90
	3	0.26	8.29	238.42	-	0.35
	6	0.53	8.02	238.15	-	0.71
	9	0.79	7.76	237.89	-	1.06
	19	1.59	6.96	237.09	-	2.11
Liquid batch	-	25.00	-	100.00	0.17 - 4.13	49.00
Unsaturated Soil Column	9	6.00	60.19	-	4.13	1.78
	14	9.00	57.19	-	4.13	2.66
	27	18.00	48.19	-	4.13	5.21

4.2.3 Unsaturated soil column experiments

A column set-up was designed to determine unsaturated soil biodegradation rates under a continuous hydrocarbon flux. The set-up consisted of two parallel soil columns, 19.5 cm in length and 3.5 cm in diameter (Figure 4.1). One of the columns was inoculated with an active culture of *A. denitrificans*, the other was amended with $HgCl_2$ (500 mg kg^{-1} soil) and therefore functioned as sterile control. The culture used for inoculation was identical to the one used in microcosms and batch experiments, and the initial inoculated biomass concentration was fixed at 4.13 mgL^{-1} for each column test. The soil columns were filled at a uniform density of 1.51 g cm^{-3}. Air dried soil (230 g) was amended with variable volumes of mineral medium with inoculum or medium with $HgCl_2$ according to the specific water-filled porosity (9%, 14% and 27% WFP, see Table 4.1). The total column volume was 153 mL, thus total pore volume corresponded to 66 mL.

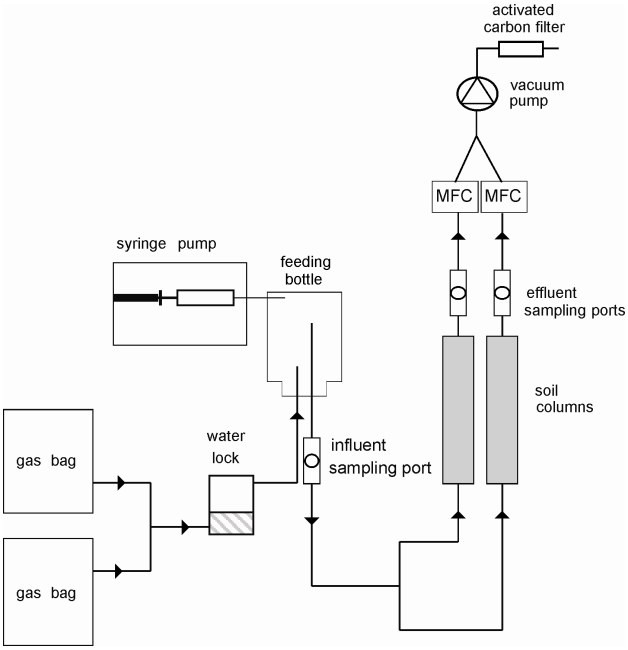

Figure 4.1 –Scheme of the unsaturated soil column set-up (MFC = Mass Flow Controller).

The experiments were conducted at 20°C. Air containing toluene was flowing in upward direction through the columns. The flow was regulated at 4.3 L d^{-1} by two mass flow controllers (Smart Mass Flow Mod. 5850S, Brooks Instrument, NL) connected by a glass capillary to a vacuum pump (Capex L2NS, Charles Austen ltd., UK). The toluene gas concentration was obtained by continuously spiking a large volume of moisturized air with a small amount of pure toluene delivered by a 2.5 mL glass syringe mounted on a syringe pump (KDS200, Kd Scientific Inc., US). Varying the rate of this syringe pump controlled the effective toluene concentration. Two 20 L gas bags (Calibond, Calibration Instruments, US) refilled daily with air at atmospheric composition diluted the toluene concentration in the 500 mL feeding bottle. Air from the gas bags passed a water lock filled with a $HgCl_2$ solution in order to moisturize the gas flow and, at the same time, avoid microbial activity in the feeding section. Mixing in the feeding bottle was ensured by letting the moisturized air flow through a needle. The columns were made of glass and all tubes and connections were made of Teflon. Influent and effluent toluene gas concentrations were monitored hourly using three glass sampling ports equipped with Viton rubber stoppers (Rubber bv., NL).

The order of magnitude of the tested contaminant flux was derived from the conceptual model presented in Chapter 3, and mimicked a continuous diffusive flux from a dissolved contaminant plume to the unsaturated zone above. For a dissolved toluene source of 1 mg L^{-1} diffusing upwards through a 1 m thick unsaturated sandy soil at 20% WFP, a diffusive toluene flux of 10 mg day^{-1} can be calculated. Given the overall gas flux of 4.3 L d^{-1} of the experimental set-up, this is equivalent to a toluene input concentration of 2.3 mg L^{-1} in the gas phase. In the 14% and 27% WFP columns

the toluene flux was doubled by increasing the influent concentration from 13 mg d^{-1} (3 mg L^{-1} influent concentration) at the start, to 26 mg d^{-1} once biodegradation was achieved and toluene concentrations were close to zero for more than 72 h. To assess more unfavorable conditions, soil at 9% WFP was exposed to a flux of 30 mg d^{-1}. However, in this experiment, the influent toluene gas concentration accidentally increased at 100 and 250 hours with values up to 35 mg L^{-1} (flux of 150 mg d^{-1}).

Each experiment lasted 10 to 15 days. At the end of each experiment, soil water content was measured by weight loss at 105°C. The measured column weight difference between the beginning and the end of the experiment was 0.03%, which proved that the set-up was robust for testing unsaturated soil conditions.

4.2.4 Analytical methods

Toluene was analyzed on a Fisons AS 8000 gas chromatograph equipped with a flame ionization detector (FID). 100 μL gas samples from soil microcosms, liquid batches and soil columns were withdrawn with a gas-tight syringe (Hamilton, US). Of these, 50 μL were injected on a chromatograph column CPSil13 (50 m x 0.32 mm; 1.2 μm). Temperature of injector, oven and detector were 200°C, 190°C and 250°C, respectively. For calibration, a BTEX standard gas mixture (Matheson Tri-Gas Inc, US) was used, containing 100 ppm of each component in nitrogen.

Oxygen and carbon dioxide concentrations were measured in 100 μL samples with a Shimadzu GC-2010 gas chromatograph equipped with a thermal conductivity detector. The gas chromatograph was equipped with two columns connected in parallel (Parabond Q: 50 m x 0.53 mm, 10 μm, Varian for oxygen and nitrogen; Molsieve 5A: 25 m x 0.53 mm, 50 μm, Varian for carbon dioxide). Oven, inlet and detector temperature were 60°C, 120°C, 150°C, respectively. Column pressure was 170 bar. The gas mixture used for calibration contained: CH_4 (50.11%), CO_2 (24.8%), N_2 (20.6%), O_2 (2.97%) and H_2 (1.52%).

Biomass concentration was measured as optical density by adsorption at 600 nm of 1 mL sample with a spectrophotometer. The optical density was related to the amount of biomass by protein measurements, assuming the total cell mass contains 55% protein by weight (Maier et al., 2000). Proteins were measured following the Bradford method (Bradford, 1976), using the Cocomassie Plus Assay kit (Thermo Scientific, US). One OD_{600} unit corresponded to 0.21 mg biomass. Biomass concentrations in soil microcosms and soil columns were calculated from toluene consumption.

4.2.5 Calculations

Conceptual model

A vapor phase contaminant in a reactive unsaturated soil layer partitions among liquid and sorbed phase. Once available to bacteria, the contaminant can be biodegraded for both biomass production and mineralization to CO_2. Assuming a yield factor (Y) of 0.5 biomass moles per mole of carbon for toluene conversion (Roels

and Kossen, 1978), the following reaction describes toluene biodegradation with biomass production:

$$C_7H_8 + 5.325O_2 + 0.7NH_3 \rightarrow 0.7C_5H_9O_{2.5}N + 3.5CO_2 + 1.9H_2O \quad (1)$$

The decrease of toluene liquid concentration due to biodegradation triggers a mass transfer from the vapor and sorbed phases to the liquid, delivering fresh substrate to the biomass. Similar processes simultaneously occur for oxygen. By measuring gas concentrations in laboratory set-ups, an overall toluene mass removal rate is determined, which has two controlling components: bioactivity and macro-scale mass transfer processes for both toluene and oxygen. The bioactivity component itself, may as well be affected by a micro-scale mass transfer component, or be entirely dependent on biomass activity only.

Assuming equilibrium partitioning, the total toluene mass in the experimental systems can be calculated from measured gaseous toluene concentrations:

$$M = C_{gas}\left(V_{gas} + \frac{V_{liq}}{H} + \frac{K_d}{H}\rho_b V_{soil}\right) \quad (2)$$

where C_{gas} (mg L^{-1}) is the measured gas concentration, H the Henry's Law constant (dimensionless), K_d the soil partition coefficient (2.4 cm^3 g^{-1} after Malina et al., 1998), ρ_b the measured soil bulk density (1.51 g cm^{-3}) and V_{gas}, V_{liq} and V_{soil} the gas, liquid and solid phase volumes respectively in L. A measured H of 0.26 was used as dimensionless ratio between liquid and gas concentration, which lies within the range of reported values (e.g. Hansen et al.,1993). Based on this, each system can be characterized by a mass distribution factor (f_M). The mass distribution factor (f_M) expresses the fraction of the total toluene mass present in the liquid phase (M_{liq} in mg) compared to the total toluene mass (M_{tot} in mg), as only the former is directly available for bacteria:

$$f_M = \frac{M_{liq}}{M_{tot}} \quad (3).$$

Calculated f_M for each set-up are given in Table 4.1, expressed as percentage.

Mass removal rates

In soil microcosms, the time during which toluene concentrations remained relatively constant was defined as a lag phase. This was followed by a steep decrease in concentrations for which the rates were calculated. In both microcosms and liquid batches, toluene concentrations decreased approximately linearly with time. Mass removal rates (r_m) in these systems were calculated as the maximum slope of the curve decreasing toluene mass versus time. The first and the last data points were always excluded from the fit as affected by higher uncertainty. A minimum of four data points were used to estimate the mass removal rate.

Toluene mass removal rates in column experiments were calculated as zero order rates once the daily toluene concentration in the effluent gas of the inoculated column varied less than 5%, and these conditions persisted for a minimum of three days, which indicated the system had reached an apparent steady state. The toluene mass removal rate was calculated within a specific time interval as:

$$r_m = \varphi * (\overline{C}_{es} - \overline{C}_{el}) \quad (4)$$

where r_m is the toluene mass removed in the column per unit time (mg h^{-1}), C_{es} and C_{el} are the average toluene gas concentration in the effluent of sterile and inoculated column respectively (mg L^{-1}) when the latter is stable, and ϕ is the gas flow (L h^{-1}).

Liquid phase normalized rates

Assuming the reaction to occur in the liquid phase only (Bouwer and Zehnder, 1993), zero order biodegradation rates in the liquid phase (r_w) were calculated by normalizing mass removal rates (r_m in mg h^{-1}) to the liquid phase volume of each system (V_{liq} in L).

$$r_w = \frac{r_m}{V_{liq}} \quad (5)$$

For the columns, this is a conservative estimation: if toluene concentrations were dropping to zero before the column outlet, the effective reactive volume would have been smaller and thus the rate higher. For this reason, the rates for column experiments are indicated as larger than the calculated liquid phase biodegradation rate using the total liquid phase volume.

Bulk volume normalized rates

Additionally, zero order biodegradation rates were reported per bulk volume (r_{bulk}), whereby the bulk volume of the set-up was considered as the reference volume. The bulk toluene biodegradation rate, r_{bulk} in mg $(Lh)^{-1}$, was calculated by normalizing the mass removal rate to the bulk volume of each set-up:

$$r_{bulk} = \frac{r_m}{V_{bulk}} \quad (6)$$

The bulk volume (V_{bulk}) equals the liquid phase volume for liquid batches, and the bulk soil volume (soil particles, water-filled pore volume, air-filled pore volume) for soil microcosms and soil column experiments. For the columns, this is a conservative estimation as mentioned above for r_w.

Biomass normalized rates

Zero order specific biodegradation rates represent the amount of substrate degraded per unit biomass. Specific biodegradation rates (r_w^{spec}) in $mg_{tol}(mg_{biomass}\ h)^{-1}$ were estimated dividing the biodegradation rate in the liquid phase (r_w in $mg_{tol}\ L^{-1}h^{-1}$) for the final biomass concentration (X in $mg_{biomass}\ L^{-1}$):

$$r_w^{spec} = \frac{r_w}{X} \quad (7)$$

As the amount of biomass in soil cannot be measured directly, it was calculated using the theoretical yield coefficient (Y) as in reaction 1. For column experiments, the produced biomass concentration (X) was calculated as:

$$X_k = \sum_{i=0}^{k} \frac{\varphi * (C_{es_i} - C_{el_i}) * \Delta t_i * Y}{V_{liq}} \quad (8)$$

where X is the biomass concentration (mg L^{-1}), C_{esi} and C_{eli} are the toluene gas concentration in the effluent of the sterile and inoculated column respectively at each time step, ϕ is the gas flow through the columns (L h^{-1}), Δt_i is the time interval between two concentration measurements in hours, Y is the yield coefficient ($mg_{biomass}/mg_{tol}$) and V_{liq} is the column liquid phase volume in L. The obtained biomass concentration versus time were averaged over the time interval for which removal rates were calculated. With r_w being a minimum value, and X not likely to be underestimated, also the r_w^{spec} for the soil columns are reported as minimum values.

Apparent first order rate constants

Apparent first order rate constants (k_{app}) were derived for the second spike in soil microcosms by fitting an exponential function to the measured gas concentrations. Again, the first and the last measured concentrations were excluded from the fit as affected by higher uncertainty.

Numerical modeling

The numerical model presented in Chapter 3 was used to simulate the observations in the soil microcosms. The model includes toluene and oxygen as components. Diffusion in gas and liquid phase, and biodegradation are modeled as kinetic processes. Instead of overall equilibrium, only local equilibrium partitioning is assumed.

Biodegradation was modeled as first order reaction in the liquid phase with a Micaelis-Menten dependency from oxygen concentrations, expressed by an oxygen half saturation constant. As oxygen was always in excess in the experiments performed, the oxygen half saturation constant was set to a very low value (0.001 mg L^{-1}) in the model. Diffusion coefficients for toluene and oxygen were taken from literature (USEPA, 2004) and partition constants were as mentioned above for mass balance calculations. The numerical model was used to simulate different controlling components on the overall biodegradation rates measured: i) mass transfer controlled, ii) microbial activity controlled, and iii) no biodegradation. The first scenario (mass transfer controlled) simulated conditions in which biodegradation was instantaneous and therefore the measured toluene removal rate was limited by the substrate supply through diffusion. The second scenario (microbial activity controlled) considered the case in which the overall toluene removal was regulated by bacterial activity, described by a best-fit liquid phase first order biodegradation rate k_w. The third scenario neglected biodegradation.

4.3 Results and Discussion

4.3.1 Liquid batches

In liquid batches, half of the toluene mass was available in the liquid phase (f_M = 49%). In the investigated concentration range, measured toluene concentrations in liquid batches could only be fitted by a zero order model (Figure 4.2 a). The average

toluene mass removal rate is 0.08 mg h^{-1} at initial biomass concentration of 0.17 mg $_{biomass}$ L^{-1} (Table 4.2), which compares well with previous findings for a mixed culture containing *A. denitrificans* (Weelink et al., 2007). At an initial biomass concentration of 4.13 mg $_{biomass}$ L^{-1}, the average toluene mass removal rate increased to 0.14 mg h^{-1} (Table 4.2).

Table 4.2 – Results for liquid mixed batches (V_{liq} = 25 mL). Column headings: C_{liq} initial toluene liquid concentration, r_m mass removal rate, r_w liquid phase biodegradation rate, r_{bulk} bulk volume biodegradation rate, X_0 initial biomass concentration, X_{final} final biomass concentration, r_w^{spec} specific liquid phase biodegradation rate.

Batch	Spike n.	C_{liq}	r_m	$r_w = r_{bulk}$	X_0	X_{final}	r_w^{spec}
		mg L^{-1}	mg h^{-1}	mg (L h)$^{-1}$	mg L^{-1}	mg L^{-1}	mg_{tol} ($mg_{biomass}$ h)$^{-1}$
L1	2	10.11	0.079	3.16	0.17	19.97	0.158
	3	6.03	0.183	7.31		40.14	0.182
L2	3	3.30	0.149	5.95	0.17	57.91	0.103
L3	2	3.66	0.099	3.95	0.17	24.19	0.163
	3	1.91	0.045	1.79		28.28	0.063
L4	2	3.53	0.043	1.73	0.17	20.21	0.086
	3	3.98	0.061	2.46	0.17	28.78	0.085
L5	2	4.49	0.050	2.00	0.17	17.88	0.112
L6	2	2.76	0.044	1.75	0.17	19.87	0.088
L7	2	5.06	0.131	5.25	4.13	20.68	0.254
	3	4.76	0.197	7.86		53.23	0.148
L8	3	2.58	0.167	6.68	4.13	34.08	0.196
L9	2	5.94	0.062	2.48	4.13	30.59	0.081
L10	2	3.69	0.125	5.02	4.13	31.29	0.160

For liquid batches, bulk volume biodegradation rates (r_{bulk}) are equivalent to liquid phase biodegradation rates (r_w). The average liquid phase biodegradation rate increases with initial biomass concentration from 3.35 ± 2.03 mg (Lh)$^{-1}$ at initial biomass concentration of 0.17 $mg_{biomass}$ L^{-1} to 5.46 ± 2.03 mg (Lh)$^{-1}$ at 4.13 mg $_{biomass}$ L^{-1}. The obtained rates are significantly lower than known toluene degraders (i.e. *Pseudomonas*), which are up to 17.65 mg (Lh)$^{-1}$ (Reardon et al., 2000).

Further, the average specific substrate degradation rates are 0.12 ± 0.04 and 0.17 ± 0.06 mg_{tol} ($mg_{biomass}$ h)$^{-1}$ at initial biomass concentrations of 0.17 and 4.13 mg L^{-1} respectively. These rates are approximately a factor four to ten lower than reported specific biodegradation rates for toluene, i.e. 0.45 mg_{tol} ($mg_{biomass}$ h)$^{-1}$(Chang et al., 1993) to 1.16 mg_{tol} ($mg_{biomass}$ h)$^{-1}$(Reardon et al., 2000).

4.3.2 Unsaturated soil microcosms

In these experiments, the unsaturated soil microcosms represent a reactive soil layer located at a certain distance from the source of the gas contamination; diffusion regulates the supply of toluene and oxygen to the microorganisms. However,

contrary to field conditions, contaminant supply is intermittent (spikes) and oxygen is in excess. In fact, measured oxygen concentrations after complete toluene consumption were 15% O_2 in volume. In the inoculated soil microcosms, f_M ranges from 0.39% at 6%WFP to 1.90% at 30%WFP. Thus, the greater part of the toluene mass is not directly available in the liquid phase.

Biodegradation occurs at all tested water-filled porosities in microcosms with *A. denitrificans* as well as in non inoculated microcosms (Figures 4.2 b, c).

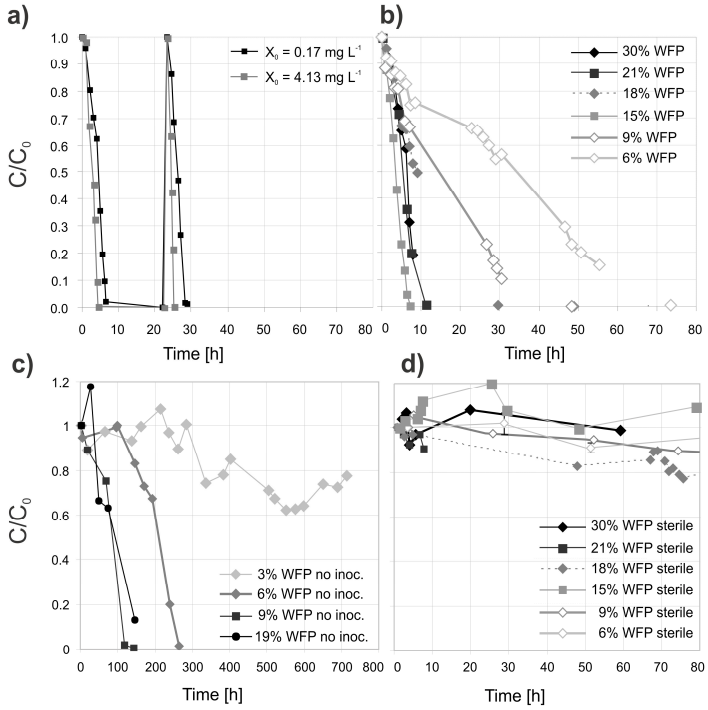

Figure 4.2 a,b,c,d – Average relative toluene gas concentrations for a) liquid batches, b) unsaturated soil microcosms inoculated with A. denitrificans, c) not inoculated unsaturated soil microcosms, d) sterile unsaturated soil microcosms at different water-filled porosity. Average gas phase C_0 are a) 2.03±0.63 mg L^{-1}, b) 1.29±0.3 mg L^{-1}, c) 1.04±0.38 mg L^{-1}, d) 0.87±0.39. Specific C_0 values are given in Table 4.2 (liquid batches) and 4.3 (soil microcosms). X_0 is the initial biomass concentration.

As expected, a shorter lag phase was observed with inoculation (18 to 165 hours at 21% and 6% WFP) compared to non inoculated conditions (27 to 216 hours at 19% and 3%WFP). This indicates that the added biomass, already adapted to toluene degradation, improves toluene biodegradation capacity. Toluene concentrations in the sterile controls decrease by a maximum of 20% only after more than 40 hours (Figure 4.2 d).

In the studied concentration range the results could be described by zero order kinetics (R^2 between 0.94 and 0.99) as well as by first order kinetics (R^2 between 0.87 and 0.98). The zero order mass removal rates range from 0.01 mg h^{-1} at 6% WFP to 0.11 mg h^{-1} at 30% WFP (Table 4.3).

Liquid phase biodegradation rates (r_w) range from 19.56 ± 3.65 mg $(Lh)^{-1}$ to 64.14 ± 8.59 mg $(Lh)^{-1}$ at initial dissolved toluene concentrations from 3.11 ± 0.43 to 7.22 ± 0.66 mg L^{-1} (Table 4.3, Figure 4.3). The range of obtained r_w is on the low end of reported rates for the same soil at 13% and 40% WFP, which were performed at ten times higher toluene concentrations (Malina et al., 1998).

Table 4.3 – Results from unsaturated soil microcosms, average values and standard deviations for each triplicate set are given. Column headings: WFP water-filled porosity, C_{liq} initial toluene liquid concentration, r_m mass removal rate, r_w liquid phase biodegradation rate, r_{bulk} bulk volume biodegradation rate, X_0 initial biomass concentration, X_{final} final biomass concentration, r_w^{spec} specific biodegradation rate, k_{app} apparent first order rate constant, $k_{app\ model}$ apparent first order rate constant as derived from the model.

** average from six identical batches; ** average from duplicates*

WFP	Spike n.	C_{liq}	r_m	r_w	r_{bulk}	X_{final}	r_w^{spec}	k_{app}	k_w data	k_{app} model	k_w model
		mg L^{-1}	mg h^{-1}	mg $(L\ h)^{-1}$	mg $(Lh)^{-1}$	mg L^{-1}	mg_{tol} $(mg_{biomass}h)^{-1}$	h^{-1}	h^{-1}	h^{-1}	h^{-1}
6%	2	5.55 ± 0.64	0.017 ± 0.0082	32.57 ± 15.42	0.86 ± 0.41	1495.16 ± 262.14	0.022 ± 0.0100	0.029	7.26	0.027	6.25
9%*	2	5.15 ± 0.44	0.032 ± 0.0043	41.03 ± 0.71	1.62 ± 0.22	740.50 ± 40.65	0.050 ± 0.0078	0.065	11.15	0.082	14.58
15%	2	3.12 ± 0.12	0.050 ± 0.0168	39.50 ± 13.36	2.49 ± 0.84	424.97 ± 62.52	0.091 ± 0.0200	0.244	26.13	0.157	20.00
	3	3.29 ± 0.19	0.081 ± 0.0108	64.14 ± 8.59	4.04 ± 0.54	694.34 ± 77.44	0.094 ±0.0233	-	-	-	-
18%	2	7.22 ± 0.66	0.063 ± 0.0246	41.49 ± 16.06	3.17 ± 1.23	528.15 ± 37.65	0.080 ± 0.0360	0.051	4.47	0.188	6.25
	3	6.37 ± 0.63	0.053 ± 0.0106	34.80 ± 6.95	2.66 ± 0.53	712.44 ± 117.12	0.050 ± 0.0125	-	-	-	-
21%**	2	5.68 ± 0.32	0.084 ± 0.0090	46.74 ± 5.02	4.18 ± 0.45	769.89 ± 67.98	0.061 ± 0.0012	0.223	16.87	0.218	14.58
	3	3.11 ± 0.43	0.035 ± 0.0065	19.56 ± 3.65	1.75 ± 0.33	350.33 ± 104.02	0.059 ± 0.0184	-	-	-	-
30%	2	4.50 ± 0.30	0.090 ± 0.0199	34.64 ± 7.67	4.49 ± 0.99	455.71 ± 79.37	0.076 ± 0.0061	0.321	16.85	0.308	14.58

From the obtained results, r_w values in soil microcosms do not show a significant variation with water-filled porosity (Figure 4.3 a). The average liquid phase biodegradation rate from all soil microcosms equals to 39.75 ± 13.79 mg $(Lh)^{-1}$. Values for r_{bulk} range from 0.86 ± 0.41 mg $(L_{bulk}\ h)^{-1}$ to 4.49 ± 0.99 mg $(L_{bulk}\ h)^{-1}$ for the triplicates at 6% and 30%WFP respectively. Even considering the relatively high standard deviation of the triplicates at 6%WFP, their r_{bulk} is still significantly lower than the rate at all other conditions (T –test $p<0.05$). At low WFP increased effective diffusion due to higher air-filled porosity should facilitate substrate and oxygen uptake and lead to higher removal rates. Conversely, we observed lower values of r_{bulk} and longer lag phases at decreasing water content (18 hours at 30%WFP to 165 hours at 6% WFP). Thus, we concluded that at water-filled porosity below 9% physiological stress was affecting bacterial activity. It was shown by Dechesne et al. (2008) that cell motility is hindered at water contents below 15%. Similarly, no toluene biodegradation at 8.7% water content in subsurface material was reported in the work of Holden et al. (2001).

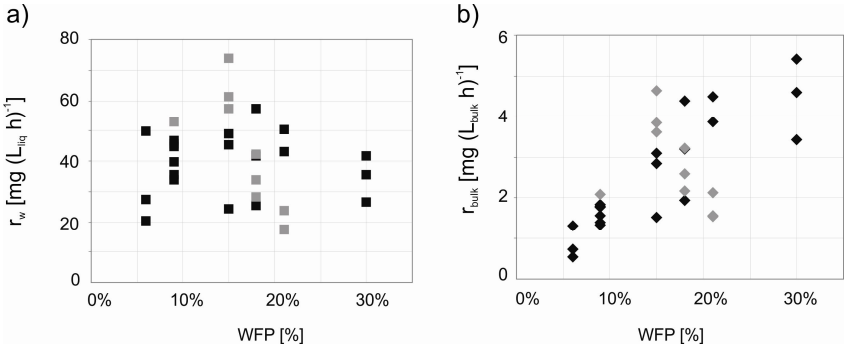

Figure 4.3 a, b – a) Zero order liquid phase biodegradation rates (r_w) versus water-filled porosity in unsaturated soil microcosms; black squares: second spike, grey squares: third spike; b) zero order bulk volume biodegradation rates (r_{bulk}) versus water-filled porosity in unsaturated soil microcosms; black diamonds: second spike, grey diamonds: third spike.

The specific substrate utilization rates (r_w^{spec}) in soil microcosms range from 0.02 ± 0.01 to 0.09 ± 0.02 mg_{tol} ($mg_{biomass}$ h)$^{-1}$, for the triplicates at 6% and at 15% WFP, respectively. The highest rate of 0.12 mg_{tol} ($mg_{biomass}$ h)$^{-1}$ is within the same order of magnitude as those reported for mixed slurries (Alvarez et al., 1991), while the average specific mass removal rate is almost an order of magnitude lower. However, the uncertainty of specific biodegradation rates is higher than liquid phase and bulk volume biodegradation rates, as true quantification of the active biomass in soil is not possible.

Apparent first order rate constants (k_{app}) ranged from 0.03 h^{-1} at 6%WFP to 0.32 h^{-1} at 30% WFP (Table 4.3). The obtained apparent first order rate constants fitted well with those obtained from the numerical model with first order liquid phase biodegradation rates (k_w) ranging from 6.25 h^{-1} at 6%WFP to 20 h^{-1} at 15% WFP (Figure 4.4 a to f). These values of k_w are one up to two order of magnitude larger than reported values for unsaturated soil microcosms (Hoehener et al., 2003), see Table 4.4.

The model results show k_{app} and k_w to be roughly related by the mass distribution factor:

$$k_w \approx k_{app} / f_M \quad (9).$$

Further, comparison between numerical model predictions and observed data showed that the mass–transfer controlled scenario did not describe the data (Figure 4 a, b, f), while the microbial activity controlled scenario did. Given the first order process, both substrate availability and bacterial activity as described by k_w are controlling toluene removal in the unsaturated microcosms.

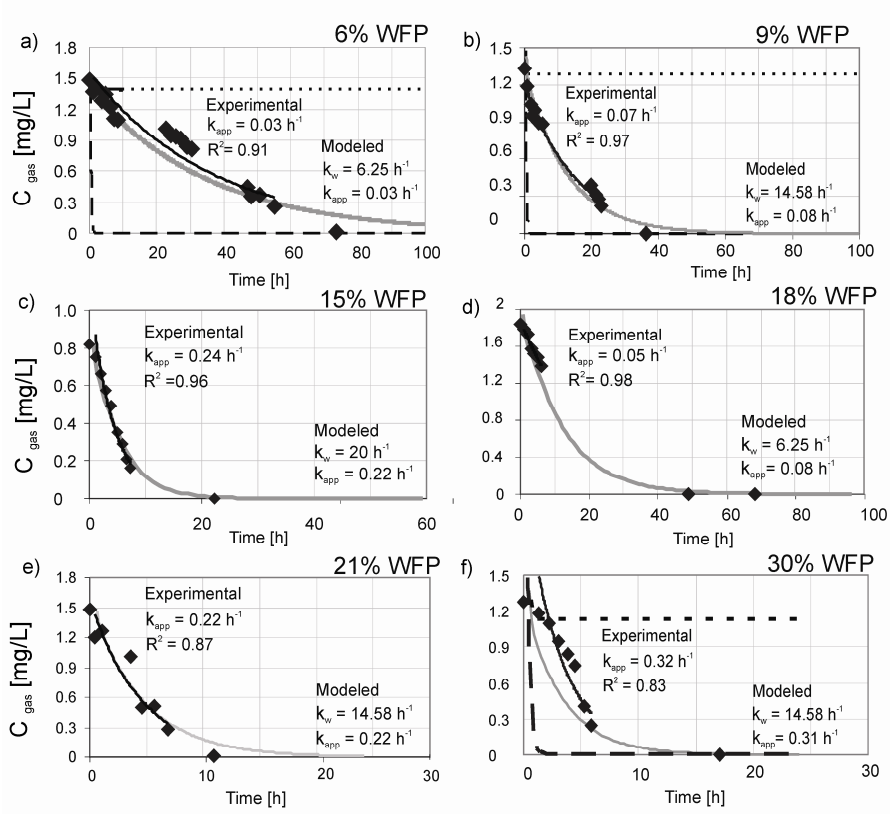

Figure 4.4 a, b, c, d, e, f - Experimental data and numerical model predictions for unsaturated soil microcosms from 6% to 30% WFP. Each plot shows: ◆ experimental data (average of triplicates), ▬ fitted exponential curve to experimental data and its k_{app}, ▬ microbial activity controlled model scenario (k_w and model k_{app} are indicated), ▪▪▪▪ no biodegradation scenario, and ▬ ▬ mass transfer controlled scenario.

Table 4.4 –Comparison between currently obtained and previously reported toluene biodegradation rates. Column headings: C_{liq} initial toluene liquid concentration, r_w zero order biodegradation rates, k_w first order liquid phase biodegradation rates, k_{app} and apparent first order rate constants for different experimental set-ups.

Set-up description (biomass source)	C_{liq} mg L^{-1} min - max	r_w mg $(L_{liq}\ h)^{-1}$ min - max	k_w h^{-1}	k_{app} h^{-1}	Reference
Liquid batch (A. denitrificans)	*0.5 - 20*	*1.73- 7.86*	-	-	*This work*
Liquid batch (mixed culture)	9	-	0.05	-	(Kelly et al., 1996) μmax
Liquid batch (*P. sp X1*)	10	-	0.54	-	(Chang et al., 1993) μmax
Liquid batch (*P. putida F1*)	43	-	0.86	-	(Reardon et al., 2000) μmax
Soil Microcosms 6% - 30% WFP	*3 - 8*	*17.40 - 73.82*	*6.25 - 20*	*0.03 - 0.3*	*This work*
Soil slurries aquifer material	50	23	-	-	(Alvarez and Vogel, 1991)
Soil microcosms 30% WFP alluvial sand	0.1	-	0.12	-	(Hoehener et al., 2003)
Soil microcosms 13% - 40% WFP uncontaminated soil	144	150.64 - 51.11	-	-	(Malina et al., 1998)
Column100% WFP liquid upflow	35	130.83	-	-	(Kelly et al., 1996) Monod no growth
Column 70% WFP pure phase + infiltration	322	-	-	0.04 - 0.08	(Tindall et al., 2005)
Column 65% WFP liquid + infiltration	13	0.13 -0.57	-	-	(Allen-King et al., 1996)
Column 50% WFP gas diffusion	154	-	-	0.06	(El-Farhan et al., 1998)
Column 40% WFP gas advection 1 Lh^{-1}	250	25.11	-	-	(Malina et al., 1998)
Column 32% WFP gas diffusion	500	-	-	1.42	(Jin et al., 1994)
Column 27% WFP gas advection 0.18 Lh^{-1}	*11 - 23*	*> 23.15 -38.43*	-	-	*This work*
Column 28% WFP gas diffusion	14	-	-	0.05	(Hoehener et al., 2003)
Column14% WFP gas advection 0.18 Lh^{-1}	*12- 21*	*> 57.15-81.53*	-	-	*This work*
Column10% WFP gas advection 0.18 Lh^{-1}	*27*	*> 176.33*	-	-	*This work*
Column 6% WFP gas diffusion	12	-	0.4 - 0.5	-	(DeVaull et al., 1997)

4.3.3 Unsaturated soil columns

In the column set-ups, f_M varied between 1.78% at 9% WFP and 5.21% at 27% WFP. Therefore the toluene fraction available in the liquid phase is slightly higher than the soil microcosms but lower than the liquid batches. The toluene concentration in the influent and the sterile effluent show that toluene was retained in the column during at least 50 h (Figure 4.5 a, c). This indicates that sorption affected the breakthrough time. Biodegradation started after 50 h at 27% WFP and after 150 h at 9% WFP. Biodegradation in the inoculated columns at 14% and 27% WFP led to toluene gas concentrations about zero in the effluent at t = 100 h (Figure 4.5 a,b), while at 9% WFP, toluene concentrations decreased to about zero after 200 hours (Figure 4.5 c).

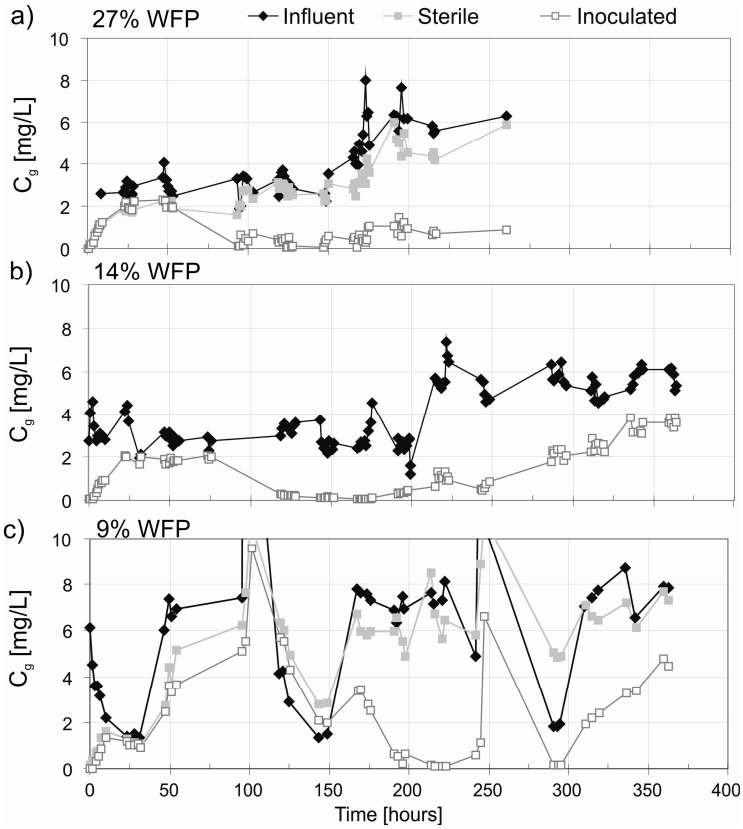

Figure 4.5 a, b, c – Toluene gas concentration as measured in the influent, sterile and inoculated columns in the experiments at 27%, 14%, 9% WFP respectively.

Minimum oxygen concentrations measured in the effluent of the inoculated columns after the onset of biodegradation were 19.7%, 20.3% and 17.8% v/v at 9%, 14% and 27% WFP respectively, thus oxygen was always in excess. In the columns at 9% and 14% WFP, the effluent concentrations started to increase after about 300

hours. As toluene and oxygen supply was continuous but the liquid phase was not refreshed, possible limitations are more likely to be related to nutrient availability.

In the column experiments, toluene was removed from the influent gas down to concentrations of about zero at all tested conditions, which suggests that the amount of toluene supplied per unit time limited the biodegradation rate. The highest mass removal rates (r_m) are 0.69 ± 0.09 mg h^{-1}, 0.73 ± 0.04 mg h^{-1}, and 1.06 ± 0.22 mg h^{-1} at 27%, 14% and 9% WFP respectively (Table 4.5). Calculated values of r_w range between ≥ 23.15 ± 1.79 mg (L h)$^{-1}$ at 27% WFP at toluene concentration of 11.44 ± 1.96 mgL^{-1} in the liquid phase, and ≥ 176.33 ± 23.47 mg (L h)$^{-1}$at 10% WFP at a toluene influent concentration of 26.81 ± 3.56 mg L^{-1} in the liquid phase (Table 4.5).

Table 4.5 – Results from unsaturated column experiments. Column headings: WFP water-filled porosity, C_{liq} toluene initial liquid concentration, r_m toluene mass removal rate, r_w liquid phase biodegradation rate, r_{bulk} bulk volume biodegradation rate, X_{final} final biomass concentration, $r_w{}^{spec}$ specific toluene liquid biodegradation rate.

WFP	C_{liq} mg L^{-1} avg ± stdev	r_m mg h^{-1} avg ± stdev	r_w mg $(L_{liq}\ h)^{-1}$ avg ± stdev	r_{bulk} mg$(L_{bulk}h)^{-1}$ avg ± stdev	X_{final} mg L^{-1} avg ± stdev	r_w^{spec} mg_{tol} $(mg_{biomass}\ h)^{-1}$ avg ± stdev
9%	26.81 ± 3.56	1.06 ± 0.22	≥ 176.33 ± 23.47	≥ 6.87 ± 0.91	1499.66 ± 482	≥ 0.118 ± 0.049
14%	11.69 ± 1.83	0.51 ± 0.09	≥ 57.15 ± 10.06	≥ 3.34 ± 0.59	700.66 ± 374	≥ 0.082 ± 0.027
	21.25 ± 2.28	0.73 ± 0.04	≥ 81.53 ± 4.23	≥ 4.76 ± 0.25	3105.42 ± 242	≥ 0.026 ± 0.017
27%	11.44 ± 1.96	0.42 ± 0.03	≥ 23.15 ± 1.79	≥ 2.71 ± 0.21	232.51 ± 123	≥ 0.100 ± 0.015
	23.14 ± 2.71	0.69 ± 0.09	≥ 38.43 ± 4.88	≥ 4.49 ± 0.57	913.99 ± 124	≥ 0.042 ± 0.039

Previously reported unsaturated soil biodegradation in diffusive column set-ups provided indications of first order kinetics (DeVaull et al., 1997; El-Farhan et al., 1998; Kelly et al., 1996; Jin et al., 1994; Tindall et al., 2005), Monod kinetics (Hoehener et al., 2003), as well as zero-order kinetics (Allen-King et al., 1996; Malina et al., 1998). When compared to published liquid phase zero order removal rates, the minimum r_w calculated for the 9% and 14% WFP columns are within the highest range of reported rates (Table 4.4).

The calculated r_{bulk} in the soil column experiments then range from ≥ 2.71 ± 0.21 mg $(L_{bulk}\ h)^{-1}$ at 27% WFP and 3 mg L^{-1} toluene influent concentration to ≥6.87 ± 0.91 mg $(L_{bulk}\ h)^{-1}$ at 10% WFP and 7 mg L^{-1} influent concentration (Table 4.5).

Calculated specific biodegradation rates ($r_w{}^{spec}$) are also minimum values, that decrease in time as a consequence of the assumed increase in biomass (eq. 8). This might support the conclusion of limitations occurring after about 300 hours. Furthermore, measured CO_2 production (not shown) is higher than what is calculated from the consumed amount of toluene, even when neglecting its partial consumption for biomass growth. Hence, other processes, i.e. organic matter degradation, are related to carbon dioxide production and probably also to biomass growth.

4.3.4 Comparison of the experimental set-ups

The conditions mimicked in these experiments refer to an unsaturated soil layer through which gaseous toluene migrates from the fringe of a contaminant plume towards the soil surface. Specifically, unsaturated soil microcosms and columns resembled the diffusion regulated transport likely to occur in the field, where the column experiments allowed for continuous supply of toluene and oxygen. Conversely, liquid batches were performed to obtain rates under optimal mass transfer conditions. The inoculum of *A. denitrificans* degraded toluene in all experiments.

In the columns, the toluene supply rate was limiting. The soil microcosms were controlled by bacterial activity and the latter appeared not to be mass transfer limited. In the microcosms, a first order process in the liquid phase could describe the measured data. In contrast to that, the liquid batches showed zero order kinetics. This indicates that they did not reflect optimal biodegradation rates. We hypothesize that either reduced oxygen and/or toluene mass transfer at the cell scale due to diffusion in the liquid phase (Harms and Zehnder, 1994), or a less favorable growth environment due to the absence of soil/water/air interfaces were limiting for the bacteria.

As for obtained zero order rates, liquid phase rates calculated for soil microcosms and soil column experiments are orders of magnitude higher than for liquid batches (Figure 4.6 a). They show no significant variation with WFP, hence bulk volume biodegradation rates (r_{bulk}) are expected to decrease with decreasing moisture. Indeed, significantly lower rates were found for soil microcosms at 6% WFP (Figure 4.3, Figure 4.6 a). These might also be explained by physiological limitations due to drought stress (Potts, 1994).

With respect to first order biodegradation rates, the k_w, which adequately described observed data, are higher than reported values (Table 4.4). Further, the derived k_w are five up to ten times higher than maximum rates used to simulate biodegradation in vapor intrusion scenarios in the modeling work of Abreu and Johnson (2006). Literature values for k_w are closer to the k_{app} that were shown to increase as a function of f_M (Table 4.4). This was confirmed by the modeling results (Figure 4.6c). It should be noted that extrapolating towards f_M equals 100% is hypothetical, as it implies a single phase liquid system for which, in this study, other limitations were found. Values of k_w did not correlate with f_M, suggesting that the bioactivity rate constant is not influenced by micro-scale mass transfer (Figure 4.6 d).

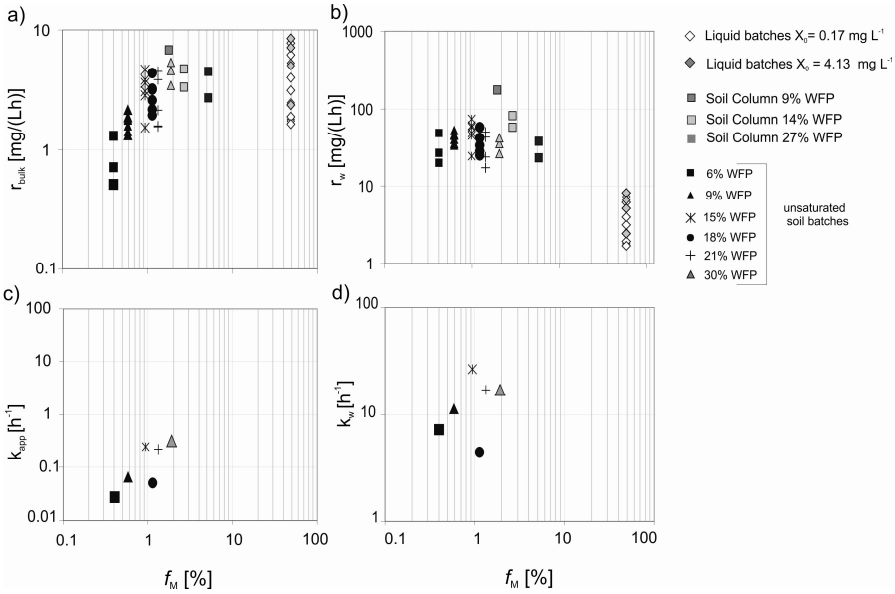

Figure 4.6 a, b, c, d – Four parameters describing biodegradation for liquid batches, unsaturated soil microcosms, and unsaturated soil column versus f_M in %. a) toluene zero order liquid phase biodegradation rates (r_w); b) toluene bulk phase toluene biodegradation rates (r_{bulk}); c) toluene apparent first order rate constants (k_{app}) for each triplicate set of soil microcosms as derived by data-fitting; d) toluene liquid phase first order biodegradation rates (k_w; $k_w = k_{app}/f_M$) for each triplicate set of soil microcosms. All axes in log scale. For model-fitted values of k_{app} and k_w see Figure 4.4 and Table 4.3.

4.3.5 Relevance to field conditions

The experiments presented in this study were performed to obtain quantitative insights on maximum biodegradation for vapor intrusion scenarios. Although toluene degraders are common at BTEX contaminated sites (Hendrickx et al., 2006), the conditions mimicked in the experiments may not correspond to the field. In fact, the experiments mimic a best case scenario for biodegradation: presence of an adapted aerobic toluene degrader, absence of oxygen or nutrient limitations, and a temperature of 20°C. Especially oxygen limitations are critical in the context of vapor intrusion, as oxygen distribution in the subsurface below a building is generally not well known (McAlary et al., 2011).

However, comparing the obtained half-lives from unsaturated soil microcosms with characteristic times for vapor intrusion can give an indication of the relative importance of biodegradation in relation to vapor intrusion. Neglecting biodegradation, based on the modeling presented in Chapter 3, 159 days are necessary for vapor concentrations to build up from a toluene source at the capillary fringe to an above ground crawl space for a soil with the same properties as the one used in the experiment. The apparent first order constants as derived from these experiments correspond to contaminant half-lives ranging from 0.09 to 0.96 days,

which are between two and three orders of magnitude faster than the transport. Thus biodegradation may significantly reduce contaminant fluxes. Moreover, the experiments show that utilizing rates obtained by liquid mixed batches to predict unsaturated soil biodegradation would substantially underestimate biodegradation rates, as these were affected by limitations not observed in unsaturated soil set-ups.

4.4 Conclusions

In this study, liquid batches did not reflect optimal conditions for biodegradation. Contrary to expectations, liquid batches showed zero order behavior and their liquid phase biodegradation rates were lower than in the other set-ups. Thus, for this case, the use of biodegradation rates from liquid batches would significantly underestimate unsaturated soil biodegradation rates.

Liquid phase first order rate constants derived from apparent first order constants obtained under conditions of partial water-filled porosity and without oxygen or nutrient limitations adequately described unsaturated soil biodegradation in soil microcosms. The liquid phase rate constant and the apparent rate constant are related through the mass distribution factor, being the fraction of the total contaminant mass present in the liquid phase. For the studied culture, first order liquid phase biodegradation rate constants range from 6.25 h^{-1} to 20 h^{-1} in soil microcosms. Conversely, apparent first order rate constants are two orders of magnitude lower.

The obtained half lives from soil microcosms are between two and three orders of magnitude faster than characteristic times derived for vapor intrusion transport neglecting biodegradation. Thus biodegradation can significantly reduce contaminant fluxes. Nevertheless, translation of these rates to field conditions requires additional consideration of limitations from biomass and oxygen availability. The proposed modeling approach can be used to derive liquid phase biodegradation rates from experimental data, and to model biodegradation in vapor intrusion scenarios.

5 Diffusion and microbial activity control aerobic vinyl chloride biodegradation in liquid and unsaturated soil microcosms

Abstract

Vinyl chloride (VC) is a widely spread carcinogenic groundwater contaminant which can accumulate at contaminated sites as a result of incomplete dechlorination of chlorinated solvents. Because of its solubility and volatility, VC is of greater concern for vapor intrusion than other common contaminants. It can be degraded under aerobic conditions both by growth related and cometabolic processes. Even though aerobic VC degradation is widely reported in literature, rates for unsaturated soil conditions are lacking.

This work aimed at obtaining biodegradation rates for the aerobic VC degrader *Mycobacterium aurum* in unsaturated soil under the condition that oxygen is not limiting. The rates were compared with those from aerobic liquid batches inoculated with the same strain. In both experimental set-ups, the dynamics of the bacterial population was monitored by quantifying the abundance of the functional gene etnE, encoding for epoxyalkane coenzyme M transferase (EaCOMT) which is used for aerobic VC metabolism.

Experiments were performed with unsaturated soil between 6% and 71% water-filled porosity (WFP) and a concentration range from 3 to 14 mg L^{-1} dissolved VC. Relatively long lag phases (14 days) were observed at the lowest WFP. Zero and first order biodegradation rates, as well as abundance of etnE gene copies, indicated that microbial growth and VC degradation were faster in unsaturated soil microcosms than in liquid batches. For zero order rates, the difference amounts to one order of magnitude. This can be at least partly related to a faster diffusive mass transfer at the micro-scale in unsaturated soil systems as compared to liquid systems. Possibly, indigenous bacteria also contributed to the VC degradation in the soil system.

This chapter has been submitted for publication as: Picone, S., Hannes, F., Grotenhuis, T., Gerritse J., Rijnaarts H., submitted. Diffusion and microbial activity control aerobic vinyl chloride biodegradation in liquid and unsaturated soil microcosms.

The number of etnE gene copies were found to be linearly related to the amount of VC degraded, with a slope of 4.05×10^5 etnE gene copies (g soil mg VC degraded)$^{-1}$. The use of etnE genes as molecular tools to monitor VC degradation is promising for applications in the field.

5.1 Introduction

Vinyl chloride (VC) is a widely spread carcinogenic groundwater contaminant (IARC, 1979). Most of VC contamination originates from its accumulation at chlorinated solvents contaminated sites after incomplete reductive dechlorination (Lorah and Voytek, 2004). As VC is a gas at normal temperature and pressure, it is of greater concern for vapor intrusion than other common groundwater pollutants such as hydrocarbons or other chlorinated ethenes, as shown by the modeling in Chapter 3 (Table 3.2). However, risk predictions are often not confirmed by indoor air or soil gas measurements (Gargini et al., 2010). A likely cause for this discrepancy is aerobic biodegradation in the unsaturated zone. Under anaerobic conditions, complete dehalogenation of VC can be performed by members of the genus *Dehalococcoides* (He et al., 2003). Anaerobic oxidation of VC to carbon dioxide has been reported under iron-manganese reducing conditions (Bradley and Chapelle, 1996). Under aerobic conditions, both co-metabolic and metabolic degradation processes are likely to occur. Aromatic hydrocarbons, propane, ethane, ethene and methane can serve as substrate for co-metabolic VC degradation (Freedman and Herz, 1996; Graham et al., 1992; Malachowsky et al., 1994; Schaefer and Bouwer, 2000). Strains of the genus *Mycobacterium* (Hartmans et al., 1985), *Pseudomonas* (Verce et al., 2000), *Nocardia* (Coleman, 2002), and indigenous soil bacteria (Davis and Carpenter, 1990) are able to grow on VC under aerobic conditions. Recent research has shown that aerobic VC degraders can be active at oxygen dissolved concentrations lower than 0.02 mg L^{-1} (Bradley and Chapelle, 2011; Gossett, 2010), which may be present in what is nominally considered an anaerobic environment.

Although literature indicates that VC aerobic biodegradation is a widespread process (Abe et al., 2009; Davis and Carpenter, 1990; Kao and Prosser, 1999; Witt et al., 2002), studies addressing this process in unsaturated soils and providing biodegradation rates are lacking. Unsaturated soils include a solid phase, a liquid phase and a gas phase. Air-filled and water-filled porosity vary with water content as a function of depth and specific soil properties (Koorevaar et al., 1983). The influence of water content on microbial activity has been extensively studied for soil respiration (Bastida et al., 2006; Linn and Doran, 1984; Skopp et al., 1990; Stark and Firestone, 1995). Research has shown that water content variation affects mass transfer of soluble substrates or nutrients and oxygen in soil macro pores (Holden et al., 1997). Two endpoints can be distinguished. At low water content, dissolved substrate availability may become limiting due to the reduction of liquid diffusion pathways (Or et al., 2007). Moreover, limitations from reduced water content can affect bacterial physiology. Specifically, at lower water content, decreased enzyme catalytic rates (Andersson and Hahn-Hagerdal, 1987) and reduced growth rates

(Potts, 1994) were observed. At high water content, the enhanced dissolved nutrients and substrate availability would be progressively overruled by reduced oxygen availability (Skopp et al., 1990). Thus, an optimum for aerobic microbial activity determined by the above mentioned endpoints is found between 50 and 60% of the water-filled porosity (Linn and Doran, 1984).

The effects of reduced water potential on unsaturated toluene biofilms showed significant limitations by diffusion through cell membranes, as well as hindering of biodegradation at the driest conditions (Holden et al., 1997; 2001). Furthermore, an important effect of moisture on substrate availability was observed by Schoefs et al. (2004) with hexadecane. In the case of VC at drier soil conditions, higher gas filled porosity increases the effective diffusion and potentially leads to enhanced VC bioavailability at soil/air interfaces. As bacteria tend to preferably adhere to soil particles (Gray et al., 1968; Stotzky, 1972) this could support even higher removal rates for highly volatile organics such as VC compared to water saturated conditions.

From a more applied point of view, the lack of specific monitoring tools complicates the assessment of aerobic biodegradation at field conditions. Aerobic metabolic growth on VC is related to a specific enzyme, epoxyalkane coenzyme M transferase (EaCOMT), located on mobile plasmids (Coleman, 2002; Danko et al., 2004), and encoded by the gene etnE (Jin and Mattes, 2010). Use of quantitative molecular techniques (qPCR), determining the abundance of the functional genes encoding for EaCOMT enzymes in groundwater samples appears a promising approach for the assessment of VC biodegradation capacity at field conditions (Begley et al., 2009; Jin and Mattes, 2010). However, a quantitative relationship between the abundance of specific genes and VC biodegradation capacity is necessary for practical applications of such molecular tools.

This study investigates the response of the aerobic VC degrader *M. aurum* to variable soil water content in unsaturated soil microcosms under the absence of oxygen limitations. The obtained biodegradation rates are compared with those from liquid batches inoculated with the same strain. Furthermore, the use of etnE gene copies was tested as monitoring tool for the dynamics of the bacterial population during the course of VC degradation.

5.2 Material and Methods

5.2.1 Inoculum and medium

Mycobacterium aurum DSM 6695 was obtained from DSMZ. Cells were grown on TSB (Trypton Soy Broth) plates from concentrated biomass stored at -80°C. The cultures were then transferred to 5 mL sterile tubes with TSB medium and 10% dextrose and incubated at 30°C. After obtaining visible growth (three days on average), the whole content of a tube was transferred to a sterile 250 mL serum bottle containing 50 mL of Brunner medium (recipe 457, DSMZ Germany) adjusted to pH 6.9 and air with VC as the only carbon and energy source. VC was added as pure gas from a gas cylinder (Praxair, US) with a glass syringe (Hamilton, US). This culture

was used as inoculum for subsequent experiments. Brunner medium was used as liquid phase in all experiments.

5.2.2 Liquid batches

Liquid batches aimed at measuring biodegradation rates under optimal macro-scale mass transfer conditions. Inoculated batches and non inoculated controls were prepared in sterile 250 mL serum bottles with 50 mL Brunner medium (Table 5.1). Batches were first spiked with VC then inoculated. Gaseous VC was added up to dissolved initial VC concentrations of 1, 3 and 7 mg L^{-1}, respectively. Triplicate inoculated batches and one non inoculated control were prepared for each concentration. Optical density at 600 nm (OD_{600}) was used as indicator for biomass concentration. Initial OD_{600} in the live batches was set to 0.01 OD_{600} units. The not inoculated control received 4 mg NaN_3. Bottles were sealed with autoclaved Viton rubber stoppers and aluminum crimp caps. Batches were incubated at 20°C, horizontally shaking at 100 rpm. VC was repetitively added after microbial consumption had depleted the VC amount in batches leading to a total degraded VC mass of approximately 1, 2 and 4 mg, at constant dissolved concentrations of 1, 3 and 7 mg L^{-1} VC, respectively. VC concentrations in the headspace were measured at regular time intervals for ten days. After each VC spike was consumed, OD_{600} was measured as growth indicator.

A second experiment was conducted to monitor the variation of etnE gene copies with VC consumption. A series of 13 identical 125 mL serum bottles was prepared with 25 mL Brunner medium and inoculated up to an initial OD_{600} of 0.01. All bottles were spiked with VC to an initial dissolved concentration of 3 mg L^{-1}, which was doubled once the first spike was consumed. VC concentrations were monitored in the headspace four times a day. Simultaneous to each VC measurement, one batch was sacrificed over 0.2 μm membrane filters (Microfil, Millipore Inc., US) for DNA extraction.

5.2.3 Unsaturated soil microcosms

Unsaturated soil microcosms were designed to mimic an unsaturated soil layer through which gaseous VC is diffusing. The large headspace in the microcosm ensures sufficient oxygen availability and functions as a monitoring volume.

The microcosms were prepared in aerobic conditions with 30 g soil in 250 mL serum bottles. The bulk soil volume corresponded to 19.9 mL. An uncontaminated sandy soil (93.3% sand, 2.8% silt, 3.9% clay, 3% organic matter – 43% porosity) sieved over a 2 mm mesh was used for the experiments. Soil was amended with a specific volume of Brunner medium up to the desired water content (Table 5.1). Microcosms were covered with aluminum foil and incubated statically in a 20°C room. Water content was expressed as water-filled porosity (WFP), corresponding to the percentage of the pore space filled with water, as this parameter is independent from soil mass (Ilstedt et al., 2000). 100% WFP identifies water saturated conditions. Conditions studied in two independent sets of experiments ranged from 6% to 71%

WFP (Table 5.1). This interval spans from dry soils (6% WFP) to optimum moisture contents for aerobic microbial activity (62% and 71%WFP). Each condition was tested in triplicate.

The microcosms at 18%, 43% and 62% WFP were inoculated with material from an active soil microcosm inoculated with *M. aurum*. The added material corresponded to 10% mass of the soil wet weight. The microcosms were prepared in two sets of triplicates, of which one was used to measure VC and etnE, and the other to monitor oxygen depletion. Microcosms were spiked at initial dissolved VC concentration of 14 mg L^{-1} with gaseous VC. Two sets of controls were prepared: one per condition without VC in order to measure oxygen consumption in absence of VC, and a non-inoculated and bio-inactivated control per condition with 0.2 mg $HgCl_2$.

The microcosms at 6%, 20% and 71% WFP were inoculated with the same liquid culture used for the liquid batches described above. The initial OD_{600} was also identical to liquid batches, and corresponded to 0.01 OD_{600} units. Initial dissolved VC concentration was 7 mg L^{-1}. An additional series of triplicates at 20% WFP was tested at 3 mg L^{-1}. In this experiment, controls were prepared with non inoculated autoclaved soil and 4 mg NaN_3, as partial VC depletion was observed in non-inoculated controls in presence of $HgCl_2$.

In the microcosms, VC concentration in the headspace was measured at regular time intervals for at least ten days. Observations were more frequent for the second experiment. After the first spike was consumed, microcosms were respiked. Once VC had again decreased to non-detect, one microcosm per condition was sub sampled in five identical 0.5 g samples for DNA extractions.

Table 5.1 – Experimental set-up.

System	%WFP	Liquid volume	Air-filled pore volume	Total batch gas volume	Initial inoculated biomass concentration	f_M
		mL	mL	mL	mg biomass L^{-1}	%
Liquid batch	-	50	-	150	12.98	20.8
	-	25	-	100	12.98	20.3
Unsaturated Soil Microcosm	18	1.59	7.07	236.93	-	0.65
	43	3.71	4.89	231.94	-	1.51
	62	5.29	3.30	233.31	-	2.16
	6	0.53	8.07	238.07	12.98	0.23
	20	1.75	6.82	236.89	12.98	0.76
	71	6.14	2.56	232.36	12.98	2.56

5.2.4 Analytical methods

Vinyl chloride was measured in the headspace by injecting a gas sample (500 μl) with a gas tight syringe (Hamilton, US) into a Varian 3800 gas chromatograph equipped with a flame ionization detector and a Porabond – Q column (0.32 mm x 25m from Varian, Middelburg, NL). External standards at five different VC concentrations in the range 0 -15 mg L^{-1} in the gas phase were used for calibration. The injector temperature was set at 200 °C and detector at 300 °C. Initial column temperature was 3 min at 50 °C, increasing to 170 °C in 3 min, to a final temperature of 220 °C at 9.25 min. Column flow was 2 mL min^{-1}.

Oxygen concentration in the microcosms was measured with two Oxydots (Oxysense Inc., US), one on the bottom and one in the headspace of the serum bottle in which the soil was incubated. As the two dots gave identical results during the first week of measurements, further only the headspace sensor was used. The oxygen concentration was read from the dots with a LED sensor at discrete time intervals based on the fluorescent decay method (ASTM, 2009). The lower detection limit was 0.03% v/v O_2.

Biomass concentrations were measured as optical density at 600 nm. Sterile Brunner medium was used as a blank for OD_{600} measurements. Optical density was related to biomass concentration by means of protein measurements using the Lowry assay (Lowry et al., 1951) in samples from the liquid cultures (one OD_{600} unit corresponded to a protein concentration of 7.14 mg L^{-1}). Assuming that biomass consists of 55% proteins (Maier et al., 2000) this corresponds to about 13 mg L^{-1} biomass.

5.2.5 Molecular techniques

DNA extraction was performed on 0.5 mL of liquid samples or 0.5 g wet weight soil using the Fast DNA Spin Kit for soil (MP Biomedicals, Eindhoven, NL), following the manufacturer's protocol.

Quantitative PCR analysis (q-PCR) was performed using an IQ 5 Real-Time PCR system (Bio-Rad). Each well contained 22 μL IQ-Supermix (Bio-Rad, Veenendaal, NL) and 3 μL of sample. Specific primers for 16S rRNA genes were described in Ritalahti et al. (2006). Settings for qPCR assays for 16S rRNA genes were as follows: 3 minutes at 94°C followed by 35 cycles consisting of of 30 seconds at 94°C, 30 seconds at 58°C, 1 min at 72°C, and a final elongation step of 5 minutes at 72°C. Samples were analyzed undiluted and 10 times diluted. For 16S rRNA genes, the calibration curve ranged from 7.29 to 7.29×10^7 gene copies μL^{-1}. UV-treated 0.2 μm filtered MilliQ water was used as a negative control.

A method was developed to amplify and clone etnE gene, which encodes for the subunit of EaCOMT. For detection of etnE genes, forward (F402: GAAGAAGCCAGTCAAGGTGT) and reverse(R538: GCTCGATCTCTTTGAAGTCC) primers were designed, based on alignments of 12 bacterial EaCoMT sequences, using the default parameters of Primer3 software (http://frodo.wi.mit.edu/). The specificity of the primers was checked using the CHECK_PROBE software of the Ribosomal Database Project (http://rdp.cme.msu.edu/) and the Basic Local Alignment Search Tool (BLAST) network service of GenBank (www.ncbi.nlm.nih.gov/BLAST/). qPCR was performed in 25-μL volumes with MilliQ water (6.5 μL), IQMIX SybrGreen (12.5 μL) (Bio-rad, Veenendaal, NL), forward primer (1.5 μL; 10 pmol μL^{-1}), reverse primer (1.5 μL; 10 pmol μL^{-1}) and template DNA (3 μl) using MicroAmp Optical 96-well reaction plates and MicroAmp Optical Caps (Applied Biosystems). A 137-bp product of the etnE gene was amplified using the following qPCR settings: 3 minutes at 95°C followed by 35 cycles of 30 seconds at 95°C, 30 seconds at 55°C, 30 seconds at 72°C, and a final step of 3 minutes at 72°C. Calibration curves for etnE genes were prepared from *M. aurum* etnE gene PCR products, ligated

in the vector pCR 2.1-TOPO (Invitrogen, Carlsbad, US), and transformed into competent *E.coli* TOP10 cells (Invitrogen, Carlsbad, US) according to manufacturer's protocol. Competent cells with the vector were incubated overnight with the presence of ampicillin and X-gal. After plasmid isolation the concentration of the plasmids was measured using a nanodrop. A control PCR was performed and the product of this PCR was checked by sequencing and gel electrophoresis. The amount of etnE gene copies was calculated using the concentration of plasmid. This resulted in standard calibration curves ranging from 1.67 to $1.67x10^7$ gene copies μL^{-1}. MilliQ water was used as a negative control. Specificity of the assay was checked using DNA extracted from pure cultures of *M. aurum*, *Pseudomonas putida*, *Acidithiobacillus ferrooxidans*, *Nitrobacter hamburgenses*, *E. coli* and *Rhodococcus ruber*, respectively. Number of gene copies in liquid and soil samples was calculated from the C_t values of the calibration curve, and extrapolated to the number of gene copies per mL or mg sample.

5.2.6 Calculations

Conceptual model

The conceptual model is identical to that presented in Chapter 4 for toluene. Gaseous VC supplied to the batches and microcosms partitions between vapor, liquid, and solid phase. Once dissolved, VC is available to bacteria, which degrade dissolved VC using oxygen as electron acceptor. The concentration gradients drive mass transfer of VC and oxygen from the gas to the liquid phase. Thus, measured VC depletion in the headspace in the experimental set-ups is a combination of biodegradation and mass transfer processes for VC and for oxygen. Such a depletion rate might differ from the actual biodegradation rate occurring in the liquid phase.

Assuming overall equilibrium, measured gas concentrations were used to estimate the total VC mass in each system using a mass balance approach. Vinyl chloride liquid concentrations were calculated from measured gas concentrations using Henry's Law constant (C_{liq}/C_{gas}). A dimensionless Henry's law constant at 20°C of 0.98 (C_{liq}/C_{gas}) was used (USEPA, 2004). The total VC mass was calculated from measured gas concentrations as follows

$$M = C_{gas}\left(V_{gas} + \frac{V_{liq}}{H} + \frac{K_d}{H}\rho_b V_{soil}\right) \quad (1)$$

where M is the total VC mass (mg), C_{gas} is the measured gas concentration (mg L^{-1}), H is the dimensionless Henry's Law constant, V_{liq} is the liquid phase volume (L), V_{gas} is the gas phase volume (L), K_d is the partitioning coefficient ($cm^3\ g^{-1}$), ρ_b is the soil bulk density ($g\ cm^{-3}$), V_{soil} is the solid phase volume (L). K_d was calculated for the soil used in the experiments from a K_{oc} of 18.6 $cm^3\ g^{-1}$ (USEPA, 2004).

Based on the mass balance, a mass distribution factor, f_M , was calculated for liquid batches and soil microcosms as the ratio between VC mass in the liquid phase and the total VC mass added to the microcosm.

$$f_M = \frac{M_{liq}}{M_{tot}} \quad (2).$$

This value is given in Table 5.1 as percentage.

Zero order biodegradation rates

Lag phases were defined as the time before 20% of the initial VC mass had been degraded. After the lag phase, VC mass removal rates (r_m) in mg h^{-1} were calculated for the steepest part of the curve VC mass versus time. Such rates were normalized for the bulk volume of each set-up to derive bulk volume biodegradation rates, r_{bulk} in mg $(Lh)^{-1}$. The bulk volume corresponds to the total serum bottle volume minus the headspace.

Assuming that biodegradation only occurs in the liquid phase (Bouwer and Zehnder, 1993), zero order biodegradation rates in the liquid phase, r_w in mg L^{-1}, were calculated by normalizing mass removal rates for the liquid phase volume of each condition. For liquid batches, specific substrate utilization rates, r_w^{spec} in mg VC (mg biomass $h)^{-1}$, were calculated by normalizing liquid phase biodegradation rates for the biomass concentration measured after VC consumption.

Apparent first order rate constants

First order apparent rate constants (k_{app} in h^{-1}) were obtained by fitting measured VC gas concentration after the lag phase to an exponential function for liquid batches and for soil microcosms.

Numerical modeling

For soil microcosms at 6%, 20% and 71% WFP, and initial C_{liq} of 7 mg L^{-1}, the apparent rate constants derived from data fitting were compared with apparent first order constants as obtained from the numerical model presented in Chapter 3. The model includes diffusion and biodegradation as kinetic processes, and only assumes local instantaneous equilibrium. Diffusion coefficients for VC were taken from the literature (USEPA, 2004), and partition coefficients were as mentioned above for mass balance calculations.

The numerical model was used to simulate different controls on the overall biodegradation rates measured: i) mass transfer controlled, ii) microbial activity controlled, iii) no biodegradation. The first scenario (mass-transfer controlled) simulated conditions in which biodegradation was instantaneous and therefore the measured VC removal rate was limited by the substrate supply through diffusion. The second scenario (microbial activity controlled) considered the case in which the overall VC removal was regulated by bacterial activity, described by a liquid phase first order biodegradation rate k_w. The third scenario neglected biodegradation.

5.3 Results

5.3.1 Liquid batches

In liquid batches, at equilibrium, 20% of the total VC mass was available in the liquid phase (f_M = 20%) and the remaining was present in the gas phase. Biodegradation of VC in liquid batches was observed after a lag phase of about 19 hours. In the range of VC concentration studied, the observed data could be described by zero order as well as first order kinetics. The R^2 values for the zero order fit, ranging between 0.91 and 0.99, were only slightly higher than the first order R^2, varying between 0.89 and 0.98. The culture of *M. aurum* degraded VC at a maximum mass removal rate of 5.46×10^{-2} mg h^{-1}, corresponding to a liquid biodegradation rate of 1.09 mg $(Lh)^{-1}$ observed for the second spike at dissolved VC concentration of 5.57 and 6.32 mg L^{-1} (Table 5.2).

Table 5.2 – Results for liquid mixed batches. Column headings: C_{liq} initial VC liquid concentration, r_m zero order mass removal rate, r_w zero order liquid phase biodegradation rate, r_{bulk} zero order bulk volume biodegradation rate, X_0 initial biomass concentration, X_{final} final biomass concentration, r_w^{spec} specific biodegradation rate.

Batch	Spike n.	C_{liq} mg L^{-1}	r_m mg h^{-1}	$r_w = r_{bulk}$ mg $(L\ h)^{-1}$	X_{final} mg L^{-1}	r_w^{spec} mg_{VC} $(mg_{biomass}\ h)^{-1}$	k_{app} h^{-1}
L1	4	0.89	0.0103	0.205	32.47	0.011	0.0956
L2	4	0.91	0.0102	0.204	29.87	0.012	0.0885
L3	1	3.55	0.0089	0.179	-	-	0.0145
	3	3.20	0.0187	0.374	40.26	0.014	0.0353
L4	1	3.37	0.0081	0.162	-	-	0.0134
	3	3.10	0.0198	0.395	37.66	0.016	0.0403
L5	1	2.99	0.0063	0.125	-	-	0.0110
	3	2.96	0.0196	0.392	37.66	0.016	0.0425
L6	1	9.32	0.0194	0.388	-	-	0.0131
	2	6.47	0.0462	0.924	68.83	0.017	0.0629
L7	1	9.11	0.0175	0.350	-	-	0.0112
	2	5.57	0.0546	1.092	63.64	0.022	0.0857
L8	1	6.74	0.0096	0.191	-	-	0.0068
	2	6.31	0.0546	1.092	66.23	0.020	0.0602
L9- L22	1	2.71	0.0057	0.226	-	-	0.0260
L9-L22	2	5.90	0.0116	0.463	-	-	0.0505

For liquid batches, the liquid phase biodegradation rate equals to the bulk volume biodegradation rate. The increase in optical density, used as indicator for biomass concentration (Table 5.2), showed that VC degradation was linked to growth. Using the estimated conversion between optical density and protein content as an indicator for biomass concentration, a yield coefficient of 0.65 ± 0.09 $mg_{biomass}/mg_{VC}$ was calculated, which compares well with reported values for growth on ethene, 0.72 $mg_{biomass}/mg_{ethene}$ (Hartmans and De Bont, 1992). The range of specific substrate utilization rates 0.016 ± 0.0038 mg_{VC} $(mg_{biomass}\ h)^{-1}$ is in line with values reported for other *Mycobacterium* strains (Coleman, 2002). Obtained apparent first

order rate constants (k_{app}) ranged between 0.0068 h^{-1} and 0.0145 h^{-1} in the first spike. Highest rates were obtained in subsequent spikes, up to a maximum value of 0.096 h^{-1} in the fourth spike. The highest value exceeds reported first order rates for VC with enrichment from a contaminated site in the work of Tiehm et al. (2008).

In the 13 identical batches (L9-L22 in Table 5.2), VC biodegradation lead to increasing 16S rRNA gene copies and etnE gene copies, indicating bacterial growth (Figure 5.1 a, b). The initial number of etnE gene copies per mL liquid was from two to three orders of magnitude larger than reported values for groundwater samples from contaminated sites (Jin and Mattes, 2010). Furthermore, etnE gene copies per mL were about two orders of magnitude lower than 16S rRNA gene copies. After consumption of 0.97 mg VC, the number of 16S rRNA and etnE gene copies per mL increased by a factor five.

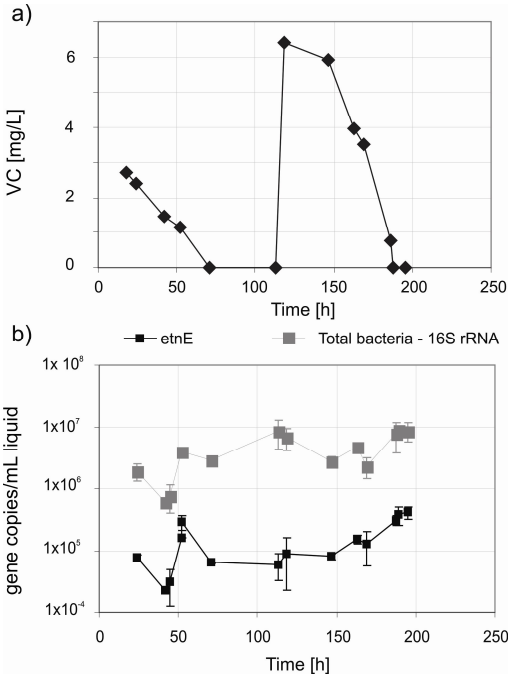

Figure 5.1 a,b – a) VC dissolved concentrations in time in 13 identical batches; b) 16s rRNA and etnE gene copies on log scale per mL liquid in 13 identical batches. Molecular data show average and standard deviation of duplicates at 10 and 100 dilutions.

5.3.2 Unsaturated soil microcosms

The fraction of VC present in the liquid phase (f_M) in the microcosms varied between 0.2% and 2.6% at 6% and 71% WFP respectively, thus approximately between a ratio of 1% and 10% of the f_M of the liquid batches. Biodegradation of VC in unsaturated soil microcosms at water-filled porosity above 18% started after a lag

period of about 100 hours, independent from the type of inoculation. Only at 6% WFP the lag phase duration increased to 350 hours (Figure 5.2).

Complete VC biodegradation occurred up to dissolved concentrations of 14 mg L^{-1} (Table 5.3). Also for the microcosms, measured data could be described by a zero order (R^2 0.86 – 0.98) as well as by a first order model (R^2 0.72 – 0.99).

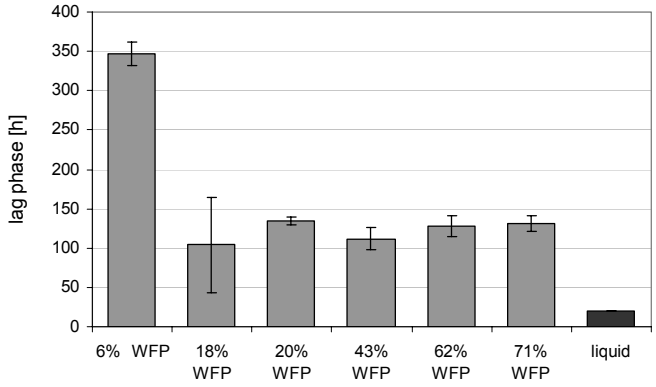

Figure 5.2 – Lag phase duration for unsaturated soil microcosms and liquid batches. Each bar represents the average and standard deviation of triplicates. The liquid triplicates gave identical results.

In the first set of experiments, at 18, 43 and 62% WFP which were inoculated with adapted soil biomass, complete VC degradation was observed also in the non inoculated controls. After repeated $HgCl_2$ addition, a second VC spike was not degraded in the non inoculated microcosms (Figure 5.3 a).

Zero order bulk volume biodegradation rates varied between 0.42 ± 0.092 mg $(Lh)^{-1}$ at 18% WFP and 0.74 ± 0.024 mg $(Lh)^{-1}$ at 43% WFP (Table 5.3). Liquid phase biodegradation rates corresponded to 12.01 ± 16.34 mg $(Lh)^{-1}$ at 18% WFP, 9.06 ± 0.30 at 43% WFP, and 5.54 ± 2.19 mg $(Lh)^{-1}$ at 62%WFP respectively.

The calculated first order apparent rate ranged between 0.014 ± 0.009 at 18% and 43% WFP, and 0.020 ± 0.012 h^{-1} at 62% WFP (Table 5.3). In the microcosms, oxygen concentrations in the headspace dropped from atmospheric values (21% v/v) to 14%, 11% and 10% v/v at 18%, 43% and 62% WFP respectively (Figure 5.3 b). As expected, a lower oxygen decrease in the headspace was observed at higher air-filled porosity. The measured oxygen decrease corresponds to a stoichiometric ratio of 2.5 mol O_2/mol VC consumed, however, an equivalent decrease of oxygen concentration was measured in microcosms without VC addition (not shown), indicating that VC degradation probably competed with organic matter degradation.

Table 5.3 – Results from two sets of experiments with unsaturated soil microcosms, average values and standard deviations for each triplicate set are given. Column headings: C_{liq} initial VC liquid concentration, r_m zero order mass removal rate, r_w zero order liquid phase biodegradation rate, r_{bulk} zero order bulk volume biodegradation rate, k_{app} apparent first order biodegradation rate, k_w first order liquid phase biodegradation rate, $k_{w\ model}$ best-fit first order liquid phase biodegradation rate from numerical model.

WFP	Spike n.	C_{liq}	r_m	r_w	r_{bulk}	k_{app}	k_w	$k_{w\ model}$
		mg L^{-1}	mg h^{-1}	mg $(L\ h)^{-1}$	mg $(L\ h)^{-1}$	h^{-1}	h^{-1}	h^{-1}
18%	1	10.75 ± 3.02	0.019± 0.0042	12.01 ± 16.34	0.42 ± 0.092	0.014 ± 0.007	2.19	-
43%	1	11.06 ± 0.56	0.034 ± 0.0011	9.06 ± 0.30	0.74 ± 0.024	0.014 ± 0.009	0.91	-
62%	1	11.12 ± 2.32	0.029 ± 0.0116	5.54 ± 2.19	0.64 ± 0.254	0.020 ± 0.012	0.93	-
	2	10.62 ± 0.25	0.028 ± 0.0020	5.26 ± 0.31	0.61 ± 0.036	-	-	-
6%	1	6.90 ± 1.06	0.014± 0.0066	27.01 ± 12.46	0.31 ± 0.145	0.014 ± 0.007	5.92	5.00
	2	6.42 ± 1.10	0.015 ± 0.0050	28.14 ± 9.07	0.33 ± 0.105	0.012 ± 0.001	5.25	-
20%	1	2.44 ± 0.094	0.010 ± 0.0002	5.86 ± 0.09	0.23 ± 0.004	0.028 ± 0.002	3.75	-
	3	3.44 ± 0.14	0.047 ± 0.0008	26.80 ± 0.47	1.03 ± 0.02	0.092 ± 0.021	12.18	-
20%	1	6.64 ± 1.01	0.018 ± 0.0014	10.11 ± 0.81	0.39 ± 0.031	0.011 ± 0.001	1.44	1.04
	2	8.53 ± 0.24	0.057 ± 0.0020	32.58 ± 1.10	1.25 ± 0.042	0.053 ± 0.001	7.07	-
71%	1	5.75 ± 0.26	0.028 ± 0.0019	3.65 ± 0.30	0.49 ± 0.041	0.050 ± 0.005	1.95	2.08
	2	7.51 ± 1.10	0.054 ± 0.0040	8.72 ± 0.63	1.16 ± 0.083	0.055 ± 0.007	2.15	-

In the second set of experiments, microcosms inoculated with a liquid inoculum were tested at 6%, 20% and 71% WFP. In these experiments, VC concentrations decreased to non-detect levels in 200 hours at 20% and 71% WFP, and 500 hours at 6% WFP respectively (Figure 5.3 c). For the microcosms with initial VC concentration from 6 to 8 mg L^{-1}, calculated zero order bulk volume biodegradation rates ranged between 0.31 ± 0.14 mg $(Lh)^{-1}$ and 0.49 ± 0.04 mg $(Lh)^{-1}$ for the first spike. Conversely, zero order liquid phase biodegradation rates decreased with increasing moisture content from 27.01 ± 12.46 mg $(Lh)^{-1}$ at 6% WFP to 3.65 ± 0.30 mg $(Lh)^{-1}$ at 71% WFP respectively. Liquid phase and bulk volume biodegradation rates increased with dissolved VC concentration, for a constant water-filled porosity of 20%WFP (Table 5.3). Zero order biodegradation rates significantly increased with increasing mass of VC consumed, for all conditions except for the driest soil microcosms (Table 5.3). First order apparent rate constants obtained from data fitting (k_{app}) varied between 0.011 ± 0.001 h^{-1} at 20% WFP and 0.050 ± 0.005 h^{-1} at 71%WFP for the first spike (Table 5.3).

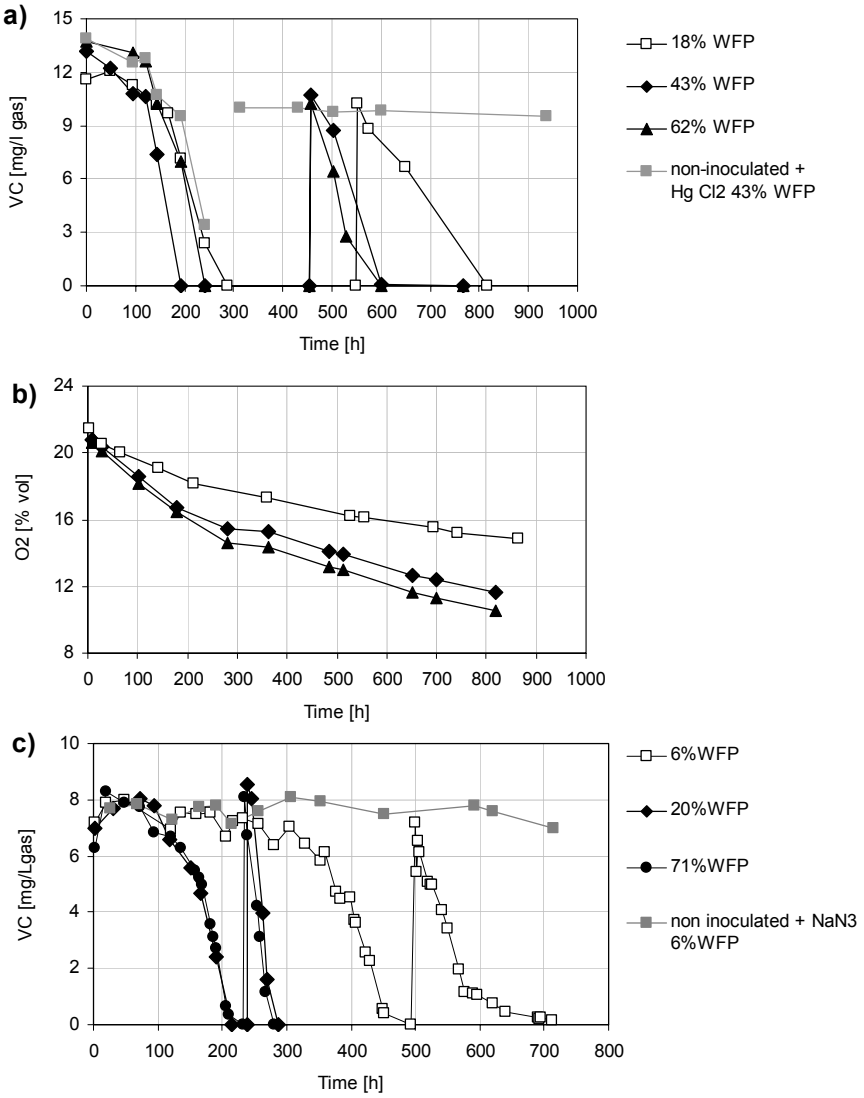

Figure 5.3 a, b, c - a) Measured VC gas concentration in time for unsaturated soil microcosms at 18, 43 and 62% WFP and initial concentration 14 mg L^{-1}; b) measured O2 concentration in % volume in unsaturated soil microcosms at 18, 43, 62% WFP; c) measured VC concentration in time in unsaturated soil microcosms at 6, 20 and 71%WFP, and initial concentration 7 mg L^{-1}.

The observed VC gas concentrations were adequately described by the numerical modeling scenario of biological activity controlled degradation, as shown by the results for the microcosms at 6%, 20% and 71% (Figure 5.4). The directly obtained k_{app} matched reasonably well with those obtained from the model (Figure 5.4). The liquid phase first order biodegradation rates that fitted the experimental data varied between 1.04 h^{-1} at 20% WFP and 5.00 h^{-1} at 6% WFP respectively.

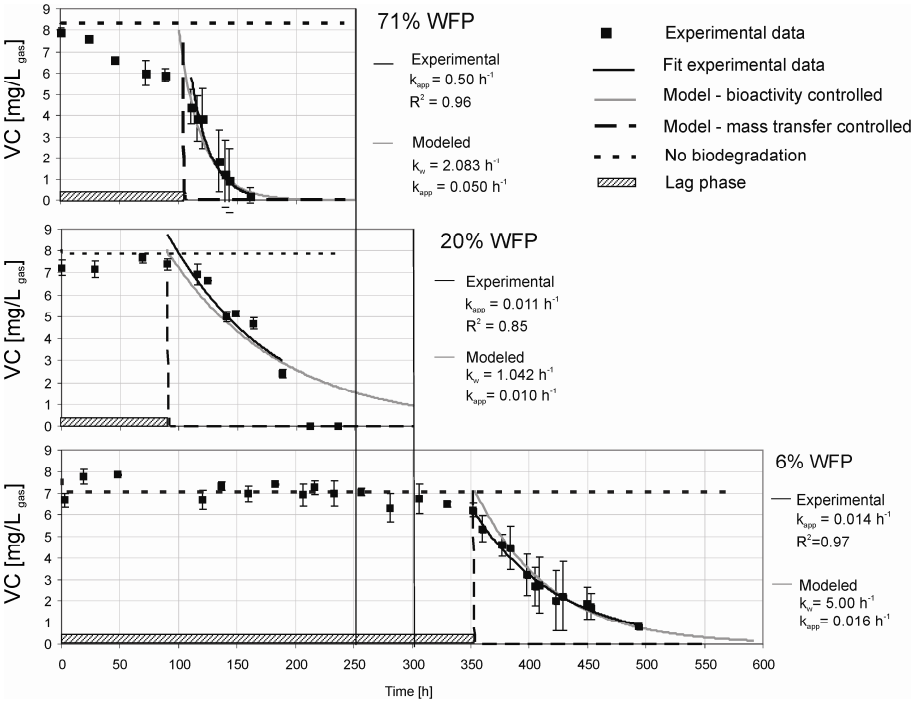

Figure 5.4 – VC measured gas concentrations (average and standard deviation of triplicates) as function of time versus numerical model predictions for soil microcosms at 6% , 20% and 71%WFP and 7 mg L^{-1} initial VC concentration, respectively.

In the soil microcosms, the number of etnE gene copies per unit soil mass was four orders of magnitude lower than 16S rRNA gene copies. 16S rRNA gene numbers do not differ significantly between VC exposed and not-exposed soil and did not show variations with increasing amount of VC degraded (Figure 5.5 a). On the contrary, etnE gene copies per g soil increased with the amount of VC consumed, and were at least two orders of magnitude more abundant in soil exposed to VC than in pristine soil (Figure 5.5 b). A factor of 4.05×10^5 etnE gene copies (g soil mg VC degraded)$^{-1}$ related the number of gene copies to the consumed amount of substrate, with an R^2 of 0.82. The intercept on the y- axes was not zero as at no VC exposure, a low concentration of etnE genes was already present in soil samples. When comparing liquid batches and soil microcosms at similar amounts of VC degraded, 16S rRNA gene copies as well as etnE gene copies were between one and two orders of magnitude more abundant in soil samples than in liquid samples (Figure 5.5 c and d).

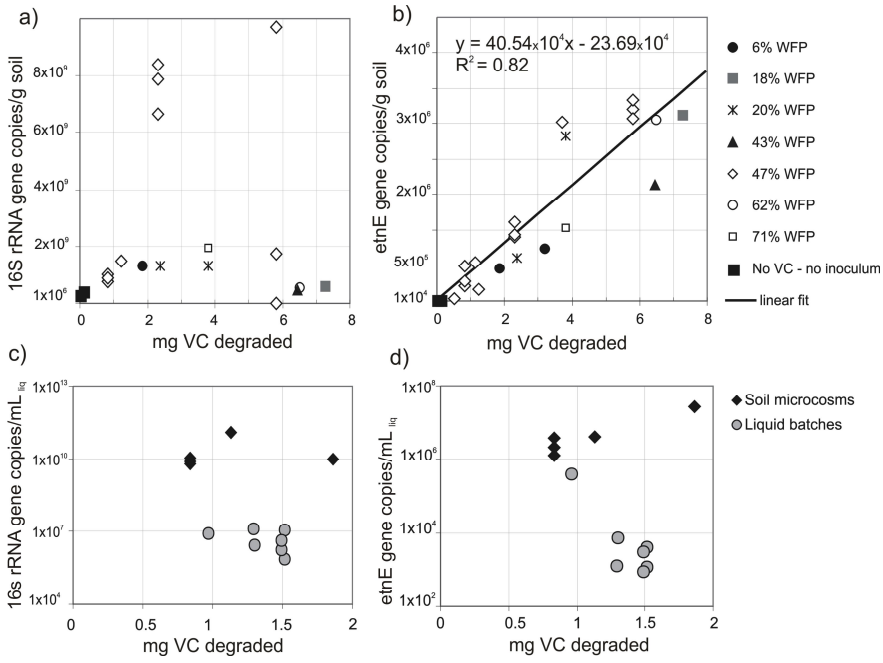

Figure 5.5 a, b, c, d – Four parameters as function of mass VC degraded (mg). a) 16s rRNA gene copies per gram soi; b) etnE gene copies per gram soil; c) 16S rRNA gene copies per mL liquid in soil microcosms and in liquid batches; d) etnE gene copies per mL liquid in soil microcosms and liquid batches.

5.3.3 Comparison of biodegradation rates

Zero order bulk volume biodegradation rates increased at higher amounts of VC degraded (Table 5.3) but did not correlate to f_M (Figure 5.6 a). This suggests that the VC degrading capacity of the biomass in the two systems is comparable. When zero order liquid phase rates are considered, a decreasing trend of liquid phase biodegradation rates with increasing f_M is observed, and the liquid batches reveal the lowest rates (Figure 5.6 b). In contrast, apparent first order rate constants (k_{app}) are two to three times higher in liquid batches than in soil microcosms (Figure 5.6 c).

As apparent rate constants result from the combination of mass transfer and biodegradation, higher values of k_{app} may be caused by either higher mass transfer, higher biomass activity, or both. Modeled values of k_w fitting the experimental data were higher at the lowest WFP tested (6% WFP), and k_w and k_{app} roughly follow the relationship (Table 5.4) :

$$k_{app}/k_w \approx f_M \qquad 3).$$

Table 5.4 - Comparison between k_w/k_{app} predicted by numerical modeling bioactivity controlled scenarios and calculated f_M values.

WFP	Model k_w/k_{app}	f_M
	-	-
6%	0.0032	0.0023
20%	0.0099	0.0076
71%	0.0240	0.0256

Assuming this is generally valid, k_w can be approximated for the non-modeled soil moisture conditions, by dividing the fitted k_{app} by f_M. This shows a decrease of liquid phase biodegradation rate constants with increasing f_M, which is consistent with the trend in r_w values decreasing with f_M as found for the zero order rates (Figure 5.6 b).

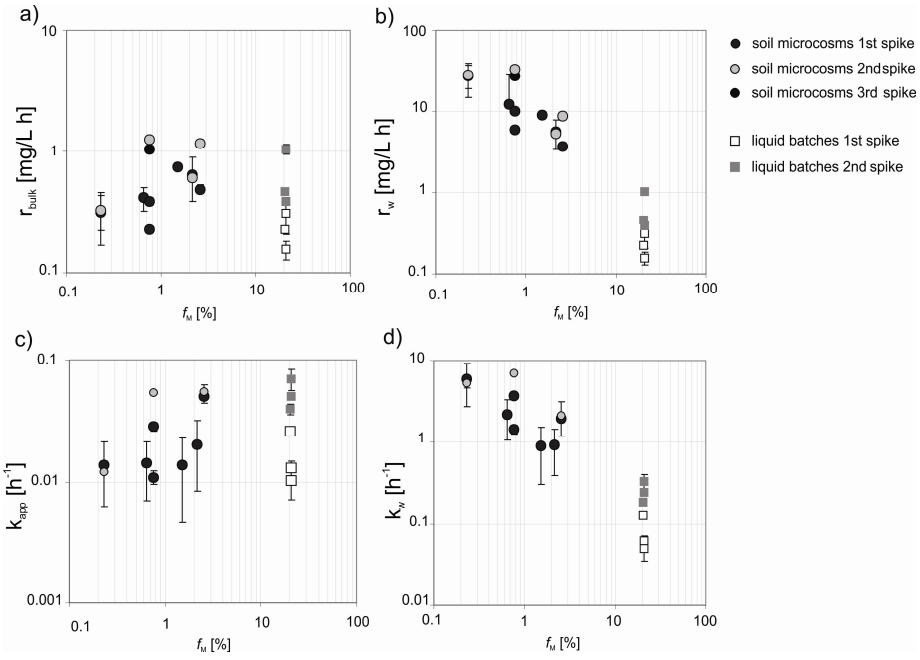

Figure 5.6 a,b,c, d – Four parameters describing biodegradation rates in liquid batches and in soil microcosms as a function of f_M. a) liquid phase biodegradation rates (r_w); b) bulk volume biodegradation rates (r_{bulk}); c) first order apparent biodegradation rates (k_{app}); d) first order liquid phase biodegradtion rates (k_w) as estimated from k_{app}.

5.4 Discussion

The experimental results reflected the performance of an identical bacterial culture of *Mycobacterium aurum* in two different systems: liquid/headspace mixed batches and static unsaturated soil/headspace microcosms. Two features distinguish them: the physical status of the biomass and the mass transfer processes by which VC is supplied to the biomass. In liquid batches, bacterial cells are suspended (Figure 5.7 a). In unsaturated soil microcosms, as in field conditions, microorganisms are located within soil pores present between soil particles surrounded by water films of variable thickness (Or et al., 2007), as shown in Figure 5.7 b. With respect to mass transfer, it is well known that mass transfer limitations may influence biodegradation to a greater extent than variations in the intrinsic biodegradation capacity (Bosma et al., 1997). Such mass transfer processes may influence the VC uptake from the biomass both at the macro-scale as well as at the micro-scale.

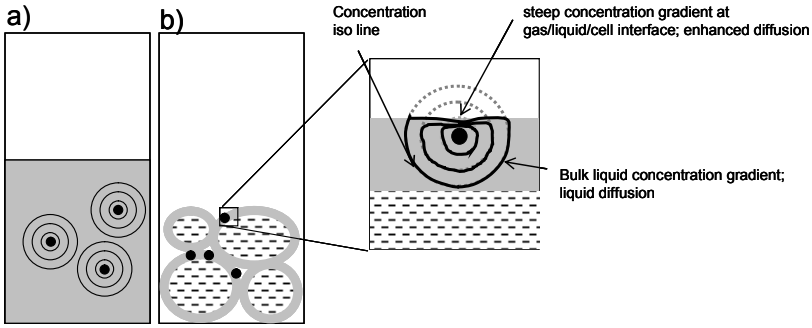

Figure 5.7 a, b – Conceptual scheme of the two experimental systems, partially after Harms and Zehnder, 1994. Black dots represent bacteria. a) liquid mixed batches (grey, liquid phase; white, gas phase; circles indicate diffusive concentration gradients), b) unsaturated soil microcosms (dashed, solid particles; grey, liquid films; white, gas phase; compressed iso-concentration lines indicate very steep concentration gradients and fast diffusion).

In the case of liquid batches, shaking should overcome mass transfer limitations at the macro-scale. Conversely, in the unsaturated soil microcosms, macro-scale mass transfer occurs through diffusion from the headspace, and VC partitioning amongst soil phases.

At the micro-scale, the concentration gradient in proximity of the cell results from the intrinsic rate of substrate uptake by the cells and the substrate diffusion to the cell. Assuming that uptake occurs from the liquid phase exclusively, liquid diffusion regulates mass transfer at the micro-scale in both systems. If at this scale substrate diffusion is not sufficient to maintain concentrations which saturate the uptake system of the cells, bacterial activity is limited by diffusion (Harms and Zehnder, 1994).

The obtained liquid phase biodegradation rates (r_w) and first order apparent rates (k_{app}) show that VC degrading biomass performed better in the unsaturated soil microcosms than in liquid batches (Fig. 5.6 b, d). Similar results were obtained for toluene biodegradation experiments in unsaturated soil microcosms and liquid

batches in Chapter 4. Furthermore, and in contrast to previous research postulating maximum general aerobic microbial activity at 50 - 60% water-filled porosity (Linn and Doran, 1984; Skopp et al., 1990), the presented experiments showed lower VC biodegradation rates in the liquid phase at increasing water-filled porosity, corresponding to higher f_M (Figure 5.6 b, d). For the soil microcosms, the comparison between numerical modeling predictions and the experimental results showed that mass transfer limitations did not play a role at the macro-scale level, as only the microbial activity controlled scenario fitted the measured data (Figure 5.4).

It appears that the lower degradation rates at higher WFP are the result of micro-scale diffusion limitations. Experimental evidence on substrate diffusion limitations of biodegradation rates was shown even for suspended cells (Caldwell and Lawrence, 1986; Harms and Zehnder, 1994).

It is well known that in porous media, the effective diffusion increases with decrease of liquid phase volume (Millington and Quirk, 1959). For a highly volatile compound such as VC, mass transfer limitations would be reduced at lower water-filled porosity, as under these conditions supply of VC is enhanced. Mass transfer of VC and oxygen by diffusion through a thin liquid film in contact with gas is more efficient than mass transfer in a liquid diffusion regulated system such as the liquid batch. Steepest substrate concentration gradients may surround the cells in unsaturated soil, compared to liquid batches (Figure 5.7 a, b).

This is in line with findings from Harms (1996), who concluded that the effective substrate diffusion controlled the final cell numbers in the degradation of distant naphthalene, and that enhanced diffusion increased biodegradation. Thus, the transition from water saturated to unsaturated conditions for VC biodegradation determines a shift from fully liquid diffusion controlled biomass activity to film-diffusion and film-thickness controlled conditions with enhanced substrate access from the gas phase. With decreasing water content, and reduced water film thickness, diffusion limitations on bioactivity are progressively lifted.

Additional explanations for the observed higher liquid phase rates the unsaturated soil microcosms as compared to the liquid batches could also be related to the biomass. Firstly, unsaturated soil could provide more favorable growth conditions. A larger particle surface area in soil microcosms could be beneficial for *M. aurum* taking into account the hydrophobicity of its cell wall (Hartmans and De Bont, 2002). Secondly, synergistic interactions could have developed with other indigenous soil bacteria, which were beneficial for aerobic VC degraders. Thirdly, in soil microcosms, other bacteria than the inoculated strain could have degraded VC. Either VC degrading enzymes located on linear plasmids (Coleman, 2002; Danko et al., 2004) were transferred to other bacteria, or bacteria able to degrade VC were already present in the non inoculated soil, as suggested by the 10^4 etnE gene copies $(g\ soil)^{-1}$ measured in not inoculated soil non exposed to VC. Fourthly, the relative contribution of other reactive species (i.e. soil organic matter, macronutrients) in the soil microcosms could have favored bioactivity.

Two stress indicators were observed at the lowest water-filled porosity tested (6% WFP): significantly longer lag phases (Figure 5.3 c), and reduced increase of biodegradation rates with increased VC consumption (Figure 5.6, second spike). This

could be related either to impaired growth or lower catabolic activity due to water stress as observed by previous research (Potts, 1994).

Detection and increase of etnE gene copies in soil microcosms allowed relating amounts of VC degraded with numbers of gene copies. This offers a tool to monitor actual VC biodegradation activity in soil and water environments. As results point out that unsaturated soils are more favorable for VC degrading bacteria due to enhanced mass transfer, restricting the monitoring of etnE genes to groundwater samples only may underestimate the potential for VC degradation in the unsaturated zone, as most cells may be attached to the soil matrix.

The present results show a relatively fast adaptation of *M. aurum* to a soil environment, which suggests that it is promising for bioaugmentation at sites where VC contamination is of concern.

5.5 Conclusions

Higher biodegradation rates in the liquid phase and higher abundance of specific functional genes related to aerobic VC degradation revealed that aerobic VC degraders performed better in unsaturated soil microcosms than in liquid batches. The zero order liquid phase rates were at least one order of magnitude higher in the unsaturated soil microcosms than in the liquid batches. Observed removal rates in unsaturated microcosms depended on soil moisture content, and appeared not to be controlled by macro-scale mass transfer. Instead, liquid diffusion at the micro-scale is postulated to be the limiting factor. Enhanced effective diffusivity with decreasing moisture content in unsaturated soil leads to higher biodegradation rates as compared to saturated conditions and liquid batches. Other factors, like available particle surface area and the potential role of indigenous bacteria or reactive soil components, could have further favored microbial activity in the soil microcosms. At the lowest water-filled porosity tested (6% WFP), evidence of water stress on microbial activity was observed.

The correlation between etnE gene copies and mass of VC degraded as demonstrated in this work, strongly promotes the use of this functional gene as a valuable tool for either assessing the aerobic VC degradation potential in the field, or to prove the efficiency of in situ techniques aimed at stimulating this. For the soil microcosms, a linear relationship could be derived between the abundance of etnE genes and the mass of VC degraded. In general, overall numbers of etnE genes were orders of magnitude higher in soil samples than in liquid batches. Thus, monitoring of aerobic VC degraders should include soil samples from the unsaturated zone to adequately quantify the presence of such bacteria in actual field situations and their contribution to reducing risks from potential VC vapor intrusion.

6 Towards an improved understanding and risk assessment of vapor intrusion

6.1 Introduction

Volatile organic compounds (VOCs) tend to partition in the gas phase at ambient temperature and pressure. The most important VOCs belong to the groups of petroleum hydrocarbons and chlorinated hydrocarbons. Subsurface contamination by such contaminants is widespread (ATSDR, 2007; EEA, 2005; Plumb, 1991; Wang et al., 2007). As these chemicals readily volatilize, they may migrate through the unsaturated zone to above ground buildings and cause risks of vapor intrusion (Little et al., 1992).

Assessment of vapor intrusion risk in the field is complicated by several interplaying factors, namely: contaminant properties, transport processes in the unsaturated zone, and biodegradation in the unsaturated zone. Contaminant properties, such as partition coefficients and diffusion coefficients, determine the distribution among soil phases and the tendency to mobilization. Transport through the unsaturated zone is determined by the presence of diffusion gradients and abrupt pressure differentials (Johnson and Ettinger, 1991; McAlary et al., 2011). Biodegradation in the unsaturated zone may reduce contaminant fluxes (Hers et al., 2000). These processes are schematized in Figure 6.1.

The direct assessment of vapor intrusion risks by means of measurements is complicated by the interplay of transport and biodegradation processes, driven by the contaminant properties. This gives rise to difficulties in obtaining the measurements and interpreting them. Commonly available vapor intrusion models still have limitations in including essential processes and system characteristics.

This leads to overestimation by predicted concentrations of up to several orders of magnitude (Provoost et al., 2009; 2010). Available models either overlook significant properties at the field scale or, conversely, are too complex to be applicable at this scale of practical application. Specifically, moisture variation, liquid diffusion, dynamic processes, and biodegradation are not adequately taken into account in existing models. Regarding biodegradation in the unsaturated zone, the lack of well-defined rate parameters is a major source of uncertainty in model

prediction, as evidenced by the wide variety of rates reported and ways of expressing them (Table 1.3, Chapter 1).

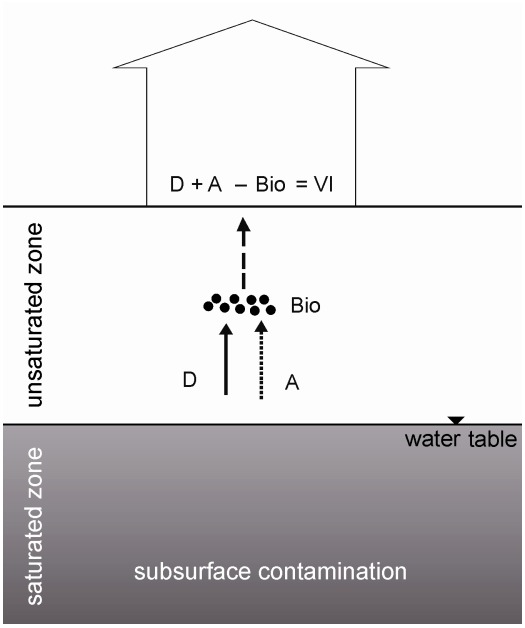

Figure 6.1 – Overview of processes determining vapor intrusion. Arrows: substrate fluxes, where solid line arrow (D), diffusion; dotted line arrow (A), advection; dashed line arrow, net flux of vapor intrusion; black dots: presence of substrate degrading bacteria; Bio: biodegradation; VI: vapor intrusion.

The research presented in this thesis addressed knowledge gaps related to transport and biodegradation of VOCs in the unsaturated zone, focusing on their influence on vapor intrusion into buildings. In a case study (Chapter 2), the need for a more mechanistic understanding of these processes was exemplified. Afterwards, numerical modeling was used to investigate the relative influence of transport and biodegradation on vapor intrusion along a one-dimensional section of subsurface underlying a building with crawl space (Chapter 3). Subsequently, laboratory experiments were performed to obtain biodegradation rates. Toluene (Chapter 4) and vinyl chloride (VC) (Chapter 5) were chosen as representative compounds for petroleum hydrocarbons and chlorinated hydrocarbons, respectively.

6.2 Critical aspects of the assessment of vapor intrusion in field situations

The field case presented in Chapter 2 dealt with a VC-contaminated shallow aquifer below a residential area. A discrepancy between indoor air concentrations as predicted by two commonly used risk assessment models, RISC (BP, 2001) and VOLASOIL (Waitz et al., 1996), and monitored concentrations was observed to be up

to several orders of magnitude. The presence of a less permeable layer (site heterogeneity) and the occurrence of biodegradation were likely to be interrupting the vapor intrusion pathway.

Similar conclusions about discrepancy between model and measurements were drawn by Provoost et al. (2009; 2010) for a larger monitoring dataset and for a range of risk assessment models. Site heterogeneity may cause i) vertical concentration gradients in the groundwater and/or pore waters, or ii) variations in air permeability. Model calculations from Atteia and Hoehener (2010), showed that predominantly clayey soils lead to 11% of the vapor fluxes predicted for sandy soils.

For the case presented in Chapter 2, additional and small scale depth-discrete site characterization data about contaminant concentrations would have been necessary in order to adapt the analytical models to a more realistic scenario. With respect to biodegradation, which can be taken into account by one of the two models used, RISC (BP, 2001), evidences from field characterization and knowledge about specific degradation rates for VC in unsaturated soils were lacking. Neglecting these two processes had a significant impact as predicted concentrations substantially overestimated measured values by several orders of magnitude for the case of VC (Chapter 2).

The indoor measurement results showed that VC is a critical compound to be measured in air due to its chemical properties. Measurements were found to be sensitive to air relative humidity. Most studies about monitoring VOCs in indoor or outdoor environments did not consider VC (e.g. Baroja et al., 2005; Srivastava et al., 2005). When VC was taken into account, it could be detected in only 6% of 1,684 indoor air samples from North American houses (Dawson and McAlary, 2009). Additionally, indoor sources alone could result in higher concentrations compared to those originating from subsurface contamination. For example, the presence of VC above risk limit concentrations (> 1 $\mu g\ m^{-3}$) was associated with house remodeling (Kurtz et al., 2010).

From the bottlenecks found in Chapter 2, complemented with the literature cited above, it is questionable whether the existing analytical capabilities are sufficient to detect VC at the low levels relevant for the adequate assessment of vapor intrusion. Firstly, it appears that methodological improvements on the sampling and analytical methods targeting the monitoring of VC in indoor air and in soil gas are necessary. Secondly, the distinction between indoor and subsurface sources remains critical. Compound specific isotopic analysis was recently used to distinguish between subsurface and indoor sources of trichloroethylene (TCE) and tetrachloroethylene (PCE) (McHugh et al., 2011). Such techniques could potentially also be valuable for cases where VC is measured if the isotopic fingerprints of the indoor sources and the subsurface would differ.

6.3 Transport in the unsaturated zone

In Chapter 3 of this thesis, a one-dimensional numerical model including vertical variations of soil moisture was presented. The model accounts for gas and liquid diffusion, advection, sorption, and aerobic biodegradation. It also allows simulating dynamic processes. By means of a sensitivity analysis, the relative importance of processes and parameters affecting vapor emissions was characterized. Results showed that the vertical distribution of the contaminant with respect to the interface between water saturated and air-filled pores has a very significant effect on risks (Table 3.2, Chapter 3) due to retarded transport by liquid diffusion. This confirms laboratory and modeling observations by other authors (Atteia and Hoehener, 2010; Parker, 2002; Popovicova and Brusseau, 1997). Vertical variations of soil moisture have a profound effect on predicted concentrations in the crawl space (Chapter 3). The thickness of the unsaturated zone has a reduced effect on vapor concentrations compared to soil moisture variations (Chapter 3).

The influence of dynamic processes, such as water table variations, was not accounted for in most of the available vapor intrusion models (Table 1.2, Chapter 1). In Chapter 3, it was shown that lowering of the water table leads to the highest risk. This brings contaminant sources into or close to the unsaturated zone, thereby reducing the protective liquid layer with slow diffusion and increasing air-filled porosity and enhanced migration due to gas diffusion. The effect of water table fluctuations on vapor concentrations is stronger if the period of the fluctuations is shorter than the characteristic time of the vapor transport process (Chapter 3). Furthermore, a water table rise may also lead to higher vapor concentrations at the top of the crawl space when dispersivity is taken into account, as dispersion reduces the transport limitations for liquid diffusion.

These findings have implications for characterizing sites with potential vapor intrusion risks, and may constrain the type of remediation technology chosen at a specific location. Processes which lead to reduced moisture in the upper portion of the soil profile, as well as processes which increase mixing in the water saturated portion on the soil profile potentially enhance vapor intrusion risks. For example, combination of remediation and aquifer thermal energy storage could potentially enhance vapor emissions as aquifer thermal energy storage systems would increase mixing. The effect of remediation on vapor intrusion would require additional research.

Based on the results presented in Chapter 3, site characterization aimed at assessing vapor intrusion risks should measure i) soil properties (including soil type, porosity, organic matter content), ii) pore water concentration of the contaminant of concern as a function of depth, iii) soil moisture content as a function of depth, and iv) oxygen concentrations in order to assess potential for biodegradation. Comparing these specific measurements with prediction from numerical models, such as the one presented in this thesis, can lead to a more robust validation of the model.

A next step to refine model prediction towards increased robustness is the introduction of i) site heterogeneity (i.e., lithological layering), and ii) interactions with the atmosphere. Lithological layering could result in high water-filled porosity

barriers. According to the model calculations presented in Chapter 3, these will have a major impact on vapor transport, as also reported by other authors (Conant et al., 1996; Johnson et al., 1999; Yu et al., 2009). Several three dimensional numerical models are available which account for site heterogeneity (Abreu and Johnson, 2005; Yao et al., 2011; Yu et al., 2009) but do not always combine it with soil moisture variations. Including interactions with the atmosphere could provide information on oxygen levels entering the subsurface. This is important as oxygen availability may be limiting biodegradation.

It appears that the focus of further research should be on model validation with detailed field data, and to a lesser extent on further refined modeling. Such validation type of studies are indeed lacking (Abreu and Johnson, 2005). For example, a thorough review of well-characterized sites compared with models that adequately take into account the relevant processes could provide a compilation of criteria for conditions in which vapor intrusion is unlikely. A recent review of reported field data for petroleum hydrocarbon sites concluded that non-NAPL sources located at a depth larger than 3 m below a building are unlikely to cause vapor intrusion (McHugh et al., 2010). This is due to attenuation by transport and sufficient soil thickness for sustaining aerobic biodegradation (McHugh et al., 2010). The results by McHugh et al. (2010) point out the relevance of an improved understanding of biodegradation at a mechanistic level, which was a focus of this thesis.

6.4 Biodegradation in the unsaturated zone

6.4.1 Mechanisms controlling biodegradation in unsaturated soils

Aerobic biodegradation in unsaturated soil microcosms was studied in laboratory experiments with toluene (Chapter 4) as model compound for petroleum hydrocarbons, and with vinyl chloride (VC, Chapter 5) as risk driver for chlorinated hydrocarbons. In order to mimic unsaturated soil conditions, experiments were conducted with static unsaturated batches (toluene and VC) and unsaturated soil columns (toluene). For safety reasons, no column experiments were performed for VC.

The type of experimental set-up influences the amount of substrate, i.e. contaminant, instantaneously available for biodegradation in the liquid phase at equilibrium. This is expressed by f_M, which is the fraction of the total contaminant mass in the system present in the liquid (mg contaminant in liquid phase/mg contaminant in the system). A similar concept is used by Hoehener et al. (2003) to derive liquid phase biodegradation rates from apparent rates, although these authors regarded it as a retardation factor.

As such, f_M is a function of several factors, namely i) the liquid volume, thus the water-filled porosity (WFP), ii) the type of experimental system, in particular the relative size of the headspace, and iii) the chemical properties of the compound. This is illustrated in Figure 6.2: for similar water-filled porosities, and for an identical

experimental set-up, the f_M, corresponding to the percentage in liquid phase, differs between toluene and VC due to their partitioning coefficients. For the same compound, e.g., toluene, f_M differs between soil microcosms and soil columns at identical WFP, because of the variation of water/soil/gas volume ratios between the two experimental set-ups. Soil column experiments more closely compare to water/soil/gas volume ratios as found in the field (Tindall et al., 2005). Soil columns can therefore be thought of as closer to the field for f_M.

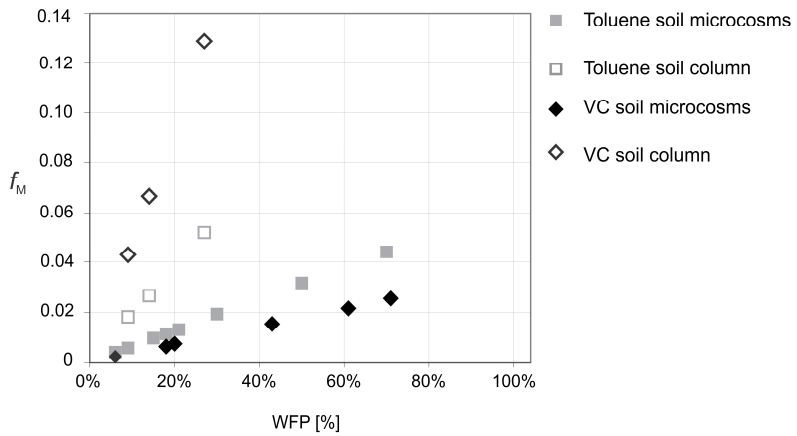

Figure 6.2 – Relationship between f_M and WFP in different experimental set-ups and for different chemicals.

Generally, in experimental set-ups, two main drivers determine overall contaminant removal: mass transfer and biodegradation. In the toluene soil columns, the regulated contaminant supply to the columns appeared to be the controlling factor on overall removal (Chapter 4). In the soil microcosms, mass transfer interplays at two different levels: at the macro-scale (the complete microcosm system) and at the micro-scale (pore scale and cell level).

Comparison of observed data with model predictions showed that for both toluene and VC experimental data were not well described by the scenario in which micro-scale biodegradation was fast and macro-scale mass transfer was limiting. Hence, micro-scale processes controlled biodegradation in the microcosms.

Micro-scale biodegradation rates in the liquid phase could be derived from the apparent rates at the macro-scale via:

$$r_w \approx r_m / V_{liq}$$

and

$$k_w \approx k_{app} / f_M$$

with r_m the overall mass removal rate, r_w the rate in the liquid phase, V_{liq} the liquid volume of the experimental system, k_{app} the apparent first order rate constant (based on overall mass removal), and k_w the liquid phase first order rate constant.

Variation of the micro-scale liquid phase rates with water-filled porosity could indicate a micro-scale influence of mass transfer on the biodegradation rates. While no clear trend can be observed for toluene, a decrease of liquid phase rates (r_w and k_w) for VC is observed at increasing water-filled porosity (Figure 6.3).

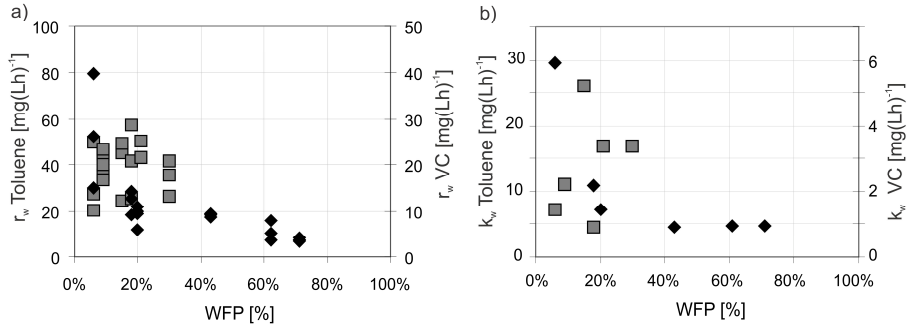

Figure 6.3 a, b – Zero order (a) and first order (b) liquid phase biodegradation rates as a function of water-filled porosity for toluene (grey squares) and for VC (black diamonds). Rates for toluene refer to right y-axes, and rates for VC refer to left y-axes; a) liquid phase zero order rates (r_w); b) first order liquid phase rate constants (k_w).

These observations could be explained by a conceptual model which compares the overall biodegradation process to an electric circuit (Figure 6.4), where the concentration gradient of the substrate (toluene or VC) induced by bacterial metabolism is compared to a potential difference, the rate of substrate supply to the bacteria is compared to the current, and mass transfer limitations are compared to resistances. Mass transfer regulated by effective diffusion operates at two levels: the macro- and micro-scale. In general, a large effective diffusion is equivalent to near absence of diffusional mass transfer limitations, and hence a small resistance. The macro-scale and micro-scale resistances are connected in series as it is assumed that the substrate has to pass from the macro-scale to the bacteria via the micro-scale.

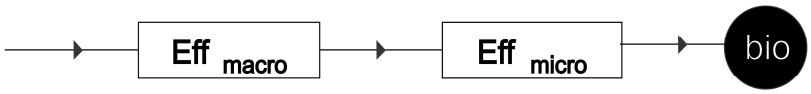

Figure 6.4 - Conceptual model of the overall biodegradation. Macro-scale and micro-scale mass transfer are resistances in series, which the substrate has to cross for biodegradation (bio) to occur. Eff macro: effective mass transfer at the macro-scale, Eff micro: effective mass transfer at the micro-scale.

Zooming in on each component of the circuit, the effective diffusion at both macro- and micro-scale results from combined liquid and gas diffusion. At the macro-scale, for unsaturated soils, the substrate can reach bacteria either by diffusing through the liquid phase or by diffusing through the gas phase. Thus, at this scale the resistances are connected in parallel (Figure 6.5) and the faster gas phase diffusion ($D_{air} \approx 10^4 D_{water}$) dominates the effective diffusion.

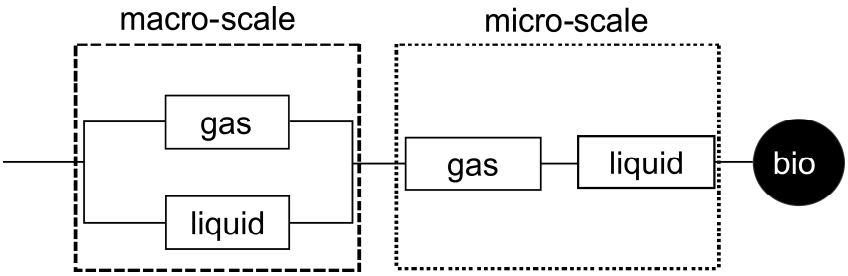

Figure 6.5 –At the macro-scale, (dashed rectangle) diffusional mass transfer results from gas and liquid diffusion connected in parallel. At the micro-scale (dotted rectangle), gas and liquid diffusion are connected in series; bio: biodegradation.

This situation differs from water saturated conditions, where the absence of a gas phase implies that the slow liquid diffusion may become limiting for bacteria (Mihelcic and Luthy, 1991; Rijnaarts et al., 1990; Scow and Hutson, 1992). At the micro-scale, where gas resides in the pore center and water is present as a thin film surrounding bacteria and soil particles, gas and liquid diffusion are two resistances connected in series (Figure 6.5). Here, the slower liquid phase diffusion dominates the effective diffusion and forms a barrier for the transfer of substrate to bacteria. Presence of a thin water film already has a significant effect in retarding the substrate supply.

The difference in behavior observed between toluene and VC can be explained starting from this conceptual model and taking into account their chemical properties. Chemical properties regulate the partitioning of each compound at the micro-scale.

Toluene is more hydrophobic than VC and has a lower Henry coefficient (H = 0.26). Hence, at the micro-scale, the majority of the toluene mass will be present as sorbed phase, and only a negligible part of the non-sorbed contaminant is present in the gas phase, even if the liquid phase volume is reduced (Figure 6.6, % toluene mass in the gas phase ≤ 3%).

Thus, for toluene, micro-scale mass transfer is likely dominated by desorption, and the effect on mass transfer of a change in micro-scale diffusion resistance with decrease in WFP may be negligible. For VC, instead, nearly half of the contaminant is non-sorbed (Figure 6.6), and mass distribution between gas and liquid is favored towards the gas phase (H = 0.98). This implies that replenishment from the gas phase and subsequent transport through the water film is more important for VC than for toluene, and increasingly so with lower WFP. Hence, for VC the gaseous-liquid supply route becomes faster at lower WFP, which appears to result in an increase of the liquid phase biodegradation rates.

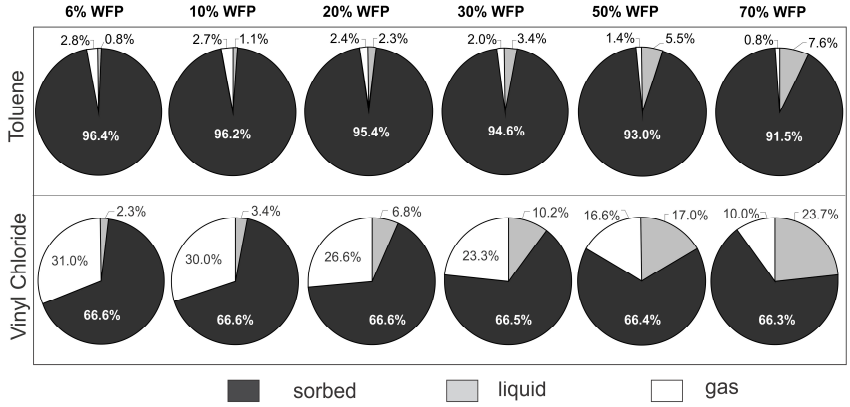

Figure 6.6 – Mass distribution within a micro-scale soil volume as a function of WFP for toluene and vinyl chloride.

An alternative explanation, also related to the change in mass distribution with WFP, lies in the possibility of direct uptake from the gas phase, as has been proposed for suspended cells for naphthalene by Hanzel et al. (2011). This, of course, would also be more relevant for VC than for toluene, and especially at low WFP.

Finally, the occurrence of physiological limitation was observed at the lowest water content (6% WFP), revealed by longer lag phases for both toluene and VC degraders. For aerobic VC degraders also indications of reduced growth were obtained at these lower WFP values. This confirms findings by previous research determining the effects of reduced soil moisture content on microbial activity (Andersson and Hahn-Hagerdal, 1987; Potts, 1994).

6.4.2 Derivation of aerobic biodegradation rates for unsaturated soils

Chapters 4 and Chapter 5 of this thesis provide an approach to derive aerobic biodegradation rates for unsaturated soils from laboratory experiments. Two important conclusions could be drawn which are relevant for further applications and for the inclusion of biodegradation in field studies.

Firstly, it is experimentally very complex to separate diffusion from reaction rates, particularly for unsaturated soil environments as water content variations may influence mass transfer. A combined experimental and modeling approach is needed to postulate feasible mechanisms explaining the observations (Chapter 4 and 5).

Secondly, for both toluene and VC, higher liquid phase biodegradation rates were obtained from unsaturated soil microcosms compared to liquid mixed batches (Figure 6.6). This is related either to improved micro-scale mass transfer or to a growth environment favoring bioactivity in the unsaturated soil systems. Micro-scale mass transfer limitations appear minimized in a soil/air/liquid system compared to a liquid system because of the presence of a sorbed stock and steeper diffusion gradients at gas/liquid interfaces. This is in line with findings from Harms and Bosma (1997), reporting denser bacterial growth on naphthalene at lower water

content. Furthermore, it is likely that an additional limitation from oxygen transfer played a role for the toluene liquid batches, which, contrary to VC, could not be described by first order kinetics. A larger oxygen amount is needed per unit mass for toluene (3.13 g O_2 for 1 g toluene) as compared to VC (1.28 g O_2 for 1 g VC). Hence, given that oxygen solubility is relatively low, it is possible that oxygen uptake from the headspace was not sufficiently fast, and limited the overall biodegradation rate in the case of toluene.

In summary, biodegradation in liquid mixed batches appears to be affected by mass transfer limitations not occurring in unsaturated soil conditions. This implies that the use of liquid phase biodegradation rates for volatile organics as derived from liquid mixed batches may significantly underestimate the role of biodegradation in unsaturated soil. If biodegradation in unsaturated systems is modeled as a process occurring only in the liquid phase, such as the modeling approach followed here, the use of rates derived from liquid batches would not be appropriate (Chapters 3, 4, 5).

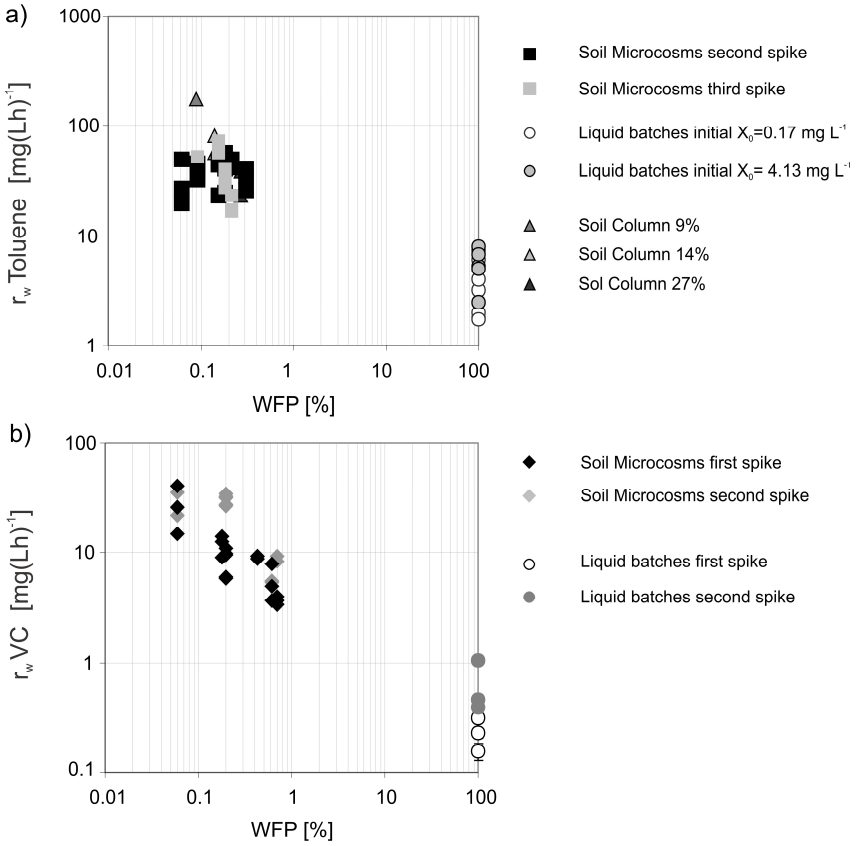

Figure 6.7 a, b – Zero order liquid phase biodegradation rates (r_w) in different experimental set-ups versus WFP (%).For comparison purposes, liquid batches are plotted as 100% WFP. a) toluene; b) VC.

6.4.3 Research needs to translate obtained rates to the field

In this thesis, biodegradation rates were derived in order to quantify the potential of biodegradation in reducing vapor intrusion risk. In order to maximize biodegradation, potential limitations such as biomass adaptation, nutrients and oxygen limitations were minimized. However, the translation of the obtained rates to field conditions requires additional studies.

The control of diffusion gradients of contaminant and oxygen on biodegradation needs to be further investigated. The microcosm experiments performed, simulated an infinitely small layer of soil for which the oxygen supply is always at its maximum and contaminant concentrations are rather high. In the field, the supply of sufficient oxygen to the biomass occurs through downward oxygen diffusion, whereas contaminant diffusion is upward (Figure 6.8). Column experiments mimicking diffusive transport of contaminant and oxygen in opposite directions could be used to obtain quantitative insights on concentration gradients by means of depth-discrete measurements.

Additionally, other oxygen consuming processes could reduce the flux available to degrade the contaminant. An example is the presence of fuel additives such as ethanol, whose rapid fermentation could reduce oxygen availability and thus increase contaminant vapor fluxes (Ruiz-Aguilar et al., 2003).

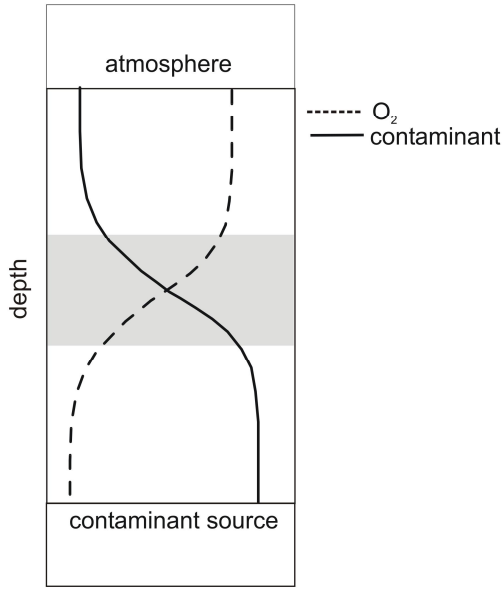

Figure 6.8 – Conditions at which biodegradation in the unsaturated could occur: presence of adapted biomass in a reactive layer (shaded grey layer), and sufficient oxygen flux from downward oxygen diffusion (dashed line) to neutralize the upward contaminant flux (solid line).

With respect to vapor intrusion, one of the major uncertainties regarding biodegradation in the field is whether and to what extent the presence of a building inhibits the supply of oxygen and therefore, whether degradation below a building is similar to degradation beside a building (McAlary et al., 2011). Lundegard and Johnson (2008) measured oxygen transport below a slab on grade foundation above a petroleum hydrocarbon contaminated aquifer in methanogenic conditions. Measured oxygen replenishment rates varied between a minimum of 200 - 500 g O_2 d^{-1} and a maximum of 2500 g O_2 d^{-1}. Assuming that the supplied oxygen is exclusively consumed for pollutant biodegradation, the minimum replenishment rate would sustain biodegradation rates four orders of magnitude larger than the maximum rates observed here for VC ($6.72x10^{-4}$ g d^{-1}) and two orders of magnitude larger than those for toluene ($3.02x10^{-2}$ g d^{-1}). Moreover, with respect to VC, recent research has shown aerobic biodegradation at nominally anoxic (Gossett, 2010) or hypoxic concentration (Bradley and Chapelle, 2011). For such conditions, other tools than contaminant and oxygen concentrations will be necessary to provide evidence of biodegradation. In this thesis, the value of the molecular tool quantifying etnE gene copies for aerobic biodegradation of VC was demonstrated (Chapter 5). This gene encodes the specific enzyme involved in the aerobic degradation of VC.

6.4.4 Role of biodegradation in reducing vapor intrusion risk

The sensitivity analysis performed by modeling in Chapter 3 showed that biodegradation may produce the same attenuation as depth of the contamination source with respect to the saturated/unsaturated zone interface. In Chapter 4 and 5 rates were obtained for unsaturated soil biodegradation for toluene and VC, which can be thought of as "maximum" potential rates as they neglect limitations from oxygen and nutrients. With the column set-up in Chapter 4, it was demonstrated that a 20 cm soil layer was able to lower contaminant concentrations roughly corresponding to fluxes equivalent to diffusion fluxes emanating from groundwater concentrations up to three times the risk limits.

To consider the implications of these results on modeling vapor intrusion, contaminant half lives derived from laboratory microcosms can be compared with characteristic times for transport. Biodegradation is at least one order of magnitude faster than the characteristic time of transport by diffusion through a 1 m thick unsaturated zone (Table 6.1). For a contaminant source located at the capillary fringe, the minimum and the maximum first order liquid phase biodegradation rates were incorporated in the numerical model presented in Chapter 3. By comparing the attenuation factors (Table 6.1) it can be seen that the effect of biodegradation is much stronger for toluene than for VC under similar transport conditions. This is because i) diffusion controlled transport is faster for VC (characteristic time 6 days) compared to toluene (characteristic time 159 days) due to lower retardation by sorption, and ii) the biodegradation rates for toluene are at least a factor four higher than those for VC.

Table 6.1 – Comparison between numerical model results with and without biodegradation with rates as obtained from experiments in Chapters 4 and 5 for toluene and VC. Column time: contaminant half lives as derived from minimum and maximum first order apparent rates (k_{app}); characteristic times for transport; column attenuation factors: attenuation factors without biodegradation and scenarios including minimum and maximum liquid phase first order rates (k_w).

Compound	Time		Attenuation factor		
	Biodegradation (half life) days	Transport to crawl space dissolved source at capillary fringe - characteristic time days	Transport no bio -	Transport + bio min rate -	Transport + bio max rate -
VC	0.48 - 2.88	6	$1.23x10^{-4}$	$6.76 x10^{-6}$	$6.69x10^{-6}$
Toluene	0.09 - 0.96	159	$2.88x10^{-4}$	$6.72 x10^{-12}$	$6.44x10^{-12}$

It is also relevant that drought related stress indicators were observed only at the driest water content tested (6% WFP), but biodegradation occurred at all conditions. Hence, in moderate climate areas, where water-filled porosity is likely to be at less extreme values (> 10% WFP) (Linn and Doran, 1984), water stress is not likely to limit biodegradation.

6.5 Implications for vapor intrusion risk assessment at contaminated sites

The main conclusions from this thesis indicate that soil moisture variations (Chapter 3) and aerobic biodegradation (Chapter 4 and 5) are crucial aspects to be jointly considered when modeling and monitoring vapor intrusion.

With respect to models, the adequacy of vapor intrusion risk assessment models could be improved by including soil moisture variation in the soil profile and aerobic biodegradation, thus complementing the findings of other authors, such as Atteia and Hoehener (2010) and Abreu et al. (2009).

As for monitoring, because of the relevance of soil moisture variations and aerobic biodegradation, specific parameters should be obtained in the field which inform about:

i) contaminant concentrations at discrete depth in the field, either in pore waters or in soil gas;

ii) oxygen concentrations to assess potential for aerobic biodegradation.

This thesis presents an approach to derive biodegradation rates from laboratory experiments and include them in models relevant for the field (Chapter 4 and 5). Additionally, the use of specific molecular tools such as the one presented in Chapter 5 for VC degrading enzymes, and the development of this type of tools for other contaminants, can provide evidence for biodegradation. Quantifying the presence of active degraders in groundwater and soil samples would further sustain the indications from field measurements of contaminant concentrations and oxygen.

This research focused on aerobically degradable compounds; however, other common volatile pollutants, such as TCE, are not easily degraded under aerobic

conditions. For this compound, more complex cometabolic processes in the unsaturated zone might be of relevance (Frascari et al., 2006), which should be addressed by further research. Presence of fuel additives, such as methyl tertiary butyl ether (MtBE), and ethanol could affect both physical behavior and biodegradation of other compounds, but studies investigating contaminant mixtures are lacking (Hoehener, 2010).

The increased knowledge about specific processes influencing vapor intrusion risks is also useful to design remedial strategies, both at the subsurface and at the building level. Mitigation systems at the building level can be implemented on existing buildings, or taken into account when brownfield redevelopment is impaired by vapor intrusion concerns (McAlary et al., 2011). Strategies applicable at the building level limit the vapor flux into the building by modifying pressure (building pressurization, sub-slab depressurization), or increasing ventilation (McAlary et al., 2011). With the model in Chapter 3, it was shown that, for the physical system described there, ventilation above 0.5 h^{-1} alone would suffice to reduce vapor emissions below risk levels according to the norms in the Netherlands (VROM, 2009). As the model is linear for concentration, extrapolation to higher source concentrations can be easily performed. Strategies at the subsurface level can either reduce the source or interrupt the pathway. It was shown in Chapter 3 that presence of a clean groundwater lens could act as a natural retarding barrier against vapor migration. A reduction of contaminant fluxes can be achieved by boosting biodegradation in the unsaturated zone. In this respect, provided that oxygen is present, bioaugmentation could be a successful technique, and the strains utilized here for toluene and VC proved to be good candidates. In particular, the VC degrader *Mycobacterium* (Chapter 5) could remain present on a longer term thanks to the adhesion mechanisms protecting it from predation by other microorganisms, and may also transfer the VC biodegrading capacity to other bacteria by exchanging DNA fragments. These processes and mechanisms involved in bacterial survival, adhesion, and molecular gene code exchanges require more and detailed research to further assess the microbiological factors in vapor intrusion attenuation.

6.6 Perspective on risk assessment for contaminated sites

Vapor intrusion risk assessment is part of a wider strategy for risk assessment at a contaminated site. Risk assessment at contaminated sites should aim at protecting receptors, while keeping societal costs of remedial actions at an acceptable level (Vegter, 2001). Neglecting processes such as reduced transport by liquid diffusion and aerobic biodegradation could lead to enhanced societal costs because of risk overestimation. This research provided an approach to account for transport limitations by liquid diffusion (Chapter 3) and aerobic biodegradation in unsaturated soils (Chapter 4 and 5).

Overall, this research contributed to new scientific knowledge on biodegradation of organic volatile compounds in unsaturated soil. However, a robust, standardized

approach to assess and quantify biodegradation in unsaturated soils in the context of vapor intrusion is still needed. Further steps are necessary to upscale the knowledge acquired in this thesis to field conditions, which include the incorporation of heterogeneity, limitations for biodegradation in the field (oxygen and temperature), and the interaction with the atmosphere.

This thesis underpinned the processes controlling vapor intrusion risks. In addition to sound scientific and technical concepts, risk perception is another important issue to be considered in managing vapor intrusion risks in existing urban areas. Risk perception is highly influenced by risk communication. Research has highlighted the need for better-developed official guidelines for communicating risks specific for contaminated soil (Wisen and Wester-Herber, 2007). Especially for vapor intrusion, which may occur in private houses, risk communication has been indicated as a crucial component of successful risk management strategies (Ivens, 2010).

In conclusion, adequate field monitoring, appropriate remedial measures, and proper risk communication should be combined for effective risk management at contaminated sites where vapor intrusion is a potential concern. The development of scientifically-based standardized protocols in each of these three aspects will provide increased transparency in the risk management process, which will improve risk perception and reduce societal costs of managing subsurface contamination.

7 References

Abe, Y., Aravena, R., Zopfi, J., Shouakar-Stash, O., Cox, E.; Roberts, J. D., Hunkeler, D. Y., 2009. Carbon and chlorine isotope fractionation during aerobic oxidation and reductive dechlorination of vinyl chloride and cis-1, 2-dichloroethene. Environmental Science and Technology, 43(1): 101-107.

Abreu, L.D.V. and Johnson, P.C., 2005. Effect of vapor source-building separation and building construction on soil vapor intrusion as studied with a three-dimensional numerical model. Environmental Science and Technology, 39(12): 4550-4561.

Abreu, L.D.V. and Johnson, P.C., 2006. Simulating the effect of aerobic biodegradation on soil vapor intrusion into buildings: influence of degradation rate, source concentration, and depth. Environmental Science and Technology, 40(7): 2304-2315.

Abreu, L.D.V., Ettinger, R. and McAlary, T., 2009. Simulated soil vapor intrusion attenuation factors including biodegradation for petroleum hydrocarbons. Ground Water Monitoring and Remediation, 29(1): 105-117.

Allen-King, R.M., Barker, J.F., Gillham, R.W. and Jensen, B.K., 1994. Substrate- and nutrient-limited toluene biotransformation in sandy soil. Environmental Toxicology and Chemistry, 13(5): 693-705.

Allen-King, R.M., Gillham, R.W., Barker, J.F. and Sudicky, E.A., 1996. Fate of dissolved toluene during steady infiltration through unsaturated soil: II. Biotransformation under nutrient-limited conditions. Journal of Environmental Quality, 25(2): 287-295.

Alvarez, P.J.J., Anid, P.J. and Vogel, T.M., 1991. Kinetics of aerobic biodegradation of benzene and toluene in sandy aquifer material. Biodegradation, 2(1): 43-51.

Alvarez, P.J.J. and Vogel, T.M., 1991. Substrate interactions of benzene, toluene, and para-xylene during microbial degradation by pure cultures and mixed culture aquifer slurries. Applied and Environmental Microbiology, 57(10): 2981-2985.

Amorosi, A., Pavesi, M., Ricci Lucchi, M., Sarti, G. and Piccin, A., 2008. Climatic signature of cyclic fluvial architecture from the Quaternary of the central Po Plain, Italy. Sedimentary Geology, 209(1-4): 58-68.

Anderson, R.T., Rooney-Varga, J.N., Gaw, C.V. and Lovley, D.R., 1998. Anaerobic benzene oxidation in the Fe(III) reduction zone of petroleum- contaminated aquifers. Environmental Science and Technology, 32(9): 1222-1229.

Andersson, E. and Hahn-Hagerdal, B., 1987. Enzyme action in polymer and salt solutions. II. Activity of penicillin acylase in poly(ethylene glycol) and potassium phosphate solutions in relation to water activity. Biochimica et Biophysica Acta - Protein Structure and Molecular Enzymology, 912(3): 325-328.

Andreoni, V. and Gianfreda, L., 2007. Bioremediation and monitoring of aromatic-polluted habitats. Applied Microbiology and Biotechnology, 76: 287-308.

Appelo, C.A.J. and Postma, D., 1994. Geochemistry, groundwater and pollution. Balkema, Rotterdam, 535 pp.

Arands, R., Lam, T., Massry, I., Berler, D.H., Muzzio, F.J. and Kosson, D.S., 1997. Modeling and experimental validation of volatile organic contaminant diffusion through an unsaturated soil. Water Resources Research, 33(4): 599-609.

ASTM, 2009. Standard Test Methods for Dissolved Oxygen in Water, American Society for Testing and Materials.

ATDSR, 1995. Toxicological Profile for Xylenes (Update). ATDSR, Atlanta, US.

ATSDR, 1994. Toxicological Profile for Toluene (Update). ATDSR, Atlanta, US.

ATSDR, 1999. Toxicological Profile for Ethylbenzene (Update). ATDSR, Atlanta, US.

ATSDR, 2007. 2007 CERCLA Priority List of Hazardous Substances, ATDSR, Atlanta, US.

Attaway, H.H. and Schmidt, M.G., 2002. Tandem biodegradation of BTEX components by two Pseudomonas sp. Current Microbiology, 45(1): 30-36.

Atteia, O. and Hoehener, P., 2010. Semianalytical model predicting transfer of volatile pollutants from groundwater to the soil surface. Environmental Science and Technology, 44: 6628-6232.

Baker, R.J., Baehr, A.L. and Lahvis, M.A., 2000. Estimation of hydrocarbon biodegradation rates in gasoline-contaminated sediment from measured respiration rates. Journal of Contaminant Hydrology, 41(1-2): 175-192.

Bakker, J., Lijzen, J.P.A. and van Wijnen, H.J., 2008. Site-specific human risk assessment of soil contamination with volatile compounds. 711701049, RIVM - National Institute for Public Health and The Environment, Bilthoven, NL.

Bastida, F., Luis Moreno, J., Teresa, H. and Garcia, C., 2006. Microbiological degradation index of soils in a semiarid climate. Soil Biology and Biochemistry, 38(12): 3463-3473.

Batterman, S., Kulshrestha, A. and Cheng, H.Y., 1995. Hydrocarbon vapor transport in low moisture soils. Environmental Science and Technology, 29(1): 171-180.

Begley, J.F., Hansen, E., Wells, A.K., Fogel, S. and Begley, G.S., 2009. Assessment and monitoring tools for aerobic bioremediation of vinyl chloride in groundwater. Remediation Journal, 20(1): 107-117.

Bird, R.B., Stewart, W.E. and Lightfoot, E.N., 1960. Transport Phenomena. Yohn Wiley and Sons, New York.

Bosma, T.N.P., Middeldorp, P.J.M., Schraa, G. and Zehnder, A.J.B., 1997. Mass transfer limitation of biotransformation: quantifying bioavailability. Environmental Science and Technology, 31(1): 248-252.

Bouwer, E.J. and Zehnder, A.J.B., 1993. Bioremediation of organic compounds - Putting microbial metabolism to work. Trends in Biotechnology, 11(8): 360-367.

Bozkurt, O., Pennel, K.G. and Suubuerg, E.M., 2009. Simulation of the vapor intrusion process for nonhomogeneous soils using a three-dimensional numerical model. Groundwater Monitoring and Remediation, 29(1): 92-104.

BP, 2001. RISC. Risk-Integrated Software for Clean-up - User's manual, British Petroleum - Amoco Oil Sunbury, UK.

Bradford, M.M., 1976. A rapid and sensitive method for the quantitation of microgram quantities of protein utilizing the principle of protein dye binding. Analytical Biochemistry, 72(1-2): 248-254.

Bradley, P.M. and Chapelle, F.H., 1996. Anaerobic mineralization of vinyl chloride in Fe(III)-reducing, aquifer sediments. Environmental Science and Technology, 30(6): 2084-2086.

Bradley, P.M. and Chapelle, F.H., 1997. Kinetics of DCE and VC mineralization under methanogenic and Fe(III)- reducing conditions. Environmental Science and Technology, 31(9): 2692-2696.

Bradley, P.M. and Chapelle, F.H., 1998. Microbial mineralization of VC and DCE under different terminal electron accepting conditions. Anaerobe, 4(2): 81-7.

Bradley, P.M. and Chapelle, F.H., 2000. Aerobic microbial mineralization of dichloroethene as sole carbon substrate. Environmental Science and Technology, 34(1): 221-223.

Bradley, P.M. and Chapelle, F.H., 2011. Microbial mineralization of dichloroethene and vinyl chloride under hypoxic conditions. Ground Water Monitoring and Remediation, 31(4): 39-49.

Brooks, H. and Corey, A.T., 1966. Properties of porous media affecting fluid flow. Journal of Irrigation and Drainage Division, 93(3): 61-88.

Brusseau, M.L., 1991. Transport of organic chemicals by gas advection in structured or heterogeneous porous media: development of a model and application to column experiments. Water Resources Research, 27(12): 3189-3199.

Caldwell, D.E. and Lawrence, J.R., 1986. Growth kinetics of Pseudomonas fluorescens microcolonies within the hydrodynamic boundary layers of surface microenvironments. Microbial Ecology, 12(3): 299-312.

Carlon, C. and Swartjes, F., 2007. Analysis of variability and reasons of differences. In: J. Pubsy (Editor), Derivation methods of soil screening values in Europe. A review of national procedures towards harmonisation opportunities. European Commission Joint Research Centre, Ispra, IT.

Chakraborty, R. and Coates, J.D., 2004. Anaerobic degradation of monoaromatic hydrocarbons. Applied Microbiology and Biotechnology, 64(4): 437-446.

Chang, M.K., Voice, T.C. and Criddle, C.S., 1993. Kinetics of competitive inhibition and cometabolism in the biodegradation of benzene, toluene, and p-xylene by two Pseudomonas isolates. Biotechnology and Bioengineering, 41(11): 1057-1065.

ChemWeek, 2008. VC product focus - Chem Week.

Chiou, C.T. and Shoup, T.D., 1985. Soil sorption of organic vapors and effects of humidity on sorptive mechanism and capacity. Environmental Science and Technology, 19(12): 1196-1200.

Chiriac, R., Carre, J., Perrodin, Y., Fine, L. and Letoffe, J.M., 2007. Characterisation of VOCs emitted by open cells receiving municipal solid waste. Journal of Hazardous Materials, 149(2): 249-263.

Choi, J.W. and Smith, J.A., 2005. Geoenvironmental factors affecting organic vapor advection and diffusion fluxes from the unsaturated zone to the atmosphere under natural conditions. Environmental Engineering Science, 22(1): 95-108.

Chowdhury, N., Marschner, P. and Burns, R., 2011. Response of microbial activity and community structure to decreasing soil osmotic and matric potential. Plant and Soil, 344(1): 241-254.

Christophersen, M.,. Broholm, M.M., Mosbæk, H., Karapanagioti, H.K., Burganos, V.N., Kjeldsen, P., 2005. Transport of hydrocarbons from an emplaced fuel source experiment in the vadose zone at Airbase Værløse, Denmark. Journal of Contaminant Hydrology, 81(1-4): 1-33.

Clement, T.P., 1997. RT3D (Version 1.0) A modular computer code for simulating Reactive multi-species Transport in 3-Dimensional groundwater systems, Pacific Northwest National Laboratory, Washington, US.

Clement, T.P., Johnson, C.D., Sun, Y., Klecka, G.M. and Bartlett, C., 2000. Natural attenuation of chlorinated ethene compounds: model development and field-scale application at the Dover site. Journal of Contaminant Hydrology, 42(2-4): 113-140.

Coleman, N.V., Mattes, T. E., Gossett, J. M., Spain, J. C., 2002. Phylogenetic and kinetic diversity of aerobic vinyl chloride-assimilating bacteria from contaminated sites. Applied and Environmental Microbiology, 68(12): 6162-71.

Conant, B.H., Gillham, R.W. and Mendoza, C.A., 1996. Vapor transport of trichloroethylene in the unsaturated zone: Field and numerical modeling investigations. Water Resources Research, 32(1): 9-22.

Danko, A.S., Luo, M., Bagwell, C.E., Brigmon, R.L. and Freedman, D.L., 2004. Involvement of linear plasmids in aerobic biodegradation of vinyl chloride. Applied and Environmental Microbiology, 70(10): 6092-6097.

Davis, J.W. and Carpenter, C.L., 1990. Aerobic biodegradation of vinyl chloride in groundwater samples. Applied and Environmental Microbiology, 56(12): 3878-3880.

Davis, J.W. and Madsen, S., 1996. Factors affecting the biodegradation of toluene in soil. Chemosphere, 33(1): 107-130.

Davis, G.B., Rayner, J.L., Trefry, M.G., Fischer, S.J. and Patterson, B.M., 2005. Measurement and modeling of temporal variations in hydrocarbon vapor behavior in a layered soil profile. Vadose Zone Journal, 4: 225-239.

Dawson, H.E. and McAlary, T., 2009. A compilation of statistics for VOCs from post-1990 indoor air concentration studies in North American residences unaffected by subsurface vapor intrusion. Ground Water Monitoring and Remediation, 29(1): 60-69.

Dechesne, A., Or, D., Gülez, G. and Smets, B.F., 2008. The porous surface model, a novel experimental system for online quantitative observation of microbial processes under unsaturated conditions. Applied and Environmental Microbiology, 74(16): 5195-5200.

Deeb, R.A. and Alvarez-Cohen, L., 1999. Temperature effects and substrate interactions during the aerobic biotransformation of BTEX mixtures by toluene-enriched consortia and Rhodococcus rhodochrous. Biotechnology and Bioengineering, 62(5): 526-536.

Deeb, R.A., Scow, K.M. and Alvarez-Cohen, L., 2000. Aerobic MTBE biodegradation: an examination of past studies, current challenges and future research directions. Biodegradation, 11(2-3): 171-186.

DeVaull, G.E., 2007. Indoor vapor intrusion with oxygen-limited biodegradation for a subsurface gasoline source. Environmental Science and Technology, 41(9): 3241-3248.

DeVaull, G.E., Ettinger, R.A., Salanitro, J.P. and Gustafson, J.B., 1997. Benzene, toluene, ethylbenzene and xylenes (BTEX) degradation in vadose zone soils during vapor transport: first-order rate constants, Proceedings of the Petroleum Hydrocarbons and Organic Chemicals in Ground Water: Prevention, Detection and Remediation Conference, API/NGWA. Ground Water Publishing Company, Westerville, Ohio, pp. 365-379.

Doucette, W.J., Hall, A.J. and Gorder, K.A., 2010. Emissions of 1,2-dichloroethane from holiday decorations as a source of indoor air contamination. Groundwater Monitoring and Remediation, 30(1): 65-71.

Dowideit, K. Scholz-Muramatsu, H., Miethling-Graff, R., Vigelahn, L., Freygang, M., Dohrmann, A.B., Tebbe, C.C., 2010. Spatial heterogeneity of dechlorinating bacteria and limiting factors for in situ trichloroethene dechlorination revealed by analyses of sediment cores from a polluted field site. FEMS Microbiology Ecology, 71(3): 444-459.

EC, 1999 Solvent Emissions Directive. European Commission.

EC, 2000. Water Framework Directive European Parliament and Council.

EC, 2006a. Thematic Strategy for Soil Protection. European Commission.

EC, 2006b. Proposal for a Directive of the European Parliament and of the Council establishing a framework for the protection of soil and amending Directive 2004/35/EC European Commission.

ECSA, 2007. White paper – perchloroethylene. ECSA European Chlorinated Solvents Association, Bruxelles, BE.

EEA, 2005. Overview of contaminants in European contaminated sites. European Environmental Agency, Copenhagen, DK.

EEA, 2007. Overview of activities causing soil contamination, European Environmental Agency, Copenhagen, DK.

El-Farhan, Y.H., Scow, K.M., De Jonge, L.W., Rolston, D.E. and Moldrup, P., 1998. Coupling transport and biodegradation of toluene and trichloroethylene in unsaturated soils. Water Resources Research, 34(3): 437-445.

EuroChlor, 2008. Chlorine Industry Review 2007-2008, Euro Chlor, Bruxelles, BE.

Fan, S. and Scow, K.M., 1993. Biodegradation of trichloroethylene and toluene by indigenous microbial populations in soil. Applied and Environmental Microbiology, 59(6): 1911-1918.

Farhadian, M., Vachelard, C., Duchez, D. and Larroche, C., 2008. In situ bioremediation of monoaromatic pollutants in groundwater: a review. Bioresource Technology, 99: 5296-5308.

Farrell, J. and Reinhard, M., 1994. Desorption of halogenated organics from model solids, sediments, and soil under unsaturated conditions. 1. Isotherms. Environmental Science and Technology, 28(1): 53-62.

Ferguson, C. Darmendrail, D., Freier, K., Jensen, B.K., Jensen, J., Kasamas, H., Urzelai, A.,
Vegter, J., 1998. Risk assessment for contaminated sites in Europe. Volume 1. Scientific basis. LQM Press, Nottingham, UK.

Ferguson, C.C., Krylov, V.V. and McGrath, P.T., 1995. Contamination of indoor air by toxic soil vapours: a screening risk assessment model. Building and Environment 30: 375-383.

Fischer, D. and Uchrin, C.G., 1996. Laboratory simulation of VOC entry in to residence basements from soil gas. Environmental Science and Technology, 30: 2598-2603.

Fitzpatrick, N.A. and Fitzgerald, J.J., 2002. An evaluation of vapor intrusion into buildings through a study of field data. Soil and Sediment Contamination, 11(4): 603-623.

Folkes, D., Wertz, W., Kurtz, J. and Kuehster, T., 2009. Observed spatial and temporal distributions of CVOCs at Colorado and New York vapor intrusion sites. Ground Water Monitoring and Remediation, 29(1): 70-80.

Frascari, D., Pinelli, D., Nocentini, M., Zannoni, A., Fedi, S., Baleani, E., Zannoni, D., Farneti, A., Battistelli, A., 2006. Long-term aerobic cometabolism of a chlorinated

solvent mixture by vinyl chloride-, methane- and propane-utilizing biomasses. Journal of Hazardous Materials, 138(1): 29-39.

Freedman, D.L. and Herz, S.D., 1996. Use of ethylene and ethane as primary substrates for aerobic cometabolism of vinyl chloride. Water Environment Research, 68(3): 320-328.

Freijer, J.I., De Jonge, H., Bouten, W. and Verstraten, J.M., 1996. Assessing mineralization rates of petroleum hydrocarbons in soils in relation to environmental factors and experimental scale. Biodegradation, 7(6): 487-500.

Freitas, J.G. and Barker, J.F., 2011. Oxygenated gasoline release in the unsaturated zone - Part 1: source zone behavior. Journal of Contaminant Hydrology, 126(3-4): 153-166.

Fugler, D. and Adomait, M., 1997. Indoor infiltration of volatile organic contaminants: measured soil gas entry rates and other research results for Canadian houses. Soil and Sediment Contamination, 6(1): 9-13.

Garbesi, K. and Sextro, R.G., 1989. Modeling and field evidence of pressure-driven entry of soil gas into a house through permeable below-grade walls. ES and T Contents, 23(12): 1481-1487.

Gargini, A., Pasini M., Picone S., Rijnaarts H. and Gaans van, P., 2010. Chlorinated hydrocarbons plumes in a residential area. Site investigation to assess indoor vapor intrusion and human health risks. In: S. Saponaro, E. Sezenna and L. Bonomo (Editors), Vapor Emission to Outdoor Air and Enclosed Spaces for Human Health Risk Assessment: Site Characterization, Monitoring and Modeling. Nova Publisher, pp. 211- 233.

Gargini, A., Pasini M., Tentoni P. and Aravena, R., 2006. Un singolare plume di cloruro di vinile in acquifero confinato: campionamento a basso flusso in sondaggi direct-push e fingerprinting isotopico preliminare. Ingegneria e Geologia degli Acquiferi, 21: 47-60.

Gennaro, V., Ceppi, M., Crosignani, P. and Montanaro, F., 2008. Reanalysis of updated mortality among vinyl and polyvinyl chloride workers: Confirmation of historical evidence and new findings. BMC Public Health, 8.

Goss, K., 2006. Prediction of the temperature dependency of Henry's law constant using poly-parameter linear free energy relationships. Chemosphere, 64(8): 1369-1374.

Gossett, J.M., 2010. Sustained aerobic oxidation of vinyl chloride at low oxygen concentrations. Environmental Science and Technology, 44(4): 1405-1411.

Graham, D.W., Korich, D.G., LeBlanc, R.P., Sinclair, N.A. and Arnold, R.G., 1992. Applications of a colorimetric plate assay for soluble methane monooxygenase activity. Applied and Environmental Microbiology, 58(7): 2231-2236.

Gray, T.R.G., Baxby, P., Hill, I.R. and Goodfellow, M., 1968. Direct observation of bacteria in soil. In: T.R.G. Gray and D. Parkinson (Editors), The Ecology of Soil Bacteria. University of Toronto Press, Toronto, pp. 171-192.

Grosse, Y., Baan, R., Straif, K., Secretan, B., El Ghissassi, F., Bouvard, V., Altieri, A., Cogliano, V., 2007. Carcinogenicity of 1,3-butadiene, ethylene oxide, vinyl chloride, vinyl fluoride, and vinyl bromide. The Lancet Oncology, 8(8): 679-680.

Hamamoto, S., Moldrup, P., Kawamoto, K. and Komatsu, T., 2009. Effect of particle size and soil compaction on gas transport parameters in variably saturated, sandy soils. Vadose Zone Journal, 8(4): 986-995.

Hansen, K.C., Zhou, Z., Yaws, C.L. and Aminabhavi, T.M., 1993. Determination of Henry's law constants of organics in dilute aqueous solutions. Journal of Chemical and Engineering Data 38 (4): 546-550.

Hanzel, J., Thullner, M., Harms, H. and Wick, L.Y., 2011. Microbial growth with vapor-phase substrate. Environmental Pollution, 159(4): 858-864.

Harms, H. and Bosma, T.N.P., 1997. Mass transfer limitation of microbial growth and pollutant degradation. Journal of Industrial Microbiology and Biotechnology, 18(2-3): 97-105.

Harms, H. and Zehnder, A.J.B., 1994. Influence of substrate diffusion on degradation of dibenzofuran and 3- chlorodibenzofuran by attached and suspended bacteria. Applied and Environmental Microbiology, 60(8): 2736-2745.

Hartmans, S., de Bont, J.A.M., Tramper, J. and Luyben, K.C.A.M., 1985. Bacterial degradation of vinyl chloride. Biotechnology Letters, 7(6): 383-388.

Hartmans, S. and De Bont, J.A.M., 1992. Aerobic vinyl chloride metabolism in Mycobacterium aurum LI. Applied and Environmental Microbiology, 58(4): 1220-1226.

He, J., Ritalahti, K.M., Aiello, M.R. and Loeffler, F.E., 2003. Complete detoxification of vinyl chloride by an anaerobic enrichment culture and identification of the reductively dechlorinating population as a Dehalococcoides species. Applied and Environmental Microbiology, 69(2): 996-1003.

He, J., Sung, Y., Krajmalnik-Brown, R., Ritalahti, K.M. and Loeffler, F.E., 2005. Isolation and characterization of Dehalococcoides sp. strain FL2, a trichloroethene (TCE)- and 1,2-dichloroethene-respiring anaerobe. Environmental Microbiology, 7(9): 1442-1450.

Heijthuijsen, J.H.F.G. and Hansen, T.A., 1986. Interspecies hydrogen transfer in co-cultures of methanol-utilizing acidogens and sulfate-reducing or methanogenic bacteria. FEMS Microbiology Letters, 38(1): 57-64.

Hendrickx, B., Junca, H., Vosahlova, J., Lindner A., Rüegg, I., Bucheli-Witschel, M., Faber, F., Egli, T., Mau, M., Schlömann, M., Brennerova, M., Brenner, V., Pieper, D.H., Top, E.M., Dejonghe, W., Bastiaens, L., Springael, D., 2006. Alternative primer sets for PCR detection of genotypes involved in bacterial aerobic BTEX degradation: distribution of the genes in BTEX degrading isolates and in subsurface soils of a BTEX contaminated industrial site. Journal of Microbiological Methods, 64(2): 250-265.

Hers, I., Atwater, J., Li, L. and Zapf-Gilje, R., 2000. Evaluation of vadose zone biodegradation of BTX vapours. Journal of Contaminant Hydrology, 46(3-4): 233-264.

Hers, I., Zapf-Gilje, R., Johnson, P.C. and Li, L., 2003. Evaluation of the Johnson and Ettinger model for prediction of indoor air quality. Ground Water Monitoring and Remediation, 23(1): 62-76.

Hers, I., Zapf-Gilje, R., Li, L. and Atwater, J., 2001. The use of indoor air measurements to evaluate intrusion of subsurface VOC vapors into buildings. Journal of the Air and Waste Management Association, 51(9): 1318-1331.

Hoehener, P., Duwig, C., Pasteris, G., Kaufmann, K., Dakhel, N., and Harms, H., 2003. Biodegradation of petroleum hydrocarbon vapors: Laboratory studies on rates and kinetics in unsaturated alluvial sand. Journal of Contaminant Hydrology, 66(1-2): 93-115.

Hoehener, P., Dakhel, N., Christophersen, M., Broholm, M. and Kjeldsen, P., 2006. Biodegradation of hydrocarbons vapors: Comparison of laboratory studies and field investigations in the vadose zone at the emplaced fuel source experiment, Airbase Værløse, Denmark. Journal of Contaminant Hydrology, 88(3-4): 337-358.

Hoehener, P., 2010. Determination of aerobic degradation rates and kinetics of gaseous hydrocarbons in soil In: K.N. Timmis and J.R. Van der Meer (Editors), Handbook of hydrocarbons and lipids microbiology Springer-Verlag, Heidelberg, DE.

Holden, P.A., Hunt, J.R. and Firestone, M.K., 1997. Toluene diffusion and reaction in unsaturated Pseudomonas putida biofilms. Biotechnology and Bioengineering, 56(6): 656-670.

Holden, P.A., Hersman, L.E. and Firestone, M.K., 2001. Water content mediated microaerophilic toluene biodegradation in arid vadose zone materials. Microbial Ecology, 42(3): 256-266.

Holden, P.A. and Fierer, N., 2005. Microbial processes in the vadose zone. Vadose Zone Journal, 4: 1-21.

Hunt, J.R., Sitar, N. and Udell, K.S., 1988. Nonaqueous phase liquid transport and cleanup. 1. Analysis of mechanisms. Water Resources Research, 24(8): 1247-1258.

IARC, 1979. Vinyl Chloride, Polyvinyl Chloride and Vinyl Chloride-Vinyl Acetate Copolymers. International Agency for Research on Cancer (IARC) - Summaries and Evaluations. Report n. 19.

IARC, 1987. Benzene. International Agency for Research on Cancer (IARC). Report n. 7.

IARC, 1995. Dry Cleaning, some chlorinated solvents and other industrial chemicals. Summary of Data Reported and Evaluation. International Agency for Research on Cancer (IARC). Report n.63.

Ilstedt U., Nordgren A. and A., M., 2000. Optimum soil water for soil respiration before and after amendment with glucose in humid tropical acrisols and a boreal mor layer. Soil Biology and Biochemistry, 32: 1591-1599.

Indulski, J.A., Sinczuk-Walczak, H., Szymczak, M. and Wesolowski, W., 1996. Neurological and neurophysiological examinations of workers occupationally exposed to organic solvent mixtures used in the paint and varnish production. International Journal of Occupational Medicine and Environmental Health, 9(3): 235-244.

Inoue, A. and Horikoshi, K., 1991. Estimation of solvent-tolerance of bacteria by the solvent parameter log P. Journal of Fermentation and Bioengineering, 71(3): 194-196.

Ivens, E., 2010. Risk communication and risk management at vapor intrusion sites - Ignore at your own risk. Air and Waste Management Association - Vapor Intrusion 2010, Chicago, US, pp. 126-154.

Janssen, M.P.M., 2003. Modeling ventilation and radon in new Dutch dwellings. Indoor Air, 13(2): 118-127.

Jewell, K.P. and Wilson, J.T., 2011. A new screening method for methane in soil gas using existing groundwater monitoring wells. Ground Water Monitoring and Remediation, 31(3): 82-94.

Jin, Y., Streck, T. and Jury, W.A., 1994. Transport and biodegradation of toluene in unsaturated soil. Journal of Contaminant Hydrology, 17(2): 111-127.

Jin, Y.O. and Mattes, T.E., 2010. A quantitative PCR assay for aerobic, vinyl chloride- and ethene-assimilating microorganisms in groundwater. Environmental Science and Technology, 44(23): 9036-9041.

Johnson, P.C. and Ettinger, R., 1991. Heuristic model for predicting the intrusion rate of contaminant vapors into buildings. Environmental Science and Technology, 25(8): 1445-1452.

Johnson, P.C., Kemblowski, M.W. and Johnson, R.L., 1999. Assessing the significance of subsurface contaminant vapor migration to enclosed spaces: site-specific alternatives to generic estimates. Soil and Sediment Contamination, 8(3): 389-421.

Johnson, R.L. and Pankow, J.F., 1992. Dissolution of dense chlorinated solvents into groundwater. 2. Source functions for pools of solvent. Environmental Science and Technology, 26(5): 896-901.

Jury, W.A., Spencer, W.F. and Farmer, W.J., 1983. Behavior assessment model for trace organics in soil: I. Model description. Journal of Environmental Quality, 12(4): 558-564.

Jury, W.A., Farmer, W.J. and Spencer, W.F., 1984a. Behavior assessment model for trace organics in soil: II. Chemical classification and parameter sensitivity. Journal of Environmental Quality, 13(4): 567-572.

Jury, W.A., Spencer, W.F. and Farmer, W.J., 1984b. Behavior assessment model for trace organics in soil: IV. Review of experimental evidence. Journal of Environmental Quality, 13(4): 580-586.

Jury, W.A., Spencer, W.F. and Farmer, W.J., 1984c. Behavior assessment model for trace organics in soil: III. Application of screening model. Journal of Environmental Quality, 13(4): 573-579.

Jury, W.A., Russo, D., Streile, G. and El Abd, H., 1990. Evaluation of volatilization by organic chemicals residing below the soil surface. Water Resources Research, 26(1): 13-20.

Kao, C.M. and Prosser, J., 1999. Intrinsic bioremediation of trichloroethylene and chlorobenzene: Field and laboratory studies. Journal of Hazardous Materials, 69(1): 67-79.

Kazumi, J., Caldwell, M.E., Suflita, J.M., Lovley, D.R. and Young, L.Y., 1997. Anaerobic degradation of benzene in diverse anoxic environments. Environmental Science and Technology, 31(3): 813-818.

Kelly, W.R., Hornberger, G.M., Herman, J.S. and Mills, A.L., 1996. Kinetics of BTX biodegradation and mineralization in batch and column systems. Journal of Contaminant Hydrology, 23(1-2): 113-132.

Khan, K.S. and Joergensen, R.G., 2006. Microbial C, N, and P relationships in moisture-stressed soils of Potohar, Pakistan. Journal of Plant Nutrition and Soil Science, 169(4): 494-500.

Klenk, I.D. and Grathwohl, P., 2002. Transverse vertical dispersion in groundwater and the capillary fringe. Journal of Contaminant Hydrology, 58(1-2): 111-128.

Koorevaar, P., Menelik, G. and Dirksen, C., 1983. Elements of Soil Physics. Developments in soil sciences, 13. Elsevier, Amsterdam, NL, 229 pp.

Kristensen, A.H., Poulsen, T.G., Mortensen, L. and Moldrup, P., 2010. Variability of soil potential for biodegradation of petroleum hydrocarbons in a heterogeneous subsurface. Journal of Hazardous Materials, 179(1-3): 573-580.

Krylov, V.V. and Ferguson, C.C., 1998. Contamination of indoor air by toxic soil vapours : The effects of subfloor ventilation and other protective measures. Building and Environment, 33(6): 331-347.

Kurtz, J.P., Wolfe, E.M., Woodland, A.K. and Foster, S.J., 2010. Evidence for increasing indoor sources of 1,2-dichloroethane since 2004 at two Colorado residential vapor intrusion sites. Ground Water Monitoring and Remediation, 30(3): 107-112.

Lahvis, M.A., 2005. Evaluation of potential vapor transport to indoor air associated with small-volume releases of oxygenated gasoline in the vadose zone. API Soil and Groundwater Research Bulletin (21): 1-4.

Lahvis, M.A. and Baehr, A.L., 1998. Documentation of R-UNSAT. A computer model for the simulation of reactive transport in the unsaturated zone U.S Geological Survey.

Lahvis, M.A., Baehr, A.L. and Baker, R.J., 1999. Quantification of aerobic biodegradation and volatilization rates of gasoline hydrocarbons near the water table under natural attenuation conditions. Water Resources Research, 35(3): 753-765.

Lee, P.K.H., Macbeth, T.W., Sorenson Jr, K.S., Deeb, R.A. and Alvarez-Cohen, L., 2008. Quantifying genes and transcripts to assess the in situ physiology of Dehalococcoides spp. in a trichloroethene-contaminated groundwater site. Applied and Environmental Microbiology, 74(9): 2728-2739.

Lee, S.K. and Lee, S.B., 2001. Isolation and characterization of a thermotolerant bacterium Ralstonia sp. strain PHS1 that degrades benzene, toluene, ethylbenzene, and o-xylene. Applied Microbiology and Biotechnology, 56(1-2): 270-275.

Lenhard, R.J., Parker, J.C. and Mishra, S., 1989. On the correspondance between Brooks-Corey and Van Genuchten models. Journal of Irrigation and Drainage Engineering, 115(4): 744-751.

Linn, D.M. and Doran, J.W., 1984. Effect of water-filled pore space on carbon dioxide and nitrous oxide production in tilled and not tilled soils. Soil Science Society of America Journal, 48(6): 1267-1272.

Little, J.C., Daisey, J.M. and Nazaroff, W.W., 1992. Transport of subsurface contaminants into buildings. Environmental Science and Technology, 26(11): 2058-2066.

Lorah, M.M. and Voytek, M.A., 2004. Degradation of 1,1,2,2-tetrachloroethane and accumulation of vinyl chloride in wetland sediment microcosms and in situ porewater: biogeochemical controls and associations with microbial communities. Journal of Contaminant Hydrology, 70(1-2): 117-145.

Loureiro, C.O., Abriola, L.M., Martin, G.E. and Sextro, R.G., 1990. Three-dimensional simulation of radon transport into houses with basements under constant negative pressure. Environmental Science and Technology, 24(9): 1338-1348.

Lowry, O.H., Rosebrough, N.J., Farr, A.L. and Randall, R.J., 1951. Protein measurement with the Folin phenol reagent. The Journal of Biological Chemistry, 193(1): 265-275.

Lundegard, P.D. and Johnson, P.C., 2004. A composite plume approach for the analysis of dissolved contaminants in ground water vs. distance from source areas. Ground Water Monitoring and Remediation, 24(3): 69-75.

Lundegard, P.D., Johnson, P.C. and Dahlen, P., 2008. Oxygen transport from the atmosphere to soil gas beneath a slab-on-grade foundation overlying petroleum-impacted soil. Environmental Science and Technology, 42(15): 5534-5540.

Luo, H., Dahlen, P., Johnson, P.C., Peargin, T. and Creamer, T., 2009. Spatial variability of soil-gas concentrations near and beneath a building overlying shallow petroleum hydrocarbon-impacted soils. Ground Water Monitoring and Remediation, 29(1): 81-91.

Maier, R.M., Pepper, I.L. and Gerba, C.P., 2000. Environmental Microbiology. Academic Press, San Diego, US.

Malachowsky, K.J., Phelps, T.J., Teboli, A.B., Minnikin, D.E. and White, D.C., 1994. Aerobic mineralization of trichloroethylene, vinyl chloride, and aromatic compounds by Rhodococcus species. Applied and Environmental Microbiology, 60(2): 542-548.

Malina, G., Grotenhuis, J.T.C., Rulkens, W.H., Mous, S.L.J. and De Wit, J.C.M., 1998. Soil vapour extraction versus bioventing of toluene and decane in bench-scale soil columns. Environmental Technology, 19(10): 977-991.

Marinelli, F. and Durnford, D.S., 1996. LNAPL thickness in monitoring wells considering hysteresis and entrapment. Ground Water, 34(3): 405-414.

Massmann, J. and Farrier, D.F., 1992. Effects of atmospheric pressure on gas transport in the vadose zone. Water Resources Research, 28: 777-791.

Mayer, A.S. and Hassanizadeh, S.M. (Editors), 2005. Soil and groundwater contamination: Nonaqueous Phase Liquids - principles and observations. Water Resources Monograph Series, 17. American Geophysical Union, Washington, US, 216 pp.

Maymo-Gatell, X.C., Y.-T.; Gossett, J. M.; Zinder, S. H., 1997. Isolation of a bacterium that reductively dechlorinates tetrachloroethene to ethene. Science 276: 1568-1571.

McAlary, T., Provoost, J. and Dawson, H.E., 2011. Vapor Intrusion. In: F.A. Swartjes (Editor), Dealing with contaminated sites. From theory towards practical application. Springer, Dordrecht, NL.

McCarthy, K.A. and Johnson, R.L., 1993. Transport of volatile organic compounds across the capillary fringe. Water Resources Research, 29(6): 1675-1683.

McDonald, G.J. and Wertz, W.E., 2007. PCE, TCE, and TCA vapors in subslab soil gas and indoor air: A case study in upstate New York. Ground Water Monitoring and Remediation, 27(4): 86-92.

McHugh, T., Conor, A.J. and Ahmad, F., 2004. An empirical analysis of the groundwater-to-indoor-air exposure pathway: the role of background concentrations in indoor air. Environmental Forensic, 5: 33-44.

McHugh, T.E., De Blanc, P.C. and Pokluda, R.J., 2006. Indoor air as a source of VOC contamination in shallow soils below buildings. Soil and Sediment Contamination, 15(1): 103-122.

McHugh, T. Davis, R., Devaull, G., Hopkins, H., Menatti, J., Peargin, T., 2010. Evaluation of vapor attenuation at petroleum hydrocarbon sites: considerations for site screening and investigation. Soil and Sediment Contamination, 19(6): 725-745.

McHugh, T., Kuder, T., Fiorenza, S., Gorder, K., Dettenmaier, E., Philp, P., 2011.Application of CSIA to distinguish between vapor intrusion and indoor sources of VOCs. Environmental Science and Technology, 45(14): 5952-5958.

Melnick, R.L., 2002. Carcinogenicity and mechanistic insights on the behavior of epoxides and epoxide-forming chemicals. Annals of the New York Academy of Sciences, pp. 177-189.

Mendoza, C.A. and Frind, E.O., 1990a. Advective-dispersive transport of dense organic vapors in the unsaturated zone. 1. Model development. Water Resources Research, 26(3): 379-387.

Mendoza, C.A. and Frind, E.O., 1990b. Advective-dispersive transport of dense organic vapors in the unsaturated zone. 2. Sensitivity analysis. Water Resources Research, 26(3): 388-398.

Mendoza, C.A. and McAlary, T.A., 1990. Modeling of ground-water contamination caused by organic solvent vapors. Ground Water, 28(2): 199-206.

Mercer, J.W. and Cohen, R.M., 1990. A review of immiscible fluids in the subsurface: properties, models, characterization and remediation. Journal of Contaminant Hydrology, 6(2): 107-163.

Mihelcic, J.R. and Luthy, R.G., 1991. Sorption and microbial degradation of naphthalene in soil-water suspensions under denitrification conditions. Environmental Science and Technology, 25(1): 169-177.

Millington, R.J. and Quirk, J.P., 1959. Permeability of porous media. Nature, 183(4658): 387-388.

Mills, W., Liu, S., Rigby, M.C. and Brenner, D., 2007. Time-variable simulation of soil vapor intrusion into a building with a combined crawl space and basement. Environmental Science and Technology, 41(14): 4993-5001.

Molinari, F., Boldrini, G., Severi, P., Dugoni, G., Rapti Caputo, D., Martinelli, G., 2007. Risorse idriche sotterranee della Provincia di Ferrara. DB-MAP, Firenze, IT.

Molins, S., Mayer, K.U., Amos, R.T. and Bekins, B.A., 2010. Vadose zone attenuation of organic compounds at a crude oil spill site - Interactions between biogeochemical reactions and multicomponent gas transport. Journal of Contaminant Hydrology, 112(1-4): 15-29.

MPA, 2010. Investigation requirements for ethanol blended fuel releases. Petroleum Remediation Program. Minnesota Pollution Control Agency, US.

Mualem, Y., 1976. A new model for predicting the hydraulic conductivity of unsaturated porous media. Water Resources Research, 12: 513-522.

Murphy, B.L. and Chan, W.R., 2011. A multi-compartment mass transfer model applied to building vapor intrusion. Atmospheric Environment, 45(37): 6650-6657.

Nazaroff, W.W., Lewis, S.R., Doyle, S.M., Moed, B.A. and Nero, A.V., 1987. Experiments on pollutant transport from soil into residential basements by pressure-driven airflow. Environmental Science and Technology, 21(5): 459-466.

Nazaroff, W.W. and Cass, G.R., 1989. Mathematical modeling of indoor aerosol dynamics. Environmental Science and Technology, 23(2): 157-166.

Niederlehner, B.R., Cairns Jr, J. and Smith, E.P., 1998. Modeling acute and chronic toxicity of nonpolar narcotic chemicals and mixtures to Ceriodaphnia dubia. Ecotoxicology and Environmental Safety, 39(2): 136-146.

Nielsen, P.H., Bjerg, P.L., Nielsen, P., Smith, P. and Christensen, T.H., 1996. In situ and laboratory determined first-order degradation rate constants of specific organic compounds in an aerobic aquifer. Environmental Science and Technology, 30(1): 31-37.

Ochiai, N., Daishima, S. and Cardin, D.B., 2003. Long-term measurement of volatile organic compounds in ambient air by canister-based one-week sampling method. Journal of Environmental Monitoring, 5(6): 997-1003.

Olson, D.A. and Corsi, R.L., 2001. Characterizing exposure to chemicals from soil vapor intrusion using a two-compartment model. Atmospheric Environment, 35(24): 4201-4209.

Ong, S.K. and Lion, L.W., 1991. Effects of soil properties and moisture on the sorption of trichloroethylene vapor. Water Research, 25(1): 29-36.

Oostrom, M., Rockhold, M.L., Thorne, P.D., Truex, M.J., Last G.V., and Rohay, V.J., 2007. Carbon tetrachloride flow and transport in the subsurface of the 216-Z-9 trench at the Hanford Site. Vadose Zone Journal, 6(4): 971-984.

Or, D., Smets, B.F., Wraith, J.M., Dechesne, A. and Friedman, S.P., 2007. Physical constraints affecting bacterial habitats and activity in unsaturated porous media - a review. Advances in Water Resources, 30(6-7): 1505-1527.

Ostendorf, D.W. and Kampbell, D.H., 1991. Biodegradation of hydrocarbon vapors in the unsaturated zone. Water Resources Research, 27(4): 453-462.

Otte, P.F., Lijzen J.P., Mennen, M.G. and Spijker, J., 2007. Richlijn voor luchtmetingen voor de risicobeoordeling van bodemverontreiniging. 711701048, RIVM - National Institute for Public Health and The Environment, Bilthoven, NL.

Parker, J.C., 2002. Modeling volatile chemical transport, biodecay, and emission to indoor air. Ground Water Monitoring and Remediation, 23(1): 107-120.

Parker, J.C., 2003. Physical processes affecting natural depletion of volatile chemicals in soil and groundwater. Vadose Zone Journal, 2: 222-230.

Pasini, M., Gargini, A., Aravena, R. and Hunkeler, D., 2008. Use of hydrogeological and geochemical methods to investigate the origin and fate of vinyl chloride in groundwater in an urban environment, Ferrara, Italy. In: M.G. Tefry (Editor), Groundwater qualty: securing groundwater quality in urban and industrial environments. IAHS pp. 102-109.

Pasteris, G., Werner, D., Kaufmann, K. and Hoehener, P., 2002. Vapor phase transport and biodegradation of volatile fuel compounds in the unsaturated zone: A large scale lysimeter experiment. Environmental Science and Technology, 36(1): 30-39.

Patterson, B.M. and Davis, G.B., 2009. Quantification of vapor intrusion pathways into a slab-on-ground building under varying environmental conditions. Environmental Science and Technology, 43(3): 650-656.

Picone, S., Gaans van, P. and Rijnaarts, H., 2007. Preliminary risk assessment at Via Caretti, Ferrara, Italy. TNO Report U-R1002/A

Plumb, I.R., 1991. The occurrence of appendix IX organic constituents in disposal site groundwater. Groundwater Monitoring and Remediation, 11(2): 157 - 164.

Popovicova, J. and Brusseau, M.L., 1997. Dispersion and transport of gas-phase contaminants in dry porous media: Effect of heterogeneity and gas velocity. Journal of Contaminant Hydrology, 28(1-2): 157-169.

Popovicova, J. and Brusseau, M.L., 1998. Contaminant mass transfer during gas-phase transport in unsaturated porous media. Water Resources Research, 34(1): 83-92.

Potts, M., 1994. Desiccation tolerance of Prokaryotes. Microbiological Reviews, 58(4): 755-805.

Poulsen, M., Lemon, L. and Barker, J.F., 1992. Dissolution of monoaromatic hydrocarbons into groundwater from gasoline- oxygenate mixtures. Environmental Science and Technology, 26(12): 2483-2489.

Powelson, D.K. and Mills, A.L., 1996. Bacterial enrichment at the gas-water interface of a laboratory apparatus. Applied and Environmental Microbiology, 62(7): 2593-2597.

Prenafeta-Boldu', F.X., Ballerstedt, H., Gerritse, J. and Grotenhuis, J.T.C., 2004. Bioremediation of BTEX hydrocarbons: Effect of soil inoculation with the toluene-growing fungus Cladophialophora sp. strain T1. Biodegradation, 15(1): 59-65.

Provoost, J., Reijnders, L., Swartjes, F., Bronders, J., Seuntjens, P., Lijzen, J., 2009. Accuracy of seven vapour intrusion algorithms for VOC in groundwater. Journal of Soil and Sediments, 9: 62-73.

Provoost, J., Bosman, A., Reijnders, L., Bronders, J., Touchant, K., Swartjes, F., 2010. Vapour intrusion from the vadose zone - seven algorithms compared. Journal of Soil and Sediments, 10: 473-483.

Rathfelder, K.M., Lang, J.R. and Abriola, L.M., 2000. A numerical model (MISER) for the simulation of coupled physical, chemical and biological processes in soil vapor extraction and bioventing systems. Journal of Contaminant Hydrology, 43(3-4): 239-270.

Reardon, K.F., Mosteller, D.C. and Bull Rogers, J.D., 2000. Biodegradation kinetics of benzene, toluene, and phenol as single and mixed substrates for Pseudomonas putida F1. Biotechnology and Bioengineering, 69(4): 385-400.

Regione Emilia Romagna&ENI-AGIP, 1998. Riserve idriche sotterranee della Regione Emilia Romagna., Firenze, IT.

Rijnaarts, H.H.M., Bachmann, A., Jumelet, J.C. and Zehnder, A.J.B., 1990. Effect of desoprtion and intraparticle mass transfer on the aerobic biomineralization of α-Hexachlorocyclohexane in a contaminated calcareous soil. Environmental Science and Technolgy, 24: 1349-1354.

Rijnaarts, H.H.M., Norde, W., Bouwer, E.J., Lyklema, J. and Zehnder, A.J.B., 1993. Bacterial adhesion under static and dynamic conditions. Applied and Environmental Microbiology, 59(10): 3255-3265.

Rivett, M.O., Wealthall, G.P., Dearden, R.A. and McAlary, T.A., 2011. Review of unsaturated-zone transport and attenuation of volatile organic compound (VOC) plumes leached from shallow source zones. Journal of Contaminant Hydrology, 123(3-4): 130-156.

Rodrigues, S.M., Pereira, M.E., Ferreira da Silva, E., Hursthouse, A.S. and Duarte, A.C., 2009. A review of regulatory decisions for enviornmental protection: Part I - Challenges in the implementation of national soil policies. Environment International, 35: 202-213.

Roels, J.A. and Kossen, N.W.F., 1978. On the modelling of microbial metabolism. In: M.J. Bull (Editor), Progress in industrial microbiology. Elsevier, Amsterdam, NL, pp. 95-203.

Ruiz-Aguilar, G.M.L., O'Reilly, K.T. and Alvarez, P.J.J., 2003. A comparison of benzene and toluene plume lengths for sites contaminated with regular vs. ethanol-amended gasoline. Ground Water Monitoring and Remediation, 23(1): 48-53.

Russel Bouling, I. and Ginn, J.S., 2003. Practical handbook of soil, vadose zone, and groundwater contamination: assessment, prevention and remediation. CRC Press, Boca Raton, US, 691 pp.

Sanders, P.F. and Hers, I., 2006. Vapor intrusion in homes over gasoline-contaminated ground water in Stafford, New Jersey. Ground Water Monitoring and Remediation, 26(1): 63-72.

Sanders, P.F. and Stern, A.H., 1994. Calculation of soil cleanup criteria for carcinogenic volatile organic compounds as controlled by the soil-to-indoor air exposure pathway. Environmental Toxicology and Chemistry, 13(8): 1367-1373.

Sanders, P.F. and Talimcioglu, N.M., 1997. Soil-to-indoor air exposure models for volatile organic compounds: the effect of soil moisture. Environmental Toxicology and Chemistry, 16(12): 2597-2604.

Schaefer, A. and Bouwer, E.J., 2000. Toluene induced cometabolism of cis-1,2-dichloroethylene and vinyl chloride under conditions expected downgradient of a permeable Fe(0) barrier. Water Research, 34(13): 3391-3399.

Schaefer, A., Harms, H. and Zehnder, A.J.B., 1998. Bacterial accumulation at the air-wate interface. Enviromental Science and Technolgy, 32: 3704-3712.

Schjønning, P., Thomsen, I.K., Moldrup, P. and Christensen, B.T., 2003. Linking soil microbial activity to water- and air-phase contents and diffusivities. Soil Science Society of America Journal, 67(1): 156-165.

Schoefs, O., Perrier, M. and Samson, R., 2004. Estimation of contaminant depletion in unsaturated soils using a reduced-order biodegradation model and carbon dioxide measurement. Applied Microbiology and Biotechnology, 64: 53-61.

Schulze-Makuch, D., 2005. Longitudinal dispersivity data and implications for scale behavior. Groundwater, 43(3): 443-456.

Scow, K.M. and Hutson, J., 1992. Effect of diffusion and sorption on the kinetics of biodegradation: theoretical considerations. Soil Science Society of America Journal, 56(1): 119-127.

Sen, T.K., 2011. Processes in pathogenic biocolloidal contaminants transport in saturated and unsaturated porous media: A review. Water, Air, and Soil Pollution, 216(1-4): 239-256.

Serrano, A. and Gallego, M., 2004. Direct screening and confirmation of benzene, toluene, ethylbenzene and xylenes in water. Journal of Chromatography A, 1045(1-2): 181-188.

Shim, H. and Yang, S.T., 1999. Biodegradation of benzene, toluene, ethylbenzene, and o-xylene by a coculture of Pseudomonas putida and Pseudomonas fluorescens immobilized in a fibrous-bed bioreactor. Journal of Biotechnology, 67(2-3): 99-112.

Silliman, S.E., Berkowitz, B., Simunek, J. and Van Genuchten, M.T., 2002. Fluid flow and solute migration within the capillary fringe. Ground Water, 40(1): 76-84.

Simunek, J., Kodesova, R., Gribb, M.M. and Van Genuchten, M.T., 1999. Estimating hysteresis in the soil water retention function from cone permeameter experiments. Water Resources Research, 35(5): 1329-1345.

Skopp, J., Jawson, M.D. and Doran, J.W., 1990. Steady-state aerobic microbial activity as a function of soil water content. Soil Science Society of America Journal, 54(6): 1619-1625.

Smith, J.A., Chiou, C.T., Kammer, J.A. and Kile, D.E., 1990. Effect of soil moisture on the sorption of trichloroethene vapor to vadose-zone soil at picatinny arsenal, New Jersey. Environmental Science and Technology, 24(5): 676-683.

Stark, J.M. and Firestone, M.K., 1995. Mechanisms for soil moisture effects on activity of nitrifying bacteria. Applied and Environmental Microbiology, 61(1): 218-221.

Staudinger, J. and Roberts, P.V., 2001. A critical compilation of Henry's law constant temperature dependence relations for organic compounds in dilute aqueous solutions. Chemosphere, 44(4): 561-576.

Stefani, M. and Vincenzi, S., 2005. The interplay of eustasy, climate and human activity in the late Quaternary depositional evolution and sedimentary architecture of the Po Delta system. Marine Geology, 222-223(1-4): 19-48.

Stoop, P., Glastra, P., Hiemstra, Y., de Vries, L. and Lembrechts, J., 1998. Results of the second Dutch national survey on radon in dwellings. 610058006, RIVM - National Institute for Public Health and The Environment, Bilthoven, NL.

Stotzky, G., 1972. Activity, ecology, and population dynamics of microorganisms in soil. CRC critical reviews in microbiology, 2(1): 59-137.

Suarez, M. and Rifai, H., 1999. Biodegradation rates for fuel hydrocarbons and chlorinated solvents in groundwater.Bioremediation Journal, 3(4): 337-362.

Swartjes, F., 2011. Approaches towards contaminated site assessment and management. In: F.A. Swartjes (Editor), Dealing with contaminated sites: from theory towards practical application. Springer Science+Business Media B.V., Dordrecht, NL, pp. 64 - 73.

Tas, N., van Eekert, M., Schraa, G., Zhou, J., de Vos, W.M, and Smidt, H., 2009. Tracking functional guilds: Dehalococcoides spp. in European river basins contaminated with hexachlorobenzene. Applied and Environmental Microbiology, 75(14): 4696-4704.

Thomson, N.R., Sykes, J.F. and Van Vliet, D., 1997. A numerical investigation into factors affecting gas and aqueous phase plumes in the subsurface. Journal of Contaminant Hydrology, 28(1-2): 39-70.

Tiehm, A., Schmidt, K.R., Pfeifer, B., Heidinger, M. and Ertl, S., 2008. Growth kinetics and stable carbon isotope fractionation during aerobic degradation of cis-1,2-dichloroethene and vinyl chloride. Water Research, 42(10-11): 2431-2438.

Tillman, J.F.D. and Weaver, J.W., 2007. Temporal moisture content variability beneath and external to a building and the potential effects on vapor intrusion risk assessment. Science of the Total Environment, 379(1): 1-15.

Tindall, J.A., Friedel, M.J., Szmajter, R.J. and Cuffin, S.M., 2005. Part 1: Vadose-zone column studies of toluene (enhanced bioremediation) in a shallow unconfined aquifer. Water, Air, and Soil Pollution, 168(1-4): 325-357.

Turczynowicz, L. and Robinson, N.I., 2001. A model to derive soil criteria for benzene migrating from soil to dwelling interior in homes with crawl spaces. Human and Ecological Risk Assessment, 7(2): 387 - 415.

USEPA, 1999. Compendium method TO-17. Determination of volatile organic compounds in ambient air using active sampling onto sorbent tubes. Cincinnati, US.

USEPA, 2001. Trichloroethylene Health Risk Assessment: synthesis and characterization. External Review Draft, Washington, D.C., US.

USEPA, 2004. User's guide for evaluating vapor intrusion into buildings, Office of Emergency and Remedial Response, Washington, DC., US.

USEPA, 2011. VOCs Technical overview. USEPA, http://www.epa.gov/iaq/voc2.html.

Vaajasaari, K., Joutti, A., Schultz, E., Selonen, S. and Westerholm, H., 2002. Comparisons of terrestrial and aquatic bioassays for oil-contaminated soil toxicity. Journal of Soils and Sediments, 2(4): 194-202.

Van der Sluijs, P. and De Gruijter, J.J., 1985. Water table classes: A method to describe seasonal fluctuation and duration of water tables on Dutch soil maps. Agricultural Water Management, 10(2): 109-125.

Van der Zaan, B., 2010. Monitoring biodegradation capacity of organic pollutants in the environment. PhD Dissertation, Wageningen University, 158 pp.

Van Der Zaan, B., Hannes, F., Hoekstra, N., Rijnaarts, H., de Vos, W.M., Smidt, H. and Gerritse, J., 2010. Correlation of Dehalococcoides 16S rRNA and chloroethene-reductive dehalogenase genes with geochemical conditions in chloroethene-contaminated groundwater. Applied and Environmental Microbiology, 76(3): 843-850.

van Leeuwen, C. and Vermeire, T., 2007. Risk Assessment of Chemicals: an Introduction. Springer, 686 pp.

van Wijnen, H. and Lijzen, J., 2006. Validation of the VOLASOIL model using air measurements from Dutch contaminated sites - Concentrations of four chlorinated compounds. 711701041, RIVM- National Institute for Public Health and The Environment, Bilthoven, NL.

Vegter, J., 2001. Sustainable contaminated land management: a risk-based land management approach. Land Contamination and Reclamation, 9(1): 95-100.

Verce, M.F., Ulrich, R.L. and Freedman, D.L., 2000. Characterization of an isolate that uses vinyl chloride as a growth substrate under aerobic conditions. Applied and Environmental Microbiology, 66(8): 3535-3542.

Vogt, C., Goedeke, S., Treutler, H.C., Weiss, H., Schirmer, H., and Richnow, H.H., 2007. Benzene oxidation under sulfate-reducing conditions in columns simulating in situ conditions. Biodegradation, 18(5): 625-636.

VROM, 2009. Circulaire Bodemsanering 2009. Ministry of Housing, Spatial Planning and the Environment of the Netherlands. Staatscourant 67, 2009.

Waitz, M., Freijer, J.I., Kreule, P. and Swartjes, F.A., 1996. The VOLASOIL risk assessment model based on CSOIL for soils contaminated with volatile compounds. 715810014 RIVM - National Institute for Public Health and The Environment, Bilthoven, NL.

Wan, J. and Wilson, J.L., 1994. Colloid transport in unsaturated porous media. Water Resources Research, 30(4): 857-864.

Wang, G. and Or, D., 2010. Aqueous films limit bacterial cell motility and colony expansion on partially saturated rough surfaces. Environmental Microbiology, 12(5): 1363-1373.

Wang, Y., Merkel, B.J., Li, Y., Ye, H., Fu, S. and Ihm, D., 2007. Vulnerability of groundwater in Quaternary aquifers to organic contaminants: A case study in Wuhan City, China. Environmental Geology, 53(3): 479-484.

Wang, Z., Fingas, M., Blenkinsopp, S., Sergy, G., Landriault, M., Sigouin, L., and Lambert, P., 1998. Study of the 25-year-old Nipisi oil spill: Persistence of oil residues and comparisons between surface and subsurface sediments. Environmental Science and Technology, 32(15): 2222-2232.

Weelink, S.A., Tan, N.C., ten Broeke, H., van Doesburg, W., Langenhoff, A., Gerritse, J., Stams, A.J., 2007. Physiological and phylogenetic characterization of a stable benzene-degrading, chlorate-reducing microbial community. FEMS Microbiology Ecology, 60(2): 312-321.

Weelink, S.A., Tan, N.C., ten Broeke, H., van den Kieboom, C., van Doesburg, W., Langenhoff, A., Gerritse, J., Junca, H., Stams, A.J., 2008. Isolation and characterization of Alicycliphilus denitrificans strain BC, which grows on benzene with chlorate as the electron acceptor. Applied and Environmental Microbiology, 74(21): 6672-6681.

Weelink, S., 2008. Degradation of benzene and other aromatic hydrocarbons by anaerobic bacteria. PhD Dissertation. University of Wageningen, 128 pp.

Werner, D. and Hoehener, P., 2001. The influence of water table fluctuations on the volatilization of contaminants from groundwater. Groundwater Quality: natural and enhanced restoration of groundwater pollution. Proceedings of the Groundwater Quality 2001 Conference, Sheffield, UK, June 200. IAHS Publication n. 275. 2002

White, M. and Oostrom, M., 2004. STOMP: Subsurface Transport Over Multiple Phases, Version 2.0: theory guide. PNNL-12030, Pacific Northwest National Laboratory, Richland, US.

WHO, 1999. Vinyl Chloride (Environmental Health Criteria 215), World Health Organization, Geneva, CH.

Wiedemeier, T.H., Rifai, H. S., Newell, C. J., and Wilson, J. T. , 1999. Natural attenuation of fuels and chlorinated solvents in the subsurface. John Wiley & Sons, New York, US.

Wieslander, G., Norback, D. and Edling, C., 1994. Occupational exposure to water based paint and symptoms from the skin and eyes. Occupational and Environmental Medicine, 51(3): 181-186.

Wisen, T. and Wester-Herber, M., 2007. Dirty soil and clean consciences: Examining communication of contaminated soil. Water, Air, and Soil Pollution, 181(1-4): 173-182.

Witt, M.E., Klecka, G.M., Lutz, E.J., Ei, T.A., Grosso, N.R., Chapelle, F.H., 2002. Natural attenuation of chlorinated solvents at Area 6, Dover Air Force Base: groundwater biogeochemistry. Journal of Contaminant Hydrology, 57(1-2): 61-80.

Yao, Y., Shen, R., Pennell, K.G. and Suuberg, E.M., 2011. Comparison of the Johnson-Ettinger vapor intrusion screening model predictions with full three-dimensional model results. Environmental Science and Technology, 45(6): 2227-2235.

Yaron, B., Calvet, C. and Prost, R., 1996. Soil pollution: processes and dynamics. Springer Verlag, Berlin, 313 pp.

Yu, S., Unger, A.J.A. and Parker, B., 2009. Simulating the fate and transport of TCE from groundwater to indoor air. Journal of Contaminant Hydrology, 107(3-4): 140-161.

Zhang, W.X. and Bouwer, E.J., 1997. Biodegradation of benzene, toluene and naphthalene in soil-water slurry microcosms. Biodegradation, 8(3): 167-175.

List of abbreviations

BDCM	Bromodichloromethane
1,1 DCE	1,1 Dichloroethylene
1,1,2,2 PCA	1,1,2,2 Tetrachloroethane
1,1,2 TCA	1,1,2,2 Trichloroethane
1,2-DCE cis	cis-1,2 Dichloroethylene
1,2-DCE trans	trans-1,2 Dichloroethylene
1,2 DCP	1,2 Dichloropropane
a.s.l.	above sea level
API	American Petroleum Institute
ARPA	Agenzia Regionale Prevenzione e Ambiente (Regional Environmental Protection Agency)
ASTM	American Society for Testing and Materials
ATSDR	Agency for Toxic Substances and Disease Registry
AVG	Average
b.g.l.	below ground level
bp	base pairs
BTEX	Benzene Toluene Ethylbenzene Xylene
cf	capillary fringe
CHC	Chlorinated Hydrocarbons
DNA	Deoxyribonucleic Acid
DNAPL	Dense Non Aqueous Phase Liquid
DSMZ	Deutsche Sammlung fuer Mikroorganismen und Zellculturen (German Collection of Microorganisms and Cell cultures)
E	East
EaCOMT	epoxyalkane coenzyme M transferase
EC	European Commission
ECSA	European Chlorinated Solvent Association
EEA	European Environmental Agency
Eh	Redox potential
etnE	gene encoding for EaCOMT
EuroChlor	European Chloroalkali Industry
FID	Flame Ionization Detector
f_M	mass distribution factor
GC	gas chromatography
H	Henry's Law Constant (dimensionless)
IARC	International Agency for Research on Cancer
IS	Indoor Sampling location
IT	Italy
K_d	Solid Liquid Partitioning Coefficient
K_{oc}	Soil Organic Carbon Partitioning Coefficient
LED	Light Emitting Diode
MAC	Maximum Allowed Concentration in groundwater referring to Italian national standards
MCD	Maximum Concentration Detected
MS	Mass Spectrometry
MtBE	Methyl tert-Butyl Ether
N	North
NAPL	Non Aqueous Phase Liquid
nd	measure below detection limit
NL	Netherlands
OD	Optical Density

PCE	Tetrachloroethylene
PH	Petroleum Hydrocarbons
ppb	part per billion
PVC	Poly Vinyl Chloride
qPCR	quantitative real time Polymerase Chain Reaction
r RNA	Ribosomal ribonucleic Acid
	RIVM Rijksinstituut voor Volksgezondheid en Milieu (National Institute for Public Health and the Environment)
S	South
SG	Soil Gas sampling location
STDEV	Standard Deviation
T (°C)	Temperature (degrees Celsius)
TAC	Tolerable Air Concentration referring to RIVM risk limits
TCE	Trichloroethylene
TNO	Nederlandse Organisatie voor Toegepast Natuurwetenschappelijk Onderzoek (Netherlands Organisation for Applied Scientific Research)
TPH	Total Petroleum Hydrocarbons
TSB	Trypton Soy Broth
UK	United Kingdom
US	United States of America
USEPA	United States Environmental Protection Agency
UV	ultraviolet
VC	Vinyl Chloride
VOC	Volatile Organic Compound
VROM	Ministerie van Volkshuisvesting, Ruimtelijke Ordening en Milieubeheer (Ministry of Housing, Spatial Planning and the Environment, the Netherlands)
W	West
WFP	Water-filled Porosity
WHO	World Health Organization
X	Biomass concentration
Y	Yield

Samenvatting

Wanneer vluchtige componenten van organische verontreinigingen in de ondergrond vanuit de verzadigde zone naar de onverzadigde zone migreren, kan accumulatie van deze vluchtige stoffen in kelders en bovengrondse ruimtes optreden. Dit proces van uitdamping wordt internationaal aangeduid met de term "vapor intrusion". Voor veel verontreinigde locaties vormt uitdamping de belangrijkste blootstellingsroute waardoor humane gezondheidsrisico's kunnen ontstaan. Toch is de inschatting van de mate waarin het proces optreedt omstreden. Vaststelling in het veld wordt bemoeilijkt door twee belangrijke factoren, die bepaald worden door de eigenschappen van de verontreiniging: transport in de onverzadigde zone en biologische afbraak in de onverzadigde zone. De algemeen beschikbare modellen voor uitdamping gaan ofwel voorbij aan relevante veld¬omstandigheden, of zijn juist te complex om op veldschaal te kunnen toepassen. Met name variatie in het vochtgehalte, diffusie in de waterfase, dynamische processen zoals grondwaterstandfluctuaties en biologische afbraak worden niet afdoende meegenomen in de bestaande modellen. Daardoor worden de concentraties van vluchtige verontreinigingen in bodemgas en binnenlucht vaak met meerdere ordegroottes overschat.

Dit proefschrift beschrijft het transport en de biologische afbraak van vluchtige organische stoffen, met name in de aerobe onverzadigde zone. Hoofddoelen waren i) karakterisatie van de transport processen die voor uitdamping van belang zijn, en ii) de kwantificering en mechanistische modelbeschrijving van biologische afbraak in de onverzadigde zone. Door een combinatie van praktische ervaring in veldsituaties, numerieke modellering en laboratorium experimenten konden de afzonderlijke, voor uitdamping relevante processen nader bestudeerd worden.

Als eerste zijn state-of-the-art monitoring technieken en beschikbare analytische modellen toegepast op een locatie waar een vinylchloride verontreiniging in het grondwater mogelijk risico van uitdamping opleverde (Hoofdstuk 2). Voorspelde en waargenomen concentraties in de binnenlucht bleken ordegroottes van elkaar te verschillen. Waarschijnlijk werd de uitdamping route onderbroken door de aanwezigheid van een slecht doorlatende laag en als gevolg van biologische afbraak. Deze factoren konden door de beschikbare risicomodellen niet worden meegenomen.

Vandaar dat vervolgens een één-dimensionaal numeriek model is ontwikkeld, dat een variabel bodemvochtgehalte, biologische afbraak en dynamische processen kan simuleren, om hiermee de effecten van fysische en chemische omstandigheden op uitdamping risico's te onderzoeken (Hoofdstuk 3). Een gevoeligheidsanalyse met dit model toonde aan dat de voorspelde binnenluchtconcentraties werden bepaald door twee factoren: i) het verticale verloop van de verontreinigings¬concentratie in de bodem, gereguleerd door de variatie in waterverzadigde porositeit en ii) aerobe biologische afbraak. Het model is in overeenstemming met eerdere bevindingen en laat zien dat de bijdrage van diffusie door de waterfase varieert met de verticale variatie in het vochtgehalte en dat hierdoor het opwaartse transport van de verontreiniging significant wordt vertraagd.

Voor het bepalen van biologische afbraaksnelheden zijn laboratorium experimenten uitgevoerd met tolueen (Hoofdstuk 4) en vinylchloride (Hoofdstuk 5) onder omstandigheden waarbij zuurstof niet limiterend was. In het geval van

tolueen zijn drie typen experimenten uitgevoerd: batchexperimenten met vloeistofcultures, microkosmos experimenten met onverzadigde bodem en kolomexperimenten met onverzadigde bodem. In het geval van vinylchloride zijn microkosmos en kolomexperimenten vergeleken. Hierbij is een nieuwe moleculaire techniek toegepast voor kwantificering van het functionele gen voor de aerobe stofwisseling van vinylchloride (etnE) in zowel bodem- als watermonsters. De resultaten voor beide stoffen laten zien dat afbraaksnelheden in de waterfase, zoals afgeleid uit batchexperimenten met vloeistofcultures, de rol van biologische afbraak significant onderschatten. De microbiële omzetting in batches met geroerde oplossingen lijkt te worden beperkt door stofoverdracht, in tegenstelling tot wat optreedt onder de omstandigheden van een onverzadigde bodem. In de onverzadigde bodem microkosmos experimenten met tolueen bleek de biologische afbraaksnelheid in de waterfase niet gerelateerd aan het bodemvochtgehalte. Voor vinylchloride daarentegen nam de afbraaksnelheid in de waterfase af met toenemend vochtgehalte. Gepostuleerd wordt dat de invloed van het vochtgehalte op stofoverdracht op de microschaal, afhangt van de chemische stofeigenschappen, die de verdeling over de verschillende fasen in het bodemsysteem bepalen. Moleculaire kwantificering van het etnE gen bleek lineair gecorreleerd met de hoeveelheid vinylchloride die was afgebroken. Dit maakt het een veelbelovende techniek voor toepassing in de praktijk.

De belangrijkste conclusies van dit proefschrift duiden erop dat zowel variatie in bodemvochtgehalte (Hoofdstuk 3) als aerobe biologische afbraak (Hoofdstuk 4 en 5) cruciaal zijn voor een adequate inschatting van uitdamping. Ze kunnen leiden tot een significante inperking van het met opgeloste vluchtige organische verontreinigingen geassocieerde risico. Hieruit kunnen specifieke en relevante aanbevelingen voor het modeleren en monitoren van uitdamping worden afgeleid. Zo zal afbraak in de onverzadigde zone sterk worden onderschat wanneer als modelparameter afbraak¬snelheden worden gebruikt die zijn afgeleid uit batchexperimenten met vloeistofcultures. Het is veel beter om hiervoor afbraak¬snelheden te gebruiken die zijn afgeleid uit experimenten met onverzadigde bodem. Bij veldmetingen moet het verticale verloop in bodemvochtgehalte, zuurstofgehalte en verontreinigingsconcentratie worden bepaald, om op adequate wijze met de voor uitdamping relevante processen rekening te kunnen houden.

Sintesi

La contaminazione di suoli ed acque sotterranee da composti organici volatili può generare intrusione ed accumulo di vapori inquinanti all'interno degli edifici (vapor intrusion). Nonostante questo processo rappresenti in molti casi la principale causa di potenziali rischi per la salute umana nei siti contaminati, le specifiche metodologie di valutazione sono controverse.

L'analisi di rischio basata sul monitoraggio in-situ risulta di difficile interpretazione a causa dell'interazione tra due processi che hanno luogo nella zona insatura, entrambi controllati dalle proprietà specifiche del contaminante: trasporto e biodegradazione. I modelli di analisi di rischio disponibili non includono alcune proprietà sito specifiche significative, o, d'altro canto, risultano troppo complessi per essere applicabili a questa scala di indagine. Nello specifico, le variazioni del grado di saturazione in acqua del suolo, la diffusione in fase liquida ed i processi dinamici come le oscillazioni della tavola d'acqua non sono adeguatamente considerati. Ne risulta che frequentemente le concentrazioni nel soil gas e nell'aria indoor calcolate dai modelli disponibili sovrastimano di diversi ordini di grandezza le concentrazioni misurate.

Questa tesi riguarda i processi di trasporto e biodegradazione di contaminanti organici volatili nella zona insatura, con particolare riguardo a situazioni di zona insatura in condizioni aerobiche. Gli obiettivi principali sono: i) la caratterizzazione dei processi che influenzano più significativamente l'intrusione di vapori; ii) la quantificazione e la descrizione meccanicistica della biodegradazione in suoli insaturi. La metodologia applicata ha previsto l'applicazione di monitoraggio in-situ, modellazione numerica ed esperimenti di laboratorio per discernere i processi ed i parametri più rilevanti.

In primo luogo, tecniche di monitoraggio all'avanguardia e modelli di analisi di rischio disponibili sono stati applicati ad un sito in cui la contaminazione delle acque sotterranee da cloruro di vinile (VC) determinava un potenziale rischio di vapor intrusion (Capitolo 2). Dall'analisi dei risultati è emersa una discrepanza di alcuni ordini di grandezza tra le stime fornite dai modelli e le concentrazioni misurate. Si è quindi ipotizzato che la presenza di un livello meno permeabile nella geologia del sottosuolo e/o la biodegradazione nella zona insatura interrompessero la migrazione dei vapori. Tali fattori non potevano infatti essere adeguatamente considerati dai modelli di analisi di rischio disponibili.

Successivamente, al fine di valutare gli effetti delle proprietà fisico-chimiche del contaminante e del sottosuolo sul rischio di vapor intrusion, è stato sviluppato un modello numerico monodimensionale che considera i seguenti parametri: le variazioni verticali del contenuto d'acqua nel suolo, la biodegradazione ed i processi dinamici (Capitolo 3). L'analisi di sensitività effettuata con il modello ha mostrato che due fattori principali controllano le concentrazioni stimate: i) la distribuzione verticale del contaminante, regolata dal contenuto d'acqua nel suolo, e ii) la biodegradazione aerobica. L'influenza della variabile contenuto d'acqua nel suolo è dovuta alla diffusione in fase liquida, che ritarda significativamente il trasporto dell'inquinante; ciò conferma precedenti risultati riportati in letteratura.

Infine, allo scopo di ottenere tassi di biodegradazione specifici per suoli insaturi, sono stati eseguiti specifici esperimenti di laboratorio con toluene (Capitolo 4) e

cloruro di vinile (Capitolo 5) in condizioni di eccesso di ossigeno. Per il toluene sono stati utilizzati esperimenti in batch, microcosmi e colonne con suolo insaturo, mentre per il cloruro di vinile batch e microcosmi con suolo insaturo. I batch per entrambi i contaminanti contenevano batteri in soluzione acquosa con i nutrienti necessari e sono stati posti in agitatore, mentre i microcosmi contenevano unicamente suolo insaturo e sono stati incubati in maniera statica. Nei microcosmi con cloruro di vinile, sono stati quantificati i geni specifici coinvolti nel metabolismo aerobico di questo composto (etnE) in campioni liquidi e di suolo. I risultati per entrambi i contaminanti hanno mostrato che l'utilizzo di tassi di biodegradazione in fase liquida derivanti dalle prove in batch sottostima significativamente il ruolo della degradazione ad opera dei batteri.

La degradazione batterica nei batch liquidi sembra influenzata da limitazioni nel trasferimento del substrato che non si verificano in condizioni di suolo insaturo. Nei microcosmi con suolo insaturo, i tassi di biodegradazione in fase liquida per il toluene non sono correlabili alle variazioni del contenuto d'acqua nel suolo. Al contrario, i tassi di biodegradazione in fase liquida per il cloruro di vinile diminuiscono all'aumentare del contenuto d'acqua nel suolo. Di conseguenza si è ipotizzato che l'influenza del contenuto d'acqua sul trasferimento di massa alla scala dei pori del suolo dipenda dalle proprietà chimiche del contaminante, che ne regolano la distribuzione tra le fasi presenti. La quantificazione del gene etnE ha mostrato una correlazione lineare con l'ammontare di cloruro di vinile degradato, e rappresenta pertanto uno strumento di notevole interesse per applicazioni in-situ.

Le principali conclusioni di questa tesi indicano che le variazioni di contenuto d'acqua nel suolo (Capitolo 3) e la biodegradazione aerobica (Capitoli 4 e 5) sono aspetti cruciali da considerare congiuntamente per la valutazione dell'intrusione di vapori. Entrambi possono contribuire ad una significativa riduzione del rischio associato alla contaminazione da contaminanti organici in fase disciolta. Da queste conclusioni si ricavano specifiche e rilevanti implicazioni per la modellazione ed il monitoraggio della vapor intrusion. Per quanto riguarda la modellazione, l'inclusione del processo di biodegradazione nella zona insatura utilizzando tassi di biodegradazione in fase liquida derivanti da esperimenti in batch liquidi può sottostimare significativamente il ruolo della biodegradazione; appare quindi più appropriato l'uso di tassi derivanti da sistemi contenenti suolo insaturo. Relativamente al monitoraggio, è opportuna la misurazione in-situ delle variazioni verticali del contenuto d'acqua nel suolo, delle concentrazioni di inquinante e di ossigeno, in modo tale da tenere in considerazione i processi chiave nel controllo dei rischi da vapor intrusion.

Acknowledgments

First of all, I would like to thank my promotor, Huub Rijnaarts for having given me the chance to perform this research. His critical look and positive attitude contributed much to the finalization of this work. Tim Grotenhuis has always been enthusiastic, encouraging, and patient in introducing me to the way of thinking of environmental technologists, for this I am grateful to him. I have much appreciated the supervision of Pauline van Gaans, our discussion were important learning moments for me.

I owe much to the guidance and support of Johan Valstar for the modeling part of this thesis. His rigorous thinking was helpful and constructive, thanks for that. I am grateful to Alette Langenhoff and Jan Gerritse for sharing their practial and theoretical knowledge on the world of bacteria, as well as for their encouragement.

Working at the laboratories of Deltares has been a pleasant and interesting experience thanks to the presence of Habiba, Fredericke, Bas, Andrè, Melike, Kathrin, and Paul. Thanks for having made time to help me out, sometimes even only with a chat. I have appreciated much the cooperation with Fredericke Hannes for the molecular work in this thesis. Equally nice was the time spent in the office at Deltares. I would like to thank Miranda, Corrie, Els and Emmy from the secretariat for their assistance throughout these years. Thanks to David, Hans, Gijs, Niels, Thomas, Sophie and Victor for the positive vibes and the encouraging chats.

I have found in the department of Environmental Technology in Wageningen a number of inspiring colleagues. Thanks to Liesbeth, Anita and Romana for their help with the burocratical part as well as to Vinnie, Katja, Jean, Bert, Hans, Ardy and Hillion for the assistance with the analytics and with thinking about the set-ups. The fellow PhD students and researchers at the department have helped me in various ways: by answering my questions, by taking care of my set-up if needed, by providing a bed after long days in the lab, by carpooling, and last but not least with good mood. Jan (and the whole Bartaceck family), Fernando, Annemiek, Roel, Cees K., Darja, Christel, Ralph, Ruud, Mieke, David, Marjolein, Tim H., Pim, Diego, Tim G., Lucia, Ricardo, Eric, Iemke, Mirjam, Ingo, Jan, Nora, Magdalena, Wijb, Martijn, Zhuobiao, thank you all. Thanks to Ale and Ste for the good time in Wageningen. Additional thanks to Claudia and Paula for sharing the stress of the last phases, and to Nora for proofreading parts of the text.

Supervising master thesis students Jinji and Michele has been a very rewarding experience. I have enjoyed working with you and am grateful for your direct and indirect input to this thesis.

I would like to thank Alex van Renesse (TNO) for his support with the VC field measurements, Sjaak van Veen (TNO Zeist) for the oxydots measurements, as well as Edward Hummelink and Harm Gooren (WUR, Soil Physic laboratory) for the guidance with the soil retention curve measurements and the tensiometers. During my fieldwork in Italy I have appreciated the supervision and support of Alessandro Gargini and Monica Pasini, thanks for that. I would as well like to thank Lorella Dall' Olio and Alberto Bassi from the Municipality of Ferrara for their cooperative attitude.

My paranimphs Kirsten and Jasperien have been important in these years. Kirsten, thanks for being an inspiring friend. Jasperien, thanks for your patience with

my Dutch and for your help in many situations. I am glad you girls are my paranimphs.

An unrenounceable source of inspiration and positive energy have been my friends. Birka&Joseph, Yukina&Willem, Galya, Öznur, Rawad, Radja, Claudia, Annerys, Jules, Daniel&Wade, Sara&Andy, Claudia P., Deger&Maria, Borja, Eli&Massi, Alessandra, Michela, Wing, Tania&Martijn, Vasilis, Vio&Micheal, Aleksandra: a huge thank to you all for the long talks at dinner tables, the interesting evenings, the "artsy" afternoons and the trips that nurtured my mind and my soul. Additional thanks to Birka for proofreading parts of the thesis, to Massi&Eli for the cover, and to Verena for having been supportive.

A special thank to Elisa, Valentina, Silvia, Sara, Alexia, Luisa for having been there for me, and to Arianna for making Berlin feel home.

Finally, I would like to thank my father Roberto with Bianca, my late grandmother Ida, my uncle Fabio with Rosy, and my aunt Graziella for their support during these years. Writing a book was one of my mother's dreams. In a way, I have accomplished what she did not have the chance to. Thanks for having inspired me with your determination and great passion for life.

About the author

Sara Picone was born in Ferrara, Italy, on 5th November 1980. She obtained her highschool diploma in 1999 at I.T.C. Marco Polo, Ferrara. In 2005, she graduated from the University of Ferrara with a MSc degree in Geology. The thesis investigated the use of geochemical tracers in the marine prodelta of the Po river, northern Italy, and was performed at the Marine Geology section of the Italian National Research Center in Bologna (IT). Afterwards she cooperated with the same research institute analyzing geochemical and sedimentological data of the Adriatic sea.

In 2006, she was granted funding for an internship at TNO Built Environment and Subsurface in Utrecht (NL). During the course of the internship, she contributed to the implementation of the vapor intrusion pathway in a GIS software. This lead to the initiation of the PhD research described in this thesis, conducted at the sub-department of Environmental Technology of Wageningen University and at Deltares.

Her interest lies in the combination of hydrogeological and microbiological knowledge to reduce the impacts of subsurface contamination in the context of urban development.

Publications

Picone S., Alvisi F., Dinelli E., Morigi C., Negri A., Ravaioli M., Vaccaro C., 2008. New insights on late Quaternary palaeogeographic setting in the Northern Adriatic Sea (Italy). Journal of Quaternary Science, 23: 5, 489-501.

Gargini A., Pasini M., Picone S., Van Gaans P., Rijnaarts H., 2010. Chlorinated hydrocarbons plumes in a residential area. Site investigation to assess indoor vapor intrusion and human health risks. In: Saponaro S., Sezenna E., Bonomo L. eds., Vapor emission to outdoor air and enclosed spaces for human health risk assessment: site characterization, monitoring and modeling. Nova Science Publishers, Inc., 211-233.

Picone S., Valstar J., Grotenhuis T., Gaans van P., Rijnaarts H., 2012. Sensitivity analysis on processes and parameters affecting vapor intrusion risk. Environmental Toxicology and Chemistry, 31: 5, 1042 – 1052.

Netherlands Research School for the
Socio-Economic and Natural Sciences of the Environment

C E R T I F I C A T E

The Netherlands Research School for the
Socio-Economic and Natural Sciences of the Environment (SENSE),
declares that

Sara Picone

born on 5 November 1980 in Ferrara, Italy

has successfully fulfilled all requirements of the
Educational Programme of SENSE.

Wageningen, 18 June 2012

the Chairman of the SENSE board

Prof. dr. Rik Leemans

the SENSE Director of Education

Dr. Ad van Dommelen

The SENSE Research School has been accredited by the Royal Netherlands Academy of Arts and Sciences (KNAW)

KONINKLIJKE NEDERLANDSE
AKADEMIE VAN WETENSCHAPPEN

The SENSE Research School declares that **Ms. Sara Picone** has successfully fulfilled all requirements of the Educational PhD Programme of SENSE with a work load of 42 ECTS, including the following activities:

SENSE PhD courses

- Environmental Research in Context
- Research Context Activity: Co-organizing Study Trip to Turkey for Sub-department Environmental Technology, Wageningen University (23-30 November 2008)
- Physical Modelling
- Basic Statistics
- Environmental Risk Assessment of Chemicals
- Biological Processes for Resource Recovery in Environmental Technology

Other PhD and MSc courses

- Risk Assessment of potentially contaminated sites
- Teaching and supervising master thesis students
- Career assessment

Educational Activities

- Co-organization symposium TNO APAT-Sustainable approaches for mega-sites management and remediation: new perspectives. Venice, Italy, 30 November – 1 December 2007
- Supervision of Internship and Master students

Oral Presentations

- Risk assessment and risk mitigation technologies for chlorinated solvents, 5 February 2008, Utrecht, The Netherlands
- Modeling vapor intrusion risk: role of biodegradation, 16 June 2009, Utrecht, The Netherlands
- Biodegradation of organic compounds in unsaturated soils: role in reducing risk from vapor intrusion, 20 – 22 January 2010, Delft, The Netherlands
- Modelling risks of vapor intrusion,22 – 24 September 2010, Salzburg, Austria
- Vapour Intrusion: role of transport and biodegradation, 14 March 2011, Utrecht, The Netherlands

SENSE Coordinator PhD Education and Research

Mr. Johan Feenstra